Biological N_2 fixation in the upwelling region off NW Iberian Peninsula: magnitude, relevance and players

Víctor Moreira Coello

Doctoral dissertation

2018

Universidade Vigo

EIDO
Escola Internacional
de Doutoramento

Universidade Vigo

International Doctoral School

Víctor Moreira Coello

DOCTORAL DISSERTATION

"Biological N_2 fixation in the upwelling region off NW Iberian Peninsula: magnitude, relevance and players"

Supervised by:

Beatriz Mouriño Carballido

Emilio Marañón Sainz

2018

The work leading to this PhD Thesis was carried out in the framework of the NICANOR (Nitrogen fixation and diffusive fluxes in the NW Iberian Peninsula, EM2013/021) project granted to B. Mouriño-Carballido by *Xunta de Galicia*, and also supported by the RADIALES project of the *Instituto Español de Oceanografía* (www.seriestemporales-ieo.net).

The PhD candidate was supported by a FPU predoctoral fellowship (FPU13/01674) from the *Ministerio de Educación, Cultura y Deporte* (Spanish Government). Research short stays in the University of Vienna (Austria) (1 month) and University of California Santa Cruz (USA) (2 months) were funded by a short stay grant (EST16/00142) from the *Ministerio de Educación, Cultura y Deporte*, as well as by a fellowship for stays in research centers from the *Universidad de Vigo* (*Axudas á investigación 2016*).

A summarized version of chapter 2 of the present PhD Thesis is currently in preparation for submission as a brief communication entitled "Effects of contamination of commercial $^{15}N_2$ gas stocks on biological N_2 fixation measurements" authored by Moreira-Coello, V., Mouriño-Carballido, B., Marañón, E., Fernández-Carrera, A., Pérez-Lorenzo M.

A modified version of chapter 3 is partially included in the published article: Moreira-Coello, V., Mouriño-Carballido, B., Marañón, E., Fernández-Carrera, A., Bode, A., and Varela, M.M. (2017). Biological N_2 Fixation in the Upwelling Region off NW Iberia: Magnitude, Relevance, and Players. *Frontiers in Marine Science* 4, 303. doi: 10.3389/fmars.2017.00303.

Chapter 4 is in part described in the article "Temporal variability of diazotroph community diversity" authored by Moreira-Coello, V., Mouriño-Carballido, B., Marañón, E., Bode, A., Sintes, E., Zehr, J.P., Turk-Kubo, K. and Varela, M.M., which has been submitted for publication.

Acknowledgements/Agradecimientos

Y casi sin darme cuenta llegué al final de este camino que comencé a andar a principios de 2014. Tengo la sensación de que estos últimos años han pasado muy rápido y que el camino ha sido corto, pero ya sabemos que el tiempo lo distorsiona todo y que cuando miramos hacia atrás siempre parece que el tiempo ha volado. La realidad es que han pasado muchas cosas y que he conocido a muchas personas que me acompañaron durante la travesía. Todas estas vivencias, experiencias y personas que se cruzaron en mi camino me han enriquecido mucho y, sin duda, es lo más valioso que me llevo. Son muchos los nombres que deberían estar aquí pero no me extenderé en una larga lista porque llenaría hojas y hojas con personas y motivos.

Gracias infinitas a mis directores de tesis, Bea y Emilio, por confiar en mí, darme esta bonita oportunidad y estar siempre dispuestos a echarme una mano. Sin vuestra ayuda, esfuerzo y consejos esta tesis no hubiera sido posible.

También quiero agradecer y reconocer el enorme trabajo de todas las personas que me han ayudado a obtener los datos que presentamos en esta tesis y que han colaborado en el proyecto. Esa es la familia NICANOR. Desde los muestreos en el mar a bordo del ya mítico Lura, pasando por el trabajo en el laboratorio, y acabando por el interminable análisis de los datos. Gracias por toda vuestra ayuda y trabajo, y por hacerlo siempre con buen humor.

Gracias a los viejos y nuevos amigos que conocí durante esta etapa. Esta tesis también es vuestra porque he compartido el camino con vosotros. Y como en algún momento habréis resistido que os haya dado la turra con los diazótrofos, os habéis ganado la coautoría!

Y por supuesto, gracias a María, siempre mi principal apoyo, a mis padres, Marité y Enrique, y mis hermanos, Vero y Quique, por estar siempre ahí, incondicionalmente.

Víctor, 12 de septiembre de 2018

Contents

1. Introduction 19
1.1. The marine nitrogen cycle 19
1.2. Biological N_2 fixation in the marine environment 22
1.3. Measurement of N_2 fixation rates 25
1.4. Relevance of biological N_2 fixation as a mechanism of new nitrogen supply 29
1.5. Diversity of N_2-fixing microorganisms 30
1.6. Environmental control factors 33
1.7. N_2 fixation in the North Atlantic ocean 35
1.8. N_2 fixation in a nitrogen-rich region: the NW Iberian upwelling system 37
1.9. Hypotheses and objectives 39
2. Effects of contamination of commercial $^{15}N_2$ gas stocks on biological N_2 fixation measurements 45
Abstract 45
2.1. Introduction 46
2.2. Materials and Methods 48
2.2.1. Contamination control test with *Tetraselmis suecica* cultures 48
2.2.2. Sampling and hydrographic measurements 49
2.2.3. N_2 fixation field measurements 50
2.2.4. Chlorophyll *a* and primary production 52
2.3. Results 53
2.3.1. Uptake of ^{15}N-contaminants by non-diazotroph organisms 53
2.3.2. Overestimation of biological N_2 fixation rates estimated in the field 54
2.4. Discussion 57
3. Magnitude, biogeochemical role and abundance of main players of N_2 fixation under contrasting hydrographic conditions 65
Abstract 65
3.1. Introduction 66
3.2. Materials and Methods 69
3.2.1. Sampling and hydrographic measurements 69
3.2.2. Inorganic nutrients, chlorophyll *a*, and primary production 70
3.2.3. Flow cytometric counting 71
3.2.4. Biological N_2 fixation 72
3.2.5. DNA samples collection and extraction 73
3.2.6. Quantification of *nifH* gene by qPCR 73

3.2.7. Double CARD-FISH assay and sampling 74
3.2.8. Epifluorescence microscopy counts of the UCYN-A–Prymnesiophyte symbiosis 76
3.2.9. Niche overlap analysis 77
3.2.10. Dissipation rates of turbulent kinetic energy and estimates of nitrate fluxes through vertical diffusion 77
3.2.11. Nitrate supply through vertical advection 78
3.3. Results 80
3.3.1. Hydrography and turbulent mixing 80
3.3.2. Nutrients, chlorophyll *a* and primary production 84
3.3.3. Picoplankton community composition 86
3.3.4. Magnitude and biogeochemical relevance of biological N_2 fixation 88
3.3.5. *nifH* gene abundances 89
3.3.6. Identification, characterization and quantification of UCYN-A–Prymnesiophyte symbiosis by double CARD-FISH 91
3.3.7. Ecological niches of diazotroph groups 91
3.4. Discussion 93
3.4.1 Magnitude and biogeochemical relevance of BNF 93
3.4.2 Players, ecological niches and contribution to BNF 95
3.5. Outlook 100
4. Temporal variability of diazotroph community composition 107
Abstract 107
4.1. Introduction 108
4.2. Materials and Methods 111
4.2.1 Hydrographic and environmental sampling 111
4.2.2. DNA Samples Collection and Extraction 112
4.2.3. *nifH* gene PCR amplification and amplicon sequencing 112
4.2.4. Bioinformatics, phylogenetic and statistical analyses 113
4.2.5. UCYN-A oligotyping 115
4.3. Results 117
4.3.1. Diazotroph community diversity and composition 117
4.3.2. Temporal variability of the diazotroph community 122
4.3.3. UCYN-A oligotypes 125
4.4. Discussion 129
4.4.1. Composition and temporal variability of the diazotroph community 129
4.4.2. Diversity, variability and ecology of UCYN-A sublineages 132

4.5. Conclusions 134
5. General discussion and conclusions 139
5.1. General discussion 139
5.1.1. Effects of contamination of commercial $^{15}N_2$ stocks on biological N_2 fixation 139
5.1.2. Magnitude and biogeochemical role of biological N_2 fixation under contrasting hydrographic regimes 139
5.1.3. Diversity, abundance, temporal variability and ecology of diazotrophs 141
5.1.4. Future studies 144
5.2. Conclusions 146
6. Appendix 153
7. References 163
8. Summary in Spanish/Resumen en español 195
8.1. Introducción 195
8.1.1. Fijación biológica de N_2 en el medio marino 195
8.1.2. Relevancia de la fijación biológica de N_2 como mecanismo de suministro de nitrógeno nuevo 196
8.1.3. Diversidad de organismos fijadores de N_2 197
8.1.4. Factores ambientales de control 199
8.1.5. Fijación de N_2 en una región rica en nitrógeno: el sistema de afloramiento del NO de la Península Ibérica 199
8.1.6. Hipótesis y objetivos 200
8.2. Resultados y discusión 202
8.2.1. Efectos de la contaminación de los stocks comerciales de $^{15}N_2$ sobre las medidas de fijación biológica de N_2 202
8.2.2. Magnitud y relevancia biogeoquímica de la fijación de N_2 bajo diferentes condiciones hidrográficas 202
8.2.3. Diversidad, abundancia, variabilidad temporal y ecología de diazótrofos . 204
8.2.4. Estudios futuros 207
8.3. Conclusiones 209

1. Introduction

1.1. The marine nitrogen cycle

Nitrogen (N) is an essential element for life and the main limiting nutrient for primary production both in terrestrial and marine ecosystems (Falkowski, 1997). It plays a key role in ocean biogeochemistry, and its complex cycling affects significantly the biogeochemical cycles of biologically important elements such as carbon (C) and phosphorus (P) (Gruber, 2008). Marine inorganic nitrogen exists in diverse chemical forms and oxidation states, which experience multiple chemical transformations that in most cases are biologically mediated (Figure 1.1).

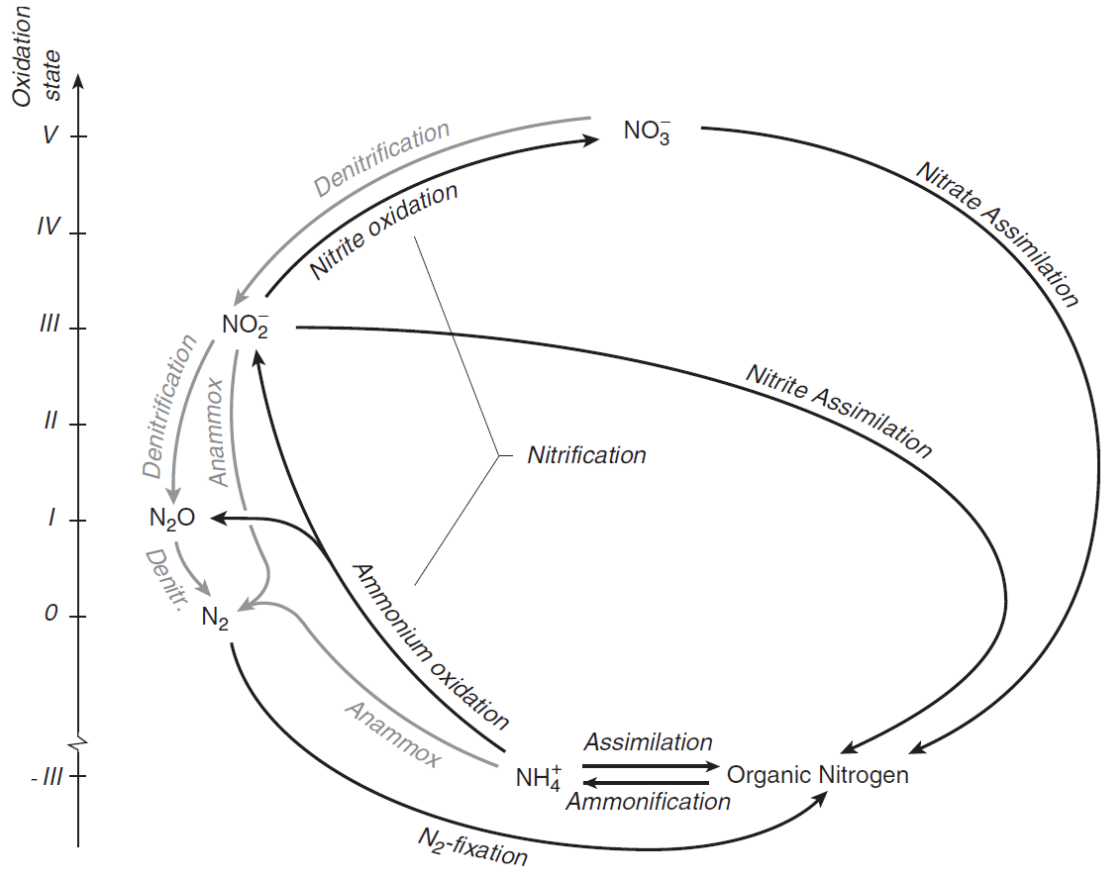

Figure 1.1. *Main nitrogen species and transformations in the marine environment. The processes indicated by grey arrows occur exclusively in anaerobic conditions. Organic nitrogen includes living and non-living particulate and non-living dissolved nitrogen. From Gruber (2008).*

In seawater, most N species are bioavailable (nitrate, NO_3^-; nitrite, NO_2^-; ammonium, NH_4^+; or dissolved organic compounds), but the most abundant (>95%) N species is

dissolved dinitrogen gas (N_2), which is not accessible to most organisms. Marine phytoplankton obtain N for growth mainly through the assimilation of nitrate and ammonium, which are important N-gain processes in the marine N cycle in quantitative terms (~8400 Tg N $year^{-1}$) (Gruber, 2008). Ammonium is the preferred N source for phytoplankton since the assimilative reduction of nitrate involves a high energetic cost (Zehr and Ward, 2002). However, nitrate is globally much more abundant than ammonium (580000 vs. 340 Tg N, respectively) (Conkright et al., 2002; Gruber, 2008). Nitrate concentrations in surface waters range from circa zero in tropical and subtropical regions to 10-35 μmol L^{-1} in temperate and cold seas (Figure 1.2). Most phytoplankton species, except *Prochlorococcus* and some *Synechococcus* strains, possess the enzymes nitrate and nitrite reductases, which catalyze the conversion of, respectively, nitrate to nitrite and nitrite to ammonium (Moore et al., 2002).

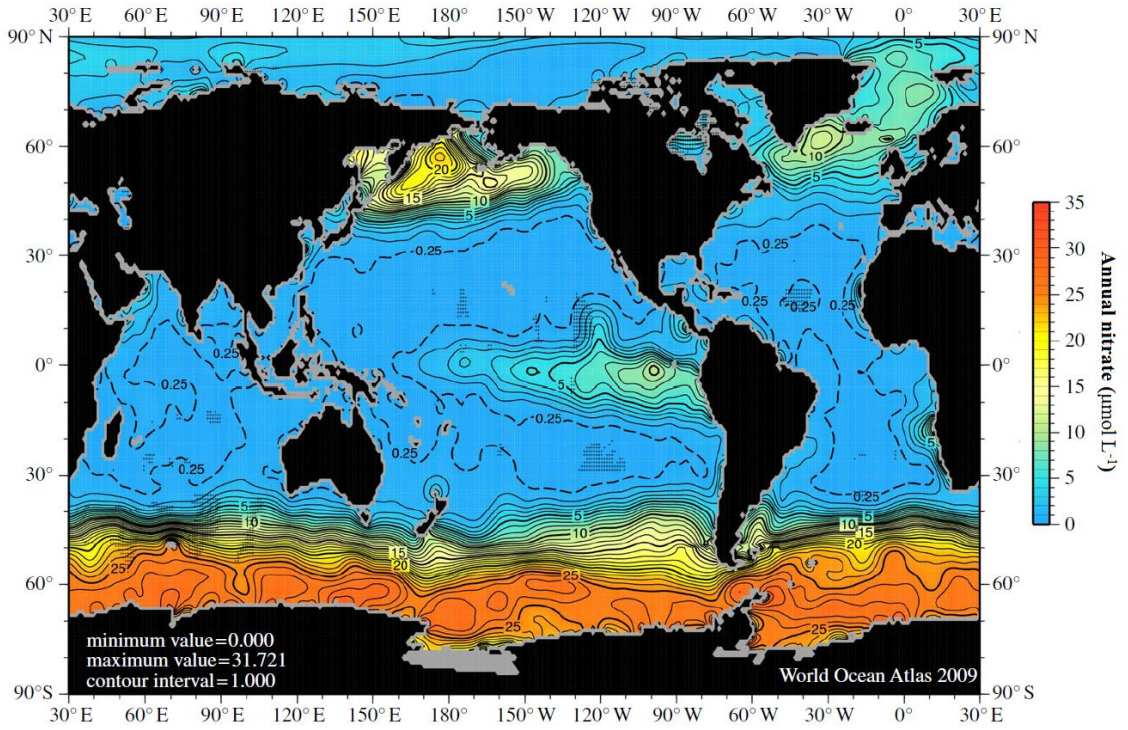

Figure 1.2. *Annual average nitrate concentration in surface waters of the global ocean. From Voss et al. (2013).*

Another important process in the marine N cycle is the remineralization of a large proportion of the organic nitrogen through ammonification and nitrification. Ammonification involves the conversion of organic N to ammonium. Nitrification consists of two steps, ammonium oxidation to nitrite, and nitrite oxidation to nitrate.

These remineralization processes, which are often coupled to the chemosynthesis of organic compounds, are performed by bacteria and archaea (Wuchter et al., 2006; Yool et al., 2007).

Denitrification and anaerobic oxidation of ammonium (anammox) are N-loss processes performed by bacteria in anaerobic conditions, such as oxygen-minimum zones (OMZs) of the water column and sediments. Both processes lead to the formation of N_2, the denitrification consuming nitrate and nitrite, and anammox consuming a combination of nitrite and ammonium.

Denitrification and nitrification produce also nitrous oxide (N_2O), a potent greenhouse gas and precursor of ozone-depleting radicals (Bange et al., 2010). Thus, due to its climatic relevance, the microbial marine pathways of N_2O production have received increased attention from the scientific community during recent decades (Voss et al., 2013).

The processes of N-loss are compensated by the transformation of atmospheric N_2 to reduced bioavailable ammonium, a process known as biological N_2 fixation, which provides the main supply of fixed N into the ocean (Gruber, 2008).

1.2. Biological N_2 fixation in the marine environment

The discovery of biological N_2 fixation in leguminous plants dates from the 19th century (Levollay, 1988). This metabolic pathway is very costly in terms of energy due to the strength of the triple bond between the two nitrogen atoms, making the biological N_2 fixation an extraordinary process due to its catalytic efficiency (Rees et al., 2005). Maybe inspired by the N_2 fixation in terrestrial systems, at the beginning of the 20th century Fritz Haber devised and patented the chemical synthesis of ammonium from atmospheric N_2. Shortly after, Carl Bosch developed the synthetic process on an industrial scale (Smil, 2001). During the last century, humans have fixed nitrogen industrially by the Haber-Bosch process to produce agricultural fertilizers, increasing the cultivation area and providing food to the increasing world population (Fowler et al., 2013). Such is the importance of this industrial procedure that, at present, the food of approximately half of the human population relies upon the production of nitrogen chemical fertilizers (Erisman et al., 2008).

Approximately 78% of atmosphere is N_2, though only a limited, but diverse, group of bacteria and archaea (termed diazotrophs) can use this large N inventory by the process of biological N_2 fixation (Karl et al., 2002). The nitrogenase enzyme is a remarkable evolutionary invention that allows to carry out this process, catalyzing the ATP-dependent reduction of N_2 to the biologically useful NH_4^+ (Zehr et al., 1998). Nitrogenase is encoded by highly conserved genes, suggesting an ancient origin since it is thought to have appeared when the Earth´s atmosphere was reducing, which could explain its inactivation in the presence of oxygen (Zehr et al., 1995). This enzyme consists of two component metalloproteins named according to their metal cofactor, the dimeric iron protein (Fe-protein) or dinitrogenase reductase, and the larger tetrameric molybdenum–iron protein (MoFe-protein) or dinitrogenase, although some diazotrophs can replace Mo by iron or vanadium (Figure 1.3) (Dixon and Kahn, 2004). The Fe-protein conducts the electron transfer to the MoFe-protein, which contains the catalytic site for the reduction. The structure of the Fe-protein is highly conserved, therefore, the *nifH* gene that encodes it is a very useful tool in diazotroph diversity studies, since it shows a low variability between the different species (Paerl and Zehr, 2000).

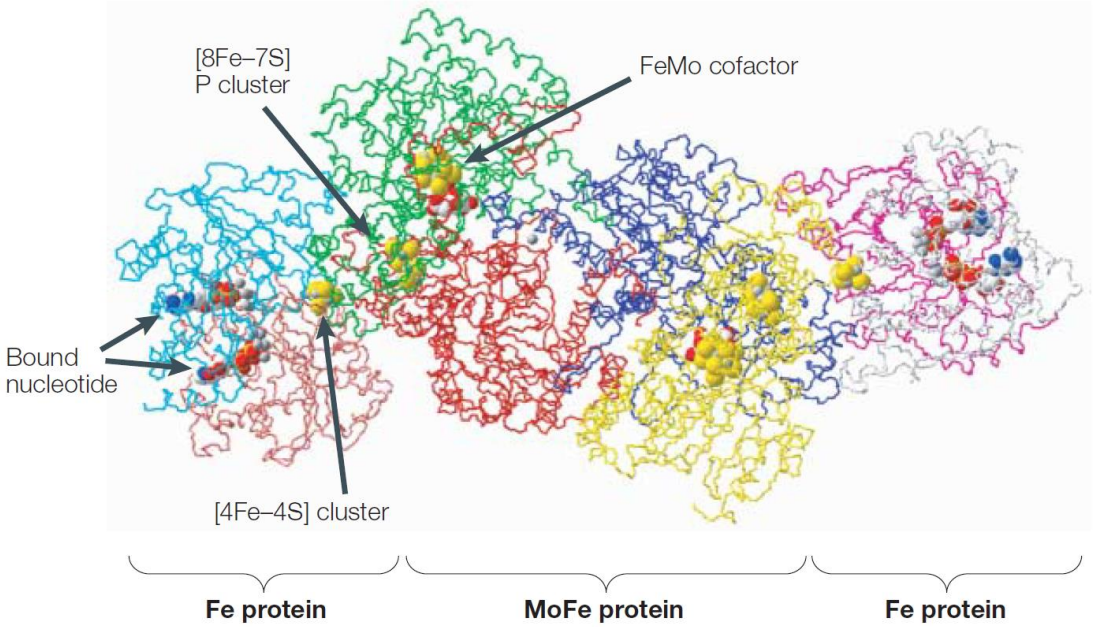

Figure 1.3. *Molecular structure of nitrogenase. The subunits of the two Fe-protein are coloured in brown, cyan, grey and magenta, whereas the subunits of MoFe-protein are coloured in yellow, green, blue and red. Bound nucleotide represents the ATP/ADP. From Dixon and Kahn (2004).*

The biological reduction of N_2 to ammonia (NH_3), catalyzed by the nitrogenase enzyme complex, has the following stoichiometry:

$$N_2 + 8H^+ + 8e^- + 16ATP \rightarrow 2NH_3 + H_2 + 16ADP + 16P_i \quad (1)$$

This process fuels phytoplankton photosynthetic activity by supplying new N as ammonium (Figure 1.4), but requires a high amount of energy (16 ATP) and reducing power (8 electrons) to break the triple bond of N_2. For this reason, the nitrogenase activity is highly regulated and controlled, for example, by nutrient concentrations (Karl et al., 2002).

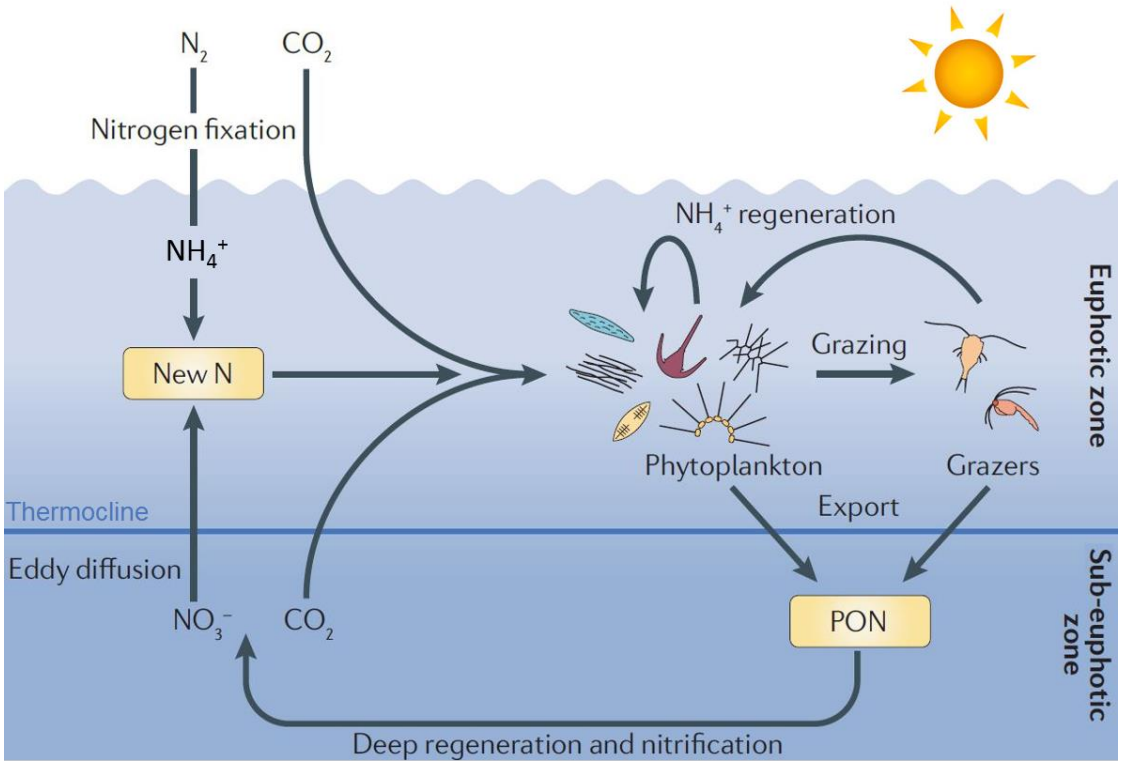

Figure 1.4. *Simplified scheme of new nitrogen inputs to surface waters in the oceanic environment through nitrogen fixation and nitrate diffusion from deep waters. PON is particulate organic nitrogen. Adapted from Sohm et al. (2011b).*

Biological N_2 fixation plays a key role in the oceanic nitrogen cycle by countering the N-loss by denitrification and anammox, thus balancing the fixed N budget (Figure 1.5). Nevertheless, there is evidence suggesting a strong imbalance between losses and inputs. The estimates point out that nitrogen losses are higher than inputs (Codispoti et al., 2001; Galloway et al., 2004; Gruber, 2004; Voss et al., 2013). Voss et al. (2013) estimated a loss of ~61 Tg N yr^{-1} in coastal systems and open ocean. Codispoti (2007) reported a deficit of ~200 Tg N yr^{-1} between denitrification sinks and biological N_2 fixation, the main source for oceanic fixed N. Denitrification takes place mainly in OMZs, where the N-losses result in N-depleted waters (N:P ratio <16) (Lam and Kuypers, 2011). The supply of these waters to the surface may favor growth and activity of diazotrophs in these regions (Deutsch et al., 2007; Karl and Letelier, 2008). However, recent findings indicate a spatial decoupling between N_2 fixation and denitrification (Knapp et al., 2016; Bonnet et al., 2017), putting into question the hypothesis of close coupling (Deutsch et al., 2007), and pointing toward iron as presumable main control factor of biological N_2 fixation (Gruber, 2016). In any case, the biogeochemical estimates on a basin or global

scale have large uncertainties, partially due to the lack of knowledge of the abundance, distribution and activity of diazotrophs over the ocean.

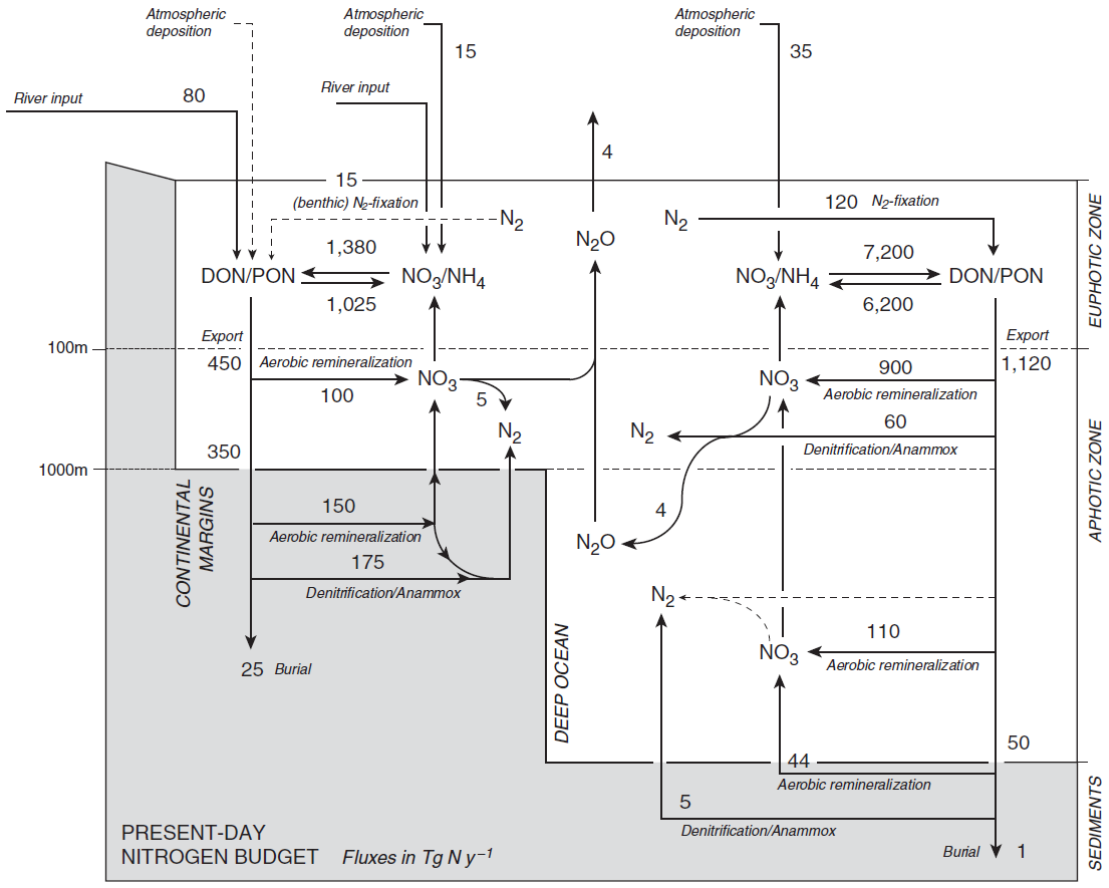

Figure 1.5. *Schematic budget of marine nitrogen cycle. Fluxes are in units of Tg N* yr^{-1}*. The level of uncertainty varies strongly between the individual fluxes, but is usually of the order of ±30%. From Gruber (2008).*

1.3. Measurement of N_2 fixation rates

Estimates of biological N_2 fixation are mainly obtained by using in vitro experimental and geochemical methods, although they can also be derived from modelling diazotroph abundances and growth rates (e.g., Goebel et al., 2007). Experimental methods are direct in vitro measurements of the N_2-fixing activity in incubations of natural planktonic samples for a certain period of time. There are two main approaches to measure experimentally the N_2 fixation: the acetylene reduction assay (ARA) (Hardy et al., 1968; Stewart et al., 1967) and the $^{15}N_2$-tracer addition technique (Montoya et al., 1996).

ARA is actually an indirect measurement of N_2 fixation that takes advantage of the low substrate specificity of the nitrogenase enzyme. It is based on the preferential reduction

of acetylene (C_2H_2) to ethylene (C_2H_4) by the nitrogenase, instead of reducing N_2 to NH_3 (Schollhorn and Burris, 1967). C_2H_2 is an analogous molecule to N_2 since both possess a triple bond, but to transform C_2H_2 reduction to N_2 fixation rates we have to apply a theoretical conversion ratio. The reduction ratios usually used are C_2H_2:N_2 = 3:1 or 4:1, which are estimated by the difference in the number of electrons needed to reduce both molecules. These conversion factors are not entirely reliable since diverse studies have shown large deviations (reviewed in Montoya et al., 1996; Postgate, 1982). Besides that, the acetylene may affect the metabolism of diazotrophs (Giller, 1987; Staal et al., 2001). Hence, the current availability of high-sensitivity and high-precision Isotope Ratio Mass Spectrometers (IRMS) and high purity $^{15}N_2$ gas, along with the development of the isotope tracer techniques, made the other principal biological method, the $^{15}N_2$-tracer assay, the most used nowadays to measure biological N_2 fixation in both terrestrial and aquatic ecosystems.

The stable isotope tracer protocol consists in the injection of a bubble of $^{15}N_2$ (98-99% ^{15}N-enriched) in a seawater sample, which is subsequently incubated for a given period of time. This technique is based on the assimilation and transformation of isotopically labelled $^{15}N_2$ gas into organic nitrogen. However, it has been demonstrated that the traditional bubble technique could underestimate the N_2 fixation rates as a result of the incomplete equilibrium between the injected gas bubble and the surrounding water in short-time incubations, leading to a lower availability of $^{15}N_2$ for diazotrophs than assumed by the method to calculate the rates (Mohr et al., 2010). The magnitude of the underestimation depends on physical properties (e.g., temperature and salinity) and incubation time, which influence the extent of the dissolution of $^{15}N_2$ in the seawater sample. In long duration incubations (~24h), the dissolution of the bubble will be higher. Likewise, the diazotroph community composition is also relevant (Benavides et al., 2013b; Großkopf et al., 2012; Mohr et al., 2010; Wilson et al., 2012). The underestimation will be lower in communities dominated by N_2-fixers with buoyancy capacity (e.g., *Trichodesmium* or *Nodularia*) because they can remain close to the bubbles, in contrast to the rest of diazotrophs that will settle to the bottom of the bottle. According to Großkopf et al. (2012), underestimation ranges from a factor of 2 in communities dominated by *Trichodesmium*, up to a factor of 7 in communities dominated by unicellular cyanobacteria. In order to attain a total equilibrium and avoid the problems associated with the incomplete dissolution, Großkopf et al. (2012) and Mohr et al. (2010) proposed

a modification to the tracer technique of Montoya et al. (1996), which consists in adding $^{15}N_2$ dissolved in seawater rather than as a bubble. However, Wannicke et al. (2018) compared the N_2 fixation rates obtained from bubble and enriched water methods, and reported insignificant underestimations of N_2 fixation rates in incubations of ~24h. Likewise, several authors have demonstrated that BNF rates may be underestimated if the ^{15}N-enrichment in the dissolved organic N is overlooked, considering only the incorporation of ^{15}N into particulate organic N (Benavides et al., 2013c; Berthelot et al., 2017; Glibert and Bronk, 1994; Konno et al., 2010). Underestimation has also been reported when glass fiber filters (GF/F, Whatman, 0.7 μm pore size) are used in the filtration after incubations with added $^{15}N_2$ tracer, due to the loss of small, unicellular diazotrophs (Bombar et al., 2018).

The accuracy of the $^{15}N_2$-tracer addition assay relies on the assumption that the ^{15}N-enrichment of the biomass is only due to the process of biological reduction of N_2. However, Dabundo et al. (2014) reported the presence of substantial concentrations of potentially bioavailable ^{15}N-contaminants ($^{15}NO_3^-/^{15}NO_2^-$ and $^{15}NH_4^+$) in some commercial $^{15}N_2$ gas stocks. The most affected commercial stocks belong to Sigma-Aldrich supplier, whereas $^{15}N_2$ from Cambridge-Isotope and Campro Scientific presumably are not contaminated or exhibit insignificant contamination. In contrast to the potential underestimations discussed above, these findings imply that the contaminant ^{15}N-species present in $^{15}N_2$ from Sigma may have caused significant overestimations in some of the N_2 fixation rates reported in the literature.

The geochemical methods are indirect approaches that allow a larger spatial and temporal resolution in the estimates of N_2 fixation. These methods are based on the chemical signatures in particulate and dissolved N pools. The approaches commonly used are the analysis of the isotopic ratio of N in samples of particles, zooplankton, etc., and the biogeochemical tracer N* (Gruber and Sarmiento, 1997; Michaels et al., 1996).

The analysis of the isotopic ratio relies on the relative abundance of the N isotopes (^{14}N and ^{15}N) in a sample in relation to the standard value in the atmospheric N_2. The parameter to express this relation is the $\delta^{15}N$:

$$\delta^{15}\mathrm{N}\ (‰) = \left[\frac{(^{15}\mathrm{N}/\,^{14}\mathrm{N})sample}{(^{15}\mathrm{N}/\,^{14}\mathrm{N})atmosphere} - 1\right] \times 1000 \quad (2)$$

where ($^{15}N/^{14}N$)atmosphere = 0.003676 (i.e., 0.366 atom%) (Montoya et al., 1996). As we can note, atmospheric N_2 is impoverished in ^{15}N. The value of $\delta^{15}N$ reflects directly the isotopic composition of the N source used by the primary producers, thus, the organic N that derives from the biological N_2 fixation will have negative $\delta^{15}N$ or ~0‰. These values help us to identify regions where the N_2 fixation is a dominant process. By contrast, when the uptake of nitrate is the main pathway of new N input, $\delta^{15}N$ will be higher since, for instance, the deep nitrate supplied to the euphotic layer by diffusive fluxes has a $\delta^{15}N$ ~4.6‰ in the oligotrophic NA (Montoya et al., 2002). Furthermore, $\delta^{15}N$ depends on the kinetic isotopic fractionation that affects all assimilation reactions of the marine N cycle, and results in an affinity for light N isotopes (^{14}N) against heavy forms (^{15}N) (Montoya et al., 2007, 2008). The weak discrimination against the heavy isotope ^{15}N explains that the zones where the N_2 fixation is an important supply of new N, the phytoplankton biomass may be slightly depleted in ^{15}N in relation to atmospheric N_2, resulting in $\delta^{15}N$ <0‰.

The tracer N* indicates the deficiency or excess of nitrate in relation to Redfield stoichiometry (C:N:P ≈ 106:16:1) (Redfield et al., 1963). This parameter is calculated from the nitrate and phosphate concentrations in the water column:

$$N^* = 0.87 \times [NO_3^-] - 16 \times [PO_4^{3-}] + 2.9 \quad (3)$$

where 0.87 and 2.9 are constants that make the global average of N* = 0, maintaining a conservative state (calculated from the database of the Geochemical Ocean Section Study–GEOSECS). Thereby, a deviation of the conservative state of N* is due to an imbalance between N_2 fixation and denitrification (Gruber and Sarmiento, 1997). An increase of the N:P ratio reaching values higher than 16 (N:P>16) could point toward a process of new N input such as N_2 fixation, whereas a decline of the N:P below the Redfield ratio (N:P<16) could indicate a nitrogen removal by denitrification. If the new N supply by vertical and horizontal mixing processes are not relevant, a N* >2.5 μmol kg^{-1} has been typically considered indicative of net N_2 fixation (Mahaffey et al., 2005).

Nonetheless, these geochemical methods have also uncertainty, since low $\delta^{15}N$ values and N* >2.5 μmol kg^{-1} could be also due to the atmospheric deposition of light fixed N stemmed from human activities such as fossil fuel combustion and fertilizers production (Baker et al., 2007; Hastings et al., 2009; Holtgrieve et al., 2011).

1.4. Relevance of biological N_2 fixation as a mechanism of new nitrogen supply

Biological N_2 fixation, along with other processes such as horizontal transport (Torres-Valdés et al., 2009; Williams and Follows, 1998), vertical diffusive (Mouriño-Carballido et al., 2011; Villamaña et al., 2017) and advective fluxes (Pitcher et al., 2010), mesoscale and submesoscale processes (Oschlies and Garçon, 1998), and atmospheric deposition (Duce et al., 2008; Mouriño-Carballido et al., 2012), supply new N to the euphotic layer. In the vast oligotrophic regions of the tropical and subtropical ocean, diazotrophs have a notable competitive advantage over the rest of phytoplankton, as they use N_2 fixation as their main N source while other inputs are scarce or absent. Considering that these oligotrophic regions occupy more than 70% of the total ocean surface (Longhurst, 1998), this diazotroph-mediated supply of new N plays a key role in CO_2 fixation, and has a large biogeochemical significance on a global scale.

Vertical turbulent diffusion is also an important mechanism of new N supply over large extensions of the open ocean (Fernández-Castro et al., 2015; Mouriño-Carballido et al., 2011; Painter et al., 2013), and in coastal regions during the summer thermal stratification. The comparison of studies quantifying simultaneously N_2 fixation versus the transport of nitrate into the surface ocean through turbulent mixing has given rise to a wide range of results. On a global scale, nitrate diffusion seems to dominate over N_2 fixation, although in some areas of the subtropical gyres N_2 fixation equals or even exceeds the new N input by nitrate diffusion (Capone et al., 2005; Fernández-Castro et al., 2015; Mouriño-Carballido et al., 2011; Painter et al., 2013). This balance highlights the major role played by the diazotrophic activity as support of the new production, which is more relevant in regions with stronger water column stability such as the Northwestern Atlantic in relation to the Northeastern Atlantic (Capone et al., 2005; Montoya et al., 2007). The global estimated N_2 fixation flux is ~120 Tg N yr^{-1} (Gruber, 2008) (Figure 1.5), which could support up to half of the global new production in oligotrophic zones (Karl et al., 1997).

Quantifying the nutrient transport into the productive euphotic layer by turbulent diffusion requires estimating the magnitude of vertical diffusivity (*Kz*) (Fernández-Castro et al., 2014), which in the ocean can be generated by a variety of processes. In surface layers, turbulence can be generated by wind stress (Moum and Smyth, 2001), ocean-atmosphere interactions (exchange of heat and freshwater fluxes), or wave processes (Langmuir circulation) (Belcher et al., 2012). Whereas in the ocean interior, turbulent diffusivity can be due to mechanical processes such as internal waves and shear

instabilities, and double-diffusion mechanisms such as the salt fingers developed in tropical and subtropical central oceans (Gargett, 1989). The implicit methodological difficulties for measuring directly microstructure turbulence and quantifying vertical mixing motivated the use of constant values of *Kz* (Capone et al., 2005) and empirical diffusivity parameterizations (Fernández-Castro et al., 2014; Planas et al., 1999). Currently, the collection of direct *Kz* estimates is made possible by instruments such as microstructure profilers (MSS, Prandke and Stips, 1998) (Figure 1.6), which allow measuring directly small-scale turbulence. In the last years, microstructure turbulence profilers have been increasingly used to measure vertical diffusivity in different regions of marine environments (e.g., Cuypers et al., 2012; Fernández-Castro et al., 2014; Hibiya et al., 2007; Jurado et al., 2012; Mouriño-Carballido et al., 2011, 2016; Villamaña et al., 2017). However, our current knowledge of turbulence magnitude in the ocean, its generation mechanisms and its large-scale distribution is still scarce.

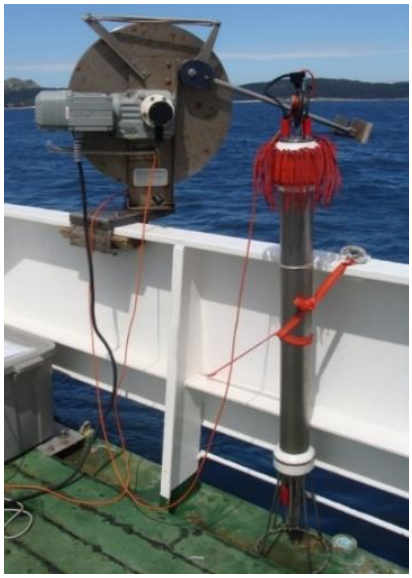

Figure 1.6. *MSS 90 multiparameter high resolution profiler (ISW Wassermesstechnik and Sea & Sun Technology GmbH, Germany) for the measurement of microstructure turbulence in aquatic environments.*

1.5. Diversity of N_2-fixing microorganisms

Diazotrophs are exclusively prokaryotic organisms (including Bacteria and Archaea), which are very diverse both in form and in function. Despite the high diversity of N_2-fixing microorganisms, those traditionally most studied in the marine environment are the colonial cyanobacterium *Trichodesmium* and the cyanobacterial symbionts of diatoms. *Trichodesmium* are non-heterocystous filamentous cyanobacteria inhabiting the

oligotrophic warm tropical and subtropical oceans, where they fix N_2 at relatively high rates and frequently form large blooms (Capone et al., 1997, 2005). Indeed, this planktonic organism is considered the major marine diazotroph due to its high abundances and N_2 fixation rates. On the basis of the cytomorphological characteristics of natural populations of *Trichodesmium*, five species have been identified (*T. erythraeum*, *T. thiebautii*, *T. tenue*, *T. hildebrandtii* and *T. contortum*) (Karl et al., 2002). However, according to genetic markers, these different species have been clustered in only two principal clades (*T. erythraeum* and the other strains) (Zehr, 2011).

The diazotrophic symbionts of diatoms are filamentous heterocystous cyanobacteria with a patchy distribution and abundance, widely distributed through the warm oligotrophic ocean and plumes of large rivers, where their hosts benefit from excess silica (Sohm et al., 2011b). These species form a chain of a few cells with a terminal heterocyst. In oceanic environments we find *Richelia*, endosymbiont of the diatoms *Rhizosolenia* and *Hemiaulus* (living within the frustule but outside the cell wall), and *Calothrix*, epibiont of the diatom *Chaetoceros* (living outside the frustule) (Zehr, 2011).

Marine diazotrophs also comprise unicellular cyanobacteria widely distributed in the global ocean (Zehr, 2011): the uncultivated group A or UCYN-A, the free-living *Crocosphaera* sp. or UCYN-B, and the presumably free-living UCYN-C, which includes cultivated cyanobacteria such as the benthic *Cyanothece* sp., morphologically similar to UCYN-B. UCYN-B has been successfully isolated from the open ocean, yielding up to ten different cultured strains (Webb et al., 2009). But in the last years UCYN-A (or *Candidatus* Atelocyanobacterium thalassa) has caught the most attention and interest since it is one of the most important members of the global diazotroph community due to its broad distribution in marine environments and relatively high N_2 fixation rates (Farnelid et al., 2016a; Martínez-Pérez et al., 2016). Unlike *Trichodesmium*, UCYN-A can be detected over a broader depth and latitudinal range (Moisander et al., 2010), even in upwelling ecosystems (Sohm et al., 2011a). This unicellular cyanobacterium lacks genes for the oxygen-evolving photosystem II, the carbon-fixation enzyme RuBisCO (ribulose bisphosphate carboxylase), the tricarboxylic acid cycle, and some pathways of amino acid and purine synthesis (Tripp et al., 2010). Thus, it lives in obligated association with a picoeukaryotic prymnesiophyte that provides it organic compounds (Figure 1.7) (Thompson et al., 2012, 2014). This single-cell symbiosis established between them is a potential model for observing the evolution of organelles in eukaryotic cells, specifically

N_2-fixing organelles (Zehr et al., 2016). Six UCYN-A sublineages (UCYN-A1 to -A6) have previously been defined based on the genetic diversity of *nifH* sequences available in the NCBI GenBank database (Farnelid et al., 2016a; Thompson et al., 2014; Turk-Kubo et al., 2017). Recent findings indicate that each of these sublineages occupy different ecological niches. For instance, UCYN-A1 dominates in the oligotrophic open ocean, whereas UCYN-A2 occurs mainly in coastal regions (Farnelid et al., 2016; Messer et al., 2015a; Thompson et al., 2014; Turk-Kubo et al., 2017).

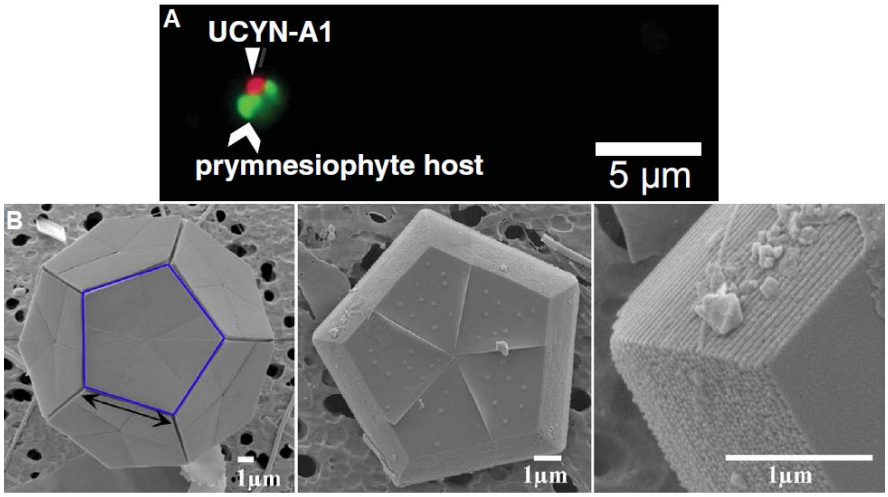

Figure 1.7. (A) *Microphotographs of the double CARD-FISH assay obtained with the epifluorescence microscope showing the Prymnesiophyte host and the associated UCYN-A1 symbiont (from Cabello et al., 2016).* ***(B)*** *Scanning Electron Microscope (SEM) images of a cell of* Braarudosphaera bigelowii *(UCYN-A2 Prymnesiophyte host) showing in detail their calcareous pentaliths (from Hagino et al., 2013).*

The planktonic diazotrophic community comprises also non-cyanobacterial diazotrophs. N_2-fixing heterotrophic bacteria include a wide range of phylogenetic groups such as Firmicutes and Proteobacteria, among others (Zehr et al., 2003b), whereas diazotrophic archaea appear to include only methanogens (Riemann et al., 2010). Even though cyanobacterial diazotrophs are traditionally considered the most important oceanic N_2-fixers, in recent years it has been demonstrated that potentially active non-cyanobacterial diazotrophs may exhibit a larger geographical and depth distribution, including the aphotic zone (Bombar et al., 2016; Delmont et al., 2018; Moisander et al., 2017). In any case, their contribution to the global marine N_2 fixation, ecological relevance and ecophysiology remain still elusive due to lack of data.

1.6. Environmental control factors

Over recent years, numerous studies have investigated the biogeography and controlling mechanisms of the oceanic biological N_2 fixation (e.g., Fernández-Castro et al., 2016; Fernández et al., 2010; Luo et al., 2014; Moore et al., 2009). The influence of the control factors depend largely on the diazotrophic community composition since each diazotrophic group has different autoecology and physiological constraints. In general, nutrients (N, P and Fe), oxygen (O_2) and temperature are commonly considered the most important controlling factors.

Due to the high energetic cost of fixing N_2 in comparison to the assimilation of dissolved inorganic nitrogen (mainly ammonium and nitrate) (Stam et al., 1987), the availability of fixed N has been traditionally considered as inhibitory for diazotrophic activity. In the case of *Trichodesmium*, additions of fixed N (nitrate) reduce or inhibit the N_2 fixation (Holl and Montoya, 2005; Mulholland et al., 1999, 2001). The activity of unicellular cyanobacteria such as UCYN-B (*Crocosphaera*) is also influenced by additions of ammonium, but not by nitrate (Dekaezemacker and Bonnet, 2011).

Low phosphorus availability in the marine environment can be a limiting factor of the N_2 fixation activity (e.g., Hynes et al., 2009; Mills et al., 2004; Sañudo-Wilhelmy et al., 2004). Considering that P occurs at low concentrations in the open ocean environment, some diazotrophs such as *Trichodesmium* or UCYN-B have acquired strategies to meet their P needs. *Trichodesmium* is able to assimilate dissolved organic phosphorus (in form of phosphomonoesters or phosphonates) (Dyhrman et al., 2002, 2006) or to maintain an intracellular reservoir of phosphate (PO_4^{3-}) in excess (Fu et al., 2005). UCYN-B has a strong capacity for scavenging P in oligotrophic systems thanks to a high-affinity PO_4^{3-} transport system, as well as genes to hydrolyze phosphomonoesters (Dyhrman et al., 2006; Dyhrman and Haley, 2006).

Iron supply correlates significantly with marine N_2 fixation (e.g., Mahaffey et al., 2003; Mills et al., 2004; Moore et al., 2009). Diazotrophs need Fe because it is an indispensable cofactor for the nitrogenase enzyme, requiring approximately 5-10 fold more Fe for growth based on N_2 fixation compared to non-diazotroph phytoplankton using ammonium (Berman-Frank et al., 2001a; Kustka et al., 2003). Fe concentration in seawater is very low, especially in oligotrophic regions (<1 nM), being mainly supplied by atmospheric dust deposition and, to a lesser extent, by vertical diffusive fluxes (Duce

and Tindale, 1991; Rijkenberg et al., 2012). Consequently, N_2-fixers have developed mechanisms to overcome the Fe limitation. For instance, *Trichodesmium* can assimilate more Fe than needed to meet its growth, as with phosphate, accumulating it in intracellular reservoirs (Chen et al., 2011). Recent studies point towards iron as the key control factor of biological N_2 fixation (Bonnet et al., 2017; Fernández et al., 2010; Knapp et al., 2016; Moore et al., 2009).

Oxygen is potentially an important limiting factor of N_2 fixation because it inhibits the nitrogenase activity (Zehr et al., 1995). By indirect mechanisms, Luo et al. (2014) identified it as one of the main predictors controlling the spatial distribution of marine N_2 fixation on a global scale. In any case, the cyanobacteria have evolved a variety of strategies to protect the nitrogenase from the photosynthetically produced O_2, including the development of heterocysts (Paerl and Zehr, 2000), the temporal segregation of N_2 fixation and photosynthesis (N_2-fixing overnight), the spatiotemporal segregation of both processes during the photoperiod, the presence of specialized cells named diazocytes where nitrogenase is found in *Trichodesmium* (Bergman et al., 2013; Berman-Frank et al., 2001b), or the autoprotection of the enzymatic complex by reducing the O_2 (Bergman et al., 1997).

Biological N_2 fixation is also related to temperature, being mainly restricted to the warm (sub)tropical ocean due to the high diazotrophic activity of *Trichodesmium* in these regions (Carpenter and Capone, 2008; Luo et al., 2014). Warm seawater leads to a relatively low O_2 solubility and increases the respiration rates, helping to maintain anoxic intracellular conditions in the case of non-heterocystous diazotrophs, such as *Trichodesmium* (Stal, 2009). Conversely, as temperature decreases, respiration also declines and O_2 solubility increases. Below a certain temperature, the O_2 diffusion within the cell would be higher than the respiration and diazotrophs would lose their ability to keep anoxic intracellular conditions. In the case of *Trichodesmium*, theoretical and empirical approaches indicate that the minimum temperature of growth is ~17ºC (Breitbarth et al., 2007; Stal, 2009). However, the connection between temperature and N_2 fixation could also be indirectly influenced by the nitrate availability, since temperature is inversely correlated to nitrate concentration (Karl et al., 2002). In any case, the presence and activity of diazotrophs in temperate and cold oceans demonstrates that N_2 fixation can also occur in the traditionally overlooked low-temperature waters (e.g.,

Benavides et al., 2011; Blais et al., 2012; Fernández-Méndez et al., 2016; Mulholland et al., 2012; Rees et al., 2009).

Finally, Hutchins et al. (2007, 2013) and Lomas et al. (2012) identified the surface CO_2 concentration, a previously neglected control factor, as a possible driver of taxon-specific diazotroph activity. These authors observed that diverse taxa of *Trichodesmium* and *Crocosphaera* respond differently to changing CO_2 partial pressures, which could induce shifts in the community favoring the better-adapted clades. This factor acquires special relevance in the current scenario of global change.

1.7. N_2 fixation in the North Atlantic ocean

The North Atlantic ocean (NA) comprises diverse biogeographical provinces with different hydrographic features. For example, this domain includes the North oligotrophic subtropical gyre, the Iberia-Canary upwelling domain, the Gulf Stream, the Equatorial upwelling region, and the Amazon and Congo Rivers plumes. In relation to the other oceanic basins, the NA is singular because it receives the highest atmospheric deposition of nutrients (Prospero et al., 1996), it has a fixed N excess and chronic P deficiency (high N:P ratios) (Ammerman et al., 2003), and it is subject to substantial nutrient supply from large rivers such as the Amazon.

The NA subtropical gyre occupies the largest area of the basin and is characterized by low surface nitrate and phosphate concentration and low primary production (Figure 1.2; Garcia et al., 2013). Nonetheless, it is fertilized through lateral transport into the gyre interior by the Gulf Stream, the subpolar gyre and the surrounding nutrient-replete regions, such as the Amazon River plume and the Northwest African and Equatorial upwelling systems (Pelegrí et al., 2006). These nutrient inputs play a key role in sustaining primary production within the subtropical gyre (e.g., Torres-Valdés et al., 2009). Likewise, the atmospheric deposition of inorganic N oxides (NO_x) and reduced N forms (NH_x) supply fixed N to the Northeastern Atlantic (0º–40ºW, NEA) since this area is located downwind from European industrialized countries (Prospero et al., 1996). NO_x and NH_x derive mainly from anthropogenic emissions due to fossil fuel combustion and agriculture fertilizers synthesis, respectively. Furthermore, the large mineral dust deposition coming from the arid NW Africa (Saharan desert) provides about 6 Tg yr^{-1} of Fe to the NA (Prospero et al., 1996), enhancing significantly the biological N_2 fixation in

this basin (e.g., Fernández et al., 2010; Mahaffey et al., 2003; Moore et al., 2009). In fact, several authors have considered that the high N:P ratios in the NA is a consequence of the stimulated diazotrophy resulting from high iron inputs (Gruber and Sarmiento, 1997; Michaels et al., 2001; Moore et al., 2009; Schlosser et al., 2014).

In the Amazon River plume and the Equatorial upwelling system, the high dissolved inorganic nitrogen and phosphate supplies promote firstly the growth of non-diazotrophic phytoplankton, which consume the nitrogen available leaving an excess of phosphate (low N:P ratio), which subsequently fuels N_2 fixation (Subramaniam et al., 2008, 2013). This positive correlation between low N:P ratios (low nitrate concentration in relation to the phosphate concentration) and diazotrophic activity has been observed in different regions of the NA, even though with some exceptions (Benavides and Voss, 2015).

The different physico-chemical characteristics of the regional environments of the low-latitude NA drive the distribution, abundance and activity of N_2-fixers (Benavides and Voss, 2015). Overall, the Northwestern Atlantic (40º–80ºW) is characterized by a stratified water column with a low N:P ratio, optimal growth conditions for *Trichodesmium* (Bergman et al., 2013). In contrast, the waters of the Northeastern Atlantic influenced by the Northwest African upwelling are characterized by receiving a larger iron supply through atmospheric deposition, as well as being richer in nitrogen, colder and more mixed. N_2-fixing unicellular cyanobacteria are abundant in this region, mainly UCYN-A, since the prevailing conditions seem to limit the growth of *Trichodesmium* (e.g., Fernández et al., 2013; Goebel et al., 2010; Langlois et al., 2005, 2008). Most studies about the distribution and abundance of diazotrophs in the NA show that *Trichodesmium* are the most abundant, followed by UCYN-A that, despite predominating in the east side, exhibit a wider distribution (Benavides and Voss, 2015).

As compared to the waters of the Northeastern Atlantic where UCYN-A predominates, the *Trichodesmium*-dominated Northwestern Atlantic exhibits a higher abundance of diazotrophs and higher N_2 fixation rates (Benavides and Voss, 2015; Montoya et al., 2007). As a result of the increasing longitudinal westward trend in the magnitude of the N_2 fixation, its contribution to new production is minor in the Northeastern Atlantic (Benavides et al., 2013a) and larger in the Northwestern Atlantic (Montoya et al., 2007). As a whole, NA provides between 10% and 25% of the global contribution to fixed N_2, being the third oceanic basin with larger contribution (Benavides and Voss, 2015). Geochemical estimates of basin-wide N_2 fixation range from 1 to ~90 Tg N yr^{-1} (Mahaffey

et al., 2005), whereas in vitro experimental methods point toward 13 Tg N yr^{-1} (Großkopf et al., 2012).

1.8. N_2 fixation in a nitrogen-rich region: the NW Iberian upwelling system

N-rich environments have traditionally been considered as inhibitory for the growth of diazotrophs and N_2-fixing activity (Holl and Montoya, 2005). However, presence and activity of diazotrophs have been observed in relatively N-rich waters, such as the East Coast of the USA (Mulholland et al., 2012), the western English Channel (Rees et al., 2009), the Arctic Ocean (Shiozaki et al., 2017, 2018), and upwelling regions such as the Benguela system (Benavides et al., 2014; Sohm et al., 2011a), the eastern equatorial Atlantic (Foster et al., 2009; Subramaniam et al., 2013; Voss et al., 2004), the region off central Chile (Fernández et al., 2015; Raimbault and Garcia, 2008) or the Taiwan Strait (Wen et al., 2017). Nevertheless, the classical paradigm about marine N_2 fixation establishes that this process is mainly constrained to the warm, nitrogen-poor waters of tropical and subtropical oceans. For this reason, most studies about N_2 fixation have been traditionally conducted in these regions (40ºS–40ºN) (Figure 1.8). In any case, the evidences found in previously overlooked environments, along with the large diversity of marine diazotrophs and their wide distribution (Farnelid et al., 2011; Riemann et al., 2010; Zehr et al., 2000, 2003b) expanded the range of environments where biological N_2 fixation may be an important process (Moisander et al., 2010).

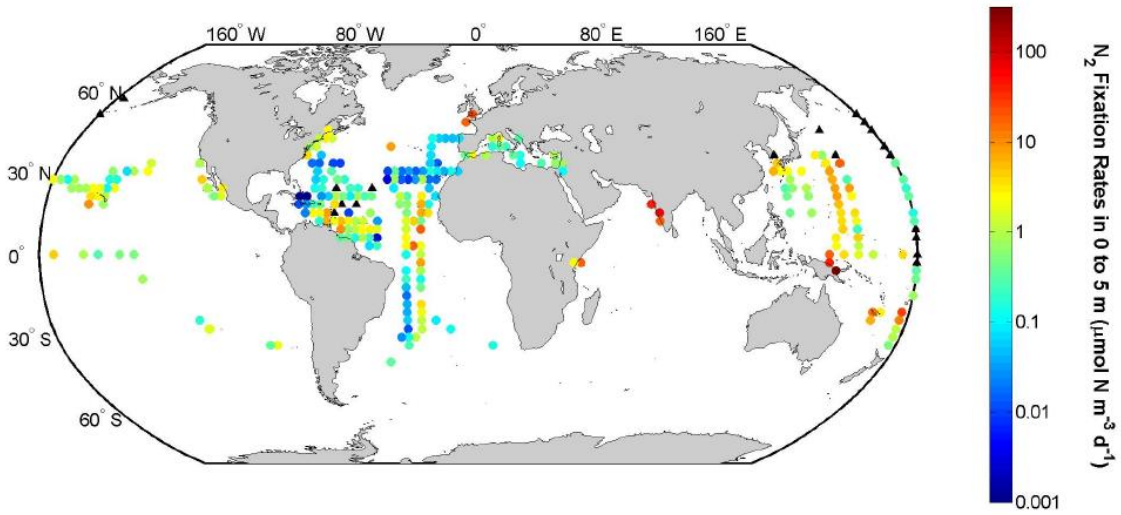

Figure 1.8. *Global distribution of surface marine N_2 fixation rates calculated by the geometric mean on 3º×3º grid. The color bar is in logarithmic scale. Zero values are indicated with black triangles. From Luo et al. (2012).*

The Northwestern Iberian Peninsula is part of the Iberia-Canary upwelling domain, one of the eastern boundary upwelling ecosystems in the global ocean (Arístegui et al., 2009). This area is characterised by the presence of coastal embayments named Rías, and the seasonal influence of wind-driven upwelling and downwelling events that induce large variability at short temporal scales (Fraga, 1981; Wooster et al., 1976). From April to September, the prevailing northerly winds cause upwelling, and the subsequent rise of cold and nutrient-rich subsurface waters into the coastal euphotic layer. These nutrient inputs, and their amplification due to remineralisation inside the Rías (Álvarez-Salgado et al., 2002; Bode et al., 1996), fuel a high phytoplankton production that sustains a rich marine ecosystem and productive fisheries (Fraga, 1981; Varela, 1992). From October to March, the prevailing southerly winds favour downwelling events (Fraga, 1981; Wooster et al., 1976). In this system, averaged chlorophyll *a* and primary production can reach up to 60±40 mg Chl *a* m^{-2} and 87±44 mg C m^{-2} h^{-1}, respectively, in conditions of high productivity (Bode et al., 1996). Most biomass corresponds usually to large phytoplankton (>10 μm), mainly chain-forming diatoms (Casas et al., 1997; Varela et al., 2001). Knowledge about diazotrophic activity in this upwelling region is limited to a single observation carried out in summer 2009, when relatively low BNF rates, mainly attributed to UCYN-A, were observed by Benavides et al. (2011) nearby Cape Silleiro (42ºN). In this survey, Agawin et al. (2014) reported that UCYN-A dominated the diazotroph community composition in the region off Cape Ghir (Northwest Africa, ~30º–31ºN) under nitrate concentrations >2 μM and temperatures circa 17ºC.

1.9. Hypotheses and objectives

The present PhD Thesis investigates for the first time, through a multidisciplinary approach, the magnitude and biogeochemical relevance of biological N_2 fixation, as well as the diversity, abundance, and temporal variability of diazotrophs in the upwelling region off NW Iberian Peninsula (Northeastern Atlantic). Furthermore, it addresses from a methodological perspective the consequences of contamination of the $^{15}N_2$ used to measure N_2 fixation. The following particular hypotheses were formulated:

1. The ^{15}N-labelled contaminants present in some commercial $^{15}N_2$ gas stocks yield significant overestimations in the biological N_2 fixation rates.
2. N_2-fixing activity occurs in the coastal upwelling region off Northwestern Iberia, although it represents a minor input of new nitrogen into the system.
3. Contrasting hydrodynamic forcing in the region through the year induces important variability in the diazotrophic community composition.

The specific objectives proposed to assess these hypotheses were:

1. To test the susceptibility of ^{15}N-contaminants to assimilation by non-diazotroph organisms, and to determine the potential overestimation of N_2 fixation rates in the field (Chapter 2).
2. To describe the seasonal variability in the magnitude of N_2 fixation, and to compare its biogeochemical role as a mechanism of new nitrogen supply versus nitrate turbulent diffusion (Chapter 3).
3. To investigate the temporal and vertical variability, in connection with the hydrodynamic forcing, of diazotroph abundance and community composition (Chapters 3 and 4).

2. Effects of contamination of commercial $^{15}N_2$ gas stocks on biological N_2 fixation measurements

Abstract

The $^{15}N_2$-tracer assay (Montoya et al., 1996) is currently, due to its high precision and sensitivity, the most used method for measuring biological N_2 fixation rates in both terrestrial and aquatic environments. The reliability of this technique depends on the purity of the commercial $^{15}N_2$ gas stocks used. However, Dabundo et al. (2014) reported the contamination of some of these stocks with bioavailable ^{15}N-labeled compounds (ammonium, nitrate and/or nitrite). Considering that the tracer assay relies on the conversion of the isotopically labelled $^{15}N_2$ into organic nitrogen, this contamination may have led to overestimated N_2 fixation rates. Therefore, we carried out laboratory and field experiments in productive waters of the temperate northwestern Iberian upwelling system in order to: 1) test the susceptibility of ^{15}N-contaminants to assimilation by non-diazotroph organisms, and 2) determine the potential overestimation of the biological N_2 fixation rates estimated in the field. Our findings indicate that the contaminant ^{15}N-compounds are assimilated by non-diazotrophs organisms, leading to an overestimation of the N_2 fixation rates up to sixteen-fold under hydrographic conditions of winter mixing. To ensure the accuracy of the estimated N_2 fixation rates, it is advisable to conduct purity control tests, such as those herein described, before using a given $^{15}N_2$ stock.

2.1. Introduction

Biological N_2 fixation is an important source of fixed-nitrogen into the ocean (Gruber, 2008). N_2 fixation rates can be estimated by modelling diazotroph biomass and growth rates (e.g., Goebel et al., 2007), using geochemical estimates (e.g., Deutsch et al., 2007; Gruber and Sarmiento, 1997), or by direct measurements. Currently, the two commonly used methods to measure directly N_2 fixation rates in the field are the $^{15}N_2$-tracer addition technique (Montoya et al., 1996) and the acetylene reduction assay (ARA) (Hardy et al., 1968; Stewart et al., 1967). Even though the $^{15}N_2$-tracer method was initially developed in the 1940s (Burris and Miller, 1941), it was soon replaced by the ARA owing to the high costs and the scarcity of instruments to measure accurately isotopic ratios (Hardy et al., 1968). Since the 1960s, ARA has allowed sensitive measurements of N_2 fixation with relatively simple experimental equipment and instrumentation. However, it is actually an indirect assay of N_2 fixation, based on the preferential reduction of acetylene (C_2H_2) to ethylene (C_2H_4) by the nitrogenase enzyme, instead of reducing N_2 to NH_3 (Schollhorn and Burris, 1967). The theoretical reduction ratios usually considered (C_2H_2:$N_2 \approx 3$:1 or 4:1) are not entirely reliable since diverse studies have shown large deviations (reviewed in Montoya et al., 1996; Postgate, 1982). Furthermore, acetylene has the potential to cause alterations on the metabolism of diazotrophs (Capone, 1993; Giller, 1987; Staal et al., 2001). Therefore, the availability of high-sensitivity and high-precision Isotope Ratio Mass Spectrometers (IRMS), and high purity $^{15}N_2$ gas, along with the development of the isotope tracer techniques made the $^{15}N_2$-tracer assay the method of choice to quantify N_2 fixation rates in both terrestrial and aquatic ecosystems.

The $^{15}N_2$-tracer technique is based on the assimilation and transformation of isotopically labelled $^{15}N_2$ into organic nitrogen in incubations of natural planktonic communities. The accuracy of this approach is based on the assumption that the ^{15}N enrichment of particulate matter can only be due to biological reduction of N_2. Nevertheless, Dabundo et al. (2014) reported the presence of substantial concentrations of ^{15}N-contaminants ($^{15}NO_3^-$, $^{15}NO_2^-$ and $^{15}NH_4^+$) in some commercial $^{15}N_2$ gas stocks from Sigma-Aldrich supplier, which may be assimilated by microorganisms. These findings imply that the contaminant ^{15}N-species may have caused significant overestimations in some of the N_2 fixation rates reported in the literature, especially in productive waters where the biomass of non-diazotrophic phytoplankton is higher than in oligotrophic regions.

The contamination of commercial $^{15}N_2$ stocks affected considerably the planning of the NICANOR project conducted in productive waters of the upwelling region off NW Iberia, which is subject to a high seasonal hydrographic variability (Bode et al., 1996; Casas et al., 1997). One of the stocks used during most 2014 experiments (lecture bottle from Sigma-Aldrich lot MBBB0968V) showed substantial contamination with bioavailable inorganic ^{15}N-species ($^{15}NH_4^+$=1900±560 μmoles per mole $^{15}N_2$, and $^{15}NO_3^-$ and/or $^{15}NO_2^-$=1.8±0.6 μmoles per mole $^{15}N_2$) (Dabundo et al., 2014). As a result, the biological N_2 fixation rates measured were greatly overestimated, reaching similar values to the highest ever reported in the (sub)tropical Atlantic and Pacific Oceans (Luo et al., 2012). Therefore, we were forced to extend the phase of field sampling, initially planned only for 2014, until the end of 2015, spanning a period of 20 months. Thereby, we were able to cover the main hydrographic stages over a seasonal cycle in this system. Concerns with the commercial $^{15}N_2$ stocks motivated the current study, in which we conducted laboratory and field experiments in order to: 1) test the susceptibility of ^{15}N-contaminants to assimilation by non-diazotroph organisms, and 2) determine the potential overestimation of the biological N_2 fixation rates estimated in the field.

2.2. Materials and Methods

2.2.1. Contamination control test with *Tetraselmis suecica* cultures

In order to investigate the potential assimilation by non-diazotrophic organisms of contaminant inorganic nitrogen species ($^{15}NO_3^-$, $^{15}NO_2^-$ or $^{15}NH_4^+$) present in $^{15}N_2$ gas stocks, the marine green alga *Tetraselmis suecica* (Kylin) Butcher was cultured in growth media equilibrated with $^{15}N_2$ from different commercial suppliers. Culture medium was f/2 for all the components (including phosphate, silicate, trace metals and vitamins, but not ammonium) except for nitrate, which was limited to f/32. We used a nitrogen-poor growth medium to favour the assimilation of the ^{15}N-contaminants presumably contained in some $^{15}N_2$ gas stocks.

Two different commercial stocks of $^{15}N_2$ gas were used to equilibrate with the culture media: Sigma-Aldrich lot MBBB0968V and Cambridge-Isotope lot I-19168A. According to Dabundo et al. (2014), the Sigma lot includes substantial contamination by ^{15}N-labelled nitrate, nitrite and ammonium. We have no data about the composition of the specific Cambridge gas lot used, but other analyzed stocks of the same commercial supplier showed negligible contamination (Dabundo et al., 2014). Two 1-L acid-cleaned clear polycarbonate bottles (Nalgene) were filled with the prepared and autoclaved growth medium using acid-washed silicone tubing and removing all air bubbles. Bottles were closed with caps with silicone septa. Using a gas-tight syringe, we injected 1.5 mL of $^{15}N_2$ gas (98 atom%) from Sigma and Cambridge stocks into each bottle. Then, injected gas and culture medium were equilibrated during 60 h by mixing of the bottles with a rotating mixer (35 rpm). All the material used in this experiment was first autoclaved, except caps with silicone septum, which were UV-sterilized prior to use.

Three 250-mL Erlenmeyer flasks were filled with 200 mL of the growth medium equilibrated with $^{15}N_2$ gas from the Sigma stock, three with medium equilibrated with $^{15}N_2$ from the Cambridge stock, and finally another three with unamended medium (control). The 9 flasks were inoculated with a stock culture of *T. suecica* (28 μg L^{-1} of initial concentration of chlorophyll *a* in each flask) and incubated during four days in a culture chamber at 21°C with an irradiance of 150 μE m^{-2} s^{-1} under a 14:10 light:dark photoperiod. Cultures were subjected to aeration through filters of 0.22 μm (Millipore) to stimulate the growth of the microalgae. We took aliquots for the determination of *in vivo* fluorescence and chlorophyll *a* concentration at the beginning of the incubation (day 0), and on days 2, 3 and 4. Filters for chlorophyll *a* quantification were extracted in 90%

acetone at 4ºC overnight and measured using the spectrofluorometric method, as described in Bode et al. (2011). The nitrate concentration of the cultures was also measured using a colorimetric test (Nitrate Pro Test Kit, Red Sea). Two days (during the exponential growth phase) and four days (during the nitrate-depleted and stationary growth phase) after inoculation, 30 mL of the cultures were filtered through 25 mm Whatman GF/F filters for the determination of the ^{15}N isotope content in the particulate organic nitrogen ($\delta^{15}N_{PN}$). After filtration, filters were dried at 40ºC during 24 h and stored at room temperature until pelletization in tin capsules. Measurements of the ^{15}N atom% of the particulate organic nitrogen were carried out with an elemental analyser combined with a continuous-flow isotope ratio mass spectrometer (FlashEA112 + Deltaplus, ThermoFinnigan), and using an acetanilide standard as reference. The precision of the analysis, expressed as the standard deviation of the ^{15}N values determined in a series of 10 standards, was 0.15‰. We also measured the nitrogen isotopic composition in three samples of the synthetic salt of nitrate ($\delta^{15}N_{NaNO3}$) used to prepare the growth media. Isotopic analyses were performed at the stable isotope facility (SAI) of the University of A Coruña (Spain).

2.2.2. Sampling and hydrographic measurements

Between February 2014 and December 2015 we carried out a total of 15 samplings during the NICANOR project (Table 2.1). Water samples from 0, 20, 40 and 70 m depth were collected with Niskin bottles on board B/O Lura at station 2 (43.42ºN, 8.44ºW; depth = 80 m) of the RADIALES time-series project (http://www.seriestemporales-ieo.com) (Figure 2.1) for the determination of biological N_2 fixation, chlorophyll *a* and primary production. This station is located in the adjacent shelf off Ría de A Coruña (Golfo Ártabro, NW Iberian Peninsula). Profiles of temperature and salinity were obtained with a CTD (Conductivity-Temperature-Depth) probe SBE25plus (SeaBird Electronics) attached to a rosette of Niskin bottles. Mixed layer depth was calculated as the depth where seawater density was 0.125 kg m^{-3} higher than the surface value.

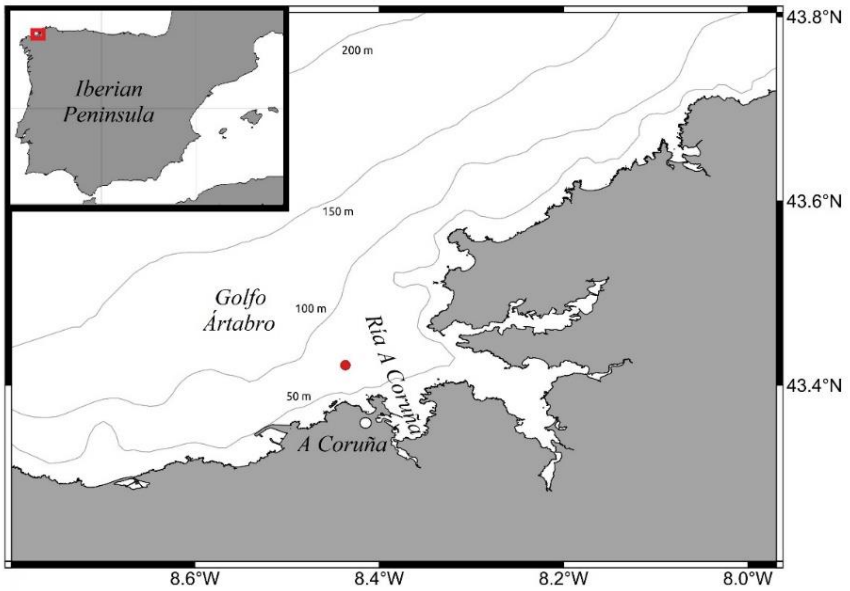

Figure 2.1. *Sampling station (red dot) located at 80 m depth in the adjacent shelf off Ría de A Coruña (Golfo Ártabro, NW Iberian Peninsula). The 50, 100, 150 and 200 m isobaths are indicated.*

2.2.3. N_2 fixation field measurements

In December 2014 we measured biological N_2 fixation rates in the field using concomitantly two $^{15}N_2$ lecture bottles, the contaminated gas from Sigma-Aldrich (stock MBBB0968V) and the presumably non-contaminated gas from Cambridge-Isotope (stock I-19168A), and compared results in order to ascertain the extent of potential overestimation of N_2 fixation rates caused by the assimilation of ^{15}N-contaminants.

Besides December 2014, we measured N_2 fixation rates in the sampling station using the contaminated $^{15}N_2$ from Sigma-Aldrich in other 6 samplings between March and September 2014 (Table 2.1). In February 2014, and between April 2015 and December 2015 we used Isotec Stable Isotopes lot TV0533 and Cambridge-Isotope Laboratories lot I-19168A, respectively, which are both $^{15}N_2$ sources presumably not contaminated according to Dabundo et al. (2014), our results with *T. suecica* cultures, as well as the N_2 fixation rates equal to zero, or below the detection limit, obtained in our field experiments.

Table 2.1. *Samplings conducted during the NICANOR project and $^{15}N_2$ stocks used to measure biological N_2 fixation rates at different depths. Asterisks indicate measurements of N_2 fixation performed with Sigma (MBBB0968V) stock.*

	Date	$^{15}N_2$ gas supplier	Depth (m) 0	20	40	70
2014	19 Feb	Isotec (TV0533)	×			
	18 March	Sigma (MBBB0968V)	×	×	×	
	15 April	Sigma (MBBB0968V)	×	×	×	
	27 May	Sigma (MBBB0968V)	×			
	19 June	Sigma (MBBB0968V)	×	×	×	
	16 July	Sigma (MBBB0968V)	×	×	×	
	4 Sept	Sigma (MBBB0968V)	×	×	×	×
	17 Dec	Sigma (MBBB0968V) & Cambridge (I-19168A)	×*	×	×	×*
2015	14 April	Cambridge (I-19168A)	×	×	×	×
	12 May	Cambridge (I-19168A)	×	×	×	×
	11 June	Cambridge (I-19168A)	×	×	×	×
	22 July	Cambridge (I-19168A)	×			
	3 Sept	Cambridge (I-19168A)	×	×	×	×
	19 Nov	Cambridge (I-19168A)	×	×	×	×
	16 Dec	Cambridge (I-19168A)	×	×	×	×

We determined N_2 fixation rates using the $^{15}N_2$-uptake technique (Montoya et al., 1996). Two sets of triplicate 2-L acid-cleaned clear polycarbonate bottles (Nalgene) were filled with water of each depth using acid-washed silicone tubing. After carefully removing all air bubbles, Nalgene bottles were closed with caps provided with silicone septa, through which 3 mL of $^{15}N_2$ gas (98 atom%) were injected with a gas-tight syringe. In December 2014 one set of bottles was injected with gas from the Sigma stock and the other set with the Cambridge gas stock. The pressure across the septum was equilibrated by allowing the excess water to escape through a syringe needle piercing the septum. Incubation bottles were gently shaken by manually inverting them fifty times, and then incubated for 24 h in refrigerated incubators equipped with a system of recirculating water. The incubation of seawater from 70 m (collected in the aphotic zone) was performed under complete darkness, by covering the incubation bottles with black duct tape and placing them inside a black opaque plastic bag. Incubations ended by filtration through 25 mm Whatman GF/F filters to obtain total N_2 fixation rates. 2-L seawater samples from each depth were also filtered at time zero for the determination of $\delta^{15}N_{PN}$. Filter drying, pelletization and isotopic ratio measurements were performed as described in the section 2.2.1. Assuming that the minimum acceptable change of $\delta^{15}N$ between the initial and the final PON sample is 4‰ (Montoya et al., 1996), and given that the detection limit of the used elemental analyser is 0.15-0.20 µg N, the detection limit of our method is approximately 0.001 nmol N L^{-1} d^{-1}. The equations of Weiss (1970) and Montoya et al.

(1996) were used to calculate the initial N_2 concentration (assuming equilibrium with atmosphere) and N_2 fixation rates, respectively.

2.2.4. Chlorophyll *a* and primary production

Chlorophyll *a* and primary production were determined at 0, 20 and 40 m depth. 150-mL samples were filtered onto Whatman GF/F filters for the total fraction. Filters for chlorophyll *a* quantification were extracted in 90% acetone at 4ºC overnight and measured using the spectrofluorometric method, as described in Bode et al. (2011). Primary production was measured by ^{14}C-uptake. Seawater samples were transferred to triplicate 300–mL polycarbonate bottles (Nalgene) (2 light and 1 dark bottles), which were spiked with 2-10 µCi of $NaH^{14}CO_3$ and incubated during 24 h in refrigerated incubators equipped with a system of recirculating water, and covered with neutral density screens to simulate the corresponding in situ irradiance. Sample filtration, filter processing and primary production calculations were conducted as described in detail in Bode et al. (2011).

2.3. Results

2.3.1. Uptake of ^{15}N-contaminants by non-diazotroph organisms

The measurements of *in vivo* fluorescence, chlorophyll *a* and nitrate concentrations allowed us to monitor the evolution of the cultures. On day 2 after inoculation, the microalgae were in exponential growth phase, and on day 4 they had reached the stationary phase and nitrate had been exhausted (Table 2.2).

Table 2.2. *Mean (±SD) of* in vivo *fluorescence, chlorophyll* a, *nitrate concentration, ^{15}N content of the particulate organic nitrogen ($\delta^{15}N_{PN}$, ‰) and ^{15}N atom% in the different treatments of* T. suecica *cultures. Asterisk indicates initial nitrate concentration in the f/32 medium culture.*

t (day)	Treatment	*In vivo* fluo (fsu)	Chl *a* (µg L^{-1})	NO_3^- (µM)	$\delta^{15}N_{PN}$ (‰ vs. air)	^{15}N atom%
0	**Control Cambridge Sigma**	~32	~28	55*	-	-
2	**Control**	61±1	127±27	-	-0.90±0.01	0.3660±0.0001
	Cambridge	61±14	120±24	-	-1.0±0.2	0.3659±0.0001
	Sigma	59±2	98±17	-	1.7±0.3	0.3669±0.0001
3	**Control**	113±3	157±16	-	-	-
	Cambridge	118±3	149±3	-	-	-
	Sigma	110±1	166±9	-	-	-
4	**Control**	155±13	120±5	≈0	-1.4±0.3	0.3658±0.0001
	Cambridge	178±6	101±11	≈0	-1.3±0.2	0.3658±0.0001
	Sigma	169±10	105±14	≈0	1.5±0.2	0.3669±0.0001

The experiments conducted in the laboratory with cultures of *T. suecica* equilibrated with $^{15}N_2$ gas from different commercial stocks showed that the treatment with the Sigma-Aldrich stock resulted in statistically significant (Kruskal-Wallis, $p<0.001$) enrichments in ^{15}N abundance of the particulate organic nitrogen ($\delta^{15}N_{PN}$ ca. 1.5‰), in relation to the treatment with the Cambridge-Isotope stock and the control ($\delta^{15}N_{PN}$ ranging from -0.90±0.01 to -1.4±0.3 ‰), both during the exponential (day 2) and stationary phases (day 4). No statistically significant (Kruskal-Wallis, $p>0.05$) differences were observed between the control and the cultures equilibrated with $^{15}N_2$ gas from the Cambridge stock (Figure 2.2).

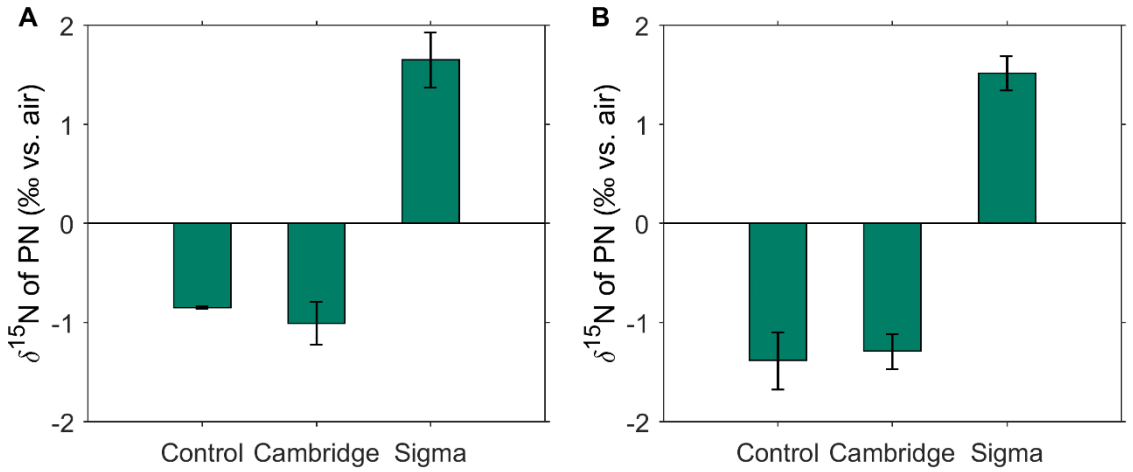

Figure 2.2. *^{15}N content of particulate organic nitrogen versus the reference value in atmospheric N_2 ($\delta^{15}N_{PN}$, ‰ vs. air) in* T. suecica *cultures equilibrated with $^{15}N_2$ gas from Cambridge-Isotope and Sigma-Aldrich commercial stocks sampled* ***(A)*** *two days (exponential growth) and* ***(B)*** *four days (stationary phase under nitrate-depleted conditions) after inoculation. Error bars represent standard deviation (n=3).*

2.3.2. Overestimation of biological N_2 fixation rates estimated in the field

The results of December 2014 were obtained under hydrographic conditions of winter mixing, which was characterized by a deep mixed layer (51 m), low chlorophyll *a* concentration (ranging from 0.2 to 0.7 mg m^{-3}) and low primary production (ranging from 4.8 to 23.5 mg C m^{-3} d^{-1}) (Figure 2.3).

N_2 fixation rates ranged from 0.02±0.01 to 0.04±0.01 µmol N m^{-3} d^{-1} using $^{15}N_2$ from the Cambridge stock, which presumably contained contaminant-free gas (Figure 2.3). The use of contaminated $^{15}N_2$ gas lecture bottles to estimate biological N_2 fixation overestimated the volumetric rates by a factor of 16. At surface waters and at 70 m depth the volumetric N_2 fixation rates were significantly higher when using $^{15}N_2$ gas from Sigma (0.4±0.1 and 0.6±0.3 µmol N m^{-3} d^{-1}, respectively) than when using the Cambridge source (0.03±0.01 and 0.04±0.01 µmol N m^{-3} d^{-1}, respectively) (Kruskal-Wallis, $p < 0.05$).

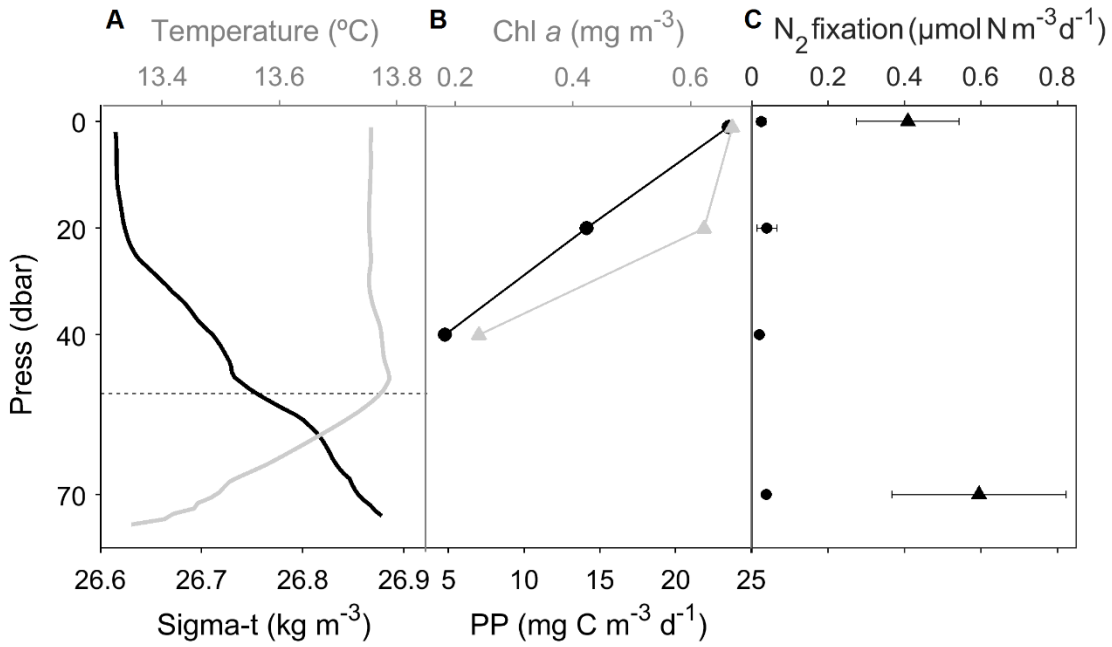

Figure 2.3. *Vertical distribution of* ***(A)*** *temperature and density (sigma-t),* ***(B)*** *chlorophyll* a *concentration (Chl* a*) (triangles) and primary production (PP) (circles), and* ***(C)*** *biological N_2 fixation rates by using contaminated $^{15}N_2$ gas from Sigma-Aldrich stock (triangles) and the presumably contaminant-free Cambridge-Isotope stock (circles), sampled in December 2014. Error bars represent standard deviation. The dashed line in the sigma-t panel indicates the mixed layer depth, estimated from an increase in water column density of 0.125 kg m^{-3} relative to surface values.*

The N_2 fixation rates measured during 2014, including the December sampling, using the contaminated Sigma stock (Table 2.1) ranged from 0.4 to 82 µmol N m^{-3} d^{-1} and they were positively correlated with the total primary production (R^2=0.423, p<0.01) and chlorophyll *a* concentration (R^2=0.583, p<0.01) (Figure 2.4). In contrast, the reliable rates obtained by using the presumably non-contaminated Cambridge and Isotec stocks did not correlate significantly with primary production (R^2=0.165, p>0.05) and chlorophyll *a* (R^2=0.109, p>0.05).

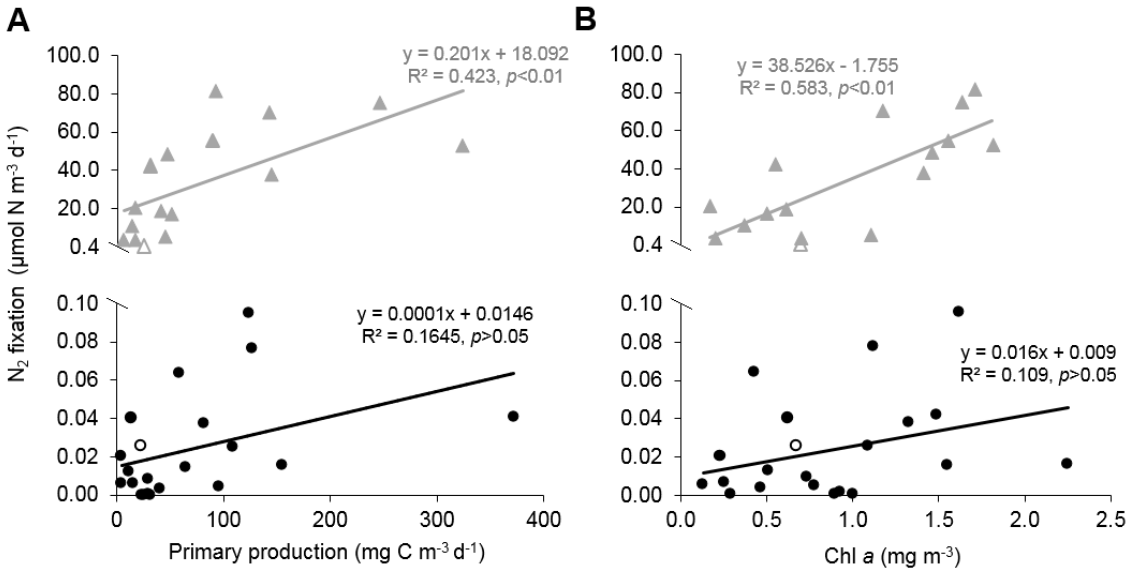

Figure 2.4. (A) *Total primary production and* ***(B)*** *chlorophyll* a *concentration versus volumetric biological N_2 fixation rates obtained by using the contaminated Sigma-Aldrich lot MBBB0968V (grey triangles), and the presumably non-contaminated Cambridge-Isotope lot I-19168A and Isotec Stable Isotopes lot TV0533 (black circles). Empty triangles and circles represent the sample at 0 m depth of December 2014, in which N_2 fixation was measured using both Sigma and Cambridge stocks. Regression lines are plotted for each data set. Only samples with chlorophyll* a *<2.5 mg m^{-3} have been represented in order to improve the data visualization, leaving out a sample with the highest chlorophyll* a *(6.5 mg m^{-3}) and primary production (396.4 mg $m^{-3}d^{-1}$), and overestimated N_2 fixation of ~72 µmol N m^{-3} d^{-1}.*

2.4. Discussion

We conducted laboratory and field experiments to assess the consequences of the contamination of $^{15}N_2$ for N_2 fixation measurements. The experiment with cultures of *T. suecica* demonstrated the uptake of contaminant ^{15}N-species by non-diazotroph organisms. Particulate organic nitrogen from the Cambridge and control cultures was ^{15}N-impoverished (negative $\delta^{15}N$ ranging from -0.9±0.01 to -1.4±0.3 ‰) since the nitrogen source for the microalgae was the synthetic salt of nitrate ($NaNO_3$) added to the growth media. The analysis of this nitrate resulted in a ^{15}N atom% (0.3656±0.0001%) below the atmospheric value of reference (0.3664%, Montoya et al., 1996) and consequently negative $\delta^{15}N$ (-1.9±0.2‰), whereas the $\delta^{15}N$ of nitrate from marine waters ranges usually between 3‰ and 6‰ (Sigman et al., 1997, 2000). The Sigma cultures were ^{15}N-enriched ($\delta^{15}N$ ca. 1.5‰) because the microalgae assimilated, in addition to the synthetic nitrate, inorganic ^{15}N-labelled species ($^{15}NH_4^+$ and $^{15}NO_3^-/^{15}NO_2^-$) present in the contaminated lecture bottle, resulting in an enrichment of up to $\delta^{15}N \approx 3$‰ in relation to Cambridge and control cultures. This interpretation assumes that the biomass of the primary producers reflects directly the isotopic composition of the nitrogen sources used for growth (e.g., NO_3^-, NO_2^- and NH_4^+), a linkage that provides insights into the oceanic nitrogen cycle processes (Montoya, 2008). In regions where N_2 fixation is an important supply of new N, the phytoplankton biomass may be slightly depleted in ^{15}N in relation to atmospheric N_2 ($\delta^{15}N < 0$‰) due to the weak discrimination against the heavy isotope ^{15}N (Montoya, 2007). This discrimination, known as kinetic isotopic fractionation, affects all metabolic reactions of the oceanic nitrogen cycle and results in an affinity for light nitrogen isotopes (^{14}N) against heavy forms (^{15}N) (Montoya, 2008). Because the fractionation only occurs while substrates are available, we extended the experiment with cultures until the nitrate was depleted in order to avoid, to the highest possible extent, fractionation effects during its uptake. We thus tried to ensure that the microalgae assimilated most of the available nitrate. This contamination control test clearly demonstrated the need to use the contaminant-free $^{15}N_2$ from the Cambridge stock for subsequent N_2 fixation measurements.

The comparison, through field estimates, of the biological N_2 fixation rates obtained simultaneously with the Sigma and Cambridge stocks showed that using contaminated $^{15}N_2$ gas overestimated the rates by up to sixteen-fold. Strikingly, the contamination of the $^{15}N_2$ gas stocks and its effects were not reported in the oceanography literature before

the study of Dabundo et al. (2014), although in studies about terrestrial N_2 fixation there are old mentions about possible contamination along with mitigation practices (De-Polli et al., 1977; Ohyama and Kumazawa, 1981). It is expected that the assimilation of dissolved inorganic nitrogen (DIN), mainly ammonium and nitrate, is preferred to the energy-costly N_2 fixation process (Stam et al., 1987). Thus, the estimates of N_2 fixation reported in the literature may be distorted depending on the commercial $^{15}N_2$ source used. Past reports obtained using $^{15}N_2$ gas from Sigma should be interpreted with caution. The commercial stocks from Cambridge-Isotope, which presumably are not contaminated or exhibit insignificant contamination (Dabundo et al., 2014), are used in most surveys and, thereby, the N_2 fixation rates reported in these studies are a priori reliable. Nonetheless, the high rates measured in N-rich temperate waters such as the western English Channel (Rees et al., 2009) or the NE American coast (Mulholland et al., 2012) are striking, although none of these authors used Sigma stocks. In the case of Mulholland et al. (2012), the authors used Cambridge stocks and detected a large abundance, among the highest ever observed, of unicellular N_2-fixing group A cyanobacteria (UCYN-A) by quantitative PCR, which may account for the high rate estimates. Additional studies should be implemented in those coastal regions to better resolve and verify the magnitude of these N_2 fixation estimates.

The overestimated N_2 fixation rates due to the contamination obtained from March to September 2014 ranged from 310 to 2260 μmol N m^{-2} d^{-1} (0.4–82 μmol N m^{-3} d^{-1}), reaching similar values to the highest ever reported in the (sub)tropical Atlantic and Pacific Oceans (Luo et al., 2012). Assuming an average carbon-specific growth rate for different cyanobacterial diazotrophs of 0.3 d^{-1} (Berman-Frank et al., 2007; Mulholland and Bernhardt, 2005; Tuit et al., 2004; Turk-Kubo et al., 2018), balanced growth in terms of carbon and nitrogen, Redfield stoichiometry for the C:N ratio of diazotrophic biomass, and that diazotrophs only use N derived from N_2 fixation, these overestimated rates would imply a depth-integrated biomass of diazotrophs ranging between 80 and 600 mg C m^{-2}. Considering that the annual average of phytoplankton biomass in the region during non-bloom conditions is typically around 2500 mg C m^{-2} (Teira et al., 2003), such diazotroph biomass would represent between 4% and 25% of the total phytoplankton biomass in the station studied in the Ría de A Coruña, which is highly unrealistic.

The overestimation extent of the N_2 fixation rates as a result of the contamination will depend on the concentration of ^{15}N-species in the used gas stock and the biomass and

primary productivity of the phytoplankton present. It is to be expected that a high production and biomass are linked to a high assimilation of nutrients, among which are the contaminants included in the stocks. Hence, phytoplankton biomass and productivity correlate positively with the overestimated N_2 fixation rates. In the coastal region under study, both phytoplankton biomass and production are subject to marked seasonal variability and influenced by upwelling pulses, which in this system induce large changes at short temporal scales (Bode et al., 1996; Casas et al., 1997; Gilcoto et al., 2017). For this reason, the overestimation will be different according to the prevailing hydrographic stage. Under high biomass and production conditions such as spring or summer blooms, the uptake rates and conversion of contaminant ^{15}N-species to organic nitrogen can be expected to be higher than in low-biomass situations. As shown in Figure 2.4, the factor of distortion and overestimation of the biological N_2 fixation rates will be probably >16 under conditions of high biomass and productivity as compared to the winter mixing situation of low biomass sampled in our experiment of December 2014. In contrast, in the widely studied oligotrophic (sub)tropical oceans, where N_2-fixers predominate, presumable inflated rates may have gone unnoticed due to the low biomass and production of non-diazotrophic phytoplankton and the high N_2 fixation rates that commonly characterize these systems. Currently, it is virtually impossible to know which previous studies report overestimated N_2 fixation estimates. In any case, considering that only one commercial brand (Sigma-Aldrich) of the three analyzed by Dabundo et al. (2014) showed substantial presence of ^{15}N-labelled contaminants, the published rates obtained with $^{15}N_2$ gas from the other two suppliers (Cambridge-Isotope and Campro Scientific) are a priori reliable. However, it would be desirable that the manufacturers improve and certify rigorous scrubbing procedures in the $^{15}N_2$ gas synthesis by catalytic oxidation of $^{15}NH_3$ (Bergersen, 1980). In the meantime, in order to ensure the reliability of future biological N_2 fixation determinations, it is advisable to use the commercial stocks presumably free of contaminants according to Dabundo et al. (2014), and to conduct control tests such as those herein described prior to use the $^{15}N_2$ lecture bottles acquired.

3. Magnitude, biogeochemical role and abundance of main players of N_2 fixation under contrasting hydrographic conditions

Abstract

The classical paradigm about marine N_2 fixation establishes that this process is mainly constrained to nitrogen-poor tropical and subtropical regions, and sustained by the colonial cyanobacterium *Trichodesmium* spp. and diatom-diazotroph associations. However, the application of molecular techniques allowed determining a high phylogenic diversity and wide distribution of marine diazotrophs, which extends the range of ocean environments where biological N_2 fixation may be relevant. Between February 2014 and December 2015, we carried out 10 one-day samplings in the upwelling system off NW Iberia in order to: 1) investigate the seasonal variability in the magnitude of N_2 fixation, 2) determine its biogeochemical role as a mechanism of new nitrogen supply, and 3) quantify the main diazotrophs in the region under contrasting hydrographic regimes. Our results indicate that the magnitude of N_2 fixation in this region was relatively low (0.001±0.002 – 0.095±0.024 µmol N m^{-3} d^{-1}), comparable to the lower-end of rates described for the subtropical NE Atlantic. Maximum rates were observed at the surface during both upwelling and relaxation conditions. The comparison with nitrate diffusive fluxes revealed the minor role of N_2 fixation (<2%) as a mechanism of new nitrogen supply into the euphotic layer. Small diazotrophs (<10 µm) were responsible for all N_2 fixation activity detected in the region. Quantitative PCR targeting the *nifH* gene revealed the highest abundances of two sublineages of *Candidatus* Atelocyanobacterium thalassa or UCYN-A (UCYN-A1 and UCYN-A2), mainly at well-lit surface waters under upwelling and relaxation conditions, and of Gammaproteobacteria γ-24774A11 at deep waters during downwelling. Maximum abundance for the three groups were up to 6.7×10^2, 1.5×10^3 and 2.4×10^4 *nifH* copies L^{-1}, respectively. Our findings demonstrate measurable N_2 fixation activity and presence of diazotrophs throughout the year in a nitrogen-rich temperate region, and outline the environmental conditions that define the ecological niches of UCYN-A and Gammaproteobacteria.

3.1. Introduction

Dinitrogen (N_2) is the most abundant form of nitrogen (N) in aquatic and terrestrial ecosystems, however only a limited, but diverse, group of bacteria and archaea (termed diazotrophs) can use this large N reservoir by the energy-costly process of biological N_2 fixation (BNF) (Karl et al., 2002). Diazotrophs possess nitrogenase, the enzyme that catalyses this process, which reduces atmospheric N_2 to bioavailable ammonium (NH_4^+). With an estimated global flux of ~120 Tg N yr^{-1}, BNF is one of the main mechanisms that supplies new N to the ocean, fueling phytoplanktonic photosynthesis and the subsequent export of organic matter into the deep waters through the 'biological carbon pump' (Gruber, 2008). The limited number of studies simultaneously quantifying BNF versus the transport of nitrate into the euphotic zone through turbulent mixing indicate that BNF can equal or even exceed nitrate diffusion in some regions of the subtropical gyres (Capone et al., 2005; Fernández-Castro et al., 2015; Mouriño-Carballido et al., 2011; Painter et al., 2013). Therefore, BNF is a key process controlling oceanic productivity, the carbon cycle, and climate (Gruber and Galloway, 2008).

Traditionally, it has been considered that marine BNF is mainly restricted to N-poor (sub)tropical regions, and sustained by the filamentous cyanobacterium *Trichodesmium* spp. and diatom-diazotroph associations. However, the development and application of molecular techniques allowed to determine an extremely high phylogenic diversity of nitrogenase genes (*nifH*) (Zehr et al., 2000). In addition to *Trichodesmium* and diatom-diazotroph associations, marine diazotrophic groups include unicellular cyanobacteria (UCYN-A, -B, -C) and non-cyanobacterial diazotrophs (heterotrophic bacteria and archaea) (Zehr et al., 2003b; Zehr, 2011). Diazotrophic heterotrophic bacteria comprise a wide range of phylogenetic groups, including Firmicutes, Alpha-, Beta-, Gamma-, Delta- and Epsilonproteobacteria (Zehr et al., 2003b).

Recently UCYN-A (or *Candidatus* Atelocyanobacterium thalassa), which lives in obligate symbiosis with picoeukaryotic prymnesiophytes (Thompson et al., 2012, 2014), has been revealed as a key component of the global diazotrophic community, since it shows a wide distribution (Farnelid et al., 2016b; Turk-Kubo et al., 2017), and relatively high N_2 fixation rates (Martínez-Pérez et al., 2016). Six different UCYN-A sublineages (UCYN-A1 to -A6) have been defined hitherto (Farnelid et al., 2016b; Thompson et al., 2014; Turk-Kubo et al., 2017). Even though UCYN-A–prymnesiophyte associations are widespread in the oceans, microscopic observations of the symbiosis are limited. The use

of a double CARD-FISH (catalyzed reporter deposition-fluorescence *in situ* hybridization) technique to target specifically UCYN-A1 and -A2 and their prymnesiophyte hosts allowed to investigate their global distribution in the major ocean basins (Cabello et al., 2016), as well as to visualize, characterize and quantify both symbiosis in open ocean regions of the North (Krupke et al., 2014, 2015) and South Atlantic (Cornejo-Castillo et al., 2016). The Gammaproteobacteria-affiliated phylotype γ-24774A11 (also named Gamma A or UMB) also exhibits a wide distribution, including contrasting marine environments in the Atlantic, Pacific and Indian Oceans (e.g. Benavides et al., s2016; Church et al., 2005; Langlois et al., 2015; Moisander et al., 2008). Gammaproteobacteria γ-24774A11 is considered one of the most important heterotrophic diazotrophs in the oligotrophic (sub)tropical regions (Moisander et al., 2014a).

Although numerous studies have investigated the biogeography and controlling mechanisms of marine BNF in recent years (e.g. Fernández-Castro et al., 2016; Luo et al., 2014; Monteiro et al., 2011; Moore et al., 2009), the limiting factors of this process are still under debate. Due to the high energetic cost of fixing N_2 in comparison to the assimilation of dissolved inorganic nitrogen (DIN) (mainly ammonium and nitrate) (Stam et al., 1987), DIN-rich environments have been considered as inhibitory for the growth of diazotrophs and BNF activity (Holl and Montoya, 2005). However, the discovery of a large diversity of organisms able to fix N_2, and their wide distribution, indicated that BNF may be more widespread than previously thought (Moisander et al., 2010). Recent studies demonstrate the presence and activity of diazotrophs in DIN-enriched environments such as the eastern tropical North Atlantic (Voss et al., 2004), the western English Channel (Rees et al., 2009), the Mekong River plume in the South China Sea (Grosse et al., 2010), the temperate NE American coast (Mulholland et al., 2012), and mesohaline temperate estuaries between the Baltic Sea and the North Sea (Bentzon-Tilia et al., 2015). Evidences of BNF have also been reported in upwelling systems such as the eastern equatorial Atlantic (Foster et al., 2009; Subramaniam et al., 2013; Voss et al., 2004), the Benguela upwelling system (Benavides et al., 2014; Sohm et al., 2011a), the region off central Chile (Fernández et al., 2015; Raimbault and Garcia, 2008) and the Taiwan Strait (Wen et al., 2017).

The NW Iberian Peninsula is part of the Iberia-Canary upwelling domain, one of the eastern boundary upwelling ecosystems in the global ocean (Arístegui et al., 2009). This area is characterised by the presence of coastal embayments named Rías and the seasonal

influence of wind-driven upwelling and downwelling events (Fraga, 1981; Wooster et al., 1976). From April to September, the prevailing northerly winds cause upwelling, and the subsequent rise of cold and nutrient-rich subsurface waters into the coastal euphotic layer. These nutrient inputs, and their amplification due to remineralisation inside the Rías (Álvarez-Salgado et al., 2002; Bode et al., 1996), fuel the high phytoplankton production that sustains a rich marine ecosystem and productive fisheries (Fraga, 1981; Varela, 1992). From October to March, the prevailing southerly winds favour downwelling events (Fraga, 1981; Wooster et al., 1976). Knowledge about diazotrophic activity in the NW Iberia region is limited to a single observation carried out in summer 2009, when relatively low BNF rates, mainly attributed to UCYN-A, were observed by Benavides et al. (2011) and Agawin et al. (2014). Here we describe the results of a survey conducted in the outer part of Ría de A Coruña between February 2014 and December 2015, which covered contrasting hydrographic regimes. Our main goals are to: 1) investigate the seasonal variability in the magnitude of BNF, 2) determine its biogeochemical role as a mechanism of new N supply, and 3) quantify the main diazotrophs.

3.2. Materials and Methods

3.2.1. Sampling and hydrographic measurements

Between February 2014 and December 2015, within the framework of the NICANOR (Nitrogen fixation and diffusive fluxes in the NW Iberian Peninsula) project, ten one-day samplings were carried out on board B/O Lura at station 2 (43.42° N, 8.44° W; depth = 80 m) of the RADIALES time-series project (www.seriestemporales-ieo.net) (Figure 2.1 in Chapter 2). This station is located in the adjacent shelf off Ría de A Coruña (Golfo Ártabro, NW Iberian Peninsula).

The samplings were designed to cover the main hydrographic stages in this system over a seasonal cycle, and spanned over a period of 20 months. To simplify the interpretation of the results, we classified the samplings into three conditions: five cruises were characterised by downwelling (February 2014, December 2014, May 2015, November 2015, and December 2015), three by upwelling (May 2014, April 2015, and June 2015), and another two by relaxation, i.e., intermediate conditions between upwelling and downwelling pulses (July 2015, and September 2015). This classification was based on the wind-driven upwelling index and the hydrographic conditions of the water column (see results). The upwelling index (I_W) was estimated by the Ekman transport ($m^3\ s^{-1}\ km^{-1}$) and computed from wind data for the sector Rías Altas (44ºN 9ºW), near Ría de A Coruña, using the NAVGEM model of Fleet Numerical Meteorology and Oceanography Center (FNMOC) (http://www.indicedeafloramiento.ieo.es), averaged over the 3 days period before each cruise. On each sampling day, profiles of temperature, salinity and fluorescence were obtained with a CTD (Conductivity-Temperature-Depth) probe SBE25plus (SeaBird Electronics) attached to a rosette of Niskin bottles. Water samples were collected for the determination of inorganic nutrients, chlorophyll *a*, primary production, biological N_2 fixation, picoplankton composition, as well as for DNA extraction. In 7 out of the 10 surveys, measurements of dissipation rates of turbulent kinetic energy were conducted using a microstructure turbulence profiler (MSS, Prandke and Stips, 1998).

In order to facilitate the comparison between hydrographic conditions, we provide mean and standard deviation for the variables quantified under the relaxation condition, despite the low number of samplings (n=2). We are aware that a higher number of samplings would be desirable to better characterize averaged physical, chemical and biological

fields in this system, where variability happens at short temporal scales of a few days (Casas et al., 1997; Gilcoto et al., 2017).

3.2.2. Inorganic nutrients, chlorophyll *a*, and primary production

Unfiltered samples for the determination of dissolved inorganic nutrients (NO_3^-, PO_4^{3-}) were collected from 3 to 7 depths in rinsed polyethylene 15-mL tubes and stored frozen at -20 °C, until further analysis by standard colorimetric methods on a segmented flow AutoAnalyzer 3 Bran Luebbe (Aminot and Kerouel, 2007). Nutrient analysis were performed at the facilities of the University of Oviedo (Spain). Data for nutrient concentrations were not available for December 2014 and April 2015. In these cases, nitrate concentration was computed from a nitrate-density (σ_t) relationship built by using all samples (n=52) collected during the sampling period. The relationship showed a linear behaviour ($NO_3^- = 9.7788 \times \sigma_t - 256.38$; $r = 0.930$; $p<0.001$) for σ_t ranging between 26.1 and 27.1 kg m^{-3}.

During all samplings except February 2014, when only the total fraction was available, size-fractionated (< and > 10 µm) chlorophyll *a* and primary production were determined at 0, 20 and 40 m. 150-mL samples were filtered onto Whatman GF/F filters for the total fraction, and onto Whatman polycarbonate filters for the >10 µm fraction. Filters for chlorophyll *a* quantification were extracted in 90% acetone at 4ºC overnight and measured using the spectrofluorometric method, as described in Bode et al. (2011). Fluorometrically determined chlorophyll *a* concentrations, ranging from 0.1 to 5.8 mg m^{-3}, were used to calibrate the fluorometer attached to the CTD-rosette (Chl $a = 0.533 \times$ fluorescence $- 0.212$; $R^2 = 0.830$, $n = 121$), which was used to plot the chlorophyll *a* distribution in February 2014, December 2014, and December 2015. In May 2014, and from April to November 2015, we used the fluorometer included in the MSS profiler (see below), also calibrated with chlorophyll *a* concentrations ranging from 0.1 to 6.5 mg m^{-3} (Chl $a = 3.520 \times$ fluorescence $- 5.125$; $R^2 = 0.770$, $n = 36$), obtained in the same station during the same sampling period. Size-fractionated primary production was measured by ^{14}C-uptake. Seawater samples were transferred to triplicate 300–mL polycarbonate bottles (Nalgene) (2 light and 1 dark bottles), which were spiked with 2-10 µCi of $NaH^{14}CO_3$ and incubated during 24 h in refrigerated incubators equipped with a system of recirculating water, and covered with neutral density screens to simulate the

corresponding in situ irradiance. Sample filtration, filter processing and primary production calculations were conducted as described in detail in Bode et al. (2011).

3.2.3. Flow cytometric counting

Samples for the determination of picoplankton abundance and cell properties were taken at 0, 40 and 70 m depth. Picoplankton samples (1.8 mL) were preserved with 1% paraformaldehyde + 0.05% glutaraldehyde (final concentration), flash-frozen in liquid N_2 for 10 min and stored at -80°C until analysis with a FACSCalibur flow cytometer (Becton-Dickinson) equipped with a laser emitting at 488 nm. To estimate the abundance of the different groups (cell mL^{-1}), calibration of the cytometer flow rate was performed before each use. A suspension (approximately 1×10^5 mL^{-1}) of fluorescent latex beads 1 μm in diameter (Molecular Probes, Life Technologies) was added to all the samples as internal standard. Two aliquots from the same sample were used for the study of picophytoplankton (0.6 ml) and heterotrophic bacteria (0.4 ml), analyzed at high (~mean 58 μL min^{-1}) and low (~mean 22 μL min^{-1}) flow rate, respectively. Before the analysis, the DNA of heterotrophic bacteria was stained with the nucleic acid fluorochrome SYTO-13 (2.5 μM; Molecular Probes, Life Technologies) in the dark for 10 min.

Autotrophic cells were separated into 2 groups of cyanobacteria (*Synechococcus* and *Prochlorococcus*) and 2 groups of picoeukaryotes (small and large), based on their orange (FL2, 585 nm) and red (FL3, >650 nm) fluorescence and side-scattered light (SSC) (Calvo-Díaz and Morán, 2006). Two groups of heterotrophic bacteria, with high and low nucleic acid content (HNA and LNA, respectively), were distinguished based on their relative green fluorescence (FL1, 530 nm), which was used as a proxy for nucleic acid content.

To estimate biovolume, we used an empirical calibration between SSC and cell diameter, assuming spherical shape for all groups. Finally, picoplankton biomass was computed using the following conversion factors of biovolume to carbon: 350 fg C μm^{-3} for heterotrophic bacteria (Bjørnsen, 1986), 230 fg C μm^{-3} for *Synechococcus*, 240 fg C μm^{-3} for *Prochlorococcus*, and 237 fg C μm^{-3} for picoeukaryotes (Worden et al., 2004).

3.2.4. Biological N_2 fixation

Water samples from 0, 20, 40 and 70 m depth were collected with Niskin bottles to determine size-fractionated (< and > 10 µm) N_2 fixation following the $^{15}N_2$-uptake technique (Montoya et al. 1996) with the modifications described in Rees et al. (2009). In February 2014, only surface water (0 m) was sampled. Triplicate 2-L acid-cleaned clear polycarbonate bottles (Nalgene) were filled directly from the Niskin bottle using acid-washed silicone tubing. After carefully removing all air bubbles, bottles were closed with caps provided with silicone septa, through which 3 mL of $^{15}N_2$ (98 atom%, Isotec Stable Isotopes lot TV0533 in February 2014, and Cambridge Isotope Laboratories lot I-19168A in the remaining samplings) were injected with a gas-tight syringe. The pressure across the septum was equilibrated by allowing the excess water to escape through a syringe needle piercing the septum. Incubation bottles were gently shaken by manually inverting them fifty times, and then incubated for 24 h in the same incubators used for primary production measurements. The incubation of seawater from 70 m (collected in the aphotic zone) was performed under complete darkness, by covering the incubation bottles with black duct tape and placing them inside a black opaque plastic bag.

Incubations ended by filtration through 25 mm Whatman GF/F filters to obtain total N_2 fixation rates. N_2 fixation rates of the <10 µm size-fraction were determined by pre-filtering the water sample through 47 mm Whatman polycarbonate filters of 10 µm pore-size, and subsequently collecting onto GF/F filters. Total and pre-filtered 2-L seawater samples from each depth were also filtered at time zero for the determination of relative abundance of N stable isotopes ($\delta^{15}N$). After filtration, filters were dried at 40°C during 24 h and stored at room temperature until pelletization in tin capsules. Measurement of particulate organic nitrogen and carbon (PON and POC) content and ^{15}N atom% were carried out with an elemental analyser combined with a continuous-flow isotope ratio mass-spectrometer (FlashEA112 + Deltaplus, ThermoFinnigan), and using an acetanilide standard as reference. The precision of the analysis, expressed as the standard deviation of the ^{15}N values determined in a series of 10 standards, was 0.15‰. Isotopic analyses were made at the stable isotope facility (SAI) of the University of A Coruña (Spain). Assuming that the minimum acceptable change of $\delta^{15}N$ between the initial and the final PON sample is 4‰ (Montoya et al., 1996), and given that the detection limit of the used elemental analyser is 0.15-0.20 µg N, the detection limit of our method is approximately 0.001 nmol N L^{-1} d^{-1}. The equations of Weiss (1970) and Montoya et al. (1996) were used

to calculate the initial N_2 concentration (assuming equilibrium with atmosphere) and N_2 fixation rates, respectively. The facts that we used the non-contaminated Cambridge stock (according to the results of *T. suecica* cultures experiments reported in the previous Chapter 2) and obtained in several samplings at different depths BNF rates equal to zero, or below the detection limit, allowed us to discard any effect of potential contamination in the commercial $^{15}N_2$ gas stocks (Dabundo et al., 2014).

Average cell-specific N_2 fixation rates by UCYN-A that would be required to explain the observed BNF rates, were calculated based on their qPCR-estimated abundances and the BNF measured, following the assumptions and calculations indicated in Turk-Kubo et al. (2014). Representative cell-specific rates for UCYN-A ranging from 0.02 to 2.6 fmol N $cell^{-1}$ h^{-1} have been directly estimated or modelled by Goebel et al. (2010). Considering these known cell-specific rates, we roughly estimated whether the UCYN-A abundances in our samples could account for the measured bulk BNF rates.

3.2.5. DNA samples collection and extraction

During all samplings except February 2014, when only the sample at 0 m was collected, seawater samples for DNA were collected at 0, 20, 40 and 70 m depth, transferred to acid-cleaned carboys using acid-washed silicone tubes and kept in darkness until further processing in the laboratory. Microbial biomass was collected by filtering 7.5-10 L of seawater through a 0.22 µm Sterivex™ filter unit (Millipore) using a peristaltic pump. The filters were preserved with 1.8 mL of lysis buffer (50mM Tris-HCl pH 8.3, 40 mM EDTA pH 8.0, 0.75 M sucrose) and stored at -80 ºC until extraction. DNA was extracted using the PowerWater® DNA Isolation Kit (MO BIO, Laboratories, Inc.), quantified and quality-checked (according to the A_{260}/A_{280} ratio) using a spectrophotometer NanoDrop 2000™ (Thermo Fisher Scientific).

3.2.6. Quantification of *nifH* gene by qPCR

The abundance of diazotrophs was determined by quantitative polymerase chain reaction (qPCR) using TaqMan primers-probe sets (PrimeTime® qPCR Assays, Integrated DNA Technologies) targeting Gammaproteobacteria-affiliated phylotype γ-24774A11 (Moisander et al., 2008, 2010), UCYN-A1 (Church et al., 2005a) and UCYN-A2 (Thompson et al., 2014). However, we are aware that the primers-probe set designed for

UCYN-A2 does not contain enough mismatches to avoid cross-hybridization with the UCYN-A3 and UCYN-A4 sublineages (Farnelid et al., 2016b). The probes were 5'FAM labelled and double-quenched with ZEN™/3'-IBFQ (Integrated DNA Technologies). The reactions were run on a MyiQ2™ Real-Time PCR Detection System (Bio-Rad Laboratories) at the *Instituto Español de Oceanografía* (IEO). Final reaction volume of 20 µL contained 10 µL PrimeTime® Gene Expression Master Mix (IDT), 2 µL DNA template, 2 µL of primers-probe set (0.5 and 0.25 µM final concentrations, respectively), and 6 µL PCR grade water (Sigma-Aldrich). Thermal cycling conditions were 95ºC for 3 min, followed by 45 cycles of 95ºC for 15 s and 60ºC for 1 min. Standards, consisting of nine 10-fold serial dilutions containing the targeted *nifH* fragments (gBlocks® Gene Fragments, IDT), were included with each qPCR run. All samples and standards were run in duplicate. Standard curves were obtained by linear regression of the threshold cycle (Ct) and $\log_{10}$ gene copies per reaction using standards ranging from 10^8 to 10^0 gene copies per reaction. Amplification efficiencies were >90 % for all reactions. No-template control sample was run in duplicate in all plates and it did not amplify in any runs. We performed inhibition tests by 2-folds and 5-folds dilutions of all samples and we concluded that our samples were not inhibited. The limit of detection (LOD) and detected but not quantified (DNQ) limits were 4 *nifH* copies L^{-1} and 41 *nifH* copies L^{-1}, respectively. Abundances below LOD were considered 0 copies L^{-1}, whereas *nifH* copies higher than LOD but less than DNQ were assigned a conservative value of 1 *nifH* copy per litre.

3.2.7. Double CARD-FISH assay and sampling

Between April and December 2015, in a total of seven cruises, seawater samples (95 mL) were collected from each cruise throughout the water column (0, 40 and 70 m depth), prefiltered through 200 µm pore-size nylon mesh and fixed with 37% formaldehyde solution (final concentration 5% v/v) for 24h at 4ºC in darkness. Subsequently, fixed samples were vacuum filtered at 100 mm Hg onto 0.6 µm pore-size polycarbonate filters (25 mm diameter; Millipore) in a filtration tower system (Millipore). Once filtered the entire sample volume, the filtration towers were rinsed with 10 mL of MilliQ water and filters were kept frozen at -80ºC until further processing.

A double CARD-FISH assay was carried out following the multi-color CARD-FISH protocol (Pernthaler et al., 2004) to target the symbiosis between UCYN-A sublineages

(Krupke et al., 2013, 2014) and their specific prymnesiophyte hosts (Cornejo-Castillo et al., 2016). Filters were embedded in 0.1% (w/v) low gelling point agarose to avoid as far as possible the cell loss, dried during 10 min at 35ºC, and treated with lysozyme (37°C, 1 h) and achromopeptidase (37°C, 0.5 h) solutions to permeabilize the cell walls. In the hybridization phase we used horseradish peroxidase (HRP) labeled oligonucleotide probes, which were specifically designed to target the 18S rRNA of eukaryotic prymnesiophyte hosts and 16S rRNA of prokaryotic UCYN-A cells under particular stringency conditions.

For the first hybridization step we used the UPRYM69 probe (5′-CACATAGGAACATCCTCC-3′), specific for the UCYN-A1 host (Cornejo-Castillo et al., 2016). The probe was combined with sequences of oligonucleotide named helpers contiguous to the probe region (Helper A-PRYM 5′-GAAAGGTGCTGAAGGAGT-3′; Helper B-PRYM 5′-AATCCCTAGTCGGCATGG-3′), and a competitor with a mismatch in the probe region (5′-CACATTGGAACATCCTCC-3′). Filter pieces were embedded in the hybridization buffer (40% deionized formamide, 0.9 M NaCl, 20mM Tris-HCl pH 8, 0.01% sodium dodecyl sulphate (SDS), and 20 mg mL^{-1} blocking reagent (Roche Diagnostic Boehringer) with a mixture of the HRP-labeled probe, helpers and competitor oligonucleotides each at 5 ng μL^{-1}, and incubated overnight at 46ºC. After hybridization, filters were rinsed during 10 min twice in washing buffer (56 mM NaCl, 5 mM EDTA, 0.01% SDS, 20 mM Tris-HCl pH 8) at 48ºC, and equilibrated in phosphate-buffered saline (PBS) buffer for 15 min at room temperature. The probe is detected by an enzymatic reaction named TSA (Tyramide Signal Amplification), which enhances the fluorescence by the covalent fixation of the Tyramide/Fluorochrome complex close to the HRP enzyme. TSA was performed for 40 min at room temperature in the dark in a buffer solution of 1× PBS, 2 M NaCl, 1 mg mL^{-1} blocking reagent, 100 mg mL^{-1} dextran sulphate, 0.0015% H_2O_2 and 4 µg mL^{-1} Alexa 488-labeled tyramide. Subsequently, filters were transferred to PBS for 20 min, rinsed with MilliQ water and air-dried. Before the second hybridization, the filters were embedded in 0.01M HCl for 10 min at room temperature in darkness to inactivate the HRP of the first probe (Pernthaler et al., 2004) and rinsed twice with MilliQ water and air-dried.

The second CARD-FISH used the probe UCYN-A732 and its corresponding helpers, targeting both UCYN-A1 and -A2 cells, and hybridization conditions described by Krupke et al. (2013). Filters were embedded in the hybridization buffer (50% formamide,

0.9 M NaCl, 20 mM Tris-HCl pH 8, 0.01% SDS, 10 mg mL^{-1} Blocking reagent and 100 mg mL^{-1} dextrane sulphate) with the probe and helpers at 0.16 ng μL^{-1}, incubated at 35ºC for 3h and rinsed at 37ºC for 15 min in a washing buffer as described above but with 9 mM NaCl. TSA was done at 46ºC in the same solution described previously but using 1 μg mL^{-1} Alexa 594-tyramide. Filters were counterstained with 5 μg mL^{-1} DAPI (4′,6-diamidino-2-phenylindole), mounted in antifading reagent (77% glycerol, 15% VECTASHIELD and 8% 20× PBS) and stored frozen until microscopic observation.

Another double CARD-FISH was also performed to target the prymnesiophyte *Braarudosphaera bigelowii* (UCYN-A2 host) and UCYN-A cells under the same hybridization and amplification conditions described above. We used the specific UBRADO69 probe (5′-CACATTGGAACATCCTCC-3′) combined with a competitor (5′-CACATAGGAACATCCTCC-3′) and the same helpers as before for UPRYM69 probe (Cornejo-Castillo et al., 2016), and the UCYN-A732 probe with its corresponding helpers.

3.2.8. Epifluorescence microscopy counts of the UCYN-A–Prymnesiophyte symbiosis

Filters from CARD-FISH assay were observed by epifluorescence microscopy (Nikon Eclipse 80i, Nikon Instruments) at 1000× under ultraviolet (DAPI signal of the cell nucleus), blue-light (green labeled host cells with Alexa 488) or green-light (red labeled UCYN-A symbionts with Alexa 594) excitations. The determination of hybridized cell abundances was performed along five transects of approximately 8 mm (~8.0 × 0.1 mm^2 each) across the filter piece, which were examined twice. A first analysis of the transect was carried out under blue light to count host cells and check the presence of associated symbionts by switching to green light. A second inspection was carried out under green light to detect free symbionts. Detection limit was about 1 cell mL^{-1} (calculated assuming only one counted cell). Cell count included only one category, labelled hosts without symbionts (non-associated hosts). Prymnesiophyte cells were only classified into one size class (4-5 μm) by measurements with the software NIS-Elements Basic Research (Nikon Instruments). Photomicrographs were taken using a Nikon DS-Fi1 camera (Nikon Instruments) attached to the microscope.

3.2.9. Niche overlap analysis

The calculations of niche overlap between different diazotrophic groups based on non-parametric kernel density functions (NO_K) were performed according to Mouillot et al. (2005):

$$NO_{K\ i,j,t} = 1 - \frac{1}{2} \int \left| f_{it}\ (x) - f_{jt}\ (x) \right| dx \quad (4)$$

where $NO_{K\ i,\ j,\ t}$ is the niche overlap between diazotrophic groups i and j for the environmental factor t, and f_{it} and f_{jt} are the kernel population density functions of factor t for species i and j, respectively. In order to correct the correlation between niche predictors, we used the estimator in a dependent sample (EDS) proposed by Kark et al. (2002).

The statistical niche differences between groups were assessed by null model permutation tests to check whether the niche overlaps were significantly lower than 100% (Geange et al., 2011). When the contribution of absolute abundance determined via qPCR for each diazotroph group exceeded that expected by chance (1/3), niche predictors for each station were selected. Statistical null distributions (the distribution of the statistic test under the null hypothesis of no niche differentiation) were generated by calculating pseudo-values through randomly permuting group labels in the corresponding data set over 10000 runs. The distributions of the average niche overlaps for the null model were then computed. Niche overlap calculations and associated null model tests were performed using the density function and the source code provided as supporting information in Geange et al. (2011). All calculations were done using R (R Core Team, 2015).

3.2.10. Dissipation rates of turbulent kinetic energy and estimates of nitrate fluxes through vertical diffusion

Measurements of dissipation rates of turbulent kinetic energy were conducted on each cruise during 6-10 vertical casts down to a maximum depth of 70 m. The microstructure turbulence profiler was equipped with 2 velocity microstructure shear sensors (type PNS98), a microstructure temperature sensor (FPO7), a sensor to measure horizontal acceleration of the profiler and a high-precision CTD probe. Fluorometrically determined chlorophyll *a* concentrations were used to calibrate the fluorometer sensor included in the MSS profiler, as previously indicated. The profiler was balanced to have negative buoyancy and a sinking velocity of ~0.4 to 0.7 m s^{-1}. The frequency of data sampling was

1024 Hz. The sensitivity of the shear sensors was checked after each use. Due to significant turbulence generation close to the ship, only the data below 5 m were considered reliable. Data processing and calculation of dissipation rates of turbulent kinetic energy (ε) was carried out with the commercial software MSSpro as described in detail in Fernández-Castro et al. (2014). The squared Brunt Väisälä frequency (N^2), a proxy for water column stratification, was computed from the CTD profiles according to the equation:

$$N^2 = -\left(\frac{g}{\rho_w}\right)\left(\frac{\partial \rho}{\partial z}\right) \quad (s^{-2}) \quad (5)$$

where g is the acceleration due to gravity (9.8 m s^{-2}), ρ_w is seawater density (1025 kg m^{-3}), and $\partial\rho/\partial z$ is the vertical potential density gradient. After averaging ε and N^2 over depth intervals of 1 m length, vertical diffusivity or mixing (Kz) was estimated as:

$$Kz = \mathrm{e}\frac{\varepsilon}{N^2} \quad (m^2 s^{-1}) \qquad (6)$$

where e is the mixing efficiency, here considered as 0.2 (Osborn, 1980).

Vertical diffusive fluxes of nitrate into the euphotic layer were calculated following the Fick's law, from the product of the nitrate gradient, obtained by linearly fitting nitrate concentrations in the 10-40 m depth layer, and the averaged Kz for the same depth interval. For those samplings in which the microstructure profiler was not deployed (February 2014, December 2014, and December 2015), estimates of Kz under similar hydrographic conditions were considered: October 2014 (for February 2014), and November 2015 (for December 2014 and December 2015). In order to quantify the biogeochemical relevance of BNF, we compared it with the supply of nitrate into the euphotic zone through vertical diffusion.

3.2.11. Nitrate supply through vertical advection

A simplified calculation of nitrate supply by vertical advection due to upwelling was computed considering the Golfo Ártabro as a single box divided into two layers (Álvarez-Salgado et al., 2000; Villamaña et al., 2017), the deeper one influenced by upwelled water and the surface layer dominated by the outgoing flow. Assuming that the bottom layer volume is conservative and stationary, the vertical advective flux (Q_Z, m^3 s^{-1}) would be equal to the incoming bottom flux (Q_B, m^3 s^{-1}), computed as the product of the upwelling index (I_W, m^3 s^{-1} km^{-1}) and the length of the mouth of the Golfo Ártabro (ca. 11.5 km).

Finally, the nitrate transport into the euphotic layer by vertical advection was computed as:

$$NO_3^- \ advective \ flux \ = \frac{Q_Z}{A_{basin}} \ [NO_3^-]_{70\ m} \qquad (7)$$

where A_{basin} is the surface area of the Golfo Ártabro (ca. 400 km^2), Q_Z is the vertical advective flux, and $[NO_3^-]_{70\ m}$ is the nitrate concentration determined at 70 m depth for each cruise in the sampling station.

3.3. Results

3.3.1. Hydrography and turbulent mixing

During our survey we encountered the main hydrographic features of a temperate coastal region subject to seasonal variability and influenced by upwelling pulses, which in this system induce large variability at short temporal scales of a few days (Bode et al., 1996; Casas et al., 1997; Gilcoto et al., 2017). During downwelling conditions, we sampled winter (February 2014 and December 2014) and autumn (November 2015 and December 2015) mixing, and also a spring transitional period under predominance of downwelling (May 2015) (Figure 3.1).

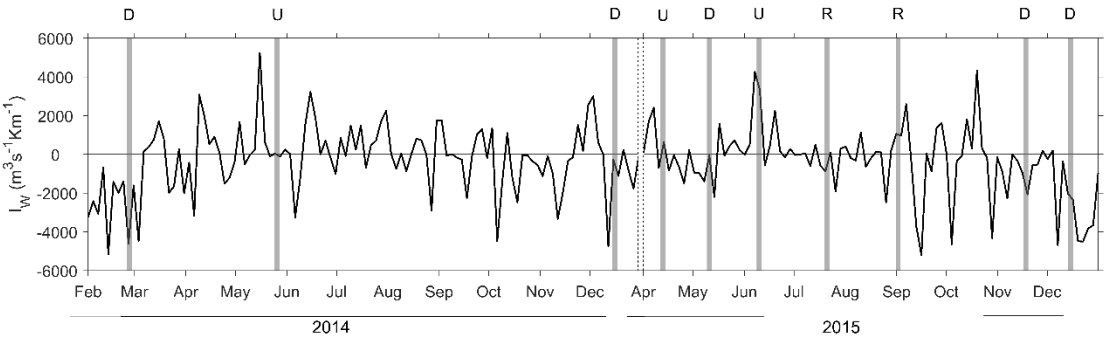

Figure 3.1. *Upwelling index (I_W) computed in the region during the sampling period covering from February 2014 to December 2014, and April 2015 to December 2015. Positive (negative) values correspond to upwelling (downwelling) due to northerly (southerly) winds. The shaded areas indicate the three days period before each sampling, and the dashed lines indicate the break between 2014 and 2015. Letters on the top indicate downwelling (D), upwelling (U) and relaxation (R) conditions.*

Autumn mixing was characterized by thermohaline mixing, whereas during winter mixing the slight haline stratification caused mixed layer depth being shallower (Figure 3.2, Table S6.1).

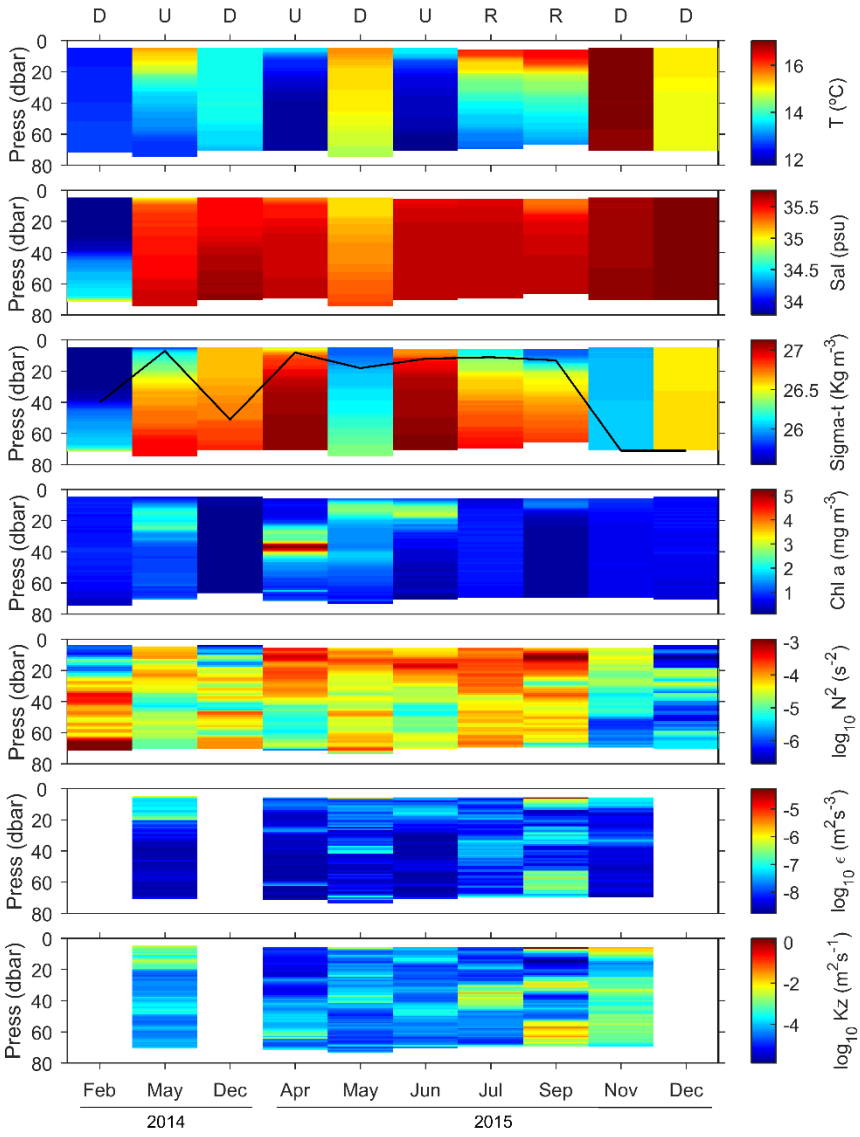

Figure 3.2. *Vertical distribution of temperature (T), salinity (Sal), density (sigma-t), chlorophyll a concentration (Chl a), squared Brunt Väisälä frequency (N^2), dissipation rates of turbulent kinetic energy (ε), and vertical diffusivity (Kz). The black line in the sigma-t panel indicates the mixed layer depth, estimated from an increase in water column density of 0.125 kg m^{-3} relative to surface values. Letters on top panel indicate the hydrographic condition sampled on each cruise (D: downwelling, U: upwelling, and R: relaxation). Chlorophyll a concentration was calculated from the calibrated fluorescence sensor included in the CTD-rosette (February 2014, December 2014, and December 2015) and the MSS profiler (May 2014, April-November 2015) (see Material and Methods).*

In May 2015, the higher vertical gradient in temperature and salinity at the surface produced that the mixed layer depth was even shallower. However, during downwelling averaged vertical stratification (determined as Brunt Väisälä frequency) between 10-40 m was relatively low (4.4±7.1 × 10^{-5} s^{-2}), and as a result the mixed layer depth was significantly deeper (50±22 m), than during upwelling and relaxation conditions (Table 3.1, Figure 3.3). Microstructure turbulence observations, which were only available for

May and November 2015, showed relatively low values of averaged vertical (10-40 m) dissipation rates of turbulent kinetic energy (ε) in both cruises (1.3-2.2 × 10^{-8} m^2 s^{-3}).

Table 3.1. *Mean (±SD) values for selected variables determined during the samplings classified as downwelling (D), upwelling (U), and relaxation (R) conditions. MLD corresponds to the mixed layer depth, estimated from an increase in water column density of 0.125 kg* m^{-3} *relative to surface values. Squared Brunt Väisälä frequency (*N^2*), dissipation rates of turbulent kinetic energy (ε), and vertical diffusivity (Kz) correspond to averaged values for the 10–40 m depth interval. The same interval was used to compute vertical* NO_3^- *gradients and diffusive fluxes. Depth-integrated values (Int) for chlorophyll a, primary production (PP), contribution of <10 µm size-fraction,* N_2 *fixation rates, Gammaproteobacteria γ-24774A11 (Gamma) and UCYN-A nifH abundances, and biomass of picoplankton groups were calculated down to 40 m. BNF contribution represents the contribution of biological* N_2 *fixation to the supply of new N (considering* N_2 *fixation plus nitrate vertical diffusion). The contribution of each group to total picoplankton biomass is also included. A nonparametric one-way ANOVA (Kruskal-Wallis) was performed to test the null hypothesis that independent groups come from distributions with equal medians (*p < 0.05; **p < 0.01; ***p < 0.001). The Bonferroni multiple comparison test was applied a posteriori to analyse the differences between every pair of groups (D, U, R). n, indicates the number of cruises included in each hydrographic condition.*

Variable	D (*n*=5)	U (*n*=3)	R (*n*=2)	Kruskal-Wallis *p*-value	Bonferroni comparisons
Upwelling Index (m^3 s^{-1} km^{-1})	-1858 ± 1585	1338 ± 1878	472 ± 1176	0.120	
Surface temperature (ºC)	14.8 ± 1.8	14.2 ± 1.1	16.3 ± 0.1	0.216	
Surface salinity	35.2 ± 0.8	35.3 ± 0.3	35.4 ± 0.2	0.700	
MLD (m)	50 ± 22	9 ± 3	12 ± 1	0.027*	D>U,R
N^2 (s^{-2}) × 10^{-5}	4.4 ± 7.1	11.7 ± 12.3	19.7 ± 21.9	0.047*	D<R
ε (m^2 s^{-3}) × 10^{-8}	1.8 ± 1.8	2.2 ± 4.6	3.0 ± 3.9	0.738	
Kz **(m^2 s^{-1}) × 10^{-4}**	4.5 ± 7.6	1.5 ± 4.2	12.0 ± 33.0	0.107	
Surface NO_3^- (µM)	3.9 ± 2.5	1.7 ± 1.8	1.2 ± 1.6	0.295	
(40 m) NO_3^- (µM)	3.3 ± 2.4	6.9 ± 3.0	5.7 ± 2.9	0.354	
Surface PO_4^{3-} (µM)	0.20 ± 0.09	0.20 ± 0.18	0.34 ± 0.01	0.181	
(40 m) PO_4^{3-} (µM)	0.39 ± 0.19	0.28 ± 0.12	0.37 ± 0.27	0.705	
NO_3^- gradient (µmol m^{-4})	15 ± 13	148 ± 41	139 ± 2	0.032*	D<U, R
NO_3^- diffusive flux (µmol m^{-2} d^{-1})	795 ± 902	2241 ± 3134	14324 ± 3063	0.106	
Surface Chl *a* (mg m^{-3})	0.9 ± 0.3	1.6 ± 0.1	0.8 ± 0.5	0.055	
Int Chl *a* (mg m^{-2})	31 ± 16	65 ± 35	20 ± 2	0.094	
% Int Chl *a* <10 µm	85 ± 8	34 ± 8	64 ± 25	0.047*	D>U, R
Int PP (mg C m^{-2} d^{-1})	1359 ± 1032	5192 ± 538	1611 ± 295	0.040*	U>D, R
% Int PP <10 µm	81 ± 8	38 ± 3	59 ± 42	0.054	
Surface N_2 fixation (µmol N m^{-3} d^{-1})	0.016 ± 0.020	0.068 ± 0.038	0.072 ± 0.008	0.085	
Int N_2 fixation (µmol N m^{-2} d^{-1})	0.7 ± 0.6	1.1 ± 0.7	0.8 ± 0.1	0.639	
Contribution BNF (%)	0.15 ± 0.20	0.65 ± 0.82	0.01	0.260	
Surface Gamma (*nifH* copies L^{-1})	2557 ± 4351	305 ± 528	1286 ± 912	0.284	
Int Gamma (*nifH* copies m^{-2} × 10^5)	145 ± 205	13 ± 23	132 ± 124	0.151	
Surface UCYN-A1 (*nifH* copies L^{-1})	33 ± 64	189 ± 31	617 ± 74	0.001**	R>D, U
Int UCYN-A1 (*nifH* cop. m^{-2} × 10^5)	1.4 ± 1.3	1.3 ± 0.2	13.0 ± 0.0	<0.001***	R>D, U
Surface UCYN-A2 (*nifH* copies L^{-1})	137 ± 240	427 ± 562	867 ± 863	0.165	
Int UCYN-A2 (*nifH* copies m^{-2} × 10^5)	7.3 ± 6.6	9.7 ± 9.8	21.0 ± 15.6	0.386	
S-picoEuk biomass (mg C m^{-2})	28 ± 12	14 ± 9	10 ± 9	0.129	
S-picoEuk contribution (%)	13 ± 5	6 ± 4	6 ± 4	0.135	
L-picoEuk biomass (mg C m^{-2})	38 ± 38	34 ± 27	13 ± 11	0.425	
L-picoEuk contribution(%)	14 ± 7	14±13	7 ± 4	0.571	
Synechococcus **biomass (mg C m^{-2})**	15 ± 7	4 ± 5	5 ± 6	0.201	
Synechococcus **contribution (%)**	7 ± 3	1 ± 1	3 ± 3	0.053	
Prochlorococcus **biomass (mg C m^{-2})**	7 ± 6	2 ± 0	2 ± 0	0.138	
Prochlorococcus **contribution(%)**	3 ± 3	1 ± 0	1 ± 0	0.262	
HNA biomass (mg C m^{-2})	96 ± 38	164 ± 56	99 ± 8	0.152	
HNA contribution (%)	43 ± 6	62 ± 10	62 ± 13	0.032*	D<U
LNA biomass (mg C m^{-2})	48 ± 23	40 ± 13	36 ± 14	0.834	
LNA contribution(%)	20 ± 3	15 ± 2	21 ± 3	0.131	

Cruises which sampled spring-summer upwelling (May 2014, April 2015, and June 2015) were characterized by shallow mixed layer depths (9±3 m) (Table 3.1, Figure 3.3). Due to the enhanced values observed in the upper 20 m in May 2014, averaged dissipation rates were slightly higher during this cruise (4.3±7.3 × 10^{-8} m^2 s^{-3}) (Figure 3.2, Table S6.1).

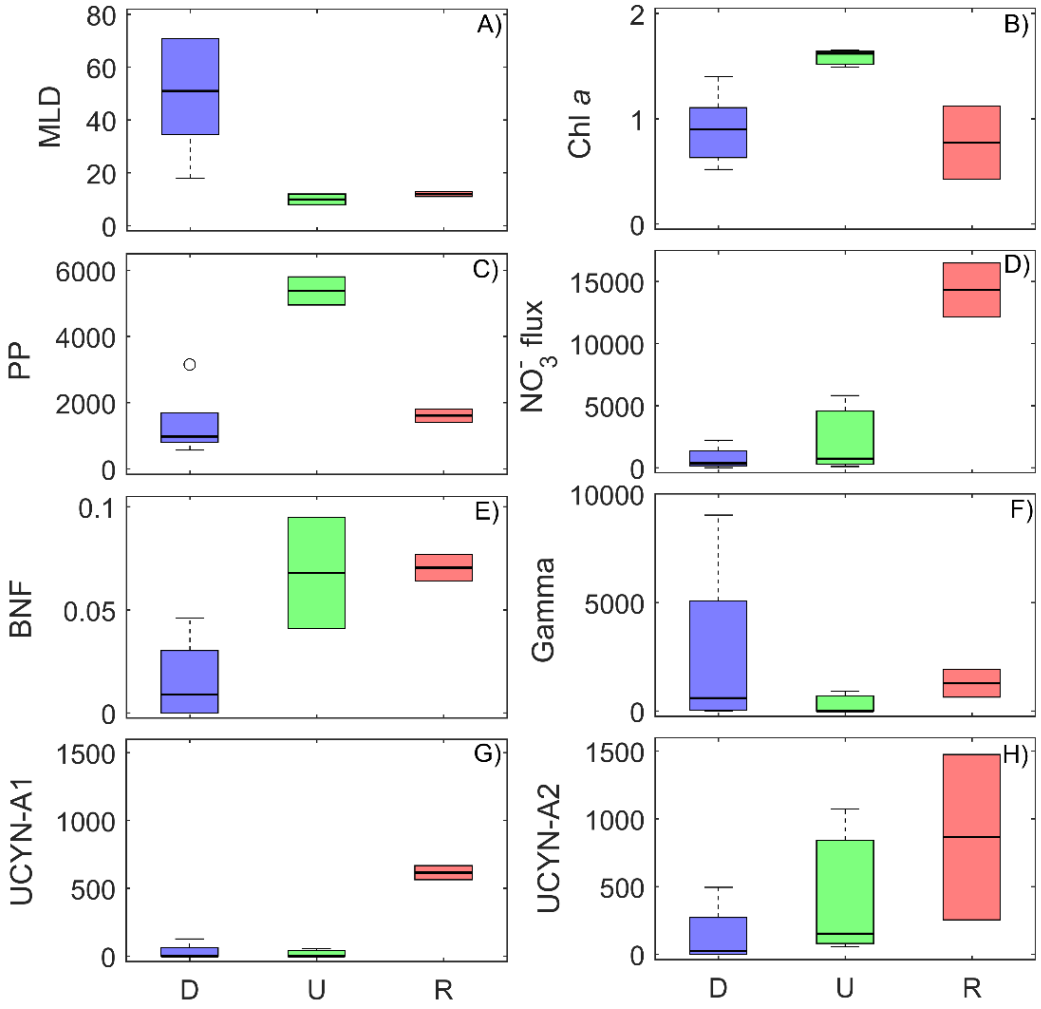

Figure 3.3. *Box-and-whisker plots of* ***(A)*** *mixed layer depth (MLD, m),* ***(B)*** *surface chlorophyll a concentration (mg* m^{-3}*),* ***(C)*** *depth-integrated (0-40 m) primary production (mg C* m^{-2} d^{-1}*),* ***(D)*** *nitrate diffusive fluxes into the euphotic layer (µmol* m^{-2} d^{-1}*),* ***(E)*** *surface biological* N_2 *fixation (BNF, µmol N* m^{-3} d^{-1}*), and surface nifH gene abundances (nifH copies* L^{-1}*) of* ***(F)*** *Gammaproteobacteria γ-24774A11 phylotype,* ***(G)*** *UCYN-A1 and* ***(H)*** *UCYN-A2. On each box, the central mark indicates the median, and the bottom and top edges of the box indicate the* 25^{th} *and* 75^{th} *percentiles, respectively. The whiskers extend to the most extreme data points not considered outliers, and the outliers are plotted individually using white circles. Letters on bottom panels indicate the hydrographic setting encountered on each sampling date (D: downwelling, U: upwelling, R: relaxation).*

Relaxation conditions included two cruises (July 2015 and September 2015), which sampled the transition between intense upwelling and downwelling events during the summer thermal stratification period (Figure 3.1). Both cruises were characterised by intense vertical stratification (19.7±21.9 × 10^{-5} s^{-2}), and shallow mixed layer depths (12±1 m) (Table 3.1, Figure 3.2). As a result of the relatively low vertical stratification and enhanced dissipation rates observed between 25-40 m depth layer, averaged vertical diffusivity (12.0±33.0 × 10^{-4} m^2 s^{-1}) was higher, although not statistically significant, than during downwelling (4.5±7.6 × 10^{-4} m^2 s^{-1}) and upwelling conditions (1.5±4.2 × 10^{-4} m^2 s^{-1}).

3.3.2. Nutrients, chlorophyll *a* and primary production

In downwelling conditions, due to the low stratification and deeper mixed layers, nitrate and phosphate vertical profiles were relatively homogeneous, whereas during upwelling, the input of cold and high-nitrate waters at depth caused significant enhanced nutrient vertical gradients (Figure 3.4). Vertical gradients of nitrate were also higher during relaxation, and the concentrations at depth of both nitrate and phosphate were higher during September 2015, compared to July 2015, due to the intensifying upwelling observed one week before the September 2015 sampling (Figure 3.1). On average, the vertical nitrate gradient between 10 and 40 m depth during upwelling (148±41 μmol m^{-4}) and relaxation (139±2 μmol m^{-4}) was significantly higher than during downwelling (15±13 μmol m^{-4}) (Table 3.1).

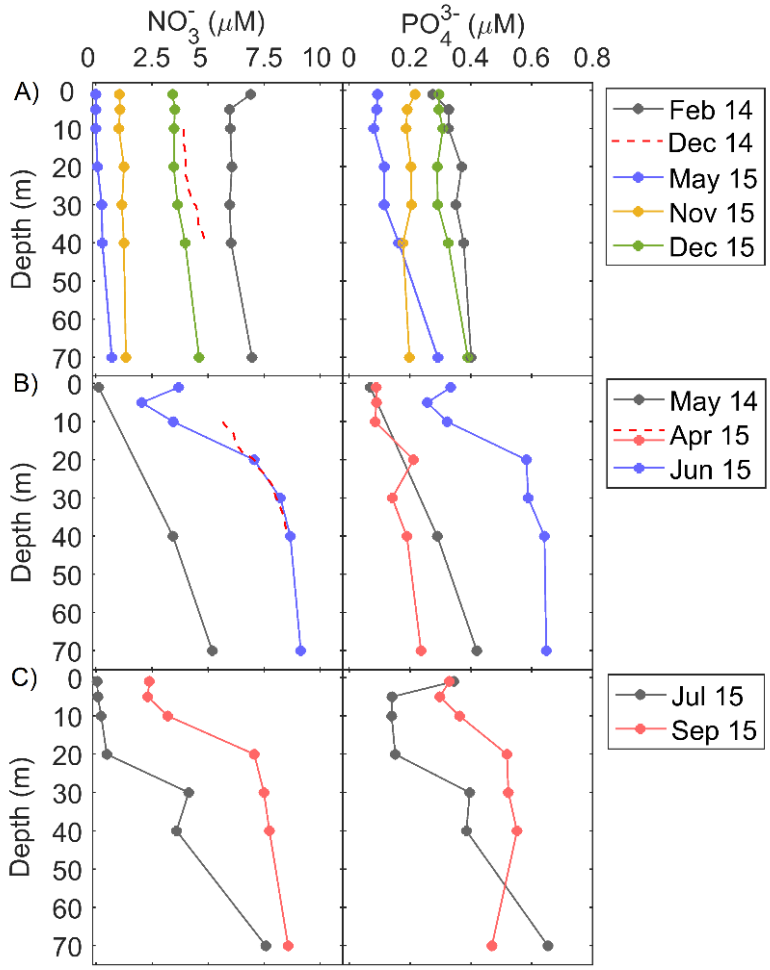

Figure 3.4. *Vertical distribution of nitrate (NO_3^-) and phosphate (PO_4^{3-}) concentration (μM) during* ***(A)*** *downwelling,* ***(B)*** *upwelling, and* ***(C)*** *relaxation conditions. Dashed line in nitrate profiles between 10-40 m depth in December 2014 and April 2015 indicate nitrate concentrations computed from the nitrate-density (σ_t) relationship (see section Material and Methods).*

Vertical profiles of total chlorophyll *a* and primary production were also homogeneous during downwelling (Figure 3.5). During these conditions depth-integrated chlorophyll *a* and primary production were, on average, relatively low (31±16 mg m^{-2} and 1359±1032 mg C m^{-2} d^{-1}, respectively), and dominated (>80%) by small (<10 μm) phytoplankton cells (Table 3.1, Figure 3.3). During upwelling the fertilization effect of deep waters stimulates phytoplankton growth, and increases the contribution of larger cells (>10 μm). Averaged depth-integrated chlorophyll *a* (65±35 mg m^{-2}) and primary production (5192±538 mg C m^{-2} d^{-1}) were slightly and significantly, respectively, higher than during downwelling and relaxation, and the contribution of larger cells to both chlorophyll *a* and primary production was higher than 60%. During relaxation depth-integrated chlorophyll *a* (20±2 mg m^{-2}) and primary production (1611±295 mg C m^{-2} d^{-1}) were relatively low.

In September 2015, small phytoplankton cells contributed more than 80% to both chlorophyll *a* and primary production, whereas in July 2015 the contribution was lower than 50%.

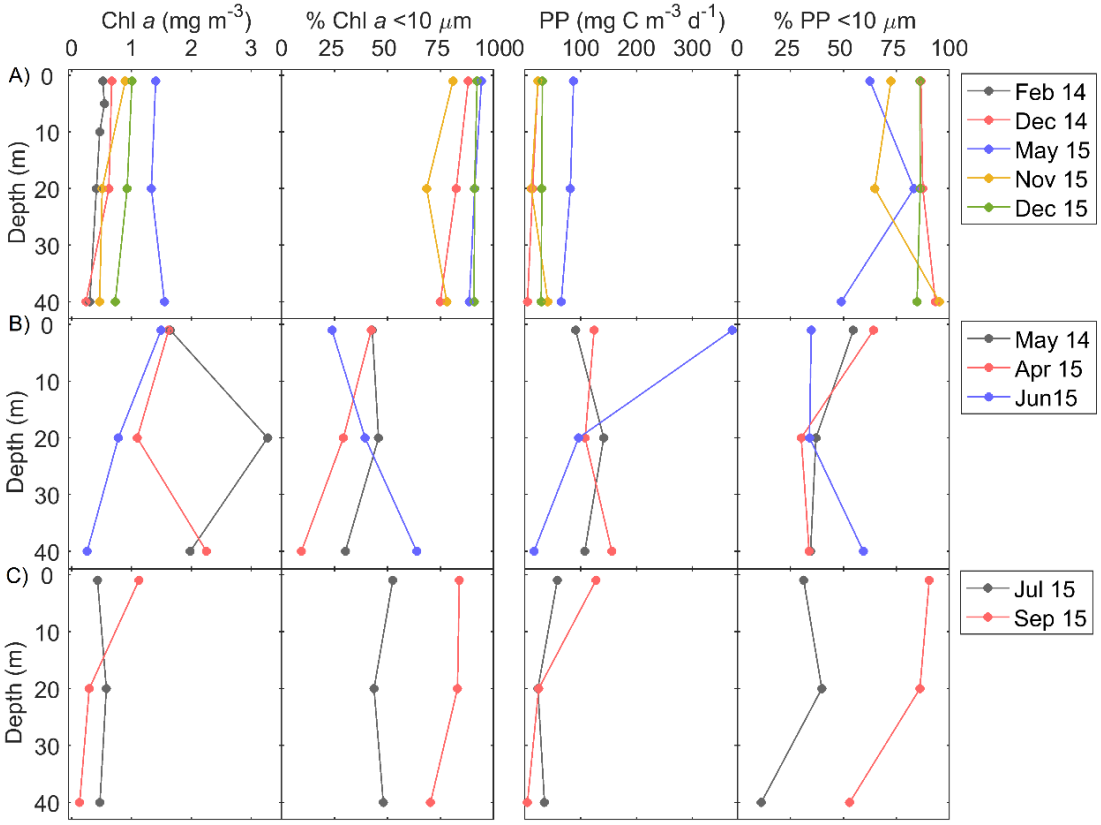

Figure 3.5. *Vertical distribution of total chlorophyll a concentration (Chl a), contribution of <10 µm size-fraction to total chlorophyll a (%), total primary production (PP), and contribution of <10 µm size-fraction to total primary production, during* ***(A)*** *downwelling,* ***(B)*** *upwelling, and* ***(C)*** *relaxation conditions.*

3.3.3. Picoplankton community composition

Flow cytometry data showed that picoplankton biomass was largely dominated by heterotrophic bacteria (HNA and LNA), followed by picoeukaryotes (large and small), and finally cyanobacteria (*Synechococcus* and *Prochlorococcus*) (Table 3.1, Table S6.1, Figure 3.6). The averaged contribution of HNA bacteria to total biomass peaked (ca. 60%) during upwelling and relaxation conditions. Consistently with the information provided by size-fractionated chlorophyll *a*, which showed the predominance of small (<10 µm) cells during downwelling (Figure 3.5), the averaged depth-integrated biomass of total picophytoplankton (i.e. large and small picoeukaryotes plus *Synechococcus* and

Prochlorococcus cyanobacteria) (88±48 mg C m^{-2}), was during this condition slightly higher than during upwelling (54±23 mg C m^{-2}) and relaxation (31±26 mg C m^{-2}).

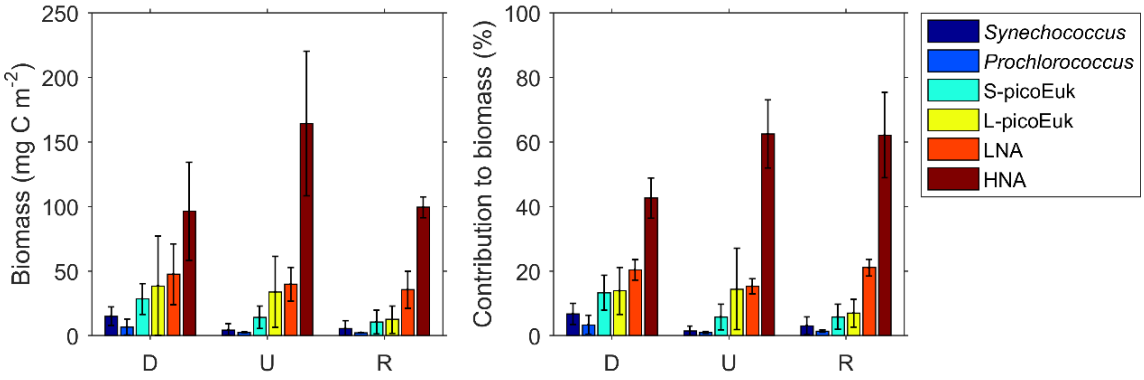

Figure 3.6. *Averaged depth-integrated biomass (left) and averaged contribution to total picoplankton biomass (right) of Synechococcus, Prochlorococcus, small (S-picoEuk) and large (L-picoEuk) picoeukaryotes, and high nucleic acid content (HNA) and low nucleic acid content (LNA) heterotrophic bacteria, during the NICANOR cruises under (D) downwelling, (U) upwelling, and (R) relaxation conditions. Error bars represent standard deviation.*

The vertical distribution of picoeukaryotic biomass, which potentially may include the UCYN-A diazotroph-prymnesiophyte host (Thompson et al., 2012, 2014), was relatively homogeneous during downwelling, with the exception of May 2015, when the highest biomass (>3 µg C L^{-1}) was observed in the upper 40 m (Figure 3.7). During upwelling conditions, the vertical distribution of picoeukaryotes biomass showed small vertical variability in May 2014, whereas in April and June 2015 enhanced values (>2 µg C L^{-1}) were observed at the surface. During relaxation, small vertical variability was observed in July 2015, whereas in September 2015 enhanced values (>1.5 µg C L^{-1}) also occurred at surface waters.

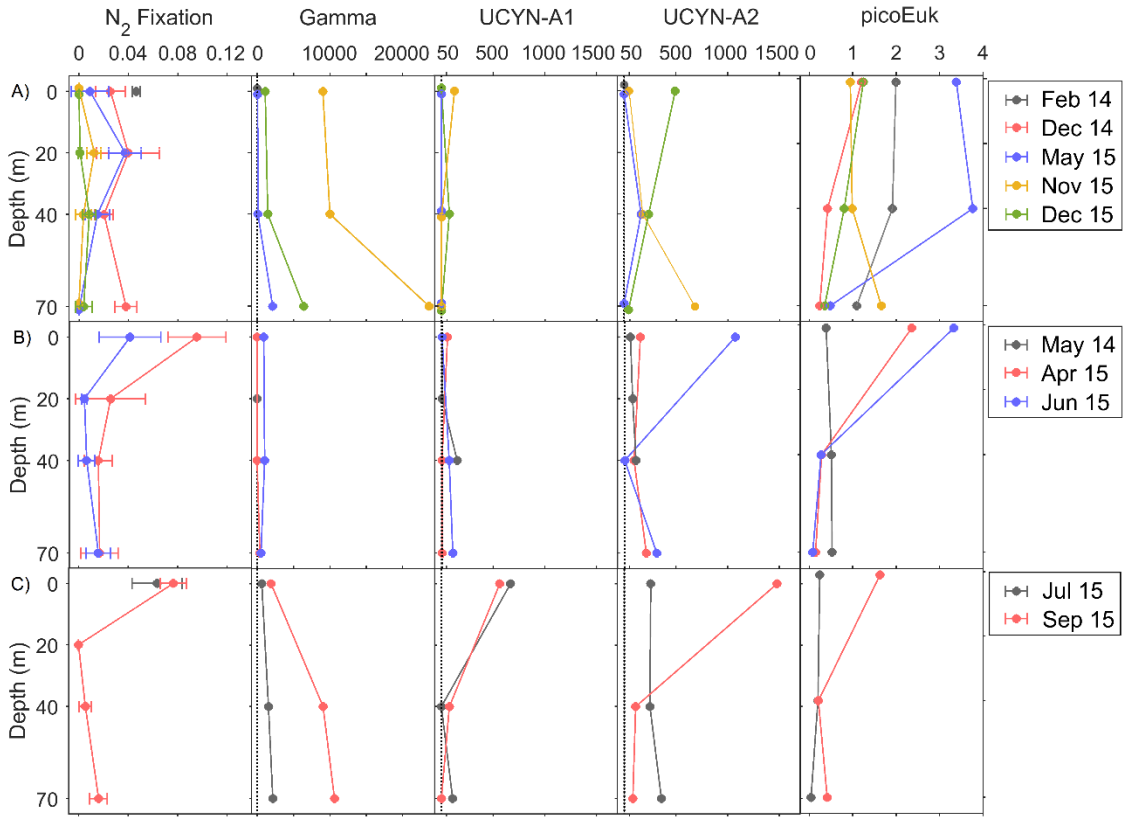

Figure 3.7. *Vertical distribution of BNF rates (µmol N m^{-3} d^{-1}), Gammaproteobacteria γ-24774A11, UCYN-A1 and UCYN-A2 nifH copies L^{-1}, and carbon biomass (µg C L^{-1}) of total (small+large) picoeukaryotes during* ***(A)*** *downwelling,* ***(B)*** *upwelling, and* ***(C)*** *relaxation conditions. Error bars in BNF panels represent standard deviation. Abundances below DNQ limit (detected but not quantified, <41 nifH copies L^{-1}) were assigned a conservative value of 1 nifH copy L^{-1}, which is indicated by a dotted line on the charts.*

3.3.4. Magnitude and biogeochemical relevance of biological N_2 fixation

No significant differences (Kruskal-Wallis, p>0.05) were found between the BNF rates corresponding to the total and small (<10 µm) size-fractions (data not shown), suggesting that small diazotrophs, presumably unicellular, were responsible for all the BNF activity detected in the region. For this reason, only BNF rates corresponding to the total size-fraction are described here. Whereas no significant differences were observed in depth-integrated rates, which ranged from 0.1±0.1 to 1.6±0.5 µmol N m^{-2} d^{-1} (Table 3.1), contrasting vertical patterns were observed during downwelling, upwelling and relaxation conditions (Figure 3.7).

During downwelling, the vertical distribution of BNF was relatively homogeneous, and no significant differences were found between the rates determined at different depths (Kruskal-Wallis, p>0.05) (Figure 3.7). Depth-integrated rates were slightly higher in

December 2014 (1.3±0.4 µmol N m^{-2} d^{-1}) and May 2015 (1.0±0.3 µmol N m^{-2} d^{-1}), compared to November 2015 (0.3±0.1 µmol N m^{-2} d^{-1}) and December 2015 (0.1±0.1 µmol N m^{-2} d^{-1}). During both upwelling and relaxation conditions, maximum rates were observed in general at the surface, decreasing between 20-40 m and slightly increasing again at 70 m. Depth-integrated rates were higher in April 2015 (1.6±0.5 µmol N m^{-2} d^{-1}, upwelling) and September 2015 (0.8±0.1 µmol N m^{-2} d^{-1}, relaxation) compared to June 2015 (0.6±0.3 µmol N m^{-2} d^{-1}, upwelling). As a result of the hydrographic patterns described, when considering all the samplings together, BNF was negatively correlated with mixed layer depth (Pearson's r=-0.364, p<0.05), whereas a positive significant relationship was found with the primary production corresponding to the small (<10 µm) size-fraction (Pearson's r=0.573, p<0.01).

Due to the increased vertical diffusivity and vertical nitrate gradient determined during relaxation conditions, averaged nitrate diffusive fluxes during these samplings were more than six-fold higher (14.3±3.1 mmol m^{-2} d^{-1}), compared to upwelling (2.2±3.1 mmol m^{-2} d^{-1}) and downwelling (0.8±0.9 mmol m^{-2} d^{-1}) conditions (Table 3.1, Figures 3.3, 3.4). These numbers were between 2-5 orders of magnitude higher than the estimates of depth-integrated BNF (0.1±0.1 – 1.6±0.5 µmol m^{-2} d^{-1}) carried out during the NICANOR samplings. From a biogeochemical perspective, the comparison between these two processes evidences that the relevance of BNF in this system, which was relatively higher during the upwelling conditions sampled in April 2015, was always <2 % (Table S6.1).

3.3.5. *nifH* gene abundances

Next Generation Sequencing library analysis of the nitrogenase gene recovered from DNA samples obtained during the NICANOR samplings unveiled that all sequences belonged to unicellular cyanobacterial and heterotrophic bacterial diazotrophs (see Chapter 4). *nifH* clusters 3 (putative anaerobes), 1G (which is comprised of mainly Gammaproteobacteria) and 1B (Cyanobacteria) were the most abundant, representing 36%, 28% and 21% of total *nifH* sequences, respectively. The other clusters represented less than 8% of relative abundances each. However, we are aware that the relative abundance of phylotypes in the *nifH* library may be influenced by factors as DNA extraction efficiency, PCR bias (Turk et al., 2011) and presence of contaminants (Goto et al., 2005; Zehr et al., 2003a). In any case, two of the most abundant diazotrophic groups were UCYN-A and Gammaproteobacteria-affiliated phylotypes (1G), thus, we used the

qPCR primers-probe sets available for quantifying UCYN-A sublineages (-A1 and -A2) and Gammaproteobacteria γ-24774A11 phylotype, widely distributed and considered one of the most important heterotrophic diazotrophs (e.g. Langlois et al., 2015; Moisander et al., 2014). The quantification of these diazotrophs allowed examining their relative importance through the year. All the abundances were above the limit of detection, except the abundance of UCYN-A1 determined at the surface in February 2014 (downwelling), and the abundances of Gammaproteobacteria determined at the surface and 40 m depth in May 2014 and April 2015 (upwelling) (Figure 3.7).

The Gammaproteobacteria phylotype was significantly more abundant than UCYN-A1 and UCYN-A2 during downwelling and relaxation (Bonferroni comparisons, $p<0.05$) (Table 3.1, Figure 3.7). Although not statistically significant, both surface ($3.1\pm5.3 \times 10^2$ *nifH* copies L^{-1}) and depth-integrated ($13\pm23 \times 10^5$ *nifH* copies m^{-2}) abundances of Gammaproteobacteria were slightly lower during upwelling, as in May 2014 and April 2015 the abundances between 0 and 40 m depth were below LOD or DNQ limits (Table S6.1, Figure 3.3). During downwelling and relaxation conditions, Gammaproteobacteria showed vertical variability, reaching maximum abundances at 70 m depth. In November 2015 (downwelling) and September 2015 (relaxation) we found the highest surface (9.0×10^3 and 1.9×10^3 *nifH* copies L^{-1}, respectively) and depth-integrated abundances (380×10^5 and 220×10^5 *nifH* copies m^{-2}, respectively) measured on all cruises.

During relaxation, UCYN-A1 abundance increased at the surface, and both surface ($6.2\pm0.7 \times 10^2$ *nifH* copies L^{-1}) and depth-integrated ($13\pm0 \times 10^5$ *nifH* copies m^{-2}) abundance were significantly higher than during downwelling (33±64 *nifH* copies L^{-1} and $1.4\pm1.3 \times 10^5$ *nifH* copies m^{-2}, respectively) and upwelling conditions ($1.9\pm0.3 \times 10^2$ *nifH* copies L^{-1} and $1.3\pm0.2 \times 10^5$ *nifH* copies m^{-2}, respectively), when the vertical distribution of this group did not exhibit important vertical variability (Table 3.1, Figure 3.7).

The abundance of UCYN-A2 was higher than UCYN-A1 (Kruskal-Wallis, $p<0.05$) and showed larger vertical variability (Figure 3.7, Table S6.1). On average, surface and depth-integrated abundances of UCYN-A2 were slightly higher during relaxation ($8.7\pm8.6 \times 10^2$ *nifH* copies L^{-1} and $21\pm16 \times 10^5$ *nifH* copies m^{-2}, respectively), compared to upwelling ($4.3\pm5.6 \times 10^2$ *nifH* copies L^{-1} and $10\pm10 \times 10^5$ *nifH* copies m^{-2}, respectively) and downwelling ($1.4\pm2.4 \times 10^2$ *nifH* copies L^{-1} and $7\pm7 \times 10^5$ *nifH* copies m^{-2}, respectively) (Table 3.1). During downwelling, higher values occurred at 70 m in November 2015 (6.9×10^2 *nifH* copies L^{-1}), and also at the surface in December 2015 (5.0×10^2 *nifH* copies

L^{-1}). During upwelling and relaxation, the maximum abundances were quantified at the surface in June 2015 (1.1×10^3 *nifH* copies L^{-1}) and September 2015 (1.5×10^3 *nifH* copies L^{-1}), respectively.

3.3.6. Identification, characterization and quantification of UCYN-A–Prymnesiophyte symbiosis by double CARD-FISH

We only detected a single *B. bigelowii* non-associated host labelled with the probe UBRADO69 in one sample, at 0 m depth in September 2015 during relaxation (1 cell of UCYN-A2 host mL^{-1}) (Figure 3.8). The host observed was within the 4-5 μm size fraction and we can discern the chloroplasts on both sides thanks to their slight red autofluorescence (marked by white arrows). However, we did not observe any UCYN-A symbiont attached to the prymnesiophyte, and neither free symbionts in the sample.

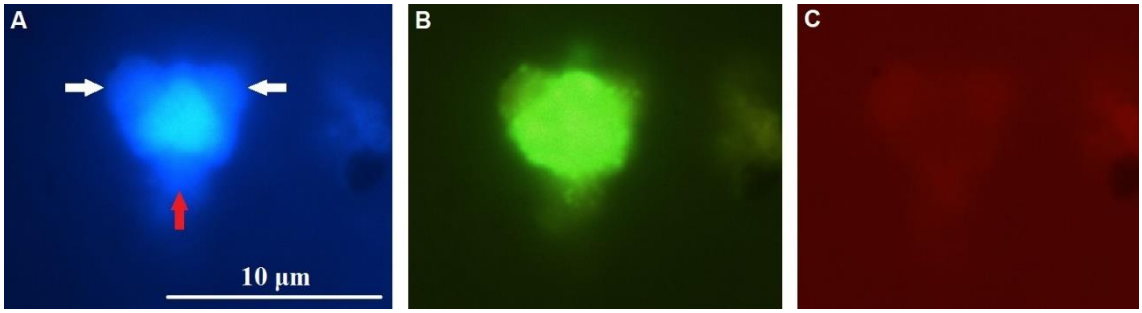

Figure 3.8. *Photomicrographs of the double CARD-FISH assay obtained with the epifluorescence microscope showing* B. bigelowii *labelled with the UBRADO69 probe without UCYN-A2 symbionts associated (sample of September 2015 at 0 m depth).* ***(A)*** *DAPI signal (blue-labelled DNA),* ***(B)*** *signal of the prymnesiophyte-specific UBRADO 69 probe (green-labelled host under blue light excitation), and* ***(C)*** *photomicrograph corresponding to the UCYN-A732 probe (if symbiont was present, red-labelled under green light excitation). White arrows in (A) indicate the position of chloroplasts on each side of the prymnesiophyte. Red arrow indicates the expected position of UCYN-A at the polar end of the cell, although in this case it was not present.*

3.3.7. Ecological niches of diazotroph groups

We finally investigated the overlapping of the ecological niches of the diazotrophs quantified by qPCR using non-parametric kernel density functions, and considering selected physical (temperature and vertical stratification), chemical (N:P ratio) and biological (chlorophyll *a* concentration) predictors. The results show a large overlapping

of the ecological niches of UCYN-A1, UCYN-A2 and Gammaproteobacteria, except when the chlorophyll *a* concentration was considered (Figure 3.9). This factor could statistically distinguish the niche partitioning between the cyanobacterial diazotroph UCYN-A2 and the heterotrophic Gammaproteobacteria (p<0.01) (Table 3.2). UCYN-A2 was more abundant under conditions of higher chlorophyll *a* concentration, whereas Gammaproteobacteria predominated at lower chlorophyll *a*.

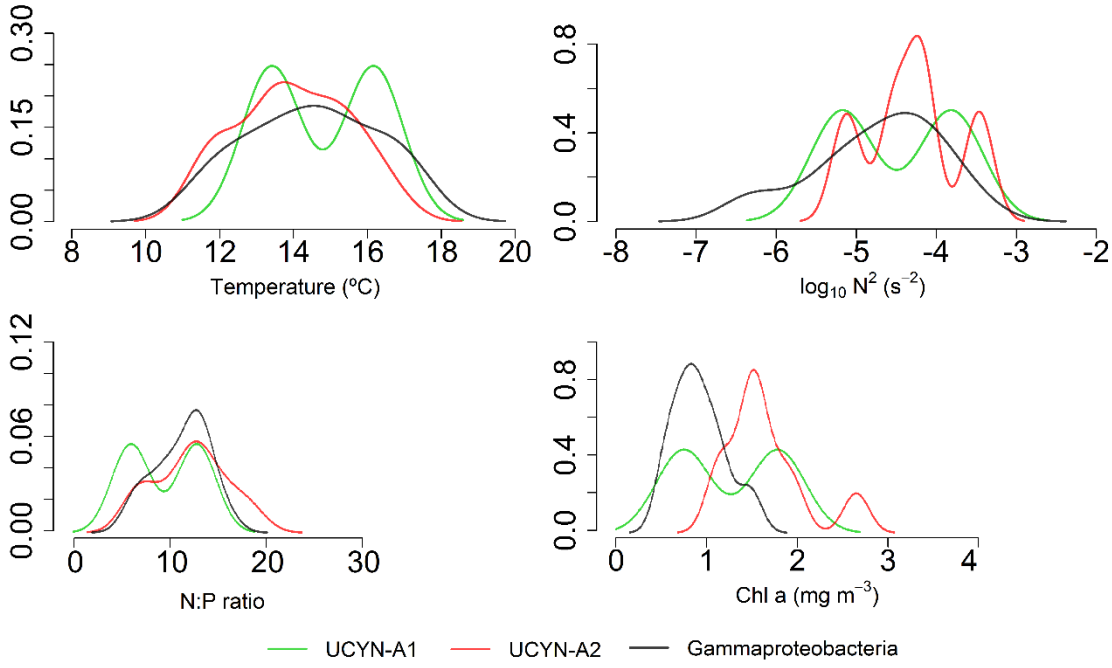

Figure 3.9. *Kernel density estimates of UCYN-A1, UCYN-A2 and Gammaproteobacteria based on the considered niche descriptors: temperature, vertical density stratification (quantified as squared Brunt Väisälä frequency, N^2), nitrate to phosphate ratio and chlorophyll* a *concentration.*

Table 3.2. *Partial weighted niche overlap (%) for each diazotroph group and environmental factor. Asterisk indicates significant differences between niches (p<0.01). N^2 is squared Brunt Väisälä frequency.*

		UCYN-A1	UCYN-A2	Gammaproteobacteria
Temperature	**UCYN-A1**	100		
	UCYN-A2	77	100	
	Gammaprot.	5980	87	100
N^2	**UCYN-A1**	100		
	UCYN-A2	70	100	
	Gammaprot.	77	72	100
N:P ratio	**UCYN-A1**	100		
	UCYN-A2	76	100	
	Gammaprot.	75		100
Chl *a*	**UCYN-A1**	100		
	UCYN-A2	56	100	
	Gammaprot.	59	32*	100

3.4. Discussion

3.4.1 Magnitude and biogeochemical relevance of BNF

Our results demonstrate the existence of detectable BNF activity (0.001±0.002 – 0.095±0.024 µmol N m^{-3} d^{-1}) under contrasting hydrographic regimes in a nitrogen-rich temperate coastal system subject to upwelling pulses. During downwelling the vertical pattern of BNF was rather homogeneous, whereas during upwelling and relaxation the BNF rates peaked in the well-lit surface waters, where we measured the highest rates of all cruises. Comparing with other studies using the same technique ($^{15}N_2$-gas tracer method, Montoya et al., 1996) and performed in similar nitrate-rich and temperate areas, our volumetric BNF rates were of similar magnitude to those measured by Benavides et al. (2011) in Cape Silleiro (NW Iberian Peninsula) in summer 2009, but between 1-3 orders of magnitude lower than those measured by Mulholland et al. (2012) in the temperate NE American coast during several summer and autumn cruises, and by Rees et al. (2009) in the western English Channel in summer. On a global context, our BNF rates estimated in the outer part of Ría de A Coruña are similar to the lower-end described for the subtropical NE Atlantic (Luo et al., 2012). Although our rates were relatively low, our results contradict the traditional paradigm about marine BNF. This view established that BNF is mainly restricted to the nitrogen-poor, warm (>20 ºC) (sub)tropical ocean, as high nutrient inputs and the relatively low surface temperatures in temperate coastal systems would not favour N_2 fixation by filamentous non-heterocystous cyanobacteria such as *Trichodesmium* (Conley et al., 2009; Howarth et al., 1988; Stal, 2009). The BNF activity detected in this study is a further evidence that high nitrate concentrations (and high N:P ratios) do not inhibit BNF activity, such as it was also observed in other upwelling regions (e.g., Benavides et al., 2014; Sohm et al., 2011a; Subramaniam et al., 2013; Voss et al., 2004; Wen et al., 2017). Indeed, recent studies demonstrated that BNF can occur upon exposure to elevated DIN (NO_x + NH_3), as long as phosphate is available (Knapp, 2012), and point towards iron as the primary control factor of BNF (Bonnet et al., 2017; Knapp et al., 2016; Moore et al., 2009). Thus, the sensitivity of marine BNF to high DIN is not clear, largely depending on the present diazotrophic taxa. Along with the wide distribution and large diversity of diazotrophs (Moisander et al., 2010; Zehr et al., 2000), our results indicate that restricting BNF measurements exclusively to oligotrophic (sub)tropical regions may result in an underestimation of the global magnitude of this flux, contributing to the apparent imbalances observed in the marine N budget (Brandes

and Devol, 2002; Codispoti, 2007; Mahaffey et al., 2005).

The contribution of BNF to new N supply into the euphotic zone was negligible (<2 %) in this system, as it was between 2 and 5 orders of magnitude lower than diffusive fluxes. These numbers represent the first estimate of the contribution of both processes in a coastal upwelling system. Few studies have simultaneously quantified BNF and nitrate diffusion (Fernández-Castro et al., 2015; Mouriño-Carballido et al., 2011; Painter et al., 2013), mainly due to the methodological difficulties to estimate vertical mixing (*Kz*) in the field, which has frequently motivated the use of constant values of *Kz* (Capone et al., 2005), and empirical parameterizations (Fernández-Castro et al., 2014; Planas et al., 1999). Capone et al. (2005) estimated in the tropical North Atlantic that BNF could equal or even exceed nitrate vertical diffusion into the euphotic zone. In the subtropical NE Atlantic, Mouriño-Carballido et al. (2011) reported a contribution of BNF to new nitrogen input of 2±2 %, whereas Painter et al. (2013) indicated that BNF represented a significant source of new N, but not as large as the diffusive fluxes. In their study across the (sub)tropical Atlantic, Pacific and Indian oceans, Fernández-Castro et al. (2015) pointed out that, on average and compared to BNF, nitrate diffusion was the main mechanism supplying new N. The magnitude of averaged nitrate diffusion estimated in our study (3.9±5.8 mmol m^{-2} d^{-1}) was slightly higher than the estimations for the subtropical NE Atlantic by Mouriño-Carballido et al. (2011) (0.8±1.3 mmol m^{-2} d^{-1}) and Painter et al. (2013) (0.06±0.02 mmol m^{-2} d^{-1}), and by Fernández-Castro et al. (2015) (0.2±0.2 mmol m^{-2} d^{-1}) in the (sub)tropical Atlantic, Pacific and Indian oceans. The range of diffusive fluxes here reported (0.1-16.5 mmol m^{-2} d^{-1}) was comparable to that obtained in a nearby coastal system (Ría de Vigo, NW Iberia) by Cermeño et al. (2016) (0.8–20.1 mmol m^{-2} d^{-1}) and Villamaña et al. (2017) (9.4–34.6 mmol m^{-2} d^{-1}).

We cannot discard that our N_2 fixation rates may be underestimated due to the use of the $^{15}N_2$-bubble addition technique (Montoya et al., 1996) instead of the modified tracer method with $^{15}N_2$-enriched seawater (Mohr et al., 2010). The magnitude of the underestimation of rates will depend on incubation time, diazotroph community composition and physical properties (e.g., temperature and salinity) (Benavides et al., 2013a; Großkopf et al., 2012b; Mohr et al., 2010; Wilson et al., 2012). However, by comparing the bubble and enriched water methods, Wannicke et al. (2018) concluded that the underestimation of N_2 fixation rates is not generalized and occurs under certain conditions since it depends mainly on incubation time and the day/night cycle in which

the diazotrophs present are active. These authors reported negligible underestimations for incubations of 24 h and observed a large consistency between N_2 fixation measurements using both methods in the studies analyzed. Likewise, several authors have demonstrated that BNF rates may be underestimated when the ^{15}N-enrichment in the dissolved organic N is overlooked, considering only the incorporation of ^{15}N into particulate organic N (Benavides et al., 2013b; Berthelot et al., 2017; Glibert and Bronk, 1994; Konno et al., 2010). Underestimation can also occur when using glass fiber filters (GF/F, Whatman, 0.7 μm pore size) to collect suspended particles by filtration after incubations with added $^{15}N_2$ tracer, due to the loss of small, unicellular diazotrophs (Bombar et al., 2018). In any case, the biogeochemical relevance of BNF in this system would be still very low since other important potential mechanisms of new N supply, such as advective vertical and horizontal transport, atmospheric deposition or internal waves (Duce et al., 2008; Oschlies and Garçon, 1998; Villamaña et al., 2017), were not considered in this study.

In order to get a rough estimation of the fertilization effect of the upwelling, we compared a simplified estimate of nitrate supply through vertical advection (see Material and Methods) with the input of nitrogen through nitrate vertical diffusion. As expected, nitrate vertical advection was the main mechanism of N supply during upwelling (79±119 mmol $m^{-2}\,d^{-1}$) and during relaxation in September 2015 (77 mmol $m^{-2}\,d^{-1}$), which was influenced by an upwelling pulse happening a few days before the sampling. This nitrogen supply was more than 180-fold higher than nitrate diffusion during upwelling, and up to 6-fold higher in September 2015. Obviously, non-upwelling situations implied higher contribution to new N supply by diffusion. In any case, the consideration of this process would decrease, even more, the contribution of BNF to the new nitrogen supply in this system. Overall, the proportion of gross primary production (GPP) that could be sustained by diazotrophy, calculated by assuming Redfield stoichiometry, would be irrelevant (<0.1 %) when compared to the proportion of GPP supported by nitrate (41.9±31.2 %) and ammonium (6.8±5.0 %) uptake rates, measured in the same region in an earlier study (Bode et al., 2004).

3.4.2 Players, ecological niches and contribution to BNF

Small diazotrophs (<10 μm), presumably unicellular, were responsible for all BNF activity detected in this region. This is consistent with analysis of the *nifH* library, which revealed that all sequences belonged to unicellular cyanobacterial and heterotrophic

diazotrophs (see Chapter 4). A large fraction of *nifH* sequences recovered belonged to Gammaproteobacteria-affiliated phylotypes of the subcluster 1G (28%) and UCYN-A (21%).

The abundance of Gammaproteobacteria γ-24774A11 phylotype (0-2.4 × 10^4 *nifH* copies L^{-1}) was significantly higher than UCYN-A1 and UCYN-A2 during downwelling and relaxation (Bonferroni comparisons, $p<0.05$). These values were in the medium-high range of global abundances reviewed by Luo et al. (2012), and by Benavides and Voss (2015) specifically from studies performed in the North Atlantic. In fact, heterotrophic diazotrophs abundances higher than 10^4 *nifH* copies L^{-1} have seldom been reported in the marine environment (e.g. Halm et al., 2012; Moisander et al., 2008). The abundance of the heterotrophic Gammaproteobacteria was positively correlated with temperature (Pearson's $r=0.473$, $p<0.05$) and mixed layer depth (Pearson's $r=0.495$, $p<0.05$), since slightly higher abundances were measured during downwelling conditions, when the water column was warmer, less stratified and with relatively low nutrient concentrations. These hydrographic features could cause the dominance of Gammaproteobacteria as the primary productivity was low and dominated by small cells, and likely sustained by regenerated nutrients (mainly nitrogen) through bacterial remineralisation of organic matter, such as it was observed previously in this region (Bode et al., 2004, 2011). The production based on bacterial recycling of nutrients may also have occurred in September 2015, when the abundance of Gammaproteobacteria increased significantly, probably fueled by the organic matter produced during the upwelling pulse happening before the sampling (Bode et al., 1996; Casas et al., 1997). These findings are consistent with Moisander et al. (2012, 2014), since they suggested that the abundance of the Gammaproteobacterial phylotype γ-24774A11 may depend on dissolved organic carbon produced by phytoplankton.

The symbiosis of UCYN-A with picoeukaryotic prymnesiophyte is present in these nitrogen-rich and relatively cold (<17ºC) waters. In contrast to Gammaproteobacteria that peaked mainly at deep waters (70 m) during downwelling conditions, UCYN-A1 and -A2 peaked in well-lit and stratified surface waters during upwelling (June 2015) and relaxation (July and September 2015). The environmental features found in the surface waters of those samplings seem to favor UCYN-A, specifically the coastal sublineage UCYN-A2 based on their highest abundances, and the photoautotroph host, which would meet its light requirements. These findings shed light on the environmental conditions

associated to the ecological niches of UCYN-A and Gammaproteobacteria within this upwelling ecosystem. Despite the differences in the described hydrographic conditions, and probably due to our limited data set, the analysis of the ecological niches by using non-parametric kernel density functions showed a large overlapping, except when chlorophyll *a* concentration was used. UCYN-A2 was more abundant under conditions of higher chlorophyll *a*, whereas Gammaproteobacteria predominates at lower chlorophyll *a* concentrations. This result seems reasonable as UCYN-A2 is a diazotroph that predominates in coastal productive regions, and Gammaproteobacteria is an important N_2-fixer in the oligotrophic open ocean.

Agawin et al. (2014) also detected UCYN-A in this same upwelling region by *nifH* sequencing. Similarly, UCYN-A1 thrived in other N-rich areas as the temperate NE American coast (Mulholland et al., 2012) and the Equatorial Atlantic upwelling region (Foster et al., 2009), as these authors demonstrated by qPCR. Furthermore, UCYN-A1 associated to its small uncultured host were detected by using CARD-FISH in the Galician Bank, an open ocean environment relatively close to our region (Cabello et al., 2016). Using the same technique, we only observed one cell of *B. bigelowii* (1 cell mL^{-1}), the UCYN-A2 host, at the surface in September 2015, when the highest abundance of UCYN-A2 was determined via qPCR (1.5×10^3 *nifH* copies L^{-1}). We would expect the abundance of the non-associated hosts to be positively related to the abundance of free UCYN-A cells, however, we did not detect any symbiont. The original symbiotic association was probably detached by rough sample manipulation and processing, as described in Cabello et al. (2016). The size of the *B. bigelowii* detected (4-5 μm) is consistent with the findings about global distribution of the UCYN-A–prymnesiophyte symbiosis reported by Cabello et al. (2016), who observed that all *B. bigelowii* cells counted (n=17) were within this size fraction. Assuming that each UCYN-A cell has one *nifH* gene copy, and considering the absolute abundances of UCYN-A1 and -A2 measured by qPCR in this study, we note that most of UCYN-A abundances were below the detection limit of the CARD-FISH technique (1000 *nifH* copies L^{-1} or 1 cell mL^{-1}), except in the surface samples of September 2015 and June 2015. We could reduce the detection limit increasing the area of count on the filter piece and the filtered sample volume. Nevertheless, both options were not operational due to the high investment of time (high effort of observation with the microscopy) and the high concentration of organic matter in the water that made difficult the filtration even with low volumes. Therefore, we conclude that the double CARD-FISH approach is not appropriate to

visualize, characterize and quantify the UCYN-A–prymnesiophyte symbiosis in this region, and in similar productive ecosystems with low symbiosis abundances. In contrast, quantitative PCR approaches allow estimating accurately *nifH* gene abundances of UCYN-A sublineages, despite not providing information about the characteristics of the relationship established such as size of the eukaryote host, number of cyanobacterial symbionts per host or degree and type of dependence between partners.

The pattern of vertical distribution of picoeukaryotes was consistent with those of UCYN-A. When the abundances of UCYN-A peaked, the biomass of the picophytoplankton also peaked (but not vice versa), although in July 2015 the pattern was not so clear. Indeed, qPCR analysis of picoeukaryotic populations sorted with flow cytometry unequivocally demonstrated that UCYN-A are associated with picoeukaryotes (Thompson et al., 2012, 2014). Furthermore, we did not find a link between UCYN-A abundance and phytoplankton biomass (chlorophyll *a*), which could be expected on the basis of the symbiotic association of UCYN-A with a photosynthetic prymnesiophyte in regions where picoplankton dominates phytoplankton biomass, such as it was previously observed in the oligotrophic (sub)tropical SW Pacific (Moisander et al., 2010). This decoupling was probably due to the fact that our study was carried out in an upwelling system, where usually most biomass corresponds to large phytoplankton (>10 μm), mainly chain-forming diatoms (Casas et al., 1997; Varela et al., 2001).

The abundance of UCYN-A2 sublineage (1–1.5 × 10^3 *nifH* copies L^{-1}) was on average 3-fold higher than that of UCYN-A1 (0–6.7 × 10^2 *nifH* copies L^{-1}). Although the differences in abundances may be due to the number of UCYN-A2 cells in symbiosis with each host, which can reach up to eleven (Thompson et al., 2014). In any case, the higher UCYN-A2 abundance is consistent with recent findings pointing out this sublineage, although globally distributed (Cabello et al., 2016; Martínez-Pérez et al., 2016), mainly inhabits coastal regions, whereas UCYN-A1 dominates in the oligotrophic open ocean (Messer et al., 2015a; Thompson et al., 2014; Turk-Kubo et al., 2017). The UCYN-A abundances detected by qPCR were in the medium-low range of global abundances reported by Luo et al. (2012) and Martínez-Pérez et al. (2016), and by Benavides and Voss (2015) from their data review of the North Atlantic. In the temperate NE American coast, Mulholland et al. (2012) showed that UCYN-A1 was the most abundant diazotroph, reaching 3.5 × 10^7 *nifH* copies L^{-1}, among the highest abundances ever observed. Several studies performed in the North Atlantic reported that, after *Trichodesmium*, UCYN-A is the most

abundant diazotrophic phylotype (Benavides et al., 2016; Benavides and Voss, 2015; Ratten et al., 2015). Even though it extends along a wide latitudinal and longitudinal range, it predominates in the eastern basin, where iron inputs by Saharan dust are higher (Benavides et al., 2013a), which favours its growth and N_2-fixing activity (Krupke et al., 2015).

Higher abundances of UCYN-A1 and UCYN-A2 determined by qPCR occurred at the well-lit surface waters under upwelling and relaxation conditions, suggesting a possible seasonal variability on the growth of the UCYN-A–prymnesiophyte symbiosis, such as it was previously observed in the (sub)tropical SW Pacific (Bonnet et al., 2015; Moisander et al., 2010). These high values coincided with the highest BNF rates, and indeed UCYN-A abundances were positively correlated with BNF rates (Pearson's r=0.534, p<0.05), consistent with the fact that small diazotrophs (<10 μm) were responsible for all BNF activity in this system. This relationship has also been observed in other regions, as the NE American coast (Mulholland et al., 2012), or the tropical SW Pacific (Bonnet et al., 2015; Turk-Kubo et al., 2015). Therefore, UCYN-A–prymnesiophyte symbiosis may be responsible for most BNF activity, or at least a large fraction, in our region, since Gammaproteobacteria abundance and BNF rates were not correlated or consistent. Turk-Kubo et al. (2014) reported that Gammaproteobacteria phylotypes do not contribute significantly to marine BNF, based on their analysis of heterotrophic cell-specific N_2 fixation rates required to explain previously reported BNF rates in different marine environments (e.g. Farnelid et al., 2013; Großkopf et al., 2012; Halm et al., 2012; Zehr et al., 2007). In our study, average cell-specific N_2 fixation rates required to account for BNF rates (see Material and Methods) ranged from 0.8 fmol N cell^{-1} h^{-1} (November 2015, 40 m) to 19.3 fmol N cell^{-1} h^{-1} (April 2015, 0 m). Therefore, in several samples UCYN-A may have been responsible for all the BNF activity, since cell-specific rates estimated for this diazotrophic group range from 0.02 to 2.6 fmol N cell^{-1} h^{-1} (Goebel et al., 2010). However, in some samples the required cell-specific rates are too high to be due solely to the UCYN-A quantified. Thus, whole BNF rates may result from small contributions from other non-cyanobacterial diazotrophs that we have not quantified by qPCR.

3.5. Outlook

Our study provides a novel assessment of the magnitude and seasonal variability of BNF, its contribution to the budget of new N inputs into the euphotic zone, and the abundance of diazotrophs in a NE Atlantic temperate upwelling region, subject to contrasting hydrographic regimes. In contrast, most studies focusing on marine BNF have been conducted in the western basin, and in the (sub)tropical North Atlantic. BNF activity and presence of diazotrophs have been demonstrated in a N-rich temperate region, even though their ecological role remains unclear. This will require further spatial–temporal studies in the zone. By calculating the geometric mean of depth-integrated BNF rates estimated during the NICANOR cruises and assuming the surface area of a 3º×3º grid cell (following Luo et al., 2012), we estimated an averaged new N input in the study area of about 0.4 Gg N yr^{-1} from planktonic BNF. In the region of the Canary Current and NW African upwelling, Benavides et al. (2011) estimated an input of 0-20 Gg N yr^{-1}, whereas Mulholland et al. (2012) estimated an input of 0.5-107 × 10^3 Gg N yr^{-1} in the temperate NE American coast (Benavides and Voss, 2015; Luo et al., 2012). The current biogeochemical relevance of BNF in our study system is negligible. However, the weakening of the Iberian coastal upwelling in the last decades (Pardo et al., 2011; Pérez et al., 2010), and the enhancement of stratification due to the warming in ocean surface waters might favour an increase of the relative importance of the diazotrophy in the future (Boyd and Doney, 2002; Doney, 2006). In any case, the study of the BNF processes and the responsible organisms in this region shed light on the ecophysiology of the present diazotrophic community. This first report of the presence of UCYN-A and Gammaproteobacteria γ-24774A11 in this region extends the geographic area where these diazotrophs grow. In contrast to Gammaproteobacteria that peaked mainly at deep waters (70 m) during downwelling conditions, UCYN-A peaked in well-lit and stratified surface waters under upwelling and relaxation conditions. These environmental features may outline the ecological niches of Gammaproteobacteria and UCYN-A, mainly UCYN-A2, in this productive region. Moreover, the phytoplanktonic biomass (Chl *a*) could differentiate the partitioning of niches between UCYN-A2 and Gammaproteobacteria, since UCYN-A2 was more abundant under conditions of higher chlorophyll *a* concentration. Our findings provide also further evidence of the co-occurrence of the UCYN-A sublineages, their wide distribution in the ocean (Farnelid et al., 2016b; Martínez-Pérez et al., 2016), as well as their ability to grow in relatively cold waters with high DIN concentrations. Considering the large diversity of marine diazotrophs, and our

limited knowledge of their physiology and ecology, sustained observational efforts throughout the ocean will be required to delimit accurately the magnitude and variability of marine BNF.

4. Temporal variability of diazotroph community composition

Abstract

Knowledge of the diversity, activity and ecology of N_2-fixing (diazotrophic) plankton is mainly limited to oligotrophic (sub)tropical oceans. However, diazotrophs are widely distributed and potentially active throughout the global ocean. Likewise, most studies are characterized by a limited understanding about the temporal variability of the diazotrophic community composition. Between February 2014 and December 2015, we carried out 9 one-day samplings in productive waters of the temperate northwestern Iberian upwelling system to investigate the temporal and vertical variability of the diazotrophic community diversity and its relationship with hydrodynamic forcing. In downwelling conditions, characterized by deeper mixed layers and a homogeneous water column, non-cyanobacterial diazotrophs belonging mainly to *nifH* clusters 1G (Gammaproteobacteria) and 3 (putative anaerobes) dominated the community. In contrast, in upwelling and relaxation conditions, affected by enhanced vertical stratification and hydrographic variability, the diazotrophic community was more heterogeneous and less diverse, with prevalence of UCYN-A (unicellular cyanobacterial diazotroph of subcluster 1B) and non-cyanobacterial diazotrophs from cluster 1G and 3. Based on oligotyping analysis of UCYN-A phylotype, UCYN-A2 sublineage was the most abundant (74%), followed by UCYN-A1 (23%) and UCYN-A4 (2%). These sublineages were mainly represented by the oligotypes oligo3 (67%), oligo1 (18%) and oligo 4 (2%), respectively. UCYN-A1 oligotypes were detected at relatively low frequencies during the three hydrographic conditions, whereas UCYN-A2 exhibited higher abundances during upwelling and relaxation. Our findings demonstrate the presence of a diverse and temporally variable diazotrophic community driven by hydrodynamic forcing.

4.1. Introduction

The large diversity of marine diazotrophs (Riemann et al., 2010; Zehr et al., 2000, 2003b) expands the range of marine environments where biological N_2 fixation (BNF) is a relevant process (Moisander et al., 2010). Besides the traditionally most studied N_2-fixing organisms, i.e. the filamentous cyanobacteria *Trichodesmium* and cyanobacterial symbionts of diatoms such as *Richelia intracellularis* (Villareal, 1992), marine diazotrophs also comprise unicellular cyanobacteria (the uncultivated group A or UCYN-A; the free-living *Crocosphaera* sp. or UCYN-B; and the presumably free-living UCYN-C, which contains cultivated cyanobacteria such as *Cyanothece* sp.), and non-cyanobacterial diazotrophs (heterotrophic Bacteria and Archaea) (Zehr et al., 2003b; Zehr, 2011). Heterotrophic bacterial diazotrophs include a large diversity of phylogenetic groups such as Proteobacteria and Verrucomicrobia, among others (Zehr et al., 2003b).

The cyanobacterium UCYN-A (or *Candidatus* Atelocyanobacterium thalassa) is one of the most important members of the global diazotroph community due to its broad distribution in marine environments and relatively high N_2 fixation rates (Farnelid et al., 2016a; Martínez-Pérez et al., 2016). It lives in association with a picoeukaryotic prymnesiophyte (Thompson et al., 2012, 2014), and the single-celled symbiosis established between them is a potential model for observing the evolution of organelles in eukaryotic cells, specifically N_2-fixing organelles (Zehr et al., 2016). Despite the ecological, biogeochemical and evolutionary relevance of UCYN-A, its low abundance in the marine environment makes its identification and quantification challenging. Regardless, a targeted approach recently adapted by Turk-Kubo et al. (2017) to define UCYN-A oligotypes, finely resolved taxonomic groups based on nucleotide positions with high variability (Eren et al., 2013), has facilitated progress in the study of its diversity and ecology. Six UCYN-A sublineages (UCYN-A1 to -A6) have previously been defined based on the genetic diversity of *nifH* sequences available in the NCBI GenBank database (Farnelid et al., 2016a; Thompson et al., 2014; Turk-Kubo et al., 2017). Recent findings indicate that each of these sublineages occupy different ecological niches (Farnelid et al., 2016a; Turk-Kubo et al., 2017).

Cyanobacterial diazotrophs have traditionally been considered to be the most important oceanic N_2-fixing organisms, however, in recent years it was demonstrated that potentially active non-cyanobacterial diazotrophs are also widespread (Bombar et al., 2016; Delmont et al., 2018; Moisander et al., 2017). Heterotrophic diazotrophs, mainly

Proteobacteria, are common and can dominate the *nifH* signatures of contrasting marine environments (Falcón et al., 2004; Farnelid et al., 2011b; Fernández-Méndez et al., 2016; Fernández et al., 2015; Moisander et al., 2014b; Riemann et al., 2010), although their contribution to marine BNF and ecological significance remain still elusive (Turk-Kubo et al., 2014).

Diazotroph communities from contrasting marine environments along the global ocean differ markedly in their composition (e.g., Farnelid et al., 2011; Zehr et al., 2003b). Although studies concerning diazotrophic diversity are not directly comparable due to different methodological approaches used, *nifH* clone libraries from open ocean show in general lower richness and diversity than libraries from the dynamic estuarine and coastal regions (Affourtit et al., 2001; Farnelid et al., 2009, 2011; Jenkins et al., 2004; Zehr et al., 2003b). The higher richness and diversity of diazotrophs found in coastal marine environments may be explained by different factors, such as nutrient availability and the allochthonous supply of diazotrophs of riverine origin (Blais et al., 2012; Fernández-Méndez et al., 2016).

Despite the high dynamic nature of diazotroph communities (Robidart et al., 2014), few studies have focused on their temporal variability in response to hydrographic and environmental changes (e.g. Church et al., 2009; Messer et al., 2015b). Therefore, the factors controlling the diversity, abundance and N_2-fixing activity of diazotrophs are not well defined (e.g. Church et al., 2008; Luo et al., 2014; Moisander et al., 2010; Monteiro et al., 2011; Moore et al., 2009). Furthermore, most studies have been conducted in the warm waters of the (sub)tropical region of the western basin of the North Atlantic Ocean (80º–40ºW), where *Trichodesmium* dominates the community (Benavides and Voss, 2015; Luo et al., 2012; Martínez-Pérez et al., 2016). Hence, little is known about the temporal and spatial distribution of the diazotroph community in temperate (>40º of latitude) cooler waters such as the nutrient-rich northwest Iberian upwelling system.

The upwelling region of the northwestern Iberian Peninsula is one of the eastern boundary upwelling ecosystems in the global ocean (Arístegui et al., 2009). It is seasonally influenced by wind-driven upwelling (from April to September) and downwelling (from October to March) events (Fraga, 1981; Wooster et al., 1976). The frequent nutrient inputs, along with their amplification due to remineralisation inside the rías (Álvarez-Salgado et al., 2002; Bode et al., 1996), fuel the primary production sustaining a rich marine ecosystem (Fraga, 1981; Varela, 1992). Therefore, in this system, high frequency

variability dominates physical, chemical and biological factors (Casas et al., 1997; Gilcoto et al., 2017; Villamaña et al., 2017). Knowledge of the presence and activity of diazotrophs in this N-rich temperate region has been limited to the observation carried out in summer 2009 by Agawin et al. (2014) and Benavides et al. (2011), who described relatively low BNF rates, mainly attributed to UCYN-A.

Herein, we extend the findings reported in Chapter 3 by describing the diazotroph community diversity (based on the nitrogenase gene, *nifH*) in the upwelling region off northwestern Iberia between February 2014 and December 2015. Our main goal was to investigate, for the first time in productive waters of an upwelling region, the temporal and vertical variability of the diazotroph community diversity, and its relationship with the hydrodynamic forcing.

4.2. Materials and Methods

4.2.1 Hydrographic and environmental sampling

Between February 2014 and December 2015, within the framework of the NICANOR (Nitrogen fixation and diffusive fluxes in the NW Iberian Peninsula) project, nine one-day samplings were carried out on board B/O Lura at station 2 (43.42° N, 8.44° W; depth = 80 m) of the RADIALES time-series project (www.seriestemporales-ieo.net). This station is located in the adjacent shelf off Ría de A Coruña (Golfo Ártabro, NW Iberian Peninsula). On each sampling day, profiles of temperature, salinity and fluorescence were obtained with a CTD (Conductivity-Temperature-Depth) probe SBE25plus (SeaBird Electronics) attached to a rosette of Niskin bottles. Water samples were collected for the determination of inorganic nutrients (NO_3^- and PO_4^{3-}), biological N_2 fixation, as well as DNA extraction. In 7 out of the 9 surveys, measurements of dissipation rates of turbulent kinetic energy were conducted using a microstructure turbulence profiler (MSS, Prandke and Stips, 1998).

The sampling dates were selected to cover contrasting hydrographic conditions in this system over a seasonal cycle, and spanned a period of 20 months. We encountered the main hydrographic features of a temperate coastal region subject to seasonal variability and influenced by upwelling pulses. To simplify the interpretation of the results, we classified the samplings into three hydrographic conditions based on the wind-driven upwelling index (see Figure 3.1 in Chapter 3) and the hydrographic conditions of the water column (see Figure 3.2 in Chapter 3): downwelling, upwelling and relaxation. During downwelling conditions, we sampled winter (February 2014) and autumn (November 2015 and December 2015) mixing, and also a spring transitional period under predominance of downwelling (May 2015). In winter, mixing was characterized by slight haline stratification, whereas in autumn thermohaline mixing dominated. In May 2014, April 2015, and June 2015 we sampled spring-summer upwelling, characterised mainly by enhanced phytoplankton biomass. Relaxation conditions included two summer cruises (July 2015 and September 2015), characterized by the transition between intense upwelling and downwelling events during the summer thermal stratification period. Hydrographic features are described in detail in Chapter 3.

4.2.2. DNA Samples Collection and Extraction

During all samplings except February 2014, when only the sample at 0 m was collected, seawater samples for DNA were collected at 0, 20, 40 and 70 m depth, transferred to acid-cleaned carboys using acid-washed silicone tubes and kept in darkness until further processing in the laboratory. Microbial biomass was collected by filtering 7.5-10 L of seawater through a 0.22 µm Sterivex™ filter unit (Millipore) using a peristaltic pump. The filters were preserved with 1.8 mL of lysis buffer (50mM Tris-HCl pH 8.3, 40 mM EDTA pH 8.0, 0.75 M sucrose) and stored at -80 ºC until extraction. DNA was extracted using the PowerWater® DNA Isolation Kit (MO BIO, Laboratories, Inc.), quantified and quality-checked (according to the A_{260}/A_{280} relation) using a spectrophotometer NanoDrop 2000™ (Thermo Fisher Scientific).

4.2.3. *nifH* gene PCR amplification and amplicon sequencing

The *nifH* gene was amplified in a total of 24 DNA samples by nested PCR using 2 sets of degenerate primers (Zehr and McReynolds, 1989; Zehr and Turner, 2001): nifH3 reverse primer (5'-ATR TTR TTN GCN GCR TA-3') and nifH4 forward primer (5'-TTY TAY GGN AAR GGN GG-3'), nifH1 forward primer (5'-TGY GAY CCN AAR GCN GA-3') and nifH2 reverse primer (5'-ADN GCC ATC ATY TCN CC-3'). The volume of the PCR reactions was 20 µL: 1 µL DNA template, forward and reverse primers (final concentration 1 µM), $MgCl_2$ (final concentration 4 mM), dNTPs mix (final concentration 0.2 mM each), Platinum® Taq DNA Polymerase (ThermoFisher Scientific, final concentration 2.5 U), BSA (final concentration 0.4 mg/mL) and PCR grade water. The first round of amplification used nifH3 and nifH4 primers and the following thermocycling conditions: initial DNA denaturation at 95ºC during 4 min, 35 cycles of denaturation at 95ºC (1 min), annealing at 45ºC (1 min) and extension at 72ºC (30 s), followed by a final extension at 72ºC (10 min) and temperature hold at 15ºC. The second round used the nifH1 and nifH2 primer set, 1 µL of PCR product from the first round as template and the following thermocycling conditions: initial denaturation at 95ºC for 4 min, 30 cycles of denaturation at 95ºC (1 min), annealing at 54ºC (1 min) and extension at 72ºC (30 s), followed by a final extension at 72ºC (10 min) and temperature hold at 15ºC. The reactions were run on a T100™ Thermal Cycler (Bio-Rad) at the Instituto Español de Oceanografía (IEO). The amplified products were purified using PCRExtract

Mini Kit (5PRIME) and quantified using a spectrophotometer NanoDrop 2000™ (Thermo Fisher Scientific).

nifH amplicon-based sequencing was performed at the facilities of IMGM Laboratories GmbH (Germany) on the Illumina MiSeq® Next Generation Sequencing technology (Illumina Inc.). Prior to sequencing, an additional PCR amplification with custom barcoded nifH1 and nifH2 primers was carried out using the same thermocycling conditions as previously described. After purification and library preparation from the barcoded PCR products, the paired-end sequencing was performed using the MiSeq® reagent kit with V2 chemistry (500 cycles). The resulting 2x250 base pairs (bp) reads were demultiplexed on the instrument.

4.2.4. Bioinformatics, phylogenetic and statistical analyses

Paired-end reads were merged, selected by length (300-400 bp) and quality filtered (Q20) using the software package PEAR (Zhang et al., 2014). Chimera removal and determination of OTU (Operational Taxonomic Unit) clusters at 92% nucleotide identity were performed by using the usearch 6.1 algorithm (Edgar et al., 2011) in QIIME (Caporaso et al., 2010b). Representative sequences from OTUs with ≥10 read counts were imported into ARB software environment (Ludwig et al., 2004) and translated into amino acid sequences. Non-*nifH* sequences, as well as sequences with stop codons or with frameshift errors were excluded from the analysis. Sequences were aligned to a reference alignment in a curated and updated *nifH* database (Heller et al., 2014) using HMMER algorithm and the Hidden Markov Model profile Fer4_NifH_fs.hmm (Finn et al., 2010). Nucleotide sequences were realigned according to the aligned amino acids in ARB. The phylogenetic affiliation of the translated OTUs into the canonical *nifH* clusters defined by Zehr et al. (2003b) was performed by BLASTx (Camacho et al., 2009) using genome-derived sequences as references from the updated and curated *nifH* database (Heller et al., 2014). We are aware that the relative abundance of phylotypes in the *nifH* Next Generation Sequencing (NGS) library may be influenced by factors such as DNA extraction efficiency, PCR bias (Farnelid et al., 2013; Turk et al., 2011) and presence of contaminants (Goto et al., 2005; Zehr et al., 2003a). In order to test if among our *nifH* sequences there were putative PCR reagent contaminants, we performed a BLASTx comparison between the representative sequences of each OTU and known contaminants

(Heller et al., 2014). To define a putative contaminant we used a conservative cut off (>92% amino acid identity, Farnelid et al., 2010). 24 minor OTUs were considered contaminants and removed from further analysis. A total of 581732 translated amino acid sequences were obtained after quality filtering, which represented 1276 OTUs. We also performed a BLASTn analysis (Camacho et al., 2009) against non-redundant NCBI nucleotide database with the representative sequences of the most abundant OTUs with the objective of identifying and naming them, determining their closest relatives (best BLASTn hit).

A neighbor-joining phylogenetic tree was constructed in ARB using the Kimura correction including the translated amino acid sequences from representative sequences of the most abundant OTUs in the *nifH* NGS library (90 OTUs, >700 sequences each, representing 83.1% of the dataset), as well as their closest relatives (determined via BLASTx). The phylogenetic tree and associated heatmap, which shows the relative abundance during each hydrographic condition for each OTU cluster, were visualized by using the Interactive Tree of Life online tool (iTOL) (Letunic and Bork, 2016). The relative abundances were shown per condition to represent the dominance of each OTU within the contrasting hydrographic regimes.

Data were analyzed and visualized by using the R packages phyloseq 1.20 (McMurdie and Holmes, 2013), vegan 2.4 (Oksanen et al., 2015) and ggcorrplot 3.4.2 (Kassambara, 2016). To allow for cross-sample comparisons, a subsampling to the minimum sequencing depth (9534 sequences) followed by the calculation of relative abundance of each OTU was applied. Chao1 richness estimator (Chao, 1984) and Shannon diversity index (Shannon, 1948) were calculated, and rarefaction curves were generated. Species accumulation curves were built using the Ugland's method (Ugland et al., 2003). A Bray-Curtis dissimilarity distance matrix was computed and visualized by Principal Coordinates Analysis (PCoA) ordination to illustrate differences in diazotroph community structure of the samples. Sample group centroids for each hydrographic condition (downwelling, upwelling and relaxation) and confidence ellipses displaying the standard deviation of centroid locations were also represented on PCoA by using betadisper function in vegan R package. A non-parametric PERMutational ANalysis Of VAriance (PERMANOVA) was conducted on the Bray-Curtis distance matrix using the adonis function in vegan R package. We tested the dependence of the distances between samples (derived from their phylogenetic composition) in relation to the factor

hydrographic conditions. Bonferroni *post hoc* tests were performed to check *nifH* compositional differences between the samples of the hydrographic conditions defined. Similarity percentages and OTUs contributions to the differences between hydrographic conditions were estimated using the similarity percentage method (SIMPER, Clarke, 1993) by simper function in vegan R package. According to SIMPER analysis, the OTUs that contributed most to the compositional differences observed between conditions were fitted through significant (p<0.05) vector overlays onto the PCoA ordination by using envfit function in vegan R package.

Raw sequence files have been submitted to the Sequence Read Archive (SRA) at the National Center for Biotechnology Information (NCBI) under SRA Accession SRP149412.

4.2.5. UCYN-A oligotyping

Oligotyping is a recently described computational method to investigate the diversity of closely related but different microbial organisms, often masked for being clustered into a single OTU, using subtle variations in gene sequences (Eren et al., 2013). This technique allows us to define oligotypes, highly refined taxa based on nucleotide positions with high variability (Shannon entropy). We have used this approach, adapted by Turk-Kubo et al. (2017), to investigate the UCYN-A diversity and define oligotypes. UCYN-A *nifH* sequences were retrieved from the quality filtered and chimera checked whole *nifH* library at 97% of OTU clustering. A total of 100686 UCYN-A *nifH* sequences were obtained and grouped into 53333 unique sequences (100% nucleotide sequence identity) by using the usearch 6.1 algorithm (Edgar et al., 2011) in QIIME (Caporaso et al., 2010b). All sequences but singletons were imported into ARB (Ludwig et al., 2004), where non-*nifH* sequences, with stop codons or with frameshift errors were removed. Sequences that passed all quality controls (96712 out of 100686) were aligned to a reference alignment in a curated and updated *nifH* database (Heller et al., 2014) using PyNAST tool (Caporaso et al., 2010a). Primer regions were trimmed in the Galaxy platform (Afgan et al., 2016). Shannon entropy analysis (Figure S6.1) and oligotyping were carried out by using the oligotyping pipeline version 2.1 (Eren et al., 2013). As described by Turk-Kubo et al. (2017), 13 nucleotide positions with the highest Shannon entropy were chosen to define oligotypes (42, 48, 75, 78, 93, 99, 102, 147, 150, 218, 244, 247, 265). To reduce noise,

each oligotype had to: (1) be present in at least one sample, (2) represent more than 0.1% of the reads for at least one sample, and (3) have a most abundant unique sequence with a minimum sequence count of 10. One sample (May 2014, 40 m) was removed from the analysis because it lacked UCYN-A oligotypes after quality filtering. UCYN-A sequences were not detected in the samples from the 70 m depth from May and June 2015. The total purity score of the analysis was 0.40. UCYN-A oligotype distribution data were also analyzed and visualized using the R package phyloseq 1.20 (McMurdie and Holmes, 2013). A subsampling was performed by (a) removing samples that had less than 100 total sequences (16 out of 21 samples remained), and (b) removing oligotypes with <100 sequence counts (26 out of 47 oligotypes remained distributed in 16 samples). A transformation to even sequencing depth was performed, followed by the calculation of a Bray-Curtis dissimilarity distance matrix between the UCYN-A oligotypes detected. Bray-Curtis ecological distances were visualized by Principal Coordinates Analysis (PCoA) according to the UCYN-A sublineages present. Oligotypes were assigned to UCYN-A sublineages, which are defined as in Thompson et al. (2014), Farnelid et al. (2016) and Turk-Kubo et al. (2017).

4.3. Results

4.3.1. Diazotroph community diversity and composition

A total of 581732 *nifH* sequences were obtained, which clustered into 1276 OTUs at 92% nucleotide identity. The total number of sequences per sample ranged from 9534 in May 2014 (40 m) to 49612 in July 2015 (0 m) (Table S6.2). However, a subsampling to the minimum sequencing depth (9534 sequences) was done to allow for beta diversity comparisons between samples. Rarefaction (Figure 4.1) and species accumulation (Figure 4.2) curves, as well as the small differences found between the Chao1 richness estimator and the number of OTUs observed (Figure 4.3), suggest that the sampling effort (number of sequences sampled) and the *nifH* library obtained were appropriate to cover and reliably characterize the overall *nifH* diversity in the region.

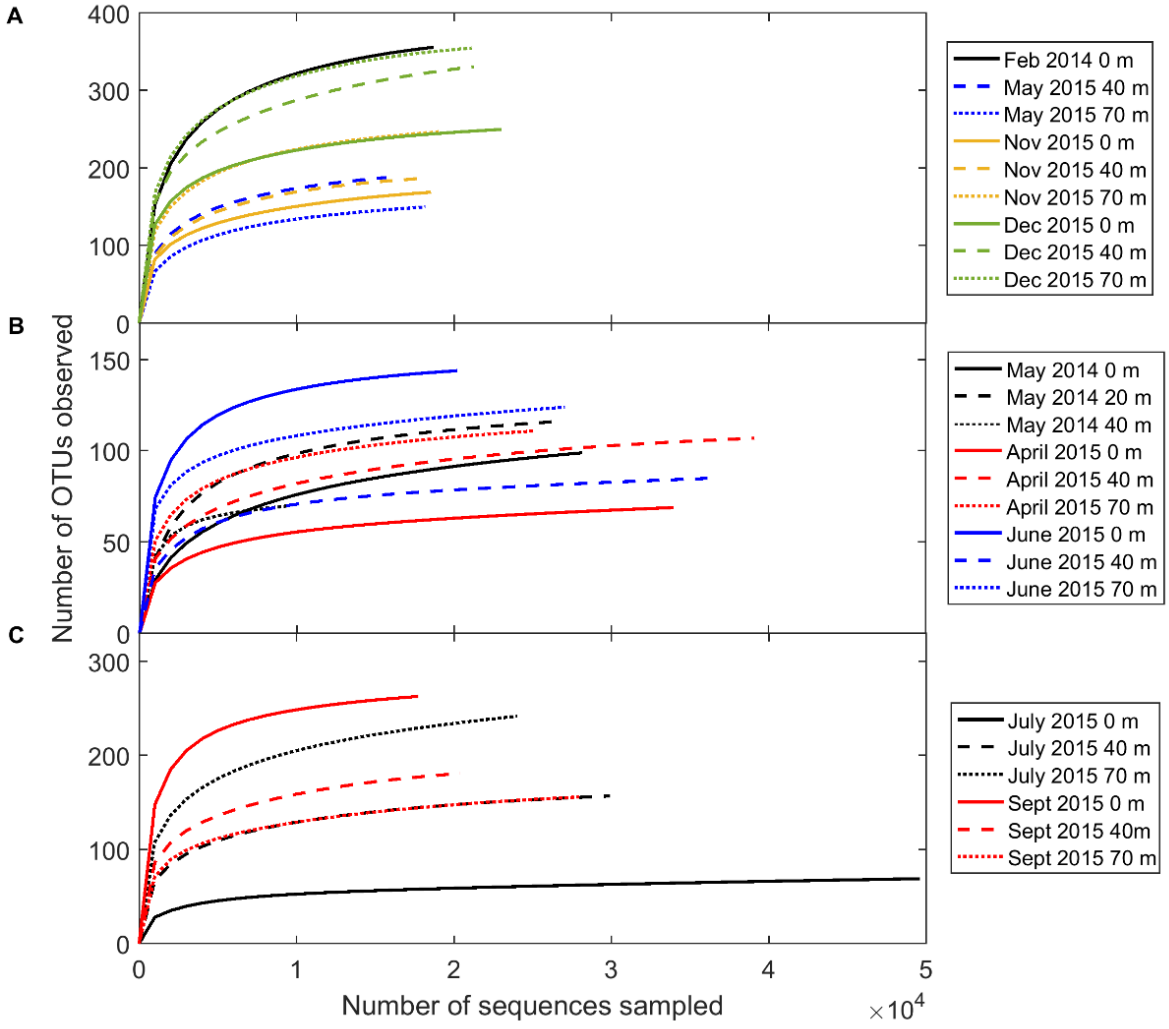

Figure 4.1. *Rarefaction curves of all samples during* ***(A)*** *downwelling,* ***(B)*** *upwelling, and* ***(C)*** *relaxation conditions based on the number of observed OTUs clustered at 92% nucleotide identity cut-off.*

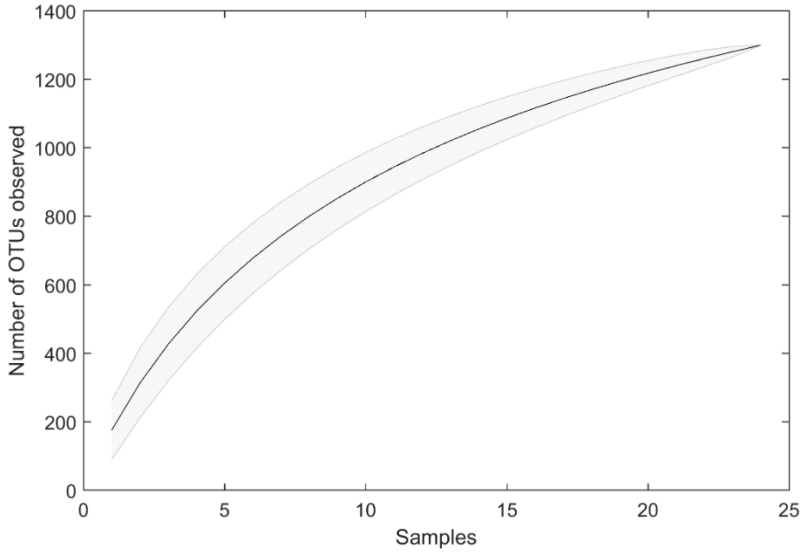

Figure 4.2. *Species accumulation curve constructed using the Ugland´s method (Ugland et al., 2003). Number of OTUs observed clustered at 92% nucleotide identity for the 24* nifH *DNA samples collected in the region. Shaded area represents standard deviation.*

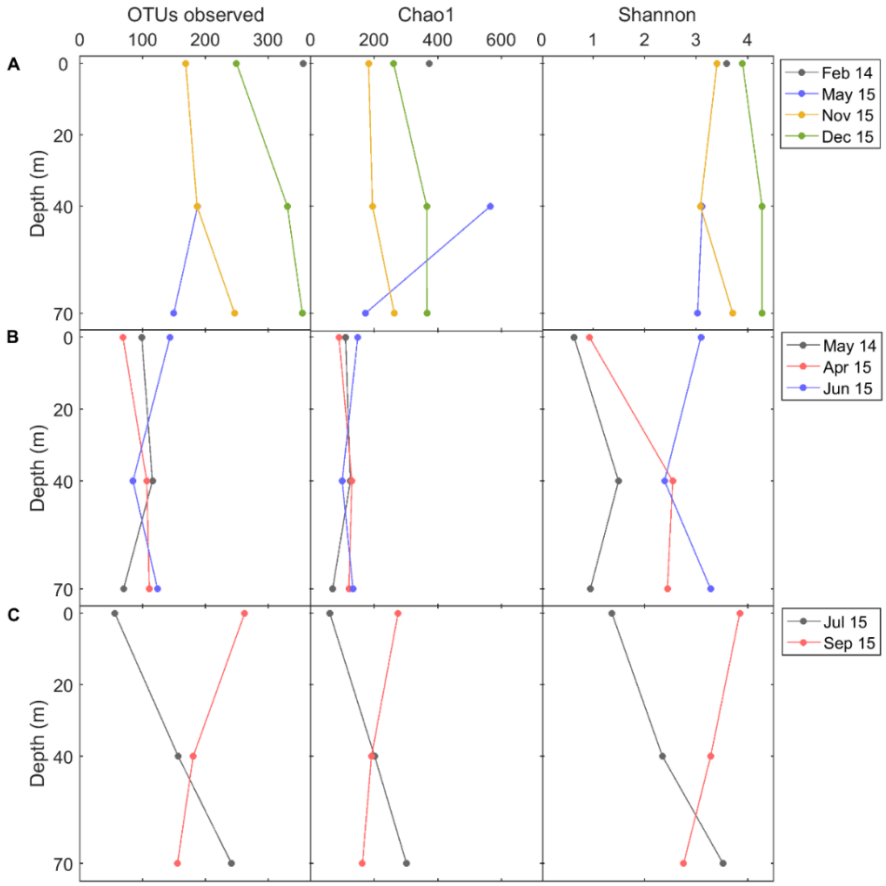

Figure 4.3. *Number of OTUs observed, Chao1 richness estimator (Chao, 1984), and Shannon diversity index (Shannon, 1948) at 92% nucleotide identity for subsamples (9534 sequences each) during* ***(A)*** *downwelling,* ***(B)*** *upwelling, and* ***(C)*** *relaxation conditions.*

Overall, the *nifH* analysis revealed that all sequences belonged to non-cyanobacterial and unicellular cyanobacterial diazotrophs. The most abundant *nifH* clusters were 3 (mainly putative anaerobes, 664 OTUs), 1G (which is comprised of mainly Gammaproteobacteria, 285 OTUs) and 1B (Cyanobacteria, 74 OTUs), which represented 36%, 28% and 21% of total sequences, respectively. We compared by BLASTn (Camacho et al., 2009) the representative sequences of Gammaproteobacterial OTUs with the sequence of the globally distributed Gammaproteobacteria-affiliated phylotype γ-24774A11 (EU052413 accession number; Moisander et al., 2008), which was quantified in these samples by using qPCR (see Chapter 3). However, we did not recover this sequence type, and Gammaproteobacterial OTUs were at most 80-82% similar at the nucleotide level. This decoupling could be due to qPCR analysis is a more accurate method targeting the γ-24774A11 phylotype than nested PCR because of using specific primers and probe or that the qPCR assay used maybe targeted other similar sequence types. The other *nifH* clusters, including 253 OTUs, each accounted for less than 8% of the total relative abundance. The diazotroph community composition in this region was uneven since few OTUs dominated (Figure 4.4).

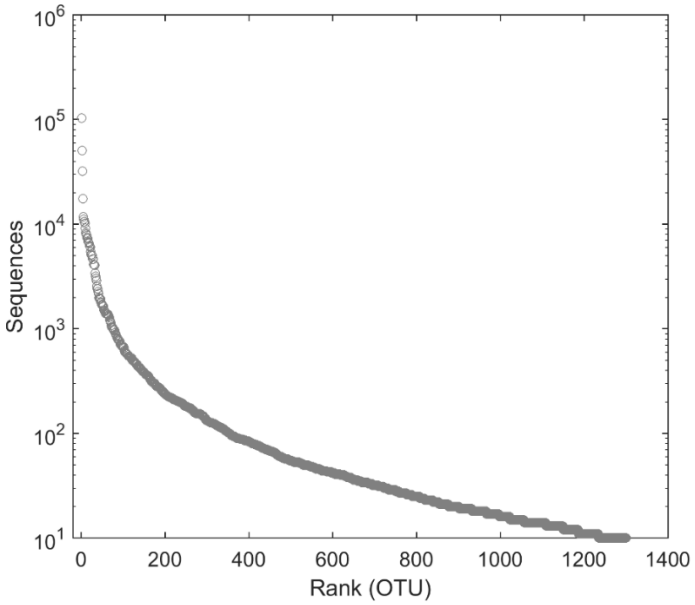

Figure 4.4. *Evenness of the OTUs distribution in the* nifH *library. Number of sequences for each OTU at 92% of nucleotide identity.*

Most *nifH* sequences belonged to OTUs affiliated with subcluster 1G, in particular with *Pseudomonas stutzeri* (Genbank accession number CP002622) as the closest cultivated relative (21% of total sequences clustered mainly in 10 OTUs, with 93-96% nucleotide identity to *P. stutzeri*), UCYN-A (subcluster 1B, 21% of total sequences clustered mostly in OTUs 0, 2854 and 338 with 100% identity to CP001842), *Opitutaceae* bacterium (cluster 3, 9% of total sequences clustered principally in OTU 1 with 94% identity to CP007053) and *Desulfovibrio aespoeensis* (cluster 3, 8% of total sequences clustered mainly in OTU 2 with 95% identity to CP002431), whereas the rest of diazotrophs represented <7% each.

We used the 90 most abundant OTUs, which accounted for 83.1% of the *nifH* sequences, to construct the phylogenetic tree of the diazotroph community present in the region (Figure 4.5). Most OTUs included in the tree (a total of 82 OTUs) belonged to *nifH* subclusters from non-cyanobacterial diazotrophs. However, although cyanobacterial OTUs were less diverse (subcluster 1B, 8 OTUs), they were very abundant, comprising a large number of sequences. Branches of cyanobacterial OTUs belonged mostly to UCYN-A, except OTU 46 which was related to *Nostoc punctiforme* (92% nucleotide identity to the best blast hit with Genbank accession number CP001037) and was only detected in surface waters during the upwelling conditions sampled in June 2015. UCYN-A OTUs were mainly represented by OTU 0 with 100% identity to CP001842. But they also included 4 UCYN-A1 OTUs (OTUs 2687, 2854, 338 and 3675), OTU 2743 and OTU 2604 with 100%, 94% and 92% identity to CP001842, respectively. OTU 0 was by far the most abundant OTU, representing 18% of the *nifH* library. OTUs affiliated with subcluster 1G were related mostly to *P. stutzeri* (92-96% identity to CP002622). OTU 1 (related with *Opitutaceae* bacterium), OTU 2 (related to *Desulfovibrio aespoeensis*) and OTU 24 (related with *P. stutzeri*) were the most abundant non-cyanobacterial OTUs, accounting for 9%, 6% and 3% of total *nifH* sequences, respectively.

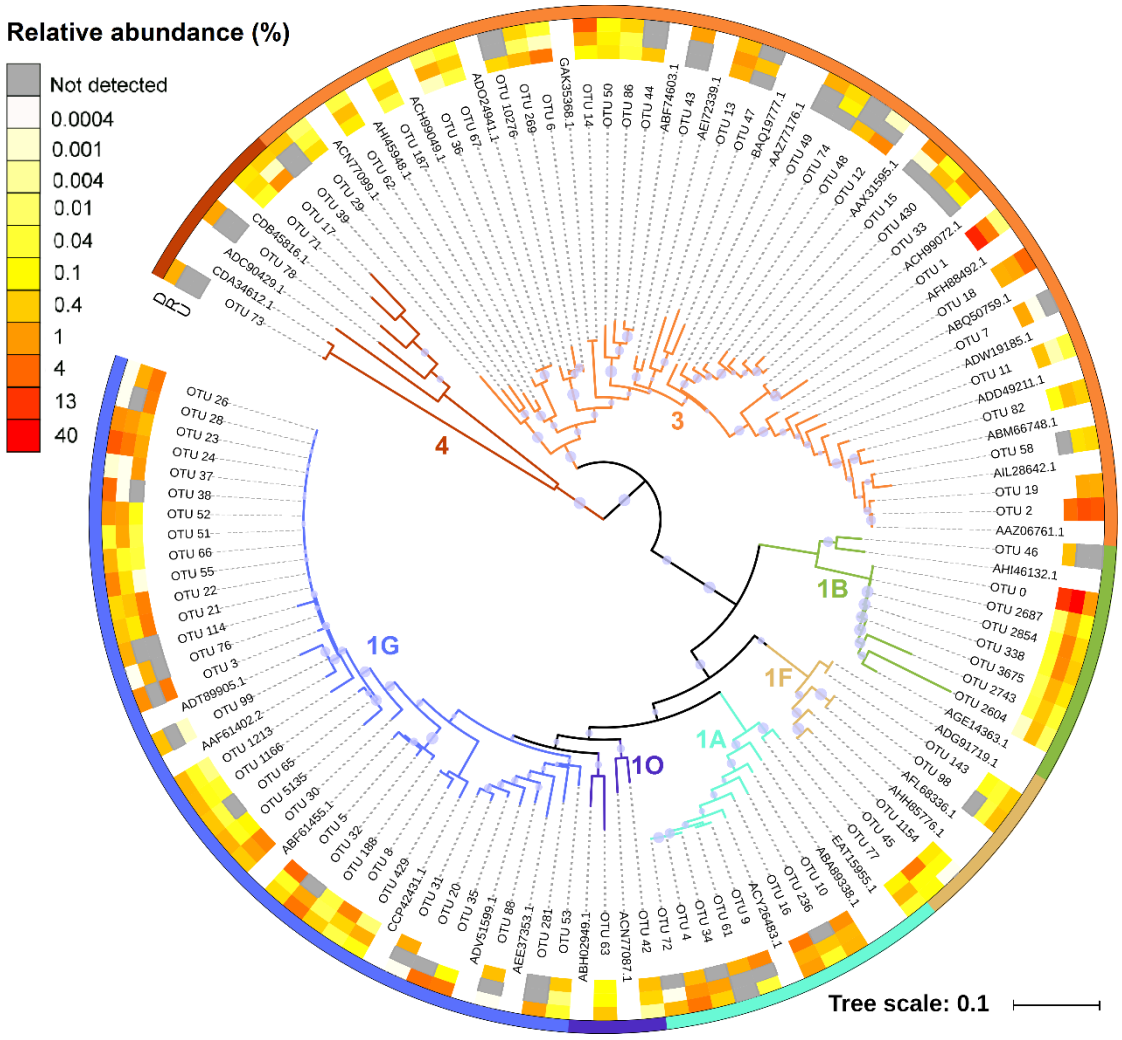

Figure 4.5. *Neighbor-joining phylogenetic tree of the 90 most abundant OTUs in the NGS library (>700 sequences each, representing 83.1% of the dataset) at 92% translated amino acid* nifH *sequence identity and their closest cultivated relatives (based on BLASTx). Canonical* nifH *clusters affiliation according to the convention defined by Zehr et al. (2003a) are indicated by coloured branches and external strip. The heatmap associated shows the relative abundance in different conditions (D, downwelling; U, upwelling; and R, relaxation) for each OTU, in which grey colour indicates no sequences detected within the OTU cluster. Accession numbers for reference sequences are indicated on the tree. Bootstrap values (1000 replicate trees) are displayed with size proportional grey circles.*

4.3.2. Temporal and vertical variability of the diazotroph community

Diazotroph community composition in this region exhibited temporal and vertical variability (Figure 4.6). At all depths during downwelling, diazotroph communities were dominated (based on relative abundance) by non-cyanobacterial diazotrophs. This group was mostly represented by *nifH* subcluster 1G (Gammaproteobacteria) (always >25%), mainly *P. stutzeri*-like sequences from OTU 24, and cluster 3 (putative anaerobes) (always >12%). In any case, no OTU dominated clearly, leading to the high *nifH* diversity observed during this hydrographic regime. During downwelling conditions, the mean number of OTUs observed (248±82 OTUs), Chao1 richness (306±127 OTUs) and Shannon diversity (3.6±0.5) were significantly higher (Bonferroni comparisons, $p<0.05$) than during upwelling (103±25 OTUs, 115±25 OTUs and 2.0±1.0, respectively), and slightly higher than during relaxation (176±74 OTUs, 200±86 OTUs and 2.9±0.9, respectively) (Figure 4.3).

In general, upwelling conditions were also dominated by non-cyanobacterial diazotrophs from subclusters 1G, mainly *P. stutzeri*-like sequences, and cluster 3 (putative anaerobes). The only exception were the surface samples of April and June 2015, where Cyanobacteria, represented mostly by UCYN-A of OTU 0, had high relative abundances (83% and 26%, respectively). Upwelling samples from May 2014 reflected a large divergence in their composition. They were characterized by a clear predominance (always >54%) of OTU 1, which are associated with cluster 3, mainly *Opitutaceae* bacterium-like taxa, which were almost absent in the rest of samples.

All depths during relaxation were characterized by increased relative abundance of subcluster 1B (Cyanobacteria) (ranging from 12% to 91%), mainly UCYN-A sequences clustered in OTU 0. Non-cyanobacterial diazotrophs were represented mostly by cluster 3 (*Desulfovibrio*-like sequences clustered mainly in OTU 2) and 1G (Gammaproteobacteria). After OTU 0, OTU 2 was the most relevant cluster during relaxation.

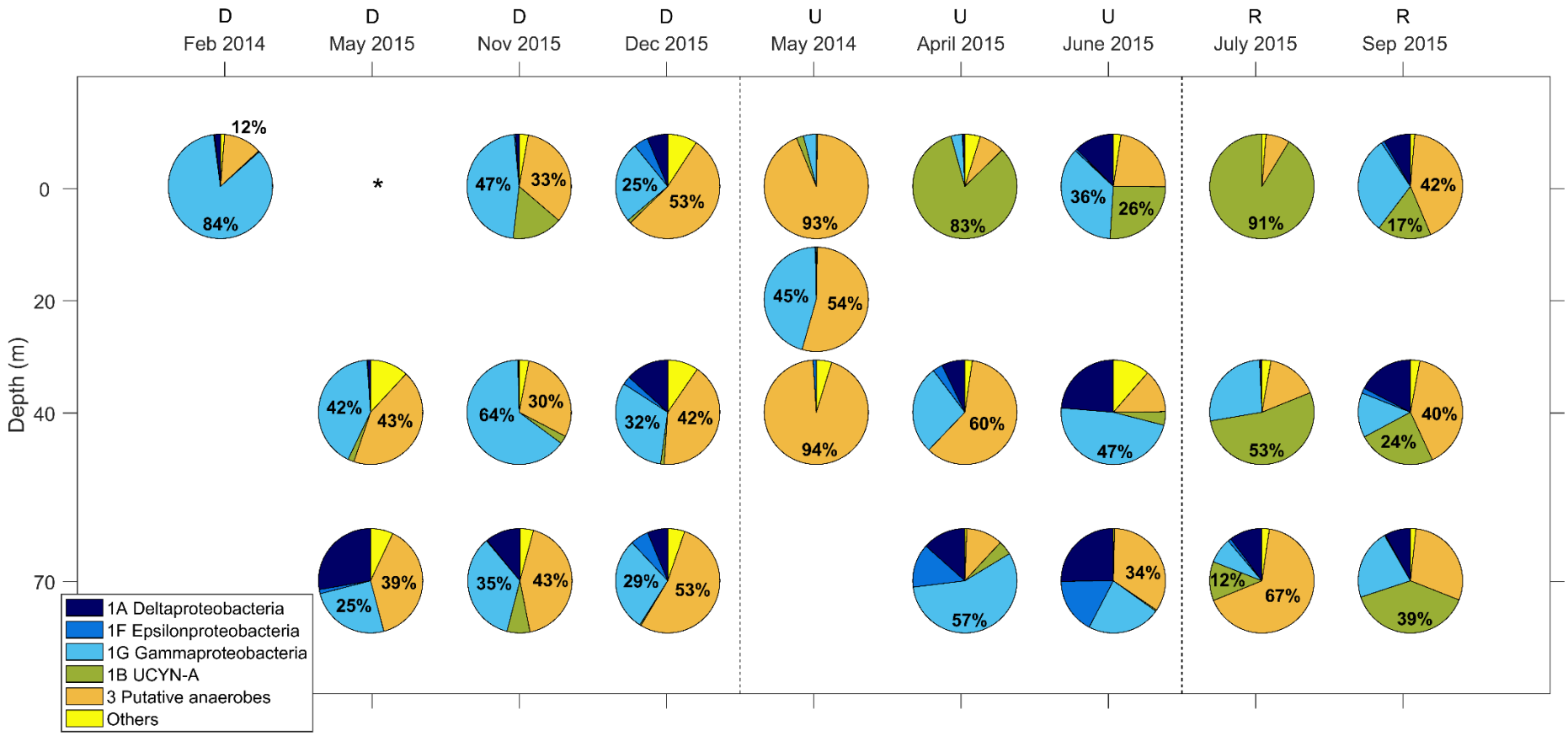

Figure 4.6. *Distribution of the most abundant* nifH *clusters in the NGS library (representing >2% of total* nifH *sequences). Phylogenetic assignments of the clusters are also indicated. 'Others' includes mainly* nifH *cluster 4. Upper characters indicate the hydrographic condition during each sampling date (D, downwelling; U, upwelling; and R, relaxation).* nifH *gene was not detected by PCR amplification in the sample from May 2015 (0 m) (indicated by asterisk). Number of sequences obtained per sample after quality filtering are shown in Table S6.2.*

The temporal variability observed in the composition of the diazotrophic community is illustrated by the Principal Coordinates Analysis (PCoA) (Figure 4.7) based on Bray-Curtis dissimilarities (Table S6.3). A higher phylogenetic similarity was observed in the samples collected during downwelling compared to upwelling and relaxation, which exhibited larger variation in their composition, mainly during upwelling, when a higher vertical variability was observed. During downwelling, the water column was characterized by homogeneous conditions and deep mixed layers. Upwelling and relaxation periods were characterized by relatively enhanced vertical stratification and a larger vertical variability in hydrographic conditions. Significant differences in *nifH* composition were observed between the three hydrographic conditions (PERMANOVA, $p<0.001$). Specifically, community composition during downwelling was significantly different from those observed during upwelling and relaxation (Bonferroni comparisons, $p<0.05$), whereas no significant differences were observed between upwelling and relaxation. As revealed by the SIMPER analysis, the compositional differences observed were mainly due to the relative contribution of the most abundant OTUs: OTU 0 (explained between 7% and 20% of variability, UCYN-A), OTU 1 (11-12%, *Opitutaceae* bacterium-like taxa), OTU 2 (3-4%, *Desulfovibrio aespoeensis*-like taxa) and OTU 24 (~3%, *P. stutzeri*-like taxa). OTU 0 correlated significantly ($r^2=0.906$, $p<0.001$), as indicated by the direction and length of its vector overlay onto PCoA, with the samples collected in relaxation and surface samples of April and June 2015 (upwelling), which were characterized by the predominance of this cluster (Figure 4.6). Vector overlay of OTU 1 showed a strong correlation ($r^2=0.859$, $p<0.001$) with the upwelling samples from May 2014 (located in upper left corner of PCoA), which were dominated by this putative anaerobe cluster. OTU 2 was a relevant cluster both in downwelling and relaxation, as shown by its vector ($r^2=0.286$, $p<0.05$). Finally, OTU 24 was very abundant in downwelling but it was also present in upwelling and relaxation samples. Thus, the correlation of its vector with downwelling samples was weaker ($r^2=0.088$, $p<0.05$).

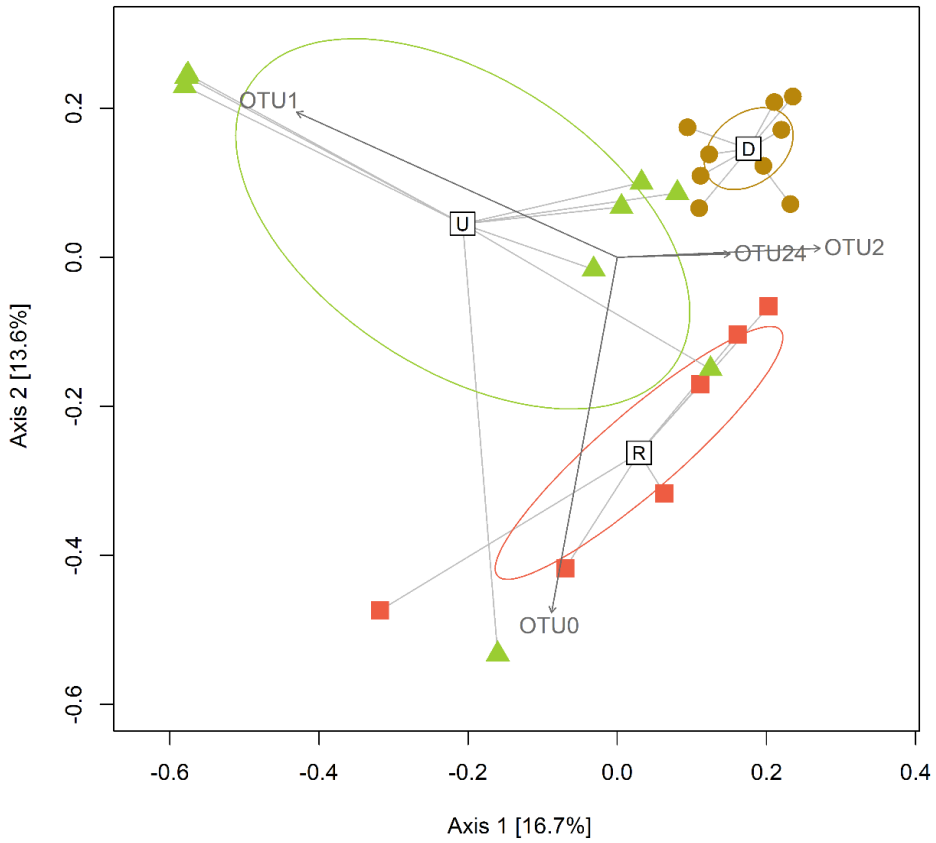

Figure 4.7. *Principal Coordinates Analysis (PCoA) based on Bray-Curtis dissimilarity distance matrix illustrating the* nifH *compositional differences between samples from downwelling (brown circles), upwelling (green triangles) and relaxation (red squares). Sample group centroids for each hydrographic condition and confidence ellipses displaying the standard deviation of centroid locations are also represented. According to SIMPER analysis, the OTUs that contributed most to the compositional differences observed between hydrographic conditions were fitted through significant ($p<0.05$) vector overlays onto the PCoA ordination. OTU 0 (UCYN-A, 100% nucleotide identity to Genbank accession number CP001842), OTU 1 (cluster 3,* Opitutaceae *bacterium-like taxa, 94% identity to CP007053), OTU 2 (cluster 3,* Desulfovibrio aespoeensis*-like, 95% identity to CP002431), and OTU 24 (subcluster 1G,* Pseudomonas stutzeri*-like, 94% identity to CP002622).*

4.3.3. UCYN-A oligotypes

Oligotyping analysis resulted in 47 UCYN-A oligotypes, which represented 95163 reads, accounting for 98.4% of all reads analyzed. Fourteen new oligotypes were defined (oligo103–116). Most oligotypes were phylogenetically affiliated with the sublineages UCYN-A2 (19 out of 47; 70785 sequences or 74.4% of data set) and UCYN-A1 (21 out of 47 oligotypes; 22305 sequences or 23.4% of data set) (Figure 4.8, Table S6.4). Four oligotypes (oligo4, 104, 108, 113; 1895 sequences or 2.0% of data set) clustered with the

UCYN-A4 sublineage defined by Farnelid et al. (2016). The remaining three oligotypes (oligo99, 109, 114; 178 sequences) did not fall into the sublineages defined to date (Turk-Kubo et al., 2017). However, because they are low in frequency (<80 read counts each), we have not created new clusters for them. All but nine minor oligotypes (oligo6, 11, 36, 37, 85, 104, 109, 111, 114) met the criteria of "convergence" since further decomposition of the oligotypes did not improve the resolution of beta diversity (Eren et al., 2013).

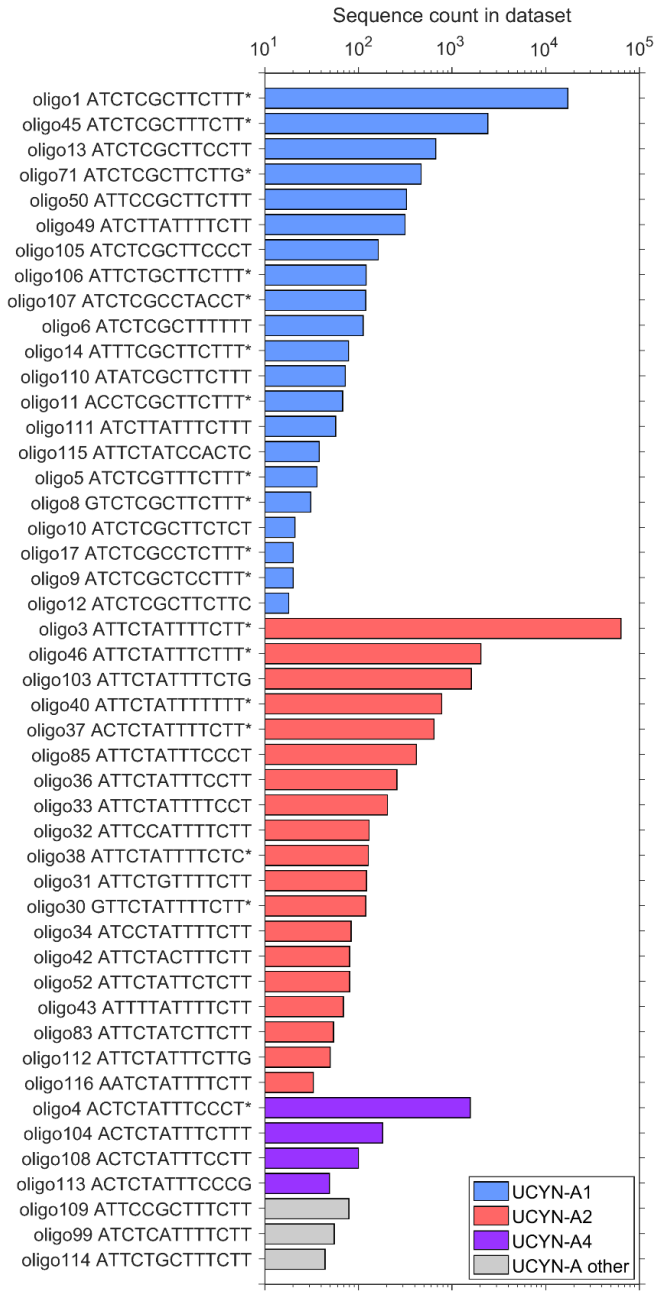

Figure 4.8. *Sequence counts for the 47 UCYN-A oligotypes. Oligotype designation and nucleotide present in each of the 13 high entropy positions are listed. Oligotypes (18 out of 47) with representative sequences that have 100% nucleotide identity to sequences submitted to NCBI's GenBank database are marked with*

an asterisk (*). 'UCYN-A other' includes oligotypes that did not fall into defined sublineages (Turk-Kubo et al., 2017). x axis in logarithmic scale.

The UCYN-A *nifH* sequences were by far dominated by oligo3, which is affiliated with the UCYN-A2 sublineage (63905 sequences; 67.2% of data set), and oligo1 affiliated to UCYN-A1 (17152 sequences; 18.0% of data set) (Figure 4.8, Table S6.4). The remaining oligotypes were always less than 2.5% of the library. Oligo3 was 90.3% of the UCYN-A2 oligotypes and accounted for over 50% of the sequences recovered in 17 out of the 21 total samples analyzed (Figure 4.9). Oligo1, the second most abundant oligotype, represented 76.9% of the UCYN-A1 oligotypes and was detected in 12 out of 21 samples at relative abundances ranging from 4% to 96%. On average, oligo3 represented 64±36% of the relative abundances of oligotypes in the samples, whereas oligo1 comprised 26±37%. Oligo1 differs from oligo3 in 7 out of 13 entropy positions.

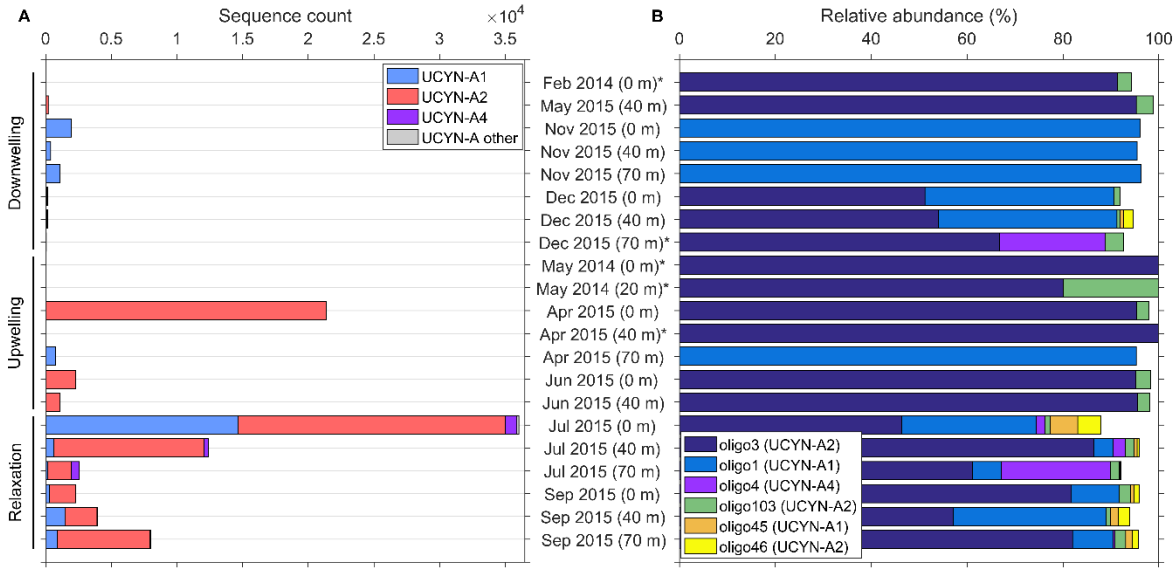

Figure 4.9. *Distribution of UCYN-A sublineages and oligotypes.* ***(A)*** *Number of sequences of UCYN-A oligotypes classified by sublineage, and* ***(B)*** *relative abundance of the six most abundant oligotypes. 'UCYN-A other' includes oligotypes that did not fall into the defined sublineages (Turk-Kubo et al., 2017). Subsampling as indicated in Materials and Methods was not applied in this figure. Samples marked with an asterisk (*) have <100 sequences.*

In general under the different hydrographic regimes the oligotype composition was dominated by UCYN-A2, mainly represented by oligo3, reaching the highest sequence absolute abundances during upwelling and relaxation (Figure 4.9). Notable exceptions to this include samples from November 2015 (downwelling), and from 70 m depth in April

2015 (upwelling). In these samples, the oligotype composition was dominated by UCYN-A1, mainly represented by oligo1, reaching >95% of relative abundances. During relaxation conditions, UCYN-A1, mostly oligo1, was also present making up lower relative abundances (4-32%). In general, a larger diversity of oligotypes was found during relaxation since minor oligotypes as oligo4 (UCYN-A4), oligo45 (UCYN-A1), oligo46 (UCYN-A2) and oligo103 (UCYN-A2), were also present in these samples (Table S6.4). UCYN-A4 oligotypes, mostly oligo4, appeared only at relatively high frequencies in July 2015 (relaxation), representing 2-23% of relative abundance, when UCYN-A2 dominated the oligotype composition. Whereas UCYN-A1 was detected at relatively low frequencies in samples collected at the three hydrographic conditions, UCYN-A2 exhibited higher abundances during upwelling and relaxation. This pattern determines the contrasting locations of their most abundant oligotypes (oligo1 and oligo3, respectively) on the PCoA ordination based on the Bray-Curtis ecological distance between oligotypes from the UCYN-A *nifH* amplicon library (Figure 4.10).

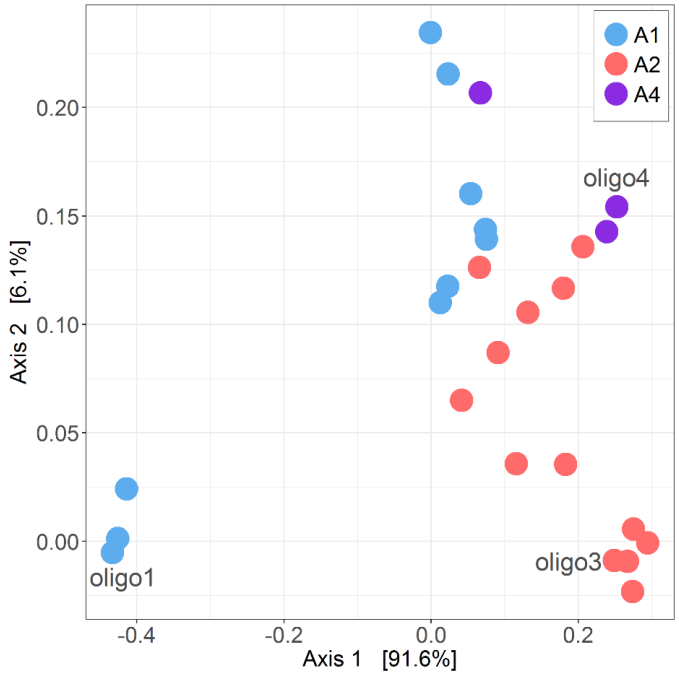

Figure 4.10. *Principal Coordinate Analysis (PCoA) illustrating the Bray-Curtis dissimilarity between UCYN-A oligotypes, which are coloured according to their sublineage (UCYN-A1, -A2 or -A4). The most abundant oligotypes of the data set, oligo1, oligo3 and oligo4 are indicated. Data set was transformed to even sampling depth after subsampling as described in Materials and Methods.*

4.4. Discussion

4.4.1. Composition and temporal variability of the diazotroph community

Our findings indicate that the diazotroph community composition in the coastal shelf region on the NW Iberian Peninsula was dominated by UCYN-A and *P. stutzeri*-like taxa (1G). These results support prior reports indicating that the UCYN-A–prymnesiophyte symbiosis is present in these relatively cold (<17ºC) and N-rich waters of the eastern basin of the North Atlantic. Agawin et al. (2014) reported the dominance of UCYN-A in the same region during a single observation in summer 2009, but in this case UCYN-A represented 95% of *nifH* sequences recovered. Furthermore, UCYN-A were also the most representative cyanobacterial diazotrophs detected by Rees et al. (2009) in the temperate waters of the Western English Channel in summer 2006. The relevance of UCYN-A was also reported in the (sub)tropical region of the NE Atlantic (e.g. Goebel et al., 2010; Langlois et al., 2005, 2008; Martínez-Pérez et al., 2016; Turk et al., 2011), where regular iron inputs by Saharan dust (Benavides et al., 2013b) promote its growth and N_2-fixing activity (Krupke et al., 2015). Similarly, UCYN-A dominated the diazotroph community, together with Proteobacteria, in the N-rich temperate NE American coast of the western basin (Mulholland et al., 2012).

Non-cyanobacterial diazotrophs, mainly from subcluster 1G (Gammaproteobacteria) and cluster 3 (putative anaerobes) are also present in these waters. Non-cyanobacterial *nifH* sequence types (mainly affiliated with clusters 1G and 1J/1K) have been reported at high relative abundances in diverse marine environments, such as the (sub)tropical South Pacific Ocean (Halm et al., 2012; Moisander et al., 2014b), the central Baltic Sea (Farnelid et al., 2013), the upwelling system of central Chile (35ºS–38.5ºS) (Fernández et al., 2015) or the N-depleted Central Arctic Ocean (Fernández-Méndez et al., 2016). Farnelid et al. (2011) showed the dominance of *nifH* cluster 1 related to Proteobacteria in surface waters of the global ocean, even in the (sub)tropical regions preferred by cyanobacteria (Zehr, 2011), as well as the preponderance of the anaerobic bacteria of cluster 3 in the cold waters (<12ºC) of the Chilean upwelling system. Farnelid et al. (2013) also reported high relative abundances of *nifH* genes related to the cluster 3 in the Baltic Sea. It has been suggested that these facultative anaerobic diazotrophs can thrive attached to particles (Church et al., 2005; Riemann et al., 2010), free-living in the oxygenated water column (Church et al., 2005; Farnelid et al., 2011) or even associated with zooplankton (Braun et al., 1999). Therefore, non-cyanobacterial diazotrophs such as

heterotrophic bacteria and archaea could occupy a wider geographical range than photosynthetic cyanobacteria, and a larger pelagic realm since they are not constrained by light (Bombar et al., 2016; Delmont et al., 2018; Moisander et al., 2017).

Our findings showed an important temporal variability in the diazotroph community composition. Overall, during downwelling, characterized by deeper mixed layers and homogeneous hydrographic conditions, the diazotroph community composition exhibited lower temporal and vertical variability and higher diversity, being mainly dominated by non-cyanobacterial diazotrophs from subcluster 1G (Gammaproteobacteria, mainly related to *P. stutzeri*) and cluster 3. Whereas during upwelling and relaxation conditions, affected by enhanced vertical stratification and larger vertical variability in the hydrographic conditions, a similar contribution of a few taxa of both non-cyanobacterial diazotrophs (Gammaproteobacteria of subcluster 1G and cluster 3) and UCYN-A was observed.

In the case of upwelling, we observed the predominance of non-cyanobacterial diazotrophs from cluster 3, specifically *Opitutaceae* bacterium-like taxa, in May 2014, and of clusters 1G (Gammaproteobacteria) and 3 in April and June 2015. Nevertheless, we found high UCYN-A relative abundances in the well-lit surface waters of these two samplings. The different stage of the upwelling may induce these *nifH* compositional differences between cruises. In April and June 2015 an intense upwelling of subsurface waters occurred just before sampling, cooling and fertilizing the water column, while in May 2014 we found a more stratified and warmer water column due to the progressive weakening of the intense upwelling pulse that occurred one to two weeks before sampling (see Chapter 3). The particular dominance of *Opitutaceae* bacterium-like taxa (cluster 3) observed exclusively in May 2014 could correspond to a specific advanced stage of marine bacterioplankton succession after an intense phytoplankton bloom, since different bacterial populations are specialized in the successive decomposition of organic substrates derived from blooms (Teeling et al., 2012).

The diazotrophic community during summer relaxation condition was characterized by an enhanced contribution of UCYN-A. This observation is consistent with the results obtained by Agawin et al. (2014) in the same region in summer 2009 under comparable hydrographic conditions. Some differences were observed in the samples collected during the two samplings carried out in relaxation (July and September 2015). In July 2015, the relative abundances of UCYN-A (52±40%) were slightly higher than in September 2015

(27±11%). In contrast, UCYN-A1 plus UCYN-A2 absolute abundances, quantified via qPCR (see Chapter 3), were higher in September 2015 than in July 2015, peaking in surface waters in both cruises. Although both samplings were characterized by relatively enhanced vertical stratification, nitrate and phosphate concentrations at deep samples were higher in September 2015, due to the upwelling pulse occurring one week before the sampling (see Chapter 3). The contrasting hydrographic features may have induced the differential *nifH* composition and UCYN-A1 and -A2 absolute abundances observed between the two cruises, as well as the predominance of small phytoplankton cells contributing significantly to both chlorophyll *a* and primary production in September 2015 (see Chapter 3).

The highest relative and absolute abundances of UCYN-A were quantified in stratified surface waters under upwelling and relaxation conditions, coinciding with the highest biological N_2 fixation rates (~0.1 μmol N m^{-3} d^{-1}) measured during this survey (reported in Chapter 3 or Moreira-Coello et al., 2017). In fact, UCYN-A relative and absolute abundances were positively correlated with N_2 fixation rates (Pearson's $r = 0.709$, $p < 0.01$ and $r = 0.534$, $p < 0.05$, respectively), consistent with the fact that small diazotrophs (<10 μm), presumably unicellular, were responsible for the diazotrophic activity in this system. This relationship has also been observed in other regions, such as the NE American coast (Mulholland et al., 2012), or the tropical SW Pacific (Bonnet et al., 2015). Therefore, UCYN-A–prymnesiophyte associations may be the main contributors to the diazotrophic activity in this region, or at least of a large fraction.

To our knowledge, this is the first study reporting temporal variability of the diazotrophic community composition in a temperate upwelling ecosystem, since most phylogenetic studies targeting the *nifH* gene in marine environments are mainly constrained to (sub)tropical regions, and characterized by a limited temporal sampling resolution. Similar to our findings, Messer et al. (2015b) provided evidence of the seasonal shift of diazotroph communities by reporting different assemblages during austral spring (dominance of Cyanobacteria, mainly *Trichodesmium* and UCYN-A) and winter (predominance of Delta- and Gammaproteobacteria) in Australian tropical waters. Church et al. (2009) observed a temporally variable diazotroph assemblage in the North Pacific Subtropical Gyre, dominated by Cyanobacteria (*Trichodesmium* and symbionts of diatoms) in summer, and unicellular diazotrophs (UCYN-A) in late winter and spring. Turk-Kubo et al. (2015) reported the succession of diazotrophs in the Noumea lagoon

(New Caledonia, tropical SW Pacific) over a 23-day period during the austral summer, and Robidart et al. (2014) demonstrated in the North Pacific Subtropical Gyre that diazotroph communities are highly variable, even at short temporal scales of a few days.

Overall, our results indicate that the diazotrophic community present in the NW Iberian upwelling system is very dynamic and responds rapidly to variations of the hydrographic conditions. This is consistent with recent findings reported by Martín-Platero et al. (2018) along the Northeast American coast. These authors reported sharp and rapid fluctuations of microbial planktonic OTUs associated with changes in the environmental conditions, suggesting that the high variability in the hydrographic features could provide short-lived but optimal conditions for the growth of different microbial communities.

4.4.2. Diversity, variability and ecology of UCYN-A sublineages

Our oligotyping analysis indicate that UCYN-A2 was by far the most abundant sublineage (74% of the data set), followed by UCYN-A1 (23%) and UCYN-A4 (2%). These UCYN-A clades were mainly represented by oligo3 (67% of data set), oligo1 (18%) and oligo 4 (2%), respectively. These oligotypes were also among the most abundant in the global UCYN-A *nifH* amplicon library analyzed by Turk-Kubo et al. (2017), although this database was mainly dominated by oligotypes affiliated to the UCYN-A1 sublineage. This UCYN-A1 prevalence observed in the global data set reflects the fact that most sampling sites were located in oligotrophic open ocean regions of the (sub)tropical Pacific and Atlantic.

Our results provide further evidence that the UCYN-A2 sublineage can be found in nutrient-rich coastal waters. Whereas UCYN-A1 was detected at relatively low frequencies in samples from the three hydrographic conditions, UCYN-A2 exhibited higher sequence counts during upwelling and relaxation, consistent with the qPCR results reported in Chapter 3. Interestingly, UCYN-A4 appeared only at relatively high frequencies during relaxation in July 2015, when UCYN-A2 dominated the oligotype composition. These results are consistent with previous findings indicating that the most abundant sublineages, UCYN-A1 and UCYN-A2, are globally distributed (Cabello et al., 2016; Martínez-Pérez et al., 2016) and co-occur frequently in coastal areas (Henke et al., 2018; Messer et al., 2015a; Turk-Kubo et al., 2015, 2017). They are also consistent with previous studies indicating that UCYN-A1 and UCYN-A3 co-occur and dominate in the

(sub)tropical open ocean, whereas UCYN-A2, sometimes co-occurring with UCYN-A4, occupy mainly coastal regions (Messer et al., 2015b, 2015a; Thompson et al., 2014; Turk-Kubo et al., 2017). Even though current data suggest that UCYN-A sublineages and their hosts probably have different physiological needs, they can co-occur within the same environment, indicating that these ecotypes may share under some circumstances a similar niche (Farnelid et al., 2016a; Thompson et al., 2014; Turk-Kubo et al., 2017).

The different global distribution and temporal variability of the closely related UCYN-A1 and -A2 lineages may be due to the adaptation of their respective prymnesiophyte hosts to specific environments, and the fact that they go through different life cycle stages (Hagino et al., 2013). UCYN-A1 and -A2 are associated with two distinct prymnesiophyte partners, an uncultured unicellular prymnesiophyte (1-3 µm) (Thompson et al., 2012) and the larger *Braarudosphaera bigelowii* (4-10 µm) (Cabello et al., 2016; Hagino et al., 2013; Thompson et al., 2014), respectively. The evolutionary divergence of UCYN-A gave rise to different ecotypes (Cornejo-Castillo et al., 2016), which could contribute to their dispersion and growth in contrasting habitats and their ability to overcome environmental changes.

4.5. Conclusions

Our findings show a highly variable diazotroph community shaped by the hydrodynamic forcing of the system, shedding light for the first time on the seasonal dynamics of diazotrophs in upwelling regions. During downwelling, which was characterized by deeper mixed layers and homogeneous hydrographic conditions, the diazotrophic community was vertically more uniform and characterized by the dominance of diverse non-cyanobacterial diazotrophs, mostly from clusters 1G (Gammaproteobacteria) and 3 (putative anaerobes). Upwelling and relaxation periods were characterized by enhanced vertical stratification, a larger vertical variability in the hydrographic features and a diazotrophic composition more heterogeneous. In these conditions, UCYN-A and non-cyanobacterial diazotrophs from cluster 3 and 1G were dominant. Within UCYN-A phylotype, UCYN-A2 sublineage was by far the most abundant, followed by UCYN-A1 and UCYN-A4. These sublineages were mainly represented by the oligotypes oligo3, oligo1 and oligo 4, respectively, among the most abundant in the global UCYN-A *nifH* library (Turk-Kubo et al., 2017). UCYN-A1 was detected at relatively low frequencies in samples collected during the three hydrographic conditions, while UCYN-A2 showed higher abundances during upwelling and relaxation. Overall, the compositional heterogeneity observed in response to the temporal shifts in environmental factors may reflect the transition of ecological niches of specific diazotrophs, since the community comprises a diverse group of organisms with different autoecology and physiological constraints. In the future, design of specific qPCR assays for the most abundant non-cyanobacterial diazotrophs found here will be needed to investigate their ecological relevance. Furthermore, higher temporal resolution approaches focusing on abundance, diversity and expression of *nifH* genes will be required to better understand the role of the short-term variability of the hydrodynamic forcing, occurring at scales of a few days in this region (Gilcoto et al., 2017), in shaping the diazotrophic community.

5.
General discussion and conclusions

5.1. General discussion

The present PhD Thesis contributes to the ecological and biogeochemical characterization of biological N_2 fixation from genes to ecosystem scale in the Galician upwelling region. We have investigated the magnitude, biogeochemical relevance and players of diazotrophic activity under contrasting hydrographic conditions, as well as the consequences of contamination of the $^{15}N_2$ gas stocks used to measure N_2 fixation rates.

5.1.1. Effects of contamination of commercial $^{15}N_2$ stocks on biological N_2 fixation

Our laboratory and field experiments demonstrated that the inorganic ^{15}N-labelled contaminants included in some commercial stocks from Sigma-Aldrich are assimilable by non-diazotrophs organisms, yielding significant ^{15}N-enrichments of the particulate organic nitrogen ($\delta^{15}N \approx 3‰$ in relation to Cambridge-Isotope and control treatments) and resulting in considerable (up to sixteen-fold) overestimations of the biological N_2 fixation rates. Therefore, the estimates of N_2 fixation reported in the literature may be distorted depending on the commercial $^{15}N_2$ source used, especially when using Sigma stocks. In any case, $^{15}N_2$ from Cambridge stocks is commonly used in most of surveys. Furthermore, considering that only one commercial brand (Sigma-Aldrich) of the three analyzed by Dabundo et al. (2014) showed substantial presence of ^{15}N-labelled contaminants, the published rates obtained with $^{15}N_2$ gas from the other two suppliers (Cambridge-Isotope and Campro Scientific) are a priori reliable. Hence, to obtain in the future reliable biological N_2 fixation measurements, it will be advisable to use the commercial stocks presumably free of contaminants according to Dabundo et al. (2014), and to perform purity control tests such as those herein described before using the $^{15}N_2$ lecture bottles acquired.

5.1.2. Magnitude and biogeochemical role of biological N_2 fixation under contrasting hydrographic regimes

Our findings demonstrate a detectable biological N_2 fixation activity (up to 0.1 μmol N m^{-3} d^{-1}) under different hydrographic regimes in a nitrogen-rich temperate coastal region subject to upwelling. The N_2 fixation rates obtained, which peaked at the surface during

both upwelling and relaxation conditions, are comparable to the lower-end of rates described for the subtropical NE Atlantic (Luo et al., 2012), and similar to those measured in the nearby Cape Silleiro (NW Iberian Peninsula) (Benavides et al., 2011b). Despite the relatively low diazotrophic activity, our results are a further evidence that high nitrate concentrations, high N:P ratios and low temperatures (<17ºC) do not suppress N_2 fixation, as also observed in other upwelling regions (e.g., Benavides et al., 2014; Sohm et al., 2011; Subramaniam et al., 2013; Voss et al., 2004; Wen et al., 2017), the coastal shelf of temperate NE America (Mulholland et al., 2012), the English Channel (Rees et al., 2009) or the Arctic Ocean (Shiozaki et al., 2017, 2018). Thus, these findings are contrary to the traditional paradigm about marine N_2 fixation, which assumes that this process is mainly constrained to the nitrogen-poor, warm (>20 ºC) (sub)tropical ocean, since the typical high nitrogen supply and the relatively low surface temperatures in temperate coastal systems would inhibit the activity of filamentous non-heterocystous cyanobacteria such as *Trichodesmium* (Conley et al., 2009; Howarth et al., 1988; Stal, 2009). The evidence of diazotrophy found in previously overlooked environments, together with the wide distribution and large diversity of N_2-fixers (Farnelid et al., 2011; Moisander et al., 2010; Riemann et al., 2010; Zehr et al., 2000, 2003b), indicate that limiting N_2 fixation surveys exclusively to oligotrophic (sub)tropical bands may result in an underestimation of the global magnitude of this flux, contributing to the apparent imbalances observed in the marine N budget (Brandes and Devol, 2002; Codispoti, 2007; Mahaffey et al., 2005; Voss et al., 2013).

From our results, we estimated an average new N input in the NW Iberia (surface area of 3º×3º grid cell) of about 0.4 Gg N yr^{-1} from planktonic N_2 fixation. The supply of new N into the euphotic layer by diazotrophic activity was between 2 and 5 orders of magnitude lower than that from nitrate diffusive fluxes. Therefore, the contribution of N_2 fixation was irrelevant (<2 %) when compared to turbulent diffusion. Likewise, the proportion of gross primary production that could be sustained by diazotrophy, calculated by assuming Redfield stoichiometry, was also negligible (<0.1 %). Our simultaneous estimates of the contribution of N_2 fixation and nitrate vertical diffusion to the input of new nitrogen are the first in a coastal upwelling system. Due to the methodological difficulties to quantify directly vertical mixing (*Kz*) in the field, few studies have concomitantly measured both processes (e.g., Fernández-Castro et al., 2015; Mouriño-Carballido et al., 2011; Painter et al., 2013), motivating the use of constant values of *Kz* (Capone et al., 2005), or empirical

parameterizations (Fernández-Castro et al., 2014; Planas et al., 1999) to estimate nitrogen diffusive fluxes. The biogeochemical relevance of N_2 fixation in this system would be still lower when considering other important new N supplies, such as advective transport due to upwelling (Pitcher et al., 2010), lateral transport (Torres-Valdés et al., 2009; Williams and Follows, 1998), or river runoff (Varela et al., 2005).

5.1.3. Diversity, abundance, temporal variability and ecology of diazotrophs

The N_2-fixing activity detected in our study region was conducted by small diazotrophs (<10 µm), presumably unicellular. This conclusion was confirmed by our analysis of the Next Generation Sequencing (Illumina MiSeq®) *nifH* library, which revealed that all sequences belonged to unicellular cyanobacterial and heterotrophic diazotrophs. Specifically, the diazotroph community composition was dominated by UCYN-A (21%) and non-cyanobacterial diazotrophs. This is consistent with previous studies reporting the predominance of UCYN-A in relatively N-rich and cold waters of temperate latitudes of NE Atlantic in summer (Agawin et al., 2014a; Rees et al., 2009). Furthermore, non-cyanobacterial diazotrophs were mainly represented by Gammaproteobacteria-affiliated phylotypes of *nifH* subcluster 1G (28%), mostly *Pseudomonas stutzeri*-like taxa, and putative anaerobic bacteria of cluster 3 (36%). Although the contribution of non-cyanobacterial diazotrophs to the marine biological N_2 fixation is still not well quantified, these potential N_2-fixers show a wider distribution than cyanobacterial diazotrophs, which highlights their possible biogeochemical importance (Bombar et al., 2016; Delmont et al., 2018; Moisander et al., 2017).

The present study reports for the first time a diverse and temporally variable diazotrophic community driven by the hydrodynamic forcing in a temperate upwelling ecosystem. Non-cyanobacterial diazotrophs belonging mainly to clusters 1G (Gammaproteobacteria, mainly related to *P. stutzeri*) and 3 (putative anaerobes) dominated the community during downwelling conditions, characterized by deeper mixed layers and a homogeneous water column. Under these hydrographic conditions, diazotroph community composition exhibited lower variability and higher diversity. Conversely, predominance of UCYN-A (mainly UCYN-A2 sublineage according to the oligotyping analysis) and a more heterogeneous diazotrophic community was observed in upwelling and relaxation, which were particularly affected by enhanced vertical stratification and larger hydrographic variability. The highest relative abundances of UCYN-A were quantified in surface

waters during these conditions. Therefore, our results point toward a dynamic diazotrophic community whose fluctuations are associated with the environmental variability. Similarly, Messer et al. (2015b) and Church et al. (2009) observed seasonal variability of the diazotroph community composition in Australian tropical waters and North Pacific Subtropical Gyre, respectively. In line with all these findings, Martin-Platero et al. (2018) demonstrated, by high-resolution time series, rapid and sharp turnover in the composition of microbial planktonic communities associated with the hydrographic variability in the temperate NE American coast.

The oligotyping approach allowed us to investigate the diversity masked inside UCYN-A OTUs and define oligotypes, highly refined taxa, which subsequently were assigned to UCYN-A sublineages. UCYN-A2 was by far the most abundant sublineage (74% of the data set), followed by UCYN-A1 (23%) and UCYN-A4 (2%), which were mainly represented by oligo3 (67% of data set), oligo1 (18%) and oligo 4 (2%), respectively. These oligotypes are among the most abundant of the global UCYN-A *nifH* amplicon library of Turk-Kubo et al. (2017), which is dominated by UCYN-A1 oligotypes because it includes mostly samples from oligotrophic open ocean regions. UCYN-A1 oligotypes were detected at relatively low frequencies during the three hydrographic conditions, while UCYN-A2 oligos exhibited higher sequence counts during upwelling and relaxation.

We also determined by quantitative PCR the absolute abundances of UCYN-A (UCYN-A1 and UCYN-A2 sublineages) and Gammaproteobacteria γ-24774A11 phylotype. The globally distributed Gammaproteobacterial phylotype exhibited highest abundances during downwelling conditions, when the water column was warmer, less stratified and with relatively low nutrient concentrations. Under these conditions, primary production was probably supported largely by nutrient regeneration through bacterial remineralisation of organic matter, as observed by Bode et al. (2004, 2011) in this same region. Moreover, Gammaproteobacteria may be favored by the organic matter produced after upwelling pulses under conditions of summer thermal stratification, such as we observed in September 2015. Indeed, Moisander et al. (2012, 2014) suggested that the Gammaproteobacterial phylotype γ-24774A11 may rely upon dissolved organic carbon produced by phytoplankton. In contrast, UCYN-A1 and -A2 exhibited highest abundances (up to 6.7×10^2 and 1.5×10^3 *nifH* copies L^{-1}, respectively) in the well-lit surface waters during upwelling and relaxation conditions, consistent with our results on

oligotype abundances. This indicates a possible seasonal variability in the growth of the UCYN-A–prymnesiophyte symbiosis, as previously observed in the (sub)tropical SW Pacific (Bonnet et al., 2015; Moisander et al., 2010). The UCYN-A absolute abundances were in the medium-low range of global abundances (Benavides and Voss, 2015; Luo et al., 2012; Martínez-Pérez et al., 2016). Specifically for the North Atlantic, UCYN-A is, after *Trichodesmium*, the most abundant diazotroph, predominating mainly in the eastern basin (Benavides et al., 2016; Benavides and Voss, 2015; Ratten et al., 2015). Overall, UCYN-A2 was significantly more abundant than UCYN-A1, both in terms of absolute abundances and in terms of relative abundances of oligotypes. This is consistent with recent findings pointing out UCYN-A2, although widespread (Cabello et al., 2016; Martínez-Pérez et al., 2016), mainly occupies coastal areas, while UCYN-A1 predominates in the oligotrophic open ocean (Henke et al., 2018; Messer et al., 2015a, 2015b; Thompson et al., 2014; Turk-Kubo et al., 2017). The contrasting global distribution of UCYN-A sublineages, as well as the temporal variability observed in this study, may be related to the physiological requirements and adaptation of their respective prymnesiophyte hosts to specific habitats and environmental conditions, and the fact that hosts go through different life cycle stages (Hagino et al., 2013). The evolutionary divergence of UCYN-A in different lineages (Cornejo-Castillo et al., 2016) may have allowed them to disperse and adapt to different environments.

In contrast to Gammaproteobacteria γ-24774A11, which peaked mainly at deep waters (70 m) during downwelling conditions, maximum abundances of UCYN-A, mainly of the coastal sublineage UCYN-A2 based on their highest absolute abundances and number of oligotype sequences, were detected in well-lit and stratified surface waters under upwelling and relaxation conditions, coinciding with the highest N_2 fixation rates. Indeed, UCYN-A abundance showed significant positive correlations with N_2 fixation, which was not the case for Gammaproteobacteria. The linkage between UCYN-A and N_2-fixing activity has also been reported in the NE American coast (Mulholland et al., 2012) and the tropical SW Pacific (Bonnet et al., 2015; Turk-Kubo et al., 2015). Hence, the UCYN-A–prymnesiophyte symbiosis is likely the main contributor to N_2-fixing activity in the NW Iberian upwelling region.

These findings shed light on the ecological niches of Gammaproteobacteria and UCYN-A in this upwelling region. In fact, the analysis of ecological niches using non-parametric kernel density functions showed that UCYN-A2 was more abundant under conditions of

higher chlorophyll *a* concentration, whereas Gammaproteobacteria predominated at lower chlorophyll *a*.

5.1.4. Future studies

In the current global change scenario, diazotrophs are undergoing important anthropogenic changes in their environment that in general could benefit their growth and activity in the future. The seawater warming, the enhancement of stratification in the global ocean and the expansion of the OMZs, which will supply N-poor waters to surface photic layer promoting the diazotroph activity (Deutsch et al., 2007; Karl and Letelier, 2008), may increase the range of geographic distribution of N_2-fixers and their global activity in the future (Deutsch et al., 2007; Doney, 2006; Hutchins and Fu, 2017; Karl and Letelier, 2008; Stramma et al., 2008). Jiang et al. (2018) forecast that the iron use efficiencies by cyanobacterial diazotrophs could increase in the future warmer Fe-deplete ocean, alleviating the prevailing iron limitation and increasing the marine N_2 fixation on a global scale. Specifically in the NW Iberia, the relative importance of diazotrophy may also increase due to the weakening of the upwelling events observed in the last decades (Pardo et al., 2011; Pérez et al., 2010). Conversely, enhanced N inputs through the increased atmospheric deposition and a larger use of agricultural fertilizers may have the opposite effect (Duce et al., 2008; Naqvi et al., 2000).

For the first time, we have demonstrated N_2-fixing activity and presence of a diverse and temporally variable diazotrophic community in a temperate upwelling region over a seasonal cycle. However, future studies with increased temporal resolution focusing on N_2 fixation rates and abundance, diversity and expression of *nifH* genes will be needed to better understand the control factors on N_2 fixation and the role of short-term variability of the environmental forcing, occurring at scales of a few days in this region (Gilcoto et al., 2017). Likewise, a higher spatial coverage including coast-ocean transects will serve to characterize the spatial variability. Studies of *nifH* expression will allow to determine the relative and absolute abundances of *nifH* transcripts for subsequently identifying the active diazotrophs in this system, distinguishing cyanobacterial from non-cyanobacterial.

Most N_2-fixing activity in the region may occur under conditions of nitrogen limitation during the summer, when the phytoplankton is limited by this element or at least it responds to its addition (Martínez-García et al., 2010). Indeed, we observed that the

highest N_2 fixation rates, which were detected in summer at surface waters, coincided with the maximum UCYN-A abundances during conditions of N:P ratio below Redfield stoichiometry (<11), relatively low chlorophyll *a* concentration (<1.5 mg m^{-3}) and relatively high stratification (log_{10} N^2 (s^{-2}) = -3.5 – -4.2) (Figure 5.1). Nevertheless, specific observational and experimental approaches, including nutrient addition assays, should be implemented to shed light on the factors driving the activity and growth of the diazotrophs present in this region, as well as to demarcate accurately the environmental conditions that define their ecological niches.

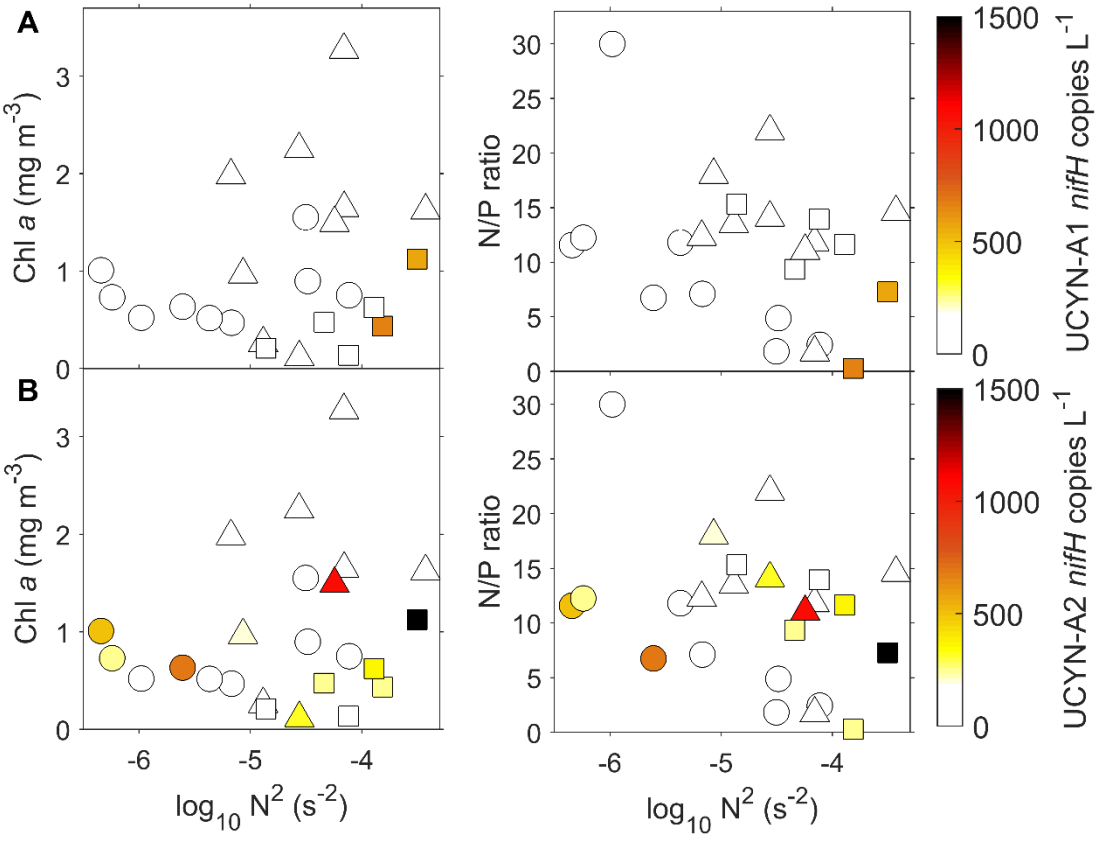

Figure 5.1. (A) *Absolute abundance of UCYN-A1 and* ***(B)*** *UCYN-A2 (nifH copies* L^{-1}*) for each sample according to water column vertical stratification (a proxy for vertical density gradient quantified as squared Brunt Väisälä frequency,* N^2*), chlorophyll* a *concentration and nitrate to phosphate ratio (N/P). Color bar represents UCYN-A absolute abundance. Empty or white symbols represent less than 250 nifH copies* L^{-1} *of UCYN-A absolute abundance. A 5-m window was used for grid-averaging* N^2 *in the vertical dimension.*

5.2. Conclusions

1. Inorganic ^{15}N-labelled contaminants included in some commercial $^{15}N_2$ gas stocks are assimilable by non-diazotrophs organisms, which can inflate the N_2 fixation rates up to sixteen-fold under hydrographic conditions of winter mixing.

2. Low N_2 fixation rates (up to 0.1 µmol N m^{-3} d^{-1}), comparable to the lower-end of rates described for the subtropical Northeastern Atlantic, were detected under different hydrographic regimes, peaking at surface waters during upwelling and relaxation conditions.

3. The contribution of N_2 fixation to new N supply into the euphotic zone was negligible as compared to nitrate diffusive fluxes (<2 %).

4. The diazotrophic community composition was dominated by putative anaerobic bacteria of *nifH* cluster 3 (relative abundance 36%), Gammaproteobacteria of subcluster 1G (28%), and unicellular cyanobacterial diazotrophs of subcluster 1B (UCYN-A, 21%).

5. The diazotrophic community showed an important temporal variability: during downwelling, when non-cyanobacterial diazotrophs from clusters 1G and 3 dominated the community, the diazotrophic community was more homogenous and diverse, whereas during upwelling and relaxation the diazotrophic community was more heterogeneous and less diverse, with prevalence of UCYN-A and clusters 1G and 3.

6. UCYN-A2 was the most abundant sublineage (74% of the data set), followed by UCYN-A1 (23%) and UCYN-A4 (2%), these clades being mainly represented by the oligotypes oligo3 (67%), oligo1 (18%) and oligo 4 (2%), respectively.

7. Gammaproteobacteria γ-24774A11 phylotype peaked (up to 2.4×10^4 *nifH* copies L^{-1}) at deep waters during downwelling, whereas the highest UCYN-A1 and -A2 abundances (up to 6.7×10^2 and 1.5×10^3 *nifH* copies L^{-1}, respectively) occurred at well-lit surface waters during upwelling and relaxation.

8. The positive correlation observed between UCYN-A abundances and N_2 fixation rates indicates that this group may be the principal active diazotroph in the region.

6. Appendix

Table S6.1. *Mean (±SD) values for selected variables determined during all the samplings classified as downwelling (D), upwelling (U), and relaxation (R) conditions. MLD corresponds to the mixed layer depth, estimated from an increase in water column density of 0.125 kg m^{-3} relative to surface values. Squared Brunt Väisälä frequency (N^2), dissipation rates of turbulent kinetic energy (ε), and vertical diffusivity (Kz) correspond to averaged values for the 10–40 m depth interval. The same interval was used to compute vertical NO_3^- gradients and diffusive fluxes. Depth-integrated values (Int) for chlorophyll (Chl* a*), primary production (PP), contribution of <10 µm size-fraction (%) to total Chl* a *and PP, N_2 fixation rates, UCYN-A and Gammaproteobacteria γ-24774A11 (Gamma A) nifH abundances, and biomass of picoplankton groups were calculated down to 40 m. BNF contribution represents the contribution of biological N_2 fixation to the supply of new N (considering N_2 fixation plus nitrate vertical diffusion). The contribution of each group to total picoplankton biomass is also included. n/a: not available. NO_3^- concentrations determined in December 2014 and April 2015 were obtained from a nitrate-density linear relationship (see corresponding section Material and Methods).*

Variable	27/2/14 D	27/5/14 U	17/12/14 D	14/4/15 U	12/5/15 D	11/6/15 U	22/7/15 R	3/9/15 R	19/11/15 D	16/12/15 D
Upwelling Index (m^3 s^{-1} km^{-1})	-3282	-12	-333	544	35	3483	-360	1303	-2602	-3108
Surface temperature (ºC)	12.5	15.5	13.8	13.55	15.6	13.6	16.2	16.4	17.1	15.1
Surface salinity	33.8	35.0	35.5	35.3	35.1	35.5	35.6	35.3	35.7	35.8
MLD (m)	40	7	51	8	18	12	11	13	71	71
N^2 (s^{-2}) × 10^{-5}	9.3 ± 13.0	4.8 ± 3.3	3.4 ± 2.5	17.6 ± 12.9	6.9 ± 5.7	12.8 ± 14.0	18.1 ± 4.2	26.2 ± 30.8	1.8 ± 1.0	0.9 ± 0.9
ε (m^2 s^{-3}) × 10^{-8}	*n/a*	4.3 ± 7.3	*n/a*	0.7 ± 0.7	2.2 ± 2.0	1.5 ± 2.0	2.0 ± 1.7	4.1 ± 5.1	1.3 ± 1.4	*n/a*
Kz **(m^2 s^{-1}) × 10^{-4}**	*n/a*	3.9 ± 6.7	*n/a*	0.1 ± 0.2	1.3 ± 1.8	0.5 ± 0.6	14.0 ± 40.0	10.0 ± 26.0	7.7 ± 9.7	*n/a*
Surface NO_3^- (µM)	6.9	0.1	3.8	1.3	< LOD	3.7	0.1	2.4	1.1	3.4
(40 m) NO_3^- (µM)	6.0	3.4	4.8	8.5	0.3	8.7	3.6	7.7	1.3	4.0
Surface PO_4^{3-} (µM)	0.28	0.07	*n/a*	0.09	0.09	0.33	0.34	0.33	0.22	0.30
(40 m) PO_4^{3-} (µM)	0.38	0.29	*n/a*	0.19	0.16	0.64	0.39	0.56	0.18	0.33
NO_3^- gradient (µmol m^{-4})	0.2	175.2	33.6	101.4	19.4	168.4	137.3	140.2	5.9	16.7
NO_3^- diffusive flux (µmol m^{-2} d^{-1})	20.8	5841.6	2232.6	125.7	221.1	755.7	16,489.4	12,158.3	392.0	1,109.7
Surface Chl *a* (mg m^{-3})	0.5	1.7	0.7	1.6	1.4	1.5	0.4	1.1	0.9	1.0
Int Chl *a* (mg m^{-2})	17	102	22	61	56	33	21	18	24	36
% Int Chl *a* <10 µm	*n/a*	42.3	83.4	25.4	91.3	34.4	46.6	82.2	75.1	91.5
Int PP (mg C m^{-2} d^{-1})	977	4810	565	4959	3157	5808	1403	1820	880	1216
% Int PP <10 µm	*n/a*	39.8	87.7	39.8	70.5	35.3	29.1	88.4	81.2	85.9
Surface N_2 fixation (µmol N m^{-3} d^{-1})	0.046 ± 0.003	*n/a*	0.025 ± 0.012	0.095 ± 0.024	0.009 ± 0.015	0.041 ± 0.025	0.066 ± 0.025	0.077 ± 0.011	0	0
Int N_2 fixation (µmol m^{-2} d^{-1})	*n/a*	*n/a*	1.3 ± 0.4	1.6 ± 0.5	1.0 ± 0.3	0.6 ± 0.3	*n/a*	0.8 ± 0.1	0.3 ± 0.1	0.1 ± 0.1
Contribution BNF (%)	*n/a*	*n/a*	0.06	1.23	0.44	0.07	*n/a*	0.01	0.07	0.01
Surface Gamma A (*nifH* copies L^{-1})	1	0	*n/a*	0	77	914	641	1931	9038	1110
Int Gamma A (*nifH* copies m^{-2} ×10^5)	*n/a*	0.02	*n/a*	0	3.7	39	44	220	380	51
Surface UCYN-A1 (*nifH* copies L^{-1})	0	1	*n/a*	54	1	1	669	565	128	1
Int UCYN-A1 (*nifH* copies m^{-2} ×10^5)	*n/a*	1.5	*n/a*	1.1	0.04	1.4	13	13	2.6	1.6
Surface UCYN-A2 (*nifH* copies L^{-1})	1	56	*n/a*	153	1	1074	256	1477	49	495
Int UCYN-A2 (*nifH* copies m^{-2} ×10^5)	*n/a*	3.2	*n/a*	4.9	3.3	21	10	32	3.7	15
S-picoEuk biomass (mg C m^{-2})	41	9	23	24	39	9	4	17	12	28
S-picoEuk contribution (%)	18	3	17	10	9	4	3	8	6	16
L-picoEuk biomass (mg C m^{-2})	37	9	10	29	104	63	5	20	27	14
L-picoEuk contribution(%)	16	3	8	12	25	28	4	10	12	8
***Synechococcus* biomass (mg C m^{-2})**	9	10	6	2	23	1	1	10	16	20
***Synechococcus* contribution (%)**	4	3	5	1	6	0	1	5	7	12
***Prochlorococcus* biomass (mg C m^{-2})**	2	2	3	2	3	3	2	2	17	8
***Prochlorococcus* contribution(%)**	1	1	2	1	1	1	2	1	8	5
HNA biomass (mg C m^{-2})	103	226	68	148	156	118	94	105	95	60
HNA contribution (%)	44	73	51	63	38	52	71	53	44	36
LNA biomass (mg C m^{-2})	41	55	22	31	85	34	25	46	51	39
LNA contribution (%)	17	18	17	13	21	15	19	23	23	23

Table S6.2. *Number of sequences obtained per sample after quality filtering and before subsampling to minimum sequencing depth to compute relative abundances.*

	Sample		Number of sequences
Downwelling	Feb 2014	0 m	18540
	May 2015	40 m	15482
		70 m	18115
	Nov 2015	0 m	18417
		40 m	18103
		70 m	18859
	Dec 2015	0 m	22106
		40 m	20433
		70 m	20193
Upwelling	May 2014	0 m	28126
		20 m	26237
		40 m	9534
	April 2015	0 m	33925
		40 m	39060
		70 m	25152
	June 2015	0 m	17961
		40 m	36019
		70 m	27050
Relaxation	Jul 2015	0 m	49612
		40 m	29774
		70 m	24011
	Sep 2015	0 m	17520
		40 m	20334
		70 m	27169
		Total	581732

Table S6.3. *Distance matrix between samples based on Bray-Curtis dissimilarity indices (%).*

	Feb 2014	**May 2015**		**Nov 2015**			**Dec 2015**			**Jul 2015**			**Sep 2015**			**May 2014**			**Apr 2015**			**Jun 2015**		
	0 m	**40 m**	**70 m**	**0 m**	**40 m**	**70 m**	**0 m**	**40 m**	**70 m**	**0 m**	**40 m**	**70 m**	**0 m**	**40 m**	**70 m**	**0 m**	**20 m**	**40 m**	**0 m**	**40 m**	**70 m**	**0 m**	**40 m**	**70 m**
	D1	**D2**	**D3**	**D4**	**D5**	**D6**	**D7**	**D8**	**D9**	**R1**	**R2**	**R3**	**R4**	**R5**	**R6**	**U1**	**U2**	**U3**	**U4**	**U5**	**U6**	**U7**	**U8**	**U9**
D1	0																							
D2	0.901	0																						
D3	0.877	0.902	0																					
D4	0.895	0.633	0.951	0																				
D5	0.803	0.887	0.925	0.875	0																			
D6	0.832	0.810	0.763	0.749	0.726	0																		
D7	0.873	0.771	0.756	0.848	0.887	0.767	0																	
D8	0.765	0.859	0.797	0.835	0.784	0.779	0.636	0																
D9	0.771	0.799	0.794	0.833	0.849	0.722	0.582	0.542	0															
R1	0.997	0.991	0.999	0.944	0.988	0.962	0.993	0.993	0.997	0														
R2	0.902	0.916	0.965	0.877	0.833	0.770	0.856	0.875	0.880	0.581	0													
R3	0.956	0.880	0.703	0.870	0.921	0.719	0.833	0.883	0.856	0.920	0.819	0												
R4	0.892	0.862	0.766	0.859	0.828	0.703	0.755	0.780	0.749	0.916	0.780	0.702	0											
R5	0.965	0.880	0.792	0.830	0.929	0.803	0.867	0.902	0.836	0.864	0.772	0.663	0.748	0										
R6	0.920	0.923	0.771	0.890	0.886	0.832	0.852	0.835	0.867	0.731	0.611	0.682	0.792	0.673	0									
U1	0.998	0.996	0.998	0.999	0.999	0.998	0.995	0.997	0.997	0.907	0.972	0.997	0.998	0.998	0.997	0								
U2	0.984	0.987	0.994	0.990	0.978	0.993	0.991	0.976	0.985	0.904	0.935	0.994	0.997	0.996	0.994	0.498	0							
U3	0.998	0.998	0.995	0.999	1.000	0.999	0.994	0.991	0.991	0.878	0.959	0.997	0.998	0.999	0.995	0.545	0.506	0						
U4	0.962	0.933	0.962	0.929	0.992	0.963	0.935	0.966	0.955	0.312	0.493	0.887	0.867	0.858	0.689	0.997	0.999	0.999	0					
U5	0.933	0.925	0.806	0.934	0.958	0.918	0.912	0.943	0.933	1.000	0.981	0.824	0.939	0.884	0.833	0.999	0.990	0.987	0.982	0				
U6	0.985	0.942	0.854	0.926	0.952	0.915	0.949	0.948	0.940	0.977	0.953	0.868	0.941	0.868	0.903	0.999	0.998	0.999	0.989	0.935	0			
U7	0.882	0.889	0.851	0.866	0.796	0.739	0.878	0.855	0.894	0.909	0.752	0.736	0.571	0.807	0.767	0.998	0.992	0.996	0.842	0.973	0.965	0		
U8	0.984	0.971	0.931	0.948	0.984	0.935	0.981	0.947	0.948	0.964	0.930	0.849	0.891	0.894	0.922	0.997	0.990	0.996	0.959	0.988	0.830	0.867	0	
U9	0.964	0.948	0.755	0.972	0.948	0.889	0.879	0.924	0.896	0.999	0.957	0.805	0.893	0.823	0.793	1.000	0.998	1.000	0.999	0.796	0.765	0.937	0.902	0

Table S6.4. *Distribution of oligotypes across samples from UCYN-A* nifH *library. Number of sequences are provided for the six most abundant oligotypes: oligo3 ATTCTATTTTCTT (100% nucleotide identity to KM012884), oligo1 ATCTCGCTTCTTT (100% identity to KM012889), oligo45 ATCTCGCTTTCTT (100% identity to LC013499), oligo46 ATTCTATTTCTTT (100% identity to KU183544), oligo103 ATTCTATTTTCTG (99% identity to KU218784) and oligo4 ACTCTATTTCCCT (100% identity to LC013598). Sequence counts for the rest of oligotypes (Other UCYN-A oligotypes) were summed for each UCYN-A sublineage detected, and the number of oligotypes represented (n) are indicated at each column. 'UCYN-A other' includes oligotypes that did not fall into the sublineages defined hitherto (Turk-Kubo et al., 2017), however, because they are low in frequency (<80 read counts each), we have not created new clusters for them.*

	Sample		UCYN-A1		UCYN-A2			UCYN-A4	Other UCYN-A oligotypes			
			oligo1	oligo45	oligo3	oligo46	oligo103	oligo4	A1 *n*=19	A2 *n*=16	A4 *n*=3	A other *n*=3
Downwelling	Feb 2014	0 m	0	0	32	0	1	0	0	2	0	0
	May 2015	40 m	0	0	183	0	7	0	0	2	0	0
	Nov 2015	0 m	1858	0	0	0	0	0	76	0	0	0
		40 m	363	0	0	0	0	0	17	0	0	0
		70 m	1024	0	1	0	0	0	40	0	0	0
	Dec 2015	0 m	64	0	83	0	2	0	4	9	0	0
		40 m	56	1	81	3	1	0	4	4	0	0
		70 m	0	0	36	0	2	12	0	3	1	0
Relaxation	Jul 2015	0 m	10300	2126	16879	1755	401	628	2203	1804	248	151
		40 m	493	73	10729	55	230	309	76	407	32	2
		70 m	151	4	1565	5	43	586	24	134	42	3
	Sep 2015	0 m	229	17	1875	26	52	0	17	73	0	3
		40 m	1246	66	2241	92	37	0	143	89	0	5
		70 m	677	112	6562	97	178	30	115	212	7	14
Upwelling	May 2014	0 m	0	0	7	0	0	0	0	0	0	0
		20 m	0	0	4	0	1	0	0	0	0	0
	Apr 2015	0 m	0	0	20391	0	557	0	1	436	0	0
		40 m	0	0	2	0	0	0	0	0	0	0
		70 m	691	0	0	0	0	0	34	0	0	0
	Jun 2015	0 m	0	0	2179	0	70	0	0	41	0	0
		40 m	0	0	1055	0	28	0	0	21	0	0
	Total		17152	2399	63905	2033	1610	1565	2754	3237	330	178

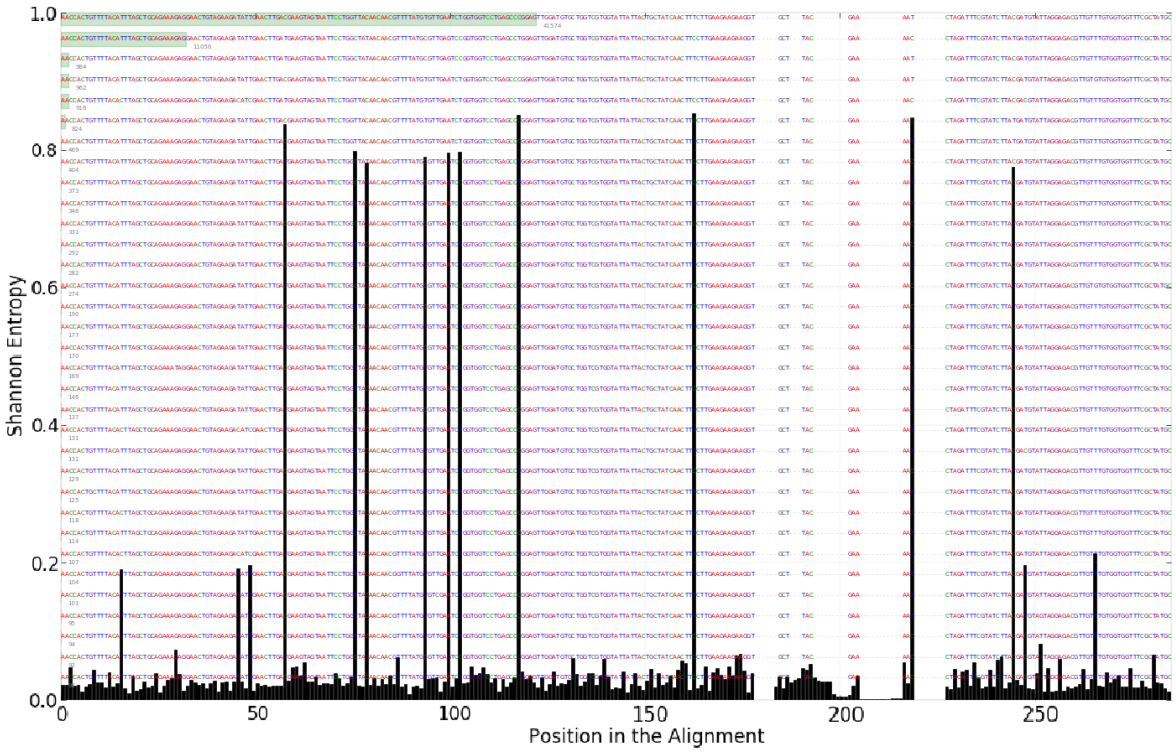

Figure S6.1. *Shannon entropy analysis showing nucleotide positions with highest variability in the data set of UCYN-A* nifH *sequences. Output plot from the oligotyping pipeline (merenlab.org/software/oligotyping/; Eren et al., 2013).*

7. References

Affourtit, J., Zehr, J.P., and Paerl, H.W. (2001). Distribution of Nitrogen-Fixing Microorganisms along the Neuse River Estuary, North Carolina. *Microb. Ecol.* 41, 114–123.

Afgan, E., Baker, D., van den Beek, M., Blankenberg, D., Bouvier, D., Čech, M., et al. (2016). The Galaxy platform for accessible, reproducible and collaborative biomedical analyses: 2016 update. *Nucleic Acids Res*. 44, W3–W10.

Agawin, N. S. R., Benavides, M., Busquets, A., Ferriol, P., Stal, L. J., and Arístegui, J. (2014). Dominance of unicellular cyanobacteria in the diazotrophic community in the Atlantic Ocean. *Limnol. Oceanogr*. 59, 623–637. doi:10.4319/lo.2014.59.2.0623.

Álvarez-Salgado, X. A., Beloso, S., Joint, I., Nogueira, E., Chou, L., Pérez, F. F., et al. (2002). New production of the NW Iberian shelf during the upwelling season over the period 1982-1999. *Deep. Res. I* 49, 1725–1739.

Álvarez-Salgado, X. A., Gago, J., Míguez, B. M., Gilcoto, M., and Pérez, F. F. (2000). Surface Waters of the NW Iberian Margin: Upwelling on the Shelf versus Outwelling of Upwelled Waters from the Rías Baixas. Estuar. *Coast. Shelf Sci.* 51, 821–837. doi:10.1006/ecss.2000.0714.

Aminot, A., and Kerouel, R. (2007). *Dosage automatique des nutriments dans les eaux marines: méthodes en flux continu*. Méthodes d'analyse en milieu marin, Ifremer, Plouzané.

Ammerman, J. W., Hood, R. R., Case, D. A., and Cotner, J. B. (2003). Phosphorus Deficiency in the Atlantic: An Emerging Paradigm in Oceanography. *Eos Trans. Am* 84, 165–170.

Arístegui, J., Barton, E. D., Álvarez-Salgado, X. A., Santos, A. M. P., Figueiras, F. G., Kifani, S., et al. (2009). Sub-regional ecosystem variability in the Canary Current upwelling. *Prog. Oceanogr*. 83, 33–48. doi:10.1016/j.pocean.2009.07.031.

Baker, A. R., Weston, K., Kelly, S. D., Voss, M., Streu, P. and Cape, J. N. (2007). Dry and wet deposition of nutrients from the tropical Atlantic atmosphere: Links to primary productivity and nitrogen fixation. *Deep-Sea Research I* 54, 1704–1720.

Bange, H., Freing, A., Kock, A. and Löscher, C. (2010). "Marine pathways to nitrous oxide", in *Nitrous oxide and climate change*, ed K. Smith (London, UK), 36–62.

Belcher, S. E., Grant, A. L. M., Hanley, K. E., Fox-Kemper, B., Roekel, L. Van, Sullivan, P. P., et al. (2012). A global perspective on Langmuir turbulence in the ocean surface boundary layer. *Geophys. Res. Lett.* 39, 1–9. doi:10.1029/2012GL052932.

Benavides, M., Agawin, N., Arístegui, J., Ferriol, P., and Stal, L. (2011). Nitrogen fixation by *Trichodesmium* and small diazotrophs in the subtropical northeast Atlantic. *Aquat. Microb. Ecol.* 65, 43–53. doi:10.3354/ame01534.

Benavides, M., Arístegui, J., Agawin, N. S. R., Álvarez-Salgado, X. A., Álvarez, M., and Troupin, C. (2013a). Low contribution of N_2 fixation to new production and excess nitrogen in the subtropical northeast Atlantic margin. *Deep Sea Res. Part I* 81, 36–48. doi: 10.1016/j.dsr.2013.07.004

Benavides, M., Arístegui, J., Agawin, N. S. R., López Cancio, J., and Hernández-León, S. (2013b). Enhancement of nitrogen fixation rates by unicellular diazotrophs vs. *Trichodesmium* after a dust deposition event in the Canary Islands. *Limnol. Oceanogr.* 58, 267–275. doi:10.4319/lo.2013.58.1.0267.

Benavides, M., Bronk, D. A., Agawin, N. S. R., Pérez-Hernández, D. M., Hernández-Guerra, A., and Arístegui, J. (2013c). Longitudinal variability of size-fractionated N_2 fixation and DON release rates along 24.5ºN in the subtropical North Atlantic. *J. Geophys. Res. Ocean.* 118, 3406–3415. doi:10.1002/jgrc.20253.

Benavides, M., Moisander, P. H., Daley, M. C., Bode, A., and Arístegui, J. (2016). Longitudinal variability of diazotroph abundances in the subtropical North Atlantic Ocean. *J. Plankton Res*. 38(3), 662-672. doi:10.1093/plankt/fbv121.

Benavides, M., Santana-Falcón, Y., Wasmund, N., and Arístegui, J. (2014). Microbial uptake and regeneration of inorganic nitrogen off the coastal Namibian upwelling system. *J. Mar. Syst.* doi:10.1016/j.jmarsys.2014.05.002.

Benavides, M., and Voss, M. (2015). Five decades of N_2 fixation research in the North Atlantic Ocean. *Front. Mar. Sci.* 2, 1–20. doi:10.3389/fmars.2015.00040.

Bentzon-Tilia, M., Traving, S. J., Mantikci, M., Knudsen-Leerbeck, H., Hansen, J. L., Markager, S., et al. (2015). Significant N_2 fixation by heterotrophs, photoheterotrophs and heterocystous cyanobacteria in two temperate estuaries. *ISME J.* 9, 273–285. doi:10.1038/ismej.2014.119.

Bergersen, F. J. (1980). "Measurements of nitrogen fixation by direct means", in *Methods for evaluating biological nitrogen fixation*, eds F. J. Bergersen, ed Wiley-Interscience (Chichester, UK), 5–110.

Bergman, B., Gallon, J. R., Rai, A. N., and Stal, L. J. (1997). N_2 Fixation by non-heterocystous cyanobacteria. *FEMS Microbiol. Rev*. 19, 139–185.

Bergman, B., Sandh, G., Lin, S., Larsson, J., and Carpenter, E. J. (2013). *Trichodesmium*-a widespread marine cyanobacterium with unusual nitrogen fixation properties. *FEMS Microbiol. Rev.* 37, 286–302. doi:10.1111/j.1574-6976.2012.00352.x.

Berman-Frank, I., Cullen, J. T., Sherrell, R. M., and Falkowski, P. G. (2001a). Iron availability, cellular iron quotas, and nitrogen fixation in *Trichodesmium*. *Limnol. Oceanogr.* 46, 1249–1260.

Berman-Frank, I., Lundgren, P., Chen, Y., Küpper, H., Kolber, Z., Bergman, B., et al. (2001b). Segregation of Nitrogen Fixation and Oxygenic Photosynthesis in the Marine Cyanobacterium *Trichodesmium*. *Science* 294, 1534–1537.

Berman-Frank, I., Quigg, A., Finkel, Z. V., Irwin, A. J., and Haramaty, L. (2007). Nitrogen-fixation strategies and Fe requirements in cyanobacteria. *Limnol. Oceanogr*. 52, 2260–2269.

Berthelot, H., Benavides, M., Moisander, P. H., Grosso, O., and Bonnet, S. (2017). High-nitrogen fixation rates in the particulate and dissolved pools in the Western Tropical Pacific (Solomon and Bismarck Seas). *Geophys. Res. Lett*. 44, 8414–8423. doi:10.1002/2017GL073856.

Bjørnsen, P. K. (1986). Automatic Determination of Bacterioplankton Biomass by Image Analysis. *Appl. Environ. Microbiol*. 51, 1199–1204.

Blais, M., Tremblay, J. É., Jungblut, A. D., Gagnon, J., Martin, J., Thaler, M., et al. (2012). Nitrogen fixation and identification of potential diazotrophs in the Canadian Arctic. *Global Biogeochem. Cycles* 26, GB3022. doi:10.1029/2011GB004096.

Blanton, J. O., Tenore, K. R., Castillejo, F., Atkinson, L. P., Schwing, F. B., and Lavin, A. (1987). Relationship of upwelling to mussel production in the Rias on the western coast of Spain. *J. Mar. Res*. 45, 497–511.

Bode, A., Anadón, R., Morán, X. A. G., Nogueira, E., Teira, E., and Varela, M. (2011). Decadal variability in chlorophyll and primary production off NW Spain. *Clim. Res.* 48, 293–305. doi:10.3354/cr00935.

Bode, A., Barquero, S., González, N., Alvarez-Ossorio, M. T., and Varela, M. (2004). Contribution of heterotrophic plankton to nitrogen regeneration in the upwelling ecosystem of A Coruña (NW Spain). *J. Plankton Res.* 26, 11–28. doi:10.1093/plankt/fbh003.

Bode, A., Casas, B., Fernández, E., Marañón, E., Serret, P., and Varela, M. (1996). Phytoplankton biomass and production in shelf waters off NW Spain: spatial and seasonal variability in relation to upwelling. *Hydrobiologia* 341, 225–234. doi:10.1007/BF00014687.

Bombar, D., Paerl, R. W., Anderson, R., and Riemann, L. (2018). Filtration via Conventional Glass Fiber Filters in $^{15}N_2$ Tracer Assays Fails to Capture All Nitrogen-Fixing Prokaryotes. *Frontiers in Marine Science*, 5, 6. doi: 10.3389/fmars.2018.00006.

Bombar, D., Paerl, R. W., and Riemann, L. (2016). Marine Non-Cyanobacterial Diazotrophs: Moving beyond Molecular Detection. *Trends Microbiol.* 24, 916–927. doi:10.1016/j.tim.2016.07.002.

Bonnet, S., Caffin, M., Berthelot, H., and Moutin, T. (2017). Hot spot of N_2 fixation in the western tropical South Pacific pleads for a spatial decoupling between N_2 fixation and denitrification. *Proc. Natl. Acad. Sci.* 114, 2800–2801. doi: 10.1073/pnas.1619514114.

Bonnet, S., Rodier, M., Turk-Kubo, K., Germineaud, C., Menkes, C., Ganachaud, A., et al. (2015). Contrasted geographical distribution of N_2 fixation rates and nifH phylotypes in the Coral and Solomon Seas (southwestern Pacific) during austral winter conditions. *Global Biogeochem. Cycles* 29, 1874–1892. doi:10.1002/2014GB005049.

Boyd, P. W., and Doney, S. C. (2002). Modelling regional responses by marine pelagic ecosystems to global climate change. *Geophys. Res. Lett.* 29, 53–1–53–4. doi: 10.1029/2001GL014130

Brandes, J. A., and Devol, A. H. (2002). A global marine-fixed nitrogen isotopic budget: Implications for Holocene nitrogen cycling. *Global Biogeochem. Cycles* 16, 0–1. doi:10.1029/2001GB001856.

Braun, S. T., Proctor, L. M., Zani, S., Mellon, M. T., and Zehr, J. P. (1999). Molecular evidence for zooplankton-associated nitrogen-fixing anaerobes based on amplification of the *nifH* gene. *FEMS Microbiol. Ecol*. 28, 273–279.

Breitbarth, E., Oschlies, A., and LaRoche, J. (2007). Physiological constraints on the global distribution of *Trichodesmium* - effect of temperature on diazotrophy. *Biogeosciences* 4, 53–61.

Burris, R. H. and Miller, C. E. (1941). Application of N^{15} to the study of biological nitrogen fixation. *Science* 93(2405), 114–115.

Cabello, A. M., Cornejo-Castillo, F. M., Raho, N., Blasco, D., Vidal, M., Audic, S., et al. (2016). Global distribution and vertical patterns of a prymnesiophyte–cyanobacteria obligate symbiosis. *ISME J.* 10, 693–706. doi:10.1038/ismej.2015.147.

Calvo-Díaz, A., and Moran, X. A. G. (2006). Seasonal dynamics of picoplankton in shelf waters of the southern Bay of Biscay. *Aquat. Microb. Ecol*. 42, 159–174. doi:10.3354/ame042159.

Camacho, C., Coulouris, G., Avagyan, V., Ma, N., Papadopoulos, J., Bealer, K., and Madden, T.L. (2009). BLAST plus: architecture and applications. *BMC Bioinformatics* 10, 1–9.

Capone, D. G. (1993). "Determination of nitrogenase activity in aquatic samples using the acetylene reduction procedure", in *Handbook of methods in aquatic microbial ecology*, eds P. F. Kemp, B. F. Sherr, E. B. Sherr and J. J. Cole, ed Lewis Publishers (Boca Raton, FL, USA), 621–631.

Capone, D. G., Burns, J. A., Montoya, J. P., Subramaniam, A., Mahaffey, C., Gunderson, T., et al. (2005). Nitrogen fixation by *Trichodesmium* spp.: An important source of new nitrogen to the tropical and subtropical North Atlantic Ocean. *Global Biogeochem. Cycles* 19, GB2024. doi:10.1029/2004GB002331.

Capone, D. G., Popa, R., Flood, B., and Nealson, K. H. (2006). Follow the nitrogen. *Science* 312, 708–709. doi:10.1126/science.1111863.

Capone, D. G., Zehr, J. P., Paerl, H. W., Bergman, B., and Carpenter, E. J. (1997). *Trichodesmium*, a Globally Significant Marine Cyanobacterium. *Science* 276, 1221–1229. doi:10.1126/science.276.5316.1221.

Caporaso, J. G., Bittinger, K., Bushman, F. D., Desantis, T. Z., Andersen, G. L., and Knight, R. (2010a). PyNAST: A flexible tool for aligning sequences to a template alignment. *Bioinformatics* 26, 266–267.

Caporaso, J.G., Kuczynski, J., Stombaugh, J., Bittinger, K., Bushman, F. D., Costello, E. K., et al. (2010b). QIIME allows analysis of high-throughput community sequencing data. *Nat. Methods* 7, 335–336.

Carpenter, E. J. and Capone, D. G. (2008). "Nitrogen Fixation in the Marine Environment", in *Nitrogen in the Marine Environment*, ed Elsevier Inc. (Amsterdam, The Netherlands), 141−198.

Casas, B., Varela, M., Canle, M., González, N., and Bode, A. (1997). Seasonal Variations of Nutrients, Seston and Phytoplankton, and Upwelling Intensity off La Coruña (NW Spain). *Estuar. Coast. Shelf Sci.* 44, 767–778. doi:10.1006/ecss.1996.0155.

Cermeño, P., Chouciño, P., Fernández-Castro, B., Figueiras, F. G., Marañón, E., Marrase, C., et al. (2016). Marine primary productivity is driven by a selection effect. *Front. Mar. Sci*. 3, 173. doi:10.3389/fmars.2016.00173.

Chao, A. (1984). Nonparametric Estimation of the Number of Classes in a Population. *Scand J Stat*. 11, 265–270.

Chen, Y., Tovar-Sanchez, A., Siefert, R. L., Sañudo-Wilhelmy, S. A., and Zhuang, G. (2011). Luxury uptake of aerosol iron by *Trichodesmium* in the western tropical North Atlantic. *Geophys. Res. Lett.* 38, L18602. doi:10.1029/2011GL048972.

Church, M. J., Björkman, K. M., Karl, D. M., Saito, M. A., and Zehr, J. P. (2008). Regional distributions of nitrogen-fixing bacteria in the Pacific Ocean. *Limnol. Oceanogr*. 53, 63–77.

Church, M. J., Jenkins, B. D., Karl, D. M., and Zehr, J. P. (2005). Vertical distributions of nitrogen-fixing phylotypes at Station ALOHA in the oligotrophic North Pacific Ocean. *Aquat. Microb. Ecol*. 38, 3–14. doi:10.3354/ame038003.

Church, M. J., Mahaffey, C., Letelier, R. M., Lukas, R., Zehr, J. P., and Karl, D. M. (2009). Physical forcing of nitrogen fixation and diazotroph community structure in the North Pacific subtropical gyre. *Global Biogeochem. Cycles* 23, GB2020.

Church, M. J., Short, C. M., Jenkins, B. D., Karl, D. M., and Zehr, J. P. (2005) Temporal patterns of nitrogenase gene (*nifH*) expression in the oligotrophic North Pacific Ocean. *Appl. Environ. Microbiol*. 71, 5362–5370.

Clarke, K. R. (1993). Non-parametric multivariate analyses of changes in community structure. *Aust. J. Ecol*. 18, 117–143.

Codispoti, L. A. (2007). An oceanic fixed nitrogen sink exceeding 400 Tg N a^{-1} vs the concept of homeostasis in the fixed-nitrogen inventory. *Biogeosciences Discuss.* 4, 233–253. doi:10.5194/bgd-3-1203-2006.

Codispoti, L. A., Brandes, J. A., Christensen, J. P., Devol, A. H., Naqvi, S. W. A., Paerl, H. W., et al. (2001). The oceanic fixed nitrogen and nitrous oxide budgets: Moving targets as we enter the anthropocene? *Sci. Mar.* 65, 85–105.

Conkright, M. E., Locarnini, R. A., Garcia, H., Brien, T. O., Boyer, T., Stephens, C., and Antonov, J. (2002). *World Ocean Atlas 2001: Objective analyses, data statistics, and figures, CD-ROM documentation, NODC Tech. Report*. National Oceanographic Data Center. Silver Spring, MD.

Conley, D. J., Paerl, H. W., Howarth, R. W., Boesch, D. F., Seitzinger, S. P., Havens, K. E., et al. (2009). Controlling eutrophication: nitrogen and phosphorus. *Science* 323, 1014–1015. doi:10.1126/science.1167755.

Cornejo-Castillo, F.M., Cabello, A. M., Salazar, G., Sánchez-Baracaldo, P., Lima-Mendez, G., Hingamp, P., et al. (2016). Cyanobacterial symbionts diverged in the late Cretaceous towards lineage-specific nitrogen fixation factories in single-celled phytoplankton. *Nat. Commun*. 7, 11071.

Cuypers, Y., Bouruet-Aubertout, P., Marec, C., and Fuda, J. L. (2012). Characterization of turbulence from a fine-scale parameterization and microstructure measurements in the Mediterranean Sea during the BOUM experiment. *Biogeosciences* 9, 3131–3149. doi:10.5194/bg-9-3131-2012.

Dabundo, R., Lehmann, M. F., Treibergs, L., Tobias, C. R., Altabet, M. A., Moisander, P. H., et al. (2014). The Contamination of Commercial $^{15}N_2$ Gas Stocks with ^{15}N–

Labeled Nitrate and Ammonium and Consequences for Nitrogen Fixation Measurements. *PLoS One* 9, e110335. doi:10.1371/journal.pone.0110335.

Delmont, T. O., Quince, C., Shaiber, A., Esen, Ö. C., Lee, S. T. M., Rappé, M. S., et al. (2018). Nitrogen-fixing populations of Planctomycetes and Proteobacteria are abundant in surface ocean metagenomes. *Nat. Microbiol.* 3, 804–813. doi:10.1038/s41564-018-0176-9.

De-Polli, H., Matsui, E., Döbereine, J., Salati, E. (1977). Confirmation of nitrogen fixation in two tropical grasses by $^{15}N_2$ incorporation. *Soil Biol and Biochem* 9, 119–123.

Dekaezemacker, J., and Bonnet, S. (2011). Sensitivity of N_2 fixation to combined nitrogen forms (NO_3^- and NH_4^+) in two strains of the marine diazotroph *Crocosphaera watsonii* (Cyanobacteria). *Mar. Ecol. Prog. Ser.* 438, 33–46. doi:10.3354/meps09297.

Deutsch, C., Sarmiento, J. L., Sigman, D. M., Gruber, N., and Dunne, J. P. (2007). Spatial coupling of nitrogen inputs and losses in the ocean. *Nature* 445, 163–167. doi:10.1038/nature05392.

Dixon, R., and Kahn, D. (2004). Genetic regulation of biological nitrogen fixation. *Nat. Rev. Microbiol.* 2, 621–631. doi:10.1038/nrmicro954.

Doney, S. C. (2006). Plankton in a warmer world. *Nature* 444, 695–696. doi:10.1029/2003GB002134.

Doney, S. C., Fabry, V. J., Feely, R. A., and Kleypas, J. A. (2009). Ocean acidification: the other CO_2 problem. *Ann. Rev. Mar. Sci.* 1, 169–192. doi:10.1146/annurev.marine.010908.163834.

Duce, R. A., LaRoche, J., Altieri, K., Arrigo, K. R., Baker, A. R., Capone, D. G., et al. (2008). Impacts of atmospheric anthropogenic nitrogen on the open ocean. *Science* 320, 893–7. doi:10.1126/science.1150369.

Duce, R. A., and Tindale, N. W. (1991). Atmospheric transport of iron and its deposition in the ocean. *Limnol. Oceanogr.* 36, 1715–1726.

Dyhrman, S. T., Chappell, P. D., Haley, S. T., Moffett, J. W., Orchard, E. D., Waterbury, J. B., et al. (2006). Phosphonate utilization by the globally important marine diazotroph *Trichodesmium*. *Nature* 439, 68–71. doi:10.1038/nature04203.

Dyhrman, S. T., and Haley, S. T. (2006). Phosphorus Scavenging in the Unicellular Marine Diazotroph *Crocosphaera watsonii*. *Appl. Enviromental Microbiol*. 72, 1452–1458. doi:10.1128/AEM.72.2.1452.

Edgar, R. C., Haas, B. J., Clemente, J. C., Quince, C., and Knight, R. (2011). UCHIME improves sensitivity and speed of chimera detection. *Bioinformatics* 27, 2194–2200.

Eren, A. M., Maignien, L., Sul, W.J., Murphy, L.G., Grim, S.L., Morrison, H.G., and Sogin, M.L. (2013). Oligotyping: Differentiating between closely related microbial taxa using 16S rRNA gene data. *Methods Ecol. Evol*. 4, 1111–1119.

Erisman, J. W., Sutton, M. A., Galloway, J., Klimont, Z., and Winiwarter, W. (2008). How a century of ammonia synthesis changed the world. *Nat. Geosci.* 1, 636–639.

Falcón, L.I., Carpenter, E.J., Cipriano, F., Bergman, B., and Capone, D.G. (2004). N_2 Fixation by Unicellular Bacterioplankton from the Atlantic and Pacific Oceans: Phylogeny and In Situ Rates. *Appl. Environ. Microbiol*. 70, 765–770.

Falkowski, P. G. (1997). Evolution of the nitrogen cycle and its influence on biological sequestration of CO_2 in the oceans. *Nature* 387: 272–273.

Farnelid, H., Andersson, A. F., Bertilsson, S., Al-Soud, W. A., Hansen, L. H., Sorensen, S., et al. (2011). Nitrogenase gene amplicons from global marine surface waters are dominated by genes of non-cyanobacteria. *PLoS One* 6. doi:10.1371/journal.pone.0019223.

Farnelid, H., Bentzon-Tilia, M., Andersson, A. F., Bertilsson, S., Jost, G., Labrenz, M., et al. (2013). Active nitrogen-fixing heterotrophic bacteria at and below the chemocline of the central Baltic Sea. *ISME J.* 7: 1413–1423.

Farnelid, H., Öberg, T., and Riemann, L. (2009). Identity and dynamics of putative N_2-fixing picoplankton in the Baltic Sea proper suggest complex patterns of regulation. *Environ. Microbiol. Rep*. 1, 145–154.

Farnelid, H., Tarangkoon, W., Hansen, G., Hansen, P.J., and Riemann, L. (2010). Putative N_2-fixing heterotrophic bacteria associated with dinoflagellate-cyanobacteria consortia in the low-nitrogen Indian Ocean. *Aquat. Microb. Ecol*. 61: 105–117.

Farnelid, H., Turk-Kubo, K., Del Carmen Muñoz-Marín, M., and Zehr, J. P. (2016). New insights into the ecology of the globally significant uncultured nitrogen-fixing symbiont UCYN-A. *Aquat. Microb. Ecol.* 77, 128–138. doi:10.3354/ame01794.

Fernández, C., Lorena González, M., Muñoz, C., Molina, V., and Farías, L. (2015). Temporal and spatial variability of biological nitrogen fixation off the upwelling system of central Chile (35–38.5ºS). *J. Geophys. Res. Ocean*. 120, 3330–3349. doi:10.1002/2014JC010410.

Fernández-Castro, B., Mouriño-Carballido, B., Benítez-Barrios, V. M., Chouciño, P., Fraile-Nuez, E., Graña, R., et al. (2014). Microstructure turbulence and diffusivity parameterization in the tropical and subtropical Atlantic, Pacific and Indian Oceans during the Malaspina 2010 expedition. *Deep. Res. Part I Oceanogr. Res. Pap.* 94, 15–30. doi:10.1016/j.dsr.2014.08.006.

Fernández-Castro, B., Mouriño-Carballido, B., Marañón, E., Chouciño, P., Gago, J., Ramírez, T., et al. (2015). Importance of salt fingering for new nitrogen supply in the oligotrophic ocean. *Nat. Commun.* 6, 1–10. doi:10.1038/ncomms9002.

Fernández-Méndez, M., Turk-Kubo, K. A., Buttigieg, P. L., Rapp, J. Z., Krumpen, T., Zehr, J. P., et al. (2016). Diazotroph Diversity in the Sea Ice, Melt Ponds, and Surface Waters of the Eurasian Basin of the Central Arctic Ocean. *Front. Microbiol*. 7, 1–18. doi:10.3389/fmicb.2016.01884.

Fernández, A., Graña, R., Mouriño-Carballido, B., Bode, A., Varela, M., Domínguez-Yanes, J. F., et al. (2013). Community N_2 fixation and *Trichodesmium* spp. abundance along longitudinal gradients in the eastern subtropical North Atlantic. *ICES J. Mar. Sci.* 70, 223–231.

Fernández, A., Mouriño-Carballido, B., Bode, A., Varela, M., and Marañón, E. (2010). Latitudinal distribution of *Trichodesmium* spp. and N_2 fixation in the Atlantic Ocean. *Biogeosciences* 7, 3167–3176. doi:10.5194/bg-7-3167-2010.

Fernández, C., Lorena González, M., Munoz, C., Molina, V., and Farías, L. (2015). Temporal and spatial variability of biological nitrogen fixation off the upwelling system of central Chile (35–38.5ºS). *J. Geophys. Res. Ocean*. 120, 3330–3349. doi:10.1002/2014JC010410.

Finn, R. D., Mistry, J., Tate, J., Coggill, P., Heger, A., Pollington, J. E., et al. (2010). Pfam: The protein families database. *Nucleic Acids Res*. 38, D211–D222.

Foster, R. A., Subramaniam, A., and Zehr, J. P. (2009). Distribution and activity of diazotrophs in the Eastern Equatorial Atlantic. *Environ. Microbiol*. 11, 741–750. doi:10.1111/j.1462-2920.2008.01796.x.

Fowler, D., Coyle, M., Skiba, U., Sutton, M. A., Cape, J. N., Reis, S., et al. (2013). The global nitrogen cycle in the twenty-first century. *Philosophical Trans. R. Soc. B* 368, 20130164. doi:http://dx.doi.org/10.1098/rstb.2013.0164.

Fraga, F. (1981). Upwelling off the Galician Coast, northwest Spain. *Coast. Upwelling* 1, 176–182. doi:10.1029/CO001p0176.

Fu, F. X., Zhang, Y., Bell, P. R. F. and Hutchins, D. A. (2005). Phosphate uptake and growth kinetics of *Trichodesmium* (Cyanobacteria) isolates from the North Atlantic Ocean and the Great Barrier Reef, Australia. *J. Phycol.* 41, 62–73.

Galloway, A. J. N., Dentener, F. J., Capone, D. G., Boyer, E. W., Howarth, R. W., Seitzinger, S. P., et al. (2004). Nitrogen cycles: past, present, and future. *Biogeochemistry* 70, 153–226. doi:10.1007/s10533-004-0370-0.

Garcia, H. E., Locarnini, R. A., Boyer, T. P., Antonov, J. I., Baranova, O. K., Zweng, M. M., et al. (2013). "Dissolved inorganic nutrients (phosphate, nitrate, silicate)," in *World Ocean Atlas* 2013, Vol. 4, eds S. Levitus and A. Mishonov (NOAA Atlas NESDIS 76), 25.

Gargett, A. E. (1989). Ocean Turbulence. *Ann. Rev. Fluid Mech*. 21, 419–451.

Geange, S. W., Pledger, S., Burns, K. C., and Shima, J. S. (2011). A unified analysis of niche overlap incorporating data of different types. *Methods in Ecology and Evolution* 2, 175–184. doi:10.1111/j.2041-210X.2010.00070.x

Gilcoto, M., Largier, J. L., Barton, E. D., Piedracoba, S., Torres, R., Graña, R., et al. (2017). Rapid response to coastal upwelling in a semienclosed bay. *Geophys. Res*. Lett. 44, 2388–2397. doi:10.1002/2016GL072416.

Giller, K. E. (1987). Use and abuse of the acetylene-reduction assay for measurement of associative nitrogen fixation. *Soil Biology & Biochemistry* 19 (6), 783–784.

Glibert, P. M., and Bronk, D. A. (1994). Release of Dissolved Organic Nitrogen by Marine Diazotrophic Cyanobacteria, *Trichodesmium* spp. *Appl. Enviromental Microbiol.* 60, 3996–4000.

Goebel, N. L., Edwards, C. A., Church, M. J., and Zehr, J. P. (2007). Modeled contributions of three types of diazotrophs to nitrogen fixation at Station ALOHA. *ISME J.*. 1, 606–619. doi:10.1038/ismej.2007.80.

Goebel, N. L., Turk, K. A., Achilles, K. M., Paerl, R., Hewson, I., Morrison, A. E., et al. (2010). Abundance and distribution of major groups of diazotrophic cyanobacteria and their potential contribution to N_2 fixation in the tropical Atlantic Ocean. *Environ. Microbiol.* 12, 3272–3289. doi:10.1111/j.1462-2920.2010.02303.x.

Goto, M., Ando, S., Hachisuka, Y., and Yoneyama, T. (2005) Contamination of diverse *nifH* and *nifH*-like DNA into commercial PCR primers. *FEMS Microbiol. Lett.* 246, 33–38. doi:10.1111/1758-2229.12070.

Großkopf, T., Mohr, W., Baustian, T., Schunck, H., Gill, D., Kuypers, M. M. M., et al. (2012). Doubling of marine dinitrogen-fixation rates based on direct measurements. *Nature* 488, 361–364. doi:10.1038/nature1133

Grosse, J., Bombar, D., Doan, H. N., Nguyen, L. N., and Voss, M. (2010). The Mekong River plume fuels nitrogen fixation and determines phytoplankton species distribution in the South China Sea during low- and high-discharge season. *Limnol. Oceanogr*. 55, 1668–1680. doi:10.4319/lo.2010.55.4.1668.

Gruber, N. (2004). "The dynamics of the marine nitrogen cycle and atmospheric CO_2", in: *Carbon-climate interactions*, eds T. Orguz and M. Follws, ed Kluwer (Dordrecht, The Netherlands), 97–148.

Gruber, N. (2008). "The marine nitrogen cycle: Overview and challenges", in *Nitrogen in the marine environment*, eds D. G. Capone, D. A. Bronk, M. R. Mulholland, E. J. Carpenter, ed Elsevier Inc. (Amsterdam, The Netherlands), 1–50.

Gruber, N., and Galloway, J. N. (2008). An Earth-system perspective of the global nitrogen cycle. *Nature* 451, 293–296. doi:10.1038/nature06592.

Gruber, N., and Sarmiento, J. L. (1997). Global patterns of marine nitrogen fixation and denitrification. *Global Biogeochem. Cycles* 11, 235–266.

Hagino, K., Onuma, R., Kawachi, M., and Horiguchi, T. (2013). Discovery of an endosymbiotic nitrogen-fixing cyanobacterium UCYN-A in *Braarudosphaera bigelowii* (Prymnesiophyceae). *PLoS One* 8. doi:10.1371/journal.pone.0081749.

Halm, H., Lam, P., Ferdelman, T. G., Lavik, G., Dittmar, T., LaRoche, J., et al. (2012). Heterotrophic organisms dominate nitrogen fixation in the South Pacific Gyre. *ISME J.*, *6*(6), 1238-1249. doi:10.1038/ismej.2011.182.

Hardy, R. W. F., Holsten, R. D., Jackson, E. K., and Burns, R. C. (1968). The acetylene-ethylene assay for N_2 fixation: laboratory and field evaluation. *Plant Physiol.* 43, 1185–1207. doi:10.1104/pp.43.8.1185.

Hastings, M. G., Jarvis, J. C., and Steig, E. J. (2009). Anthropogenic Impacts on Nitrogen Isotopes of Ice-Core Nitrate. *Science* 324, 1288.

Heller, P., Tripp, H. J., Turk-Kubo, K., and Zehr, J. P. (2014). ARBitrator: a software pipeline for on-demand retrieval of auto-curated *nifH* sequences from GenBank. *Bioinformatics* 30, 2883–2890.

Henke, B. A., Turk-Kubo, K. A., Bonnet, S., and Zehr, J. P. (2018). Distributions and Abundances of Sublineages of the N_2-Fixing Cyanobacterium *Candidatus* Atelocyanobacterium thalassa (UCYN-A) in the New Caledonian Coral Lagoon. *Front. Microbiol*. 9, 1–14.

Hibiya, T., Nagasawa, M., and Niwa, Y. (2007). Latitudinal dependence of diapycnal diffusivity in the thermocline observed using a microstructure profiler. *Geophys. Res. Lett.* 34, L24602. doi:10.1029/2007GL032323.

Holl, C. M., and Montoya, J. P. (2005). Interactions between nitrate uptake and nitrogen fixation in continuous cultures of the marine diazotroph *Trichodesmium* (Cyanobacteria). *J. Phycol*. 41, 1178–1183. doi:10.1111/j.1529-8817.2005.00146.x.

Holtgrieve, G. W., Schindler, D. E., Hobbs, W. O., Leavitt, P. R., Ward, E. J., Bunting, L., et al. (2011). A Coherent Signature of Anthropogenic Nitrogen Deposition to Remote Watersheds of the Northern Hemisphere. *Science* 334, 1545–1548. doi:10.1126/science.1212267.

Howarth, R. W., Marino, R., Lane, J., and Cole, J. J. (1988). Nitrogen fixation in freshwater, estuarine, and marine ecosystems. 1. Rates and importance. *Limnol. Oceanogr*. 33, 669–687. doi:10.4319/lo.1988.33.4_part_2.0669.

Hutchins, D. A., Fu, F. X., Webb, E. A., Walworth, N., and Tagliabue, A. (2013). Taxon-specific response of marine nitrogen fixers to elevated carbon dioxide concentrations. *Nat. Geosci.* 6, 790–795. doi:10.1038/ngeo1858.

Hutchins, D. A., and Fu, F. (2017). Microorganisms and ocean global change. *Nat. Microbiol.* 2, 1–11. doi:10.1038/nmicrobiol.2017.58.

Hutchins, D. A., Fu, F., Zhang, Y., Warner, M. E., Feng, Y., Portune, K., et al. (2007). CO2 control of *Trichodesmium* N_2 fixation, photosynthesis, growth rates, and elemental ratios: Implications for past, present, and future ocean biogeochemistry. *Limnol. Oceanogr.* 52, 1293–1304.

Hynes, A. M., Chappell, P. D., Dyhrman, S. T., Doney, S. C., and Webb, E. A. (2009). Cross-basin comparison of phosphorus stress and nitrogen fixation in *Trichodesmium*. *Limnol. Oceanogr.* 54, 1438–1448.

IPCC (2014). Climate Change 2014: Synthesis Report. Contribution of Working Groups I, II and III to the Fifth Assessment Report of the Intergovernmental Panel on Climate Change [Core Writing Team, R.K. Pachauri and L.A. Meyer (eds.)]. IPCC, Geneva, Switzerland, 151 pp.

Jenkins, B.D., Steward, G.F., Short, S.M., Ward, B.B., and Zehr, J. P. (2004). Fingerprinting Diazotroph Communities in the Chesapeake Bay by Using a DNA Macroarray. *Appl. Environ. Microbiol*. 70, 1767–1776.

Jiang, H.-B., Fu, F.-X., Rivero-Calle, S., Levine, N. M., Sañudo-Wilhelmy, S. A., Qu, P.-P., et al. (2018). Ocean warming alleviates iron limitation of marine nitrogen fixation. *Nat. Clim. Chang*. 8, 709–712. doi:10.1038/s41558-018-0216-8.

Jickells, T. D., An, Z. S., Andersen, K. K., Baker, A. R., Bergametti, G., Brooks, N., et al. (2005). Global Iron Connections Between Desert Dust, Ocean Biogeochemistry, and Climate. *Science* 308, 67–71. doi:10.1126/science.1105959.

Jurado, E., van der Woerd, H. J., and Dijkstra, H. A. (2012). Microstructure measurements along a quasi-meridional transect in the northeastern Atlantic Ocean. *J. Geophys. Res.* 117, C04016. doi:10.1029/2011JC007137.

Kark, S., Mukerji, T., Safriel, U. N., Noy-Meir, I., Nissani, R., and Darvasi, A. (2002). Peak morphological diversity in an ecotone unveiled in the chukar partridge by a novel Estimator in a Dependent Sample (EDS). *Journal of Animal Ecology* 71, 1015–1029. doi: 10.1046/j.1365-2656.2002.00665.x

Karl, D., Letelier, R., Tupas, L., Dore, J., Christian, J., and Hebel, D. (1997). The role of nitrogen fixation in biogeochemical cycling in the subtropical North Pacific Ocean. *Nature* 388, 533–538. doi:10.1038/41474.

Karl, D. M., and Letelier, R. M. (2008). Nitrogen fixation-enhanced carbon sequestration in low nitrate, low chlorophyll seascapes. *Mar. Ecol. Prog. Ser.* 364, 257–268. doi:10.3354/meps07547.

Karl, D., Michaels, A., Bergman, B., Capone, D., Carpenter, E., Letelier, R., et al. (2002). Dinitrogen fixation in the world's oceans. *Biogeochemistry* 57/58, 47–98.

Khatiwala, S., Tanhua, T., Fletcher, S. M., Gerber, M., Doney, S. C., Graven, H. D., et al. (2013). Global ocean storage of anthropogenic carbon. *Biogeosciences* 10, 2169–2191. doi:10.5194/bg-10-2169-2013.

Knapp, A. N. (2012). The sensitivity of marine N_2 fixation to dissolved inorganic nitrogen. *Front. Microbiol.* 3, 1–14. doi:10.3389/fmicb.2012.00374.

Knapp, A. N., Casciotti, K. L., Berelson, W. M., Prokopenko, M. G., and Capone, D. G. (2016). Low rates of nitrogen fixation in eastern tropical South Pacific surface waters. *Proc. Natl. Acad. Sci.* 113, 4398–4403. doi:10.1073/pnas.1515641113.

Konno, U., Tsunogai, U., Komatsu, D. D., Daita, S., Nakagawa, F., Tsuda, A., et al. (2010). Determination of total N_2 fixation rates in the ocean taking into account both the particulate and filtrate fractions. *Biogeosciences* 7, 2369–2377. doi:10.5194/bg-7-2369-2010.

Krupke, A., Mohr, W., Laroche, J., Fuchs, B. M., Amann, R. I., and Kuypers, M. M. M. (2015). The effect of nutrients on carbon and nitrogen fixation by the UCYN-A – haptophyte symbiosis. *ISME J.* 9, 1635–1647. doi:10.1038/ismej.2014.253.

Kustka, A. B., Sañudo, S. A., Carpenter, E. J., Capone, D., Burns, J., and Sunda, W. G. (2003). Iron requirements for dinitrogen- and ammonium-supported growth in cultures of *Trichodesmium* (IMS 101): Comparison with nitrogen fixation rates and iron: carbon ratios of field populations. *Limnol. Oceanogr*. 48, 1869–1884.

Lam, P. and Kuypers, M. M. M. (2011). Microbial nitrogen cycling processes in oxygen minimum zones. *Annu. Rev. Mar. Sci*., 3, 317–345, doi:10.1146/annurev-marine-120709-142814

Landolfi, A., Koeve, W., Dietze, H., Kähler, P., and Oschlies, A. (2015). A new perspective on environmental controls. *Geophys. Res. Lett*. 42, 4482–2289. doi:10.1002/2015GL063756.Abstract.

Langlois, R., Großkopf, T., Mills, M., Takeda, S., and LaRoche, J. (2015). Widespread distribution and expression of Gamma A (UMB), an uncultured, diazotrophic, γ-proteobacterial *nifH* phylotype. *PLoS One* 10, 1–17. doi:10.1371/journal.pone.0128912.

Langlois, R. J., Hümmer, D., and LaRoche, J. (2008). Abundances and distributions of the dominant *nifH* phylotypes in the Northern Atlantic Ocean. *Appl. Environ. Microbiol*. 74, 1922–1931. doi:10.1128/AEM.01720-07.

Langlois, R. J., Laroche, J., and Raab, P. A. (2005). Diazotrophic Diversity and Distribution in the Tropical and Subtropical Atlantic Ocean. *Appl. Environ. Microbiol.* 71, 7910–7919. doi:10.1128/AEM.71.12.7910.

Letunic, I. and Bork, P. (2016). Interactive tree of life (iTOL) v3: an online tool for the display and annotation of phylogenetic and other trees. *Nucleic Acids Res*. 44, W242–W245.

Levollay, J. (1988). L'azote et la vie; l'ouvre de Jean Baptiste Boussingault. *Vies Scientifiques*, CR5, 59–72.

Lomas, M. W., Hopkinson, B. M., Losh, J. L., Ryan, D. E., Shi, D. L., Xu, Y., et al. (2012). Effect of ocean acidification on cyanobacteria in the subtropical North Atlantic. *Aquat. Microb. Ecol.* 66, 211–222. doi:10.3354/ame01576.

Longhurst, A. (1998). *"Ecological geography of the sea"*, ed Academic Press (San Diego, USA).

Ludwig, W., Strunk, O., Westram, R., Richter, L., Meier, H., Yadhukumar, A., et al. (2004) ARB: A software environment for sequence data. *Nucleic Acids Res*. 32, 1363–1371.

Luo, Y. W., Doney, S. C., Anderson, L. A., Benavides, M., Bode, A., Bonnet, S., et al. (2012). Database of diazotrophs in global ocean: abundances, biomass and nitrogen fixation rates. *Earth Syst. Sci. Data Discuss*. 5, 47–106. doi:10.5194/essd-4-47-2012.

Luo, Y. W., Lima, I. D., Karl, D. M., Deutsch, C. A., and Doney, S. C. (2014). Data-based assessment of environmental controls on global marine nitrogen fixation. *Biogeosciences* 11, 691–708. doi:10.5194/bg-11-691-2014.

Mahaffey, C., Michaels, A. F., and Capone, D. G. (2005). The conundrum of Marine N_2 Fixation. *Am. J. Sci.* 305, 546–595. doi:10.2475/ajs.305.6-8.546.

Mahaffey, C., Williams, R. G., Wolff, G. A., Mahowald, N., Anderson, W., and Woodward, M. (2003). Biogeochemical signatures of nitrogen fixation in the eastern North Atlantic. *Geophys. Res. Lett.* 30, 1300. doi:10.1029/2002GL016542.

Malakoff, D. (2012). Researchers struggle to assess responses to ocean acidification. *Science* 338, 27–28. doi: 10.1126/science.338.6103.27

Martín-Platero, A. M., Cleary, B., Kauffman, K., Preheim, S. P., McGillicuddy, D. J., Alm, E. J., and Polz, M. F. (2018). High resolution time series reveals cohesive but short-lived communities in coastal plankton. *Nat. Commun*. 9, 1–11.

Martínez-García, S., Fernández, E., Álvarez-Salgado, X. A., González, J., Lønborg, C., Marañón, E., Morán, X. A. and Teira, E. (2010). Differential responses of phytoplankton and heterotrophic bacteria to organic and inorganic nutrient additions in coastal waters off the NW Iberian Peninsula. *Marine Ecology Progress Series*, 416, 17–33. doi: 10.3354/meps08776.

Martínez-Pérez, C., Mohr, W., Löscher, C. R., Dekaezemacker, J., Littmann, S., Yilmaz, P., et al. (2016). The small unicellular diazotrophic symbiont, UCYN-A, is a key player in the marine nitrogen cycle. *Nat. Microbiol*. 1, 16163. doi:10.1038/nmicrobiol.2016.163.

McMurdie, P. J. and Holmes, S. (2013). Phyloseq: An R Package for Reproducible Interactive Analysis and Graphics of Microbiome Census Data. *PLoS One* 8, e61217.

Messer, L. F., Doubell, M., Jeffries, T. C., Brown, M. V. and Seymour, J. R. (2015a). Prokaryotic and diazotrophic population dynamics within a large oligotrophic inverse estuary. *Aquat. Microb. Ecol.* 74, 1–15.

Messer, L.F., Mahaffey, C., M Robinson, C., Jeffries, T.C., Baker, K.G., Bibiloni Isaksson, J., et al. (2015b). High levels of heterogeneity in diazotroph diversity and activity within a putative hotspot for marine nitrogen fixation. *ISME J.* 10, 1–15.

Michaels, A. F., Karl, D. M., and Capone, D. G. (2001). Element Stoichiometry, New Production and Nitrogen Fixation. *Oceanography* 14, 68–77.

Michaels, A. F., Olson, D., Sarmiento, J. L., Ammerman, J. W., Fanning, K., Jahnke, R., et al. (1996). Inputs, losses and transformations of nitrogen and phosphorus in the pelagic North Atlantic Ocean. *Biogeochemistry* 35, 181–226.

Mills, M. M., Ridame, C., Davey, M., La Roche, J., and Geider, R. J. (2004). Iron and phosphorus co-limit nitrogen fixation in the eastern tropical North Atlantic. *Nature* 429, 292–294.

Mohr, W., Großkopf, T., Wallace, D. W. R., and LaRoche, J. (2010). Methodological underestimation of oceanic nitrogen fixation rates. *PLoS One* 5, 1–7. doi:10.1371/journal.pone.0012583.

Moisander, P. H., Beinart, R. A, Hewson, I., White, A. E., Johnson, K. S., Carlson, C. A, et al. (2010). Unicellular cyanobacterial distributions broaden the oceanic N_2 fixation domain. *Science* 327, 1512–1514. doi:10.1126/science.1185468.

Moisander, P. H., Beinart, R. A., Voss, M., and Zehr, J. P. (2008). Diversity and abundance of diazotrophic microorganisms in the South China Sea during intermonsoon. *ISME J.* 2, 954–967. doi:10.1038/ismej.2008.84.

Moisander, P. H., Benavides, M., Bonnet, S., Berman-Frank, I., White, A. E., and Riemann, L. (2017). Chasing after Non-cyanobacterial Nitrogen Fixation in Marine Pelagic Environments. *Front. Microbiol*. 8, 1736. doi:10.3389/fmicb.2017.01736.

Moisander, P. H., Serros, T., Paerl, R. W., Beinart, R. A., and Zehr, J. P. (2014). Gammaproteobacterial diazotrophs and *nifH* gene expression in surface waters of the South Pacific Ocean. *ISME J.* 8, 1962–1973. doi:10.1038/ismej.2014.49.

Monteiro, F. M., Dutkiewicz, S., and Follows, M. J. (2011). Biogeographical controls on the marine nitrogen fixers. *Global Biogeochem. Cycles* 25, 1–8. doi:10.1029/2010GB003902.

Montoya, J. P. (2007). "Natural abundance of ^{15}N in marine planktonic ecosystems", in *Stable isotopes in ecology and environmental science*, ed Blackwell (New Jersey, USA).

Montoya, J. P. (2008). "Nitrogen Stable Isotopes in Marine Environments", in *Nitrogen in the Marine Environment*, ed Elsevier Inc. (Amsterdam, The Netherlands). doi: 10.1016/B978-0-12-372522-6.00001-3

Montoya, J. P., Carpenter, E. J., and Capone, D. G. (2002). Nitrogen fixation and nitrogen isotop abundance in zooplankton of the oligotrophic North Atlantic. *Limnol. Oceanogr.* 47, 1617–1628. doi:10.4319/lo.2002.47.6.1617.

Montoya, J. P., Voss, M., and Capone, D. G. (2007). Spatial variation in N_2-fixation rate and diazotroph activity in the Tropical Atlantic. *Biogeosciences* 4, 369–376. doi:10.5194/bg-4-369-2007.

Montoya, J. P., Voss, M., Kahler, P., and Capone, D. G. (1996). A Simple, High-Precision, High-Sensitivity Tracer Assay for N_2 Fixation. *Appl. Environ. Microbiol.* 62, 986–993.

Moore, C. M., Mills, M. M., Achterberg, E. P., Geider, R. J., LaRoche, J., Lucas, M. I., et al. (2009). Large-scale distribution of Atlantic nitrogen fixation controlled by iron availability. *Nat. Geosci.* 2, 867–871. doi:10.1038/ngeo667.

Moore, L. R., Post, A. F., Rocap, G., and Chisholm, S. W. (2002). Utilization of different nitrogen sources by the marine cyanobacteria *Prochlorococcus* and *Synechococcus*. *Limnol. Oceanogr*. 47, 989–996.

Moreira-Coello, V., Mouriño-Carballido, B., Marañón, E., Fernández-Carrera, A., Bode, A., and Varela, M.M. (2017). Biological N_2 Fixation in the Upwelling Region off NW Iberia: Magnitude, Relevance, and Players. *Front. Mar. Sci.* 4, 303.

Mouillot, D., Stubbs, W., Faure, M., Dumay, O., Tomasini, J. A., Wilson, J. B., and Chi, T. D. (2005). Niche overlap estimates based on quantitative functional traits: a new family of non-parametric indices. *Oecologia* 145, 345–353, https://doi.org/10.1007/s00442-005-0151-z

Moum, J. N. and Smyth, W. D. (2001). *Upper Ocean Mixing*. Academic Press (Oxford, UK), 3093.

Mouriño-Carballido, B., Graña, R., Fernández, A., Bode, A., Varela, M., Domínguez, J. F., et al. (2011). Importance of N_2 fixation vs. nitrate eddy diffusion along a latitudinal transect in the Atlantic Ocean. *Limnol. Oceanogr*. 56, 999–1007. doi:10.4319/lo.2011.56.3.0999.

Mouriño-Carballido, B., Hojas, E., Cermeño, P., Chouciño, P., Fernández-Castro, B., Latasa, M., et al. (2016). Nutrient supply controls picoplankton community structure during three contrasting seasons in the northwestern Mediterranean Sea. *Mar. Ecol. Prog. Ser.* 543, 1–19. doi:10.3354/meps11558.

Mouriño-Carballido, B., Pahlow, M., and Oschlies, A. (2012). High sensitivity of ultra-oligotrophic marine ecosystems to atmospheric nitrogen deposition. *Geophys. Res. Lett.* 39, 1–6. doi:10.1029/2011GL050606.

Mulholland, M. R., and Bernhardt, P. W. (2005). The effect of growth rate, phosphorus concentration, and temperature on N_2 fixation, carbon fixation, and nitrogen release in continuous cultures of *Trichodesmium* IMS101. *Limnol. Oceanogr*. 50, 839–849.

Mulholland, M. R., Bernhardt, P. W., Blanco-Garcia, J. L., Mannino, A., Hyde, K., Mondragon, E., et al. (2012). Rates of dinitrogen fixation and the abundance of diazotrophs in North American coastal waters between Cape Hatteras and Georges Bank. *Limnol. Oceanogr*. 57, 1067–1083. doi:10.4319/lo.2012.57.4.1067.

Mulholland, M., Ohki, K. and Capone, D. G. (1999). Nitrogen utilization and metabolism relative to patterns of N_2 fixation in cultures of *Trichodesmium* NIBB 1067. *J. Phycol*. 35, 977–988.

Mulholland, M., Ohki, K. and Capone, D. G. (2001). Nutrient controls on nitrogen uptake and metabolism by natural populations and cultures of *Trichodesmium* (cyanobacteria). *J. Phycol.* 37, 1001–1009.

Ohyama, T., and Kumazawa, K. (1981). A simple method for the preparation, purification and storage of $^{15}N_2$ gas for biological nitrogen fixation studies. *Soil Sci. Plant Nutr*. 27, 263–265. doi:10.1080/00380768.1981.10431278.

Osborn, T. R. (1980). Estimates of the Local Rate of Vertical Diffusion from Dissipation Measurements. *J. Phys. Oceanogr*. 10(1), 83–89.

Oschlies, A., and Garçon, V. (1998). Eddy-induced enhancement of primary production in a model of the North Atlantic Ocean. *Nature* 394, 266–269. doi:10.1038/28373.

Paerl, H. W., Zehr, J. P. (2000). "Marine nitrogen fixation", in *Microbial Ecology of the Oceans*, eds D. L. Kirchman, ed Wiley-Liss (New York, USA), 387−426.

Painter, S. C., Patey, M. D., Forryan, A., and Torres-Valdes, S. (2013). Evaluating the balance between vertical diffusive nitrate supply and nitrogen fixation with reference

to nitrate uptake in the eastern subtropical North Atlantic Ocean. *J. Geophys. Res. Ocean.* 118, 5732–5749. doi:10.1002/jgrc.20416.

Pardo, P. C., Padín, X. A., Gilcoto, M., Farina-Busto, L., and Pérez, F. F. (2011). Evolution of upwelling systems coupled to the long-term variability in sea surface temperature and Ekman transport. *Clim. Res.* 48, 231–246. doi:10.3354/cr00989.

Pelegrí, J. L., Marrero-Díaz, A., and Ratsimandresey, A. W. (2006). Nutrient irrigation of the North Atlantic. *Prog. Oceanogr*. 70, 366–406. doi: 10.1016/j.pocean.2006.03.018

Pérez, F. F., Padín, X. A., Pazos, Y., Gilcoto, M., Cabanas, M., Pardo, P. C., et al. (2010). Plankton response to weakening of the Iberian coastal upwelling. *Glob. Chang. Biol*. 16, 1258–1267. doi:10.1111/j.1365-2486.2009.02125.x.

Pernthaler, A., Pernthaler, J., and Amann, R. (2004). Sensitive multi-color fluorescence in situ hybridization for the identification of environmental microorganisms. *Molecular Microbial Ecology Manual* 3: 2613–2627.

Pitcher, G. C., Figueiras, F. G., Hickey, B. M., and Moita, M. T. (2010). The physical oceanography of upwelling systems and the development of harmful algal blooms. *Prog. Oceanogr*. 85, 5–32. doi:10.1016/j.pocean.2010.02.002.

Planas, D., Agustí, S., Duarte, C. M., Granata, T. C., and Merino, M. (1999). Nitrate uptake and diffusive nitrate supply in the Central Atlantic. *Limnol. Oceanogr*. 44, 116–126. doi:10.4319/lo.1999.44.1.0116.

Postgate, J. R. (1982). *The fundamentals of nitrogen fixation*. Cambridge University Press, London.

Prandke, H., and Stips, A. (1998). Test measurements with an operational microstructure turbulence profiler: Detection limit of dissipation rates. *Aquat. Sci*. 60, 191–209.

Prospero, J. M., Barrett, K., Church, T., Dentener, F., Duce, R. A., Galloway, J. N., et al. (1996). Atmospheric deposition of nutrients to the North Atlantic Basin. *Biogeochemistry* 35, 27–73.

R Core Team: R: A Language and Environment for Statistical Computing, http://www.r-project.org/, 2015.

Raimbault, P., and Garcia, N. (2008). Evidence for efficient regenerated production and dinitrogen fixation in nitrogen-deficient waters of the South Pacific Ocean: impact on new and export production estimates. *Biogeosciences* 5, 323–338. doi:10.5194/bg-5-323-2008.

Ratten, J. M., LaRoche, J., Desai, D. K., Shelley, R. U., Landing, W. M., Boyle, E., et al. (2015). Sources of iron and phosphate affect the distribution of diazotrophs in the North Atlantic. *Deep. Res. Part II Top. Stud. Oceanogr.* 116, 332–341. doi:10.1016/j.dsr2.2014.11.012.

Redfield, A. C., Ketchum, B. H. and Richards, F. A. (1963). "The influence of organisms on the composition of seawater", in *The sea: Ideas and observations on progress in the study of the seas*, Vol. 2, ed Interescience Publishers (New York, USA), 26–77.

Rees, D. C., Akif Tezcan, F., Haynes, C. A., Walton, M. Y., Andrade, S., Einsle, O., et al. (2005). Structural basis of biological nitrogen fixation. *Philos. Trans. R. Soc.* 363, 971–984. doi:10.1098/rsta.2004.1539.

Rees, A., Gilbert, J., and Kelly-Gerreyn, B. (2009). Nitrogen fixation in the western English Channel (NE Atlantic Ocean). *Mar. Ecol. Prog. Ser.* 374, 7–12. doi:10.3354/meps07771.

Riemann, L., Farnelid, H., and Steward, G. F. (2010). Nitrogenase genes in non-cyanobacterial plankton: Prevalence, diversity and regulation in marine waters. *Aquat. Microb. Ecol.* 61, 235–247. doi:10.3354/ame01431.

Rijkenberg, M. J. A., Steigenberger, S., Powell, C. F., van Haren, H., Patey, M. D., Baker, A. R., et al. (2012). Fluxes and distribution of dissolved iron in the eastern (sub-) tropical North Atlantic Ocean. *Global Biogeochem. Cycles* 26, GB3004. doi:10.1029/2011GB004264.

Robidart, J.C., Church, M.J., Ryan, J.P., Ascani, F., Wilson, S.T., Bombar, D., et al. (2014). Ecogenomic sensor reveals controls on N_2-fixing microorganisms in the North Pacific Ocean. *ISME J.* 8, 1175–1185.

Sañudo-Wilhelmy, S. A., Tovar-Sanchez, A., Fu, F.-X., Capone, D. G., Carpenter, E. J., and Hutchins, D. A. (2004). The impact of surface-adsorbed phosphorus on phytoplankton Redfield stoichiometry. *Nature* 432, 897–901. doi:10.1029/2001JB001696.

Shannon, C. E. (1948). A mathematical theory of communication. *Bell Syst. Tech* 27, 379–423.

Schlosser, C., Klar, J. K., Wake, B. D., Snow, J. T., Honey, D. J., Woodward, E. M. S., et al. (2014). Seasonal ITCZ migration dynamically controls the location of the (sub)tropical Atlantic biogeochemical divide. *Proc. Natl. Acad. Sci. U. S. A.* 111, 1438–1442. doi:10.1073/pnas.1318670111.

Schollhorn, R., and Burris, R. H. (1967). Acetylene as a competitive inhibitor of N_2 fixation. *Proc. Natl. Acad. Sci*. 58, 213–216. doi:10.1073/pnas.58.1.213.

Shi, D., Kranz, S. A., Kim, J.-M., and Morel, F. M. M. (2012). Ocean acidification slows nitrogen fixation and growth in the dominant diazotroph *Trichodesmium* under low-iron conditions. *Proc. Natl. Acad. Sci*. 109, E3094–E3100. doi:10.1073/pnas.1216012109/-/DCSupplemental.www.pnas.org/cgi/doi/10.1073/pnas.1216012109.

Shiozaki, T., Bombar, D., Riemann, L., Hashihama, F., Takeda, S., Yamaguchi, T., et al. (2017). Basin scale variability of active diazotrophs and nitrogen fixation in the North Pacific, from the tropics to the subarctic Bering Sea. *Global Biogeochem. Cycles* 31, 996–1009. doi:10.1002/2017GB005681.

Shiozaki, T., Fujiwara, A., Ijichi, M., Harada, N., Nishino, S., Nishi, S., et al. (2018). Diazotroph community structure and the role of nitrogen fixation in the nitrogen cycle in the Chukchi Sea (western Arctic Ocean). *Limnol. Oceanogr*. doi:10.1002/lno.10933.

Sigman, D. M., Altabet, M. A., McCorkle, D. C., Francois, R., and Fischer, G. (2000). The $\delta^{15}N$ of nitrate in the Southern Ocean: Nitrogen cycling and circulation in the ocean interior. *J. Geophys. Res. Ocean*. 105, 19599–19614. doi:10.1029/2000JC000265.

Sigman, D. M., Altabet, M. A., Michener, R., McCorkle, D. C., Fry, B. and Holmes, R. M. (1997). Natural abundance-level measurement of the nitrogen isotopic composition of oceanic nitrate: an adaptation of the ammonia diffusion method. *Marine Chemistry* 57, 227– 242.

Smil, V. (2001). *Enriching the earth. Fritz Haber, Carl Bosch, and the transformation of world food production*. Cambridge, MA: The MIT Press.

Sohm, J. A., Hilton, J. A., Noble, A. E., Zehr, J. P., Saito, M. A., and Webb, E. A. (2011a). Nitrogen fixation in the South Atlantic Gyre and the Benguela Upwelling System. *Geophys. Res. Lett*. 38, 1–6. doi:10.1029/2011GL048315.

Sohm, J. A., Webb, E. A., and Capone, D. G. (2011b). Emerging patterns of marine nitrogen fixation. *Nat. Rev. Microbiol*. 9, 499–508. doi:10.1038/nrmicro2594.

Staal, M., te Lintel-Hekkert, S., Harren, F., and Stal, L. (2001). Nitrogenase activity in cyanobacteria measured by the acetylene reduction assay: a comparison between batch incubation and on-line monitoring. *Environ. Microbiol*. 3, 343–351. doi:10.1046/j.1462-2920.2001.00201.x.

Stal, L. J. (2009). Is the distribution of nitrogen-fixing cyanobacteria in the oceans related to temperature? *Environ. Microbiol.* 11, 1632–1645. doi:10.1111/j.1758-2229.2009.00016.x.

Stam, H., Stouthamer, A. H., and van Verseveld, H. W. (1987). Hydrogen metabolism and energy costs of nitrogen fixation. *FEMS Microbiol. Rev*. 46, 73–92.

Stewart, W. D. P., Fitzgerald, G. P., and Burris, R. H. (1967). In situ studies on N_2 fixation using the acetylene reduction technique. *Proc Natl Acad Sci* 58, 2071–2078.

Stramma, L., Johnson, G. C., Sprintall, J., and Mohrholz, V. (2008). Expanding Oxygen-Minimum Zones in the Tropical Oceans. *Science* 320, 655–658. doi:10.1126/science.1153847.

Subramaniam, A., Mahaffey, C., Johns, W., and Mahowald, N. (2013). Equatorial upwelling enhances nitrogen fixation in the Atlantic Ocean. *Geophys. Res. Lett.* 40, 1766–1771. doi:10.1002/grl.50250.

Subramaniam, A., Yager, P. L., Carpenter, E. J., Mahaffey, C., Björkman, K., Cooley, S., et al. (2008). Amazon River enhances diazotrophy and carbon sequestration in the tropical North Atlantic Ocean. *Proc. Natl. Acad. Sci*. 105, 10460–10465. doi:10.1029/2006GB002751.

Teeling, H., Fuchs, B.M., Becher, D., Klockow, C., Gardebrecht, A., Bennke, C. M., et al. (2012). Substrate-controlled succession of marine bacterioplankton populations induced by a phytoplankton bloom. *Science* 336, 608–611.

Teira, E., Abalde, J., Álvarez-Ossorio, M. T., Bode, A., Cariño, C., Cid, Á., Fernández, E., González, N., Lorenzo, J., Valencia, J. and Varela, M. (2003). Plankton carbon

budget in a coastal wind-driven upwelling station off A Coruña (NW Iberian Peninsula). *Marine Ecology Progress Series*, 265, 31–43.

Thompson, A., Carter, B. J., Turk-Kubo, K., Malfatti, F., Azam, F., and Zehr, J. P. (2014). Genetic diversity of the unicellular nitrogen-fixing cyanobacteria UCYN-A and its prymnesiophyte host. *Environ. Microbiol.* 16, 3238–3249. doi:10.1111/1462–2920.12490. doi:10.1111/1462-2920.12490.

Thompson, A. W., Foster, R. A., Krupke, A., Carter, B. J., Musat, N., Vaulot, D., et al. (2012). Unicellular Cyanobacterium Symbiotic with a Single-Celled Eukaryotic Alga. *Science* 337, 1546–1550.

Thorpe, S.A. (2004). Recent developments in the study of ocean turbulence. *Annu. Rev. Earth Planet. Sci.* 20(32), 91–109. doi: 10.1146/annurev.earth.32.071603.152635

Torres-Valdés, S., Roussenov, V. M., Sanders, R., Reynolds, S., Pan, X., Mather, R., et al. (2009). Distribution of dissolved organic nutrients and their effect on export production over the Atlantic Ocean. *Global Biogeochem. Cycles* 23, 1–16. doi:10.1029/2008GB003389.

Tripp, H. J., Bench, S. R., Turk, K. A., Foster, R. A., Desany, B. A., Niazi, F., et al. (2010). Metabolic streamlining in an open-ocean nitrogen-fixing cyanobacterium. *Nature* 464, 90–94. doi:10.1038/nature08786.

Tuit, C., Waterbury, J., and Ravizza, G. (2004). Diel variation of molybdenum and iron in marine diazotrophic cyanobacteria. *Limnol. Ocean.* 49, 978–990.

Turk-Kubo, K. A., Farnelid, H. M., Shilova, I. N., Henke, B., and Zehr, J. P. (2017). Distinct ecological niches of marine symbiotic N_2-fixing cyanobacterium *Candidatus* Atelocyanobacterium thalassa sublineages. *J. Phycol.* 53, 451–461. doi:10.1111/jpy.12505.

Turk-Kubo, K. A., Karamchandani, M., Capone, D. G., and Zehr, J. P. (2014). The paradox of marine heterotrophic nitrogen fixation: abundances of heterotrophic diazotrophs do not account for nitrogen fixation rates in the Eastern Tropical South Pacific. *Environmental Microbiology*, 16(10), 3095–3114. doi: 10.1111/1462-2920.12346.

Turk, K., Rees, A. P., Zehr, J. P., Pereira, N., Swift, P., Shelley, R., Lohan, M., Woodward, E. M. S. and Gilbert, J. (2011) Nitrogen fixation and nitrogenase (*nifH*) expression in tropical waters of the eastern North Atlantic. *ISME J.* 5, 1201–1212.

Ugland, K. I., Gray, J. S., and Ellingsen, K. E. (2003). The species–accumulation curve and estimation of species richness. *J. Anim. Ecol*. 72, 888–897.

Varela, M. (1992). Upwelling and phytoplankton ecology in Galician (NW Spain) rias and shelf waters. *Boletín Inst. Español Oceanogr*. 8: 57–74.

Varela, M., Prego, R., Belzunce, M. J., and Salas, F. M. (2001). Inshore-offshore differences in seasonal variations of phytoplankton assemblages: The case of a Galician Ria Alta (Ria de A Coruña) and its adjacent shelf (NW of Spain). *Cont. Shelf Res*. 21, 1815–1838. doi:10.1016/S0278-4343(01)00032-2.

Villamaña, M., Mouriño-Carballido, B., Marañón, E., Cermeño, P., Chouciño, P., da Silva, J. C. B., et al. (2017). Role of internal waves on mixing, nutrient supply and phytoplankton community structure during spring and neap tides in the upwelling ecosystem of Ría de Vigo (NW Iberian Peninsula). *Limnol. Ocean*. 62, 1014–1030. doi:10.1002/lno.10482.

Villareal, T. A. (1992). "Marine nitrogen-fixing diatom-cyanobacterial symbioses", in *Marine Pelagic Cyanobacteria. Trichodesmium and other diazotrophs*, ed Kluwer Academic Press (Dordrecht, The Netherlands), 163–175.

Voss, M., Bange, H. W., Dippner, J. W., Middelburg, J. J., Montoya, J. P., and Ward, B. (2013). The marine nitrogen cycle: recent discoveries, uncertainties and the potential relevance of climate change. *Philos. Trans. R. Soc.* 368, 20130121.

Voss, M., Croot, P., Lochte, K., Mills, M., and Peeken, I. (2004). Patterns of nitrogen fixation along 10ºN in the tropical Atlantic. *Geophys. Res. Lett*. 31, L23S09. doi:10.1029/2004GL020127.

Wannicke, N., Benavides, M., Dalsgaard, T., Dippner, J. W., Montoya, J. P., and Voss, M. (2018). New Perspectives on Nitrogen Fixation Measurements Using $^{15}N_2$ Gas. *Frontiers in Marine Science*, 5, 120. doi: 10.3389/fmars.2018.00120.

Webb, E. A., Ehrenreich, I. M., Brown, S. L., Valois, F. W., Waterbury, J. B. (2009). Phenotypic and genotypic characterization of multiple strains of the diazotrophic

cyanobacterium *Crocosphaera watsonii* isolated from the open ocean. *Environ. Microbiol*. 11, 338–348.

Weiss, R. F. (1970). The solubility of nitrogen, oxygen and argon in water and seawater. *Deep. Res*. 17, 721–735.

Wen, Z., Lin, W., Shen, R., Hong, H., Kao, S.-J., and Shi, D. (2017). Nitrogen fixation in two coastal upwelling regions of the Taiwan Strait. *Sci. Rep.* 7, 17601. doi:10.1038/s41598-017-18006-5.

Williams, R. G., and Follows, M. J. (1998). The Ekman transfer of nutrients and maintenance of new production over the North Atlantic. *Deep. Res. Part I Oceanogr. Res. Pap.* 45, 461–489. doi:10.1016/S0967-0637(97)00094-0.

Wilson, S. T., Bottjer, D., Church, M. J., Karl, D. M., Böttjer, D., Church, M. J., et al. (2012). Comparative assessment of nitrogen fixation methodologies, conducted in the oligotrophic North Pacific Ocean. *Appl. Environ. Microbiol*. 78, 6516–6523. doi:10.1128/AEM.01146-12.

Wooster, W. S., Bakun, A. and McClain, D.R. (1976). The seasonal upwelling cycle along the eastern boundary of the North Atlantic. *J. Mar. Res.* 34, 131–146.

Worden, A. Z., Nolan, J. K., and Palenik, B. (2004). Assessing the dynamics and ecology of marine picophytoplankton: The importance of the eukaryotic component. *Limnol. Oceanogr*. 49, 168–179. doi:10.4319/lo.2004.49.1.0168.

Wuchter, C., Abbas, B., Coolen, M. J. L., Herfort, L., van Bleijswijk, J., Timmers, P., et al. (2006). Archaeal nitrification in the ocean. *Proc. Natl. Acad. Sci*. 14, 12317–12322.

Yool, A., Martin, A. P., Fernández, C., and Clark, D. R. (2007). The significance of nitrification for oceanic new production. *Nature* 447, 999–1002. doi:10.1038/nature05885.

Zehr, J. P. (2011). Nitrogen fixation by marine cyanobacteria. *Trends Microbiol*. 19, 162–173. doi:10.1016/j.tim.2010.12.004.

Zehr, J. P., Carpenter, E. J., and Villareal, T. A. (2000). New perspectives on nitrogen-fixing microrganisms in tropical and subtropical oceans. *Trends Microbiol*. 8, 68–73.

Zehr, J. P., Crumbliss, L. L., Church, M. J., Omoregie, E. O., and Jenkins, B. D. (2003a) Nitrogenase genes in PCR and RT-PCR reagents: Implications for studies of diversity of functional genes. *BioTechniques* 35, 996–1005.

Zehr, J., Jenkins, B., Short, S., and Steward, G. (2003b). Nitrogenase gene diversity and microbial community structure: a cross-system comparison. *Environ. Microbiol*. 5, 539–554.

Zehr, J. P. and McReynolds, L. A. (1989). Use of degenerate oligonucleotides for amplification of the *nifH* gene from the marine cyanobacterium *Trichodesmium thiebautii*. *Appl. Environ. Microbiol*. 55, 2522–2526.

Zehr, J. P., Mellon, M., Braun, S., Litaker, W., Steppe, T., and Paerl, H. W. (1995). Diversity of Heterotrophic Nitrogen Fixation Genes in a Marine Cyanobacterial Mat. *Appl. Environ. Microbiol*. 61, 2527–2532.

Zehr, J. P., Mellon, M. T., and Zani, S. (1998). New nitrogen-fixing microorganisms detected in oligotrophic oceans by amplification of nitrogenase (*nifH*) genes. *Appl. Environ. Microbiol*. 64, 3444–3450. doi:PMC106745.

Zehr, J. P., Montoya, J. P., Jenkins, B. D., Hewson, I., Mondragon, E., Short, C. M., et al. (2007). Experiments linking nitrogenase gene expression to nitrogen fixation in the North Pacific subtropical gyre. *Limnol Oceanogr* 52: 169–183.

Zehr, J. P., Shilova, I. N., Farnelid, H. M., Muñoz-Marín, M. C., and Turk-Kubo, K. A. (2016). Unusual marine unicellular symbiosis with the nitrogen-fixing cyanobacterium UCYN-A. *Nat. Microbiol*. 2, 16214. doi:10.1038/nmicrobiol.2016.214.

Zehr, J. P. and Turner, P. J. (2001). Nitrogen Fixation: Nitrogenase Genes and Gene Expression. *Methods Microbiol*. 30, 271–286.

Zehr, J. P., and Ward, B. B. (2002). Nitrogen Cycling in the Ocean: New Perspectives on Processes and Paradigms. *Appl. Environ. Microbiol*. 68, 1015–1024. doi:10.1128/AEM.68.3.1015.

Zhang, J., Kobert, K., Flouri, T., and Stamatakis, A. (2014). PEAR: A fast and accurate Illumina Paired-End reAd mergeR. *Bioinformatics* 30, 614–620.

8.
Summary in Spanish/Resumen en español

8.1. Introducción

8.1.1. Fijación biológica de N_2 en el medio marino

El nitrógeno (N) es un elemento esencial para la vida y el principal nutriente limitante de la producción primaria en ecosistemas acuáticos y terrestres (Falkowski, 1997). Tiene un papel clave en la compleja biogeoquímica del océano ya que afecta significativamente a los ciclos biogeoquímicos de otros elementos importantes como el carbono y el fósforo (Gruber, 2008). La mayoría de formas de N que se encuentran en el agua de mar están biodisponibles (nitrato, NO_3^-; nitrito, NO_2^-; amonio, NH_4^+; o compuestos orgánicos disueltos). Sin embargo, la más abundante es el nitrógeno molecular (N_2), el cual no es accesible a la mayoría de los organismos. Solamente un limitado, pero diverso, grupo de bacterias y arqueas conocido como diazótrofos pueden utilizar este gran reservorio de N mediante la fijación de N_2 (Karl et al., 2002).

La enzima nitrogenasa es una destacable invención evolutiva puesto que permite llevar a cabo el proceso de fijación biológica de N_2, catalizando la reducción de N_2 al biológicamente asimilable NH_4^+, una reacción altamente dependiente de energía (ATP) (Zehr et al., 1998). La nitrogenasa está codificada por genes muy conservados, indicando que tiene un origen muy antiguo ya que se cree que apareció cuando la atmósfera terrestre era reductora, lo que podría explicar su inactivación en presencia de oxígeno (Zehr et al., 1995). Este complejo enzimático está constituido por dos metaloproteínas: dinitrogenasa y dinitrogenasa reductasa. La dinitrogenasa reductasa es una proteína dimérica cuyo cofactor metálico es el hierro (Fe), mientras que la dinitrogenasa es tetramérica y el cofactor metálico es el molibdeno (Mo), aunque algunos diazótrofos pueden reemplazarlo por Fe o vanadio (Dixon and Kahn, 2004). La estructura de la dinitrogenasa reductasa está altamente conservada ya que muestra escasa variabilidad entre las diferentes especies de diazótrofos. Por ello, el gen que la codifica (*nifH*) es una herramienta muy útil para los estudios de diversidad diazotrófica (Paerl y Zehr, 2000).

La reducción biológica de N_2 catalizada por la nitrogenasa tiene la siguiente estequiometría:

$$N_2 + 8H^+ + 8e^- + 16ATP \rightarrow 2NH_3 + H_2 + 16ADP + 16P_i \quad (1)$$

Este proceso estimula la actividad fotosintética del fitoplancton debido al suministro de N nuevo en forma de amonio, pero requiere una alta cantidad de energía (16 ATP) y poder

reductor (8 electrones) para romper el triple enlace del N_2. Por este motivo, la actividad de la nitrogenasa está regulada y controlada, por ejemplo, por la concentración de nutrientes (Karl et al., 2002).

8.1.2. Relevancia de la fijación biológica de N_2 como mecanismo de suministro de nitrógeno nuevo

La fijación biológica de N_2, junto con otros procesos como el transporte horizontal (Torres-Valdés et al., 2009; Williams and Follows, 1998), flujos verticales difusivos (Mouriño-Carballido et al., 2011) y advectivos (Pitcher et al., 2010), procesos de mesoescala y submesoescala (Oschlies and Garçon, 1998) o deposición atmosférica (Duce et al., 2008; Mouriño-Carballido et al., 2012), suministran N nuevo a la capa eufótica. Los diazótrofos tienen una notable ventaja competitiva sobre el resto de especies de fitoplancton en las vastas regiones oligotróficas de los océanos porque pueden usar la fijación de N_2 como principal fuente de N cuando los otros aportes son escasos o están ausentes. Teniendo en cuenta que las regiones oligotróficas ocupan más del 70% de la superficie total del océano (Longhurst, 1998), este suministro de N nuevo mediado por organismos tiene un papel clave en la productividad oceánica, el ciclo del carbono y el clima (Gruber and Galloway, 2008).

La difusión turbulenta vertical es uno de los principales mecanismos de suministro de N nuevo en grandes extensiones del océano abierto (Fernández-Castro et al., 2015; Mouriño-Carballido et al., 2011; Painter et al., 2013) y en regiones costeras durante los periodos de estratificación térmica de verano. Los estudios que han cuantificado simultáneamente la fijación de N_2 frente al transporte de nitrato hacia la superficie a través de mezcla turbulenta, han dado lugar a un amplio rango de resultados. A escala global, la difusión de nitrato parece dominar sobre la fijación de N_2, aunque en algunas áreas de los giros subtropicales la fijación de N_2 iguala o incluso excede la entrada de N nuevo a través de la difusión (Capone et al., 2005; Fernández-Castro et al., 2015; Mouriño-Carballido et al., 2011; Painter et al., 2013). El flujo global estimado de suministro de N nuevo al océano a través de la fijación biológica de N_2 es de ~120 Tg N a^{-1} (Gruber, 2008), que podría llegar a sustentar la mitad de la producción primaria nueva en regiones oligotróficas (Karl et al., 1997).

Para cuantificar el transporte de nutrientes hacia la capa eufótica mediante difusión turbulenta vertical es necesario estimar la magnitud de la difusividad vertical (*Kz*) (Fernández-Castro et al., 2014). Las dificultades metodológicas implícitas para medir directamente la turbulencia de microestructura y cuantificar el flujo difusivo de nutrientes motivó el uso de valores constantes de *Kz* (Capone et al., 2005) y parametrizaciones empíricas de la difusividad (Fernández-Castro et al., 2014; Planas et al., 1999). Actualmente, las estimas de *Kz* a partir de observaciones son posibles gracias a instrumentos como los perfiladores de microestructura (MSS, Prandke and Stips, 1998) que permiten medir directamente la turbulencia de pequeña escala.

En los últimos años los perfiladores de turbulencia de microestructura han sido usados con frecuencia para medir difusividad vertical en diferentes regiones del medio marino (e.g., Cuypers et al., 2012; Fernández-Castro et al., 2014; Hibiya et al., 2007; Jurado et al., 2012; Mouriño-Carballido et al., 2011, 2016; Villamaña et al., 2017). Sin embargo, actualmente nuestro conocimiento de la turbulencia en el océano, sus mecanismos de generación y su distribución a escala global es todavía escaso.

8.1.3. Diversidad de organismos fijadores de N_2

Los diazótrofos son exclusivamente organismos procariotas (bacterias y arqueas) muy diversos tanto en forma como en función. A pesar de la alta diversidad de microorganismos fijadores, los que se han estudiado tradicionalmente en el medio marino son la cianobacteria colonial *Trichodesmium* y los simbiontes cianobacterianos de diatomeas. *Trichodesmium* es una cianobacteria filamentosa no heterocística que se encuentra en los cálidos y oligotróficos océanos tropicales y subtropicales, donde fijan N_2 a tasas relativamente altas y donde forman frecuentemente grandes proliferaciones (Capone et al., 1997, 2005). De hecho, este organismo planctónico es considerado el principal diazótrofo marino debido a sus altas abundancias y elevadas tasas de fijación. Los simbiontes diazótrofos de diatomeas son cianobacterias filamentosas heterocísticas con una distribución y abundancia irregulares, ampliamente distribuidas a lo largo del océano tropical y subtropical y plumas de grandes ríos, donde las diatomeas se benefician del exceso de sílice (Sohm et al., 2011b). Estas especies forman una cadena de unas pocas células con un heterocisto terminal. En el océano podemos encontrar a *Richelia*, endosimbionte de las diatomeas *Rhizosolenia* y *Hemiaulus* (viviendo dentro del frústulo

pero en la parte externa de la pared celular), y *Calothrix*, epibionte de la diatomea *Chaetoceros* (viviendo sobre la parte externa del frústulo) (Zehr, 2011).

Los diazótrofos marinos también incluyen a cianobacterias unicelulares distribuidas globalmente (Zehr, 2011): UCYN-A o grupo A no cultivado, UCYN-B o *Crocosphaera* sp. y UCYN-C, probablemente de vida libre, que comprende a cianobacterias cultivadas como la bentónica *Cyanothece* sp. En los últimos años, UCYN-A (o *Candidatus* Atelocyanobacterium thalassa) ha despertado un gran interés ya que es uno de los miembros más importantes de la comunidad diazótrofa global debido a su amplia distribución en el medio marino y sus tasas de fijación de N_2 relativamente altas (Farnelid et al., 2016; Martínez-Pérez et al., 2016). A diferencia de *Trichodesmium*, UCYN-A puede ser detectada a lo largo de un rango latitudinal más amplio y a mayores profundidades (Moisander et al., 2010), incluso en ecosistemas de afloramiento (Sohm et al., 2011a). Esta cianobacteria unicelular carece de genes para el fotosistema II, la enzima RuBisCO (ribulosa bifosfato carboxilasa) para la fijación de carbono, el ciclo del ácido tricarboxílico y algunas rutas metabólicas para la síntesis de aminoácidos y purinas (Tripp et al., 2010). Por tanto, vive en obligada asociación con una primnesiofita picoeucariota que le proporciona compuestos orgánicos (Thompson et al., 2012, 2014). La simbiosis unicelular que se establece entre ellos es un modelo muy interesante para observar la evolución de orgánulos en células eucariotas, concretamente orgánulos fijadores de N_2 (Zehr et al., 2016). Seis sublinajes de UCYN-A (UCYN-A1 hasta -A6) han sido definidos previamente en base a la diversidad genética de las secuencias *nifH* disponibles en la base de datos del NCBI GenBank (Farnelid et al., 2016; Thompson et al., 2014; Turk-Kubo et al., 2017). Hallazgos recientes indican que estos sublinajes ocupan diferentes nichos ecológicos. Por ejemplo, UCYN-A1 domina en el océano abierto oligotrófico, mientras que UCYN-A2 se encuentra principalmente en regiones costeras (Farnelid et al., 2016; Messer et al., 2015a; Thompson et al., 2014; Turk-Kubo et al., 2017).

La comunidad diazótrofa planctónica engloba también a diazótrofos no cianobacterianos. Las bacterias heterótrofas fijadoras de N_2 incluyen un amplio rango de grupos filogenéticos como Firmicutes y Proteobacteria, entre otros (Zehr et al., 2003b), mientras que las arqueas diazótrofas parecen incluir sólo a metanógenos (Riemann et al., 2010). Aunque las cianobacterias son tradicionalmente consideradas los fijadores más importantes, en años recientes se ha demostrado que diazótrofos no cianobacterianos potencialmente activos podrían tener una mayor distribución geográfica y en profundidad

(Bombar et al., 2016; Delmont et al., 2018; Moisander et al., 2017). En cualquier caso, actualmente se desconocen muchos detalles sobre su contribución a la fijación de N_2 global, relevancia ecológica y ecofisiología.

8.1.4. Factores ambientales de control

En los últimos años numerosos estudios han investigado la biogeografía y mecanismos de control de la fijación de N_2 en el medio marino (e.g., Fernández-Castro et al., 2016; Fernández et al., 2010; Luo et al., 2014; Moore et al., 2009). La influencia de los factores de control depende en gran medida de la composición de la comunidad diazótrofa presente ya que cada grupo diazótrofo tiene diferente autoecología y distintas limitaciones fisiológicas. En general, nutrientes (N, P y Fe), oxígeno (O_2) y temperatura son comúnmente considerados los factores de control más importantes, aunque el alcance de la influencia de cada uno de ellos está todavía en debate.

8.1.5. Fijación de N_2 en una región rica en nitrógeno: el sistema de afloramiento del NO de la Península Ibérica

Debido al alto coste energético de fijar N_2 en comparación con la asimilación de nitrógeno inorgánico disuelto (principalmente amonio y nitrato) (Stam et al., 1987), la disponibilidad de N fijado siempre se ha considerado como inhibidora de la actividad diazótrofa. Sin embargo, estudios recientes demuestran la presencia y actividad de diazótrofos en aguas relativamente ricas en N, como la costa este de los EEUU (Mulholland et al., 2012), el oeste del Canal Inglés (Rees et al., 2009), el Océano Ártico (Shiozaki et al., 2017, 2018), y regiones de afloramiento como el sistema de Benguela (Benavides et al., 2014; Sohm et al., 2011a), el este del Atlántico Ecuatorial (Foster et al., 2009; Subramaniam et al., 2013; Voss et al., 2004), la costa central de Chile (Fernández et al., 2015; Raimbault and Garcia, 2008) o el Estrecho de Taiwán (Wen et al., 2017). Sin embargo, el paradigma clásico sobre fijación de N_2 establece que este proceso está principalmente limitado a las aguas cálidas y pobres en N de los océanos tropicales y subtropicales. Por este motivo, la mayoría de estudios sobre fijación de N_2 se han llevado a cabo en estas regiones (40ºS–40ºN). En cualquier caso, las evidencias de fijación encontradas en áreas previamente no estudiadas, junto con la gran diversidad de diazótrofos marinos y su amplia distribución (Farnelid et al., 2011; Riemann et al., 2010;

Zehr et al., 2000, 2003b) expandió el rango de ambientes donde la fijación de N_2 puede ser un proceso importante (Moisander et al., 2010).

El NO de la Península Ibérica está caracterizado por la presencia de entrantes denominados Rías y la influencia estacional de eventos de afloramiento y hundimiento generados por el viento que producen una gran variabilidad a escalas temporales cortas (Fraga, 1981; Wooster et al., 1976). Desde abril a septiembre, los vientos prevalentes del norte causan afloramientos, que consisten en el ascenso de aguas subsuperficiales frías y ricas en nutrientes hacia la capa superficial. Estas entradas de nutrientes, junto con su amplificación debido a la remineralización dentro de las Rías (Álvarez-Salgado et al., 2002; Bode et al., 1996), estimulan una elevada producción fitoplanctónica que sostiene un rico ecosistema marino y pesquerías muy productivas (Fraga, 1981; Varela, 1992). Desde octubre a marzo, los vientos prevalentes del sur favorecen eventos de hundimiento (Fraga, 1981; Wooster et al., 1976). El conocimiento sobre la actividad diazótrofa en esta región de afloramiento está limitado a una única observación realizada en verano de 2009 (Benavides et al., 2011). En este estudio se observaron tasas de fijación de N_2 relativamente bajas y principalmente atribuidas a UCYN-A en las proximidades de Cabo Silleiro (42ºN). En esa misma campaña, Agawin et al. (2014) observaron que UCYN-A dominó la composición de la comunidad diazótrofa en un área próxima al Cabo de Aguer (NO de África, ~30º–31ºN), bajo concentraciones de nitrato que superan los 2 μM y temperaturas de aproximadamente 17ºC.

8.1.6. Hipótesis y objetivos

La presente Tesis Doctoral investiga por primera vez, a través de un estudio multidisciplinar, la magnitud y relevancia biogeoquímica de la fijación biológica de N_2, así como la diversidad, abundancia y variabilidad temporal de diazótrofos en la región de afloramiento del NO de la Península Ibérica (Atlántico NE). Además, aborda desde una perspectiva metodológica las consecuencias de la contaminación del $^{15}N_2$ usado para medir tasas de fijación de N_2. Las hipótesis formuladas fueron:

1. Los contaminantes marcados con ^{15}N que están presentes en algunos stocks comerciales de $^{15}N_2$ producen sobreestimaciones en las tasas de fijación biológica de N_2.

2. Existe una actividad de fijación de N_2 detectable en la región costera de afloramiento del NO de la Península Ibérica, aunque representa una entrada menor de nitrógeno nuevo en el sistema.

3. El forzamiento hidrodinámico que caracteriza a la región de estudio a lo largo del año induce una importante variabilidad en la composición de la comunidad diazótrofa.

Para comprobar estas hipótesis se propusieron los siguientes objetivos específicos:

1. Comprobar la susceptibilidad a la asimilación de los contaminantes marcados con ^{15}N por organismos no diazótrofos, y determinar la potencial sobreestimación de las tasas de fijación N_2 (Capítulo 2).

2. Describir la variabilidad estacional de la magnitud de la fijación de N_2, y comparar su relevancia biogeoquímica como mecanismo de suministro de N nuevo frente a la difusión turbulenta de nitrato (Capítulo 3).

3. Investigar la relación entre la variabilidad en el forzamiento hidrodinámico y los cambios en la composición de la comunidad de diazótrofos y las abundancias de los principales grupos (Capítulos 3 y 4).

8.2. Resultados y discusión

8.2.1. Efectos de la contaminación de los stocks comerciales de $^{15}N_2$ sobre las medidas de fijación biológica de N_2

Nuestros resultados demostraron que los contaminantes inorgánicos marcados con ^{15}N, que se encuentran en algunos stocks comerciales de Sigma-Aldrich son asimilables por organismos no diazótrofos, produciendo enriquecimientos significativos en ^{15}N del nitrógeno orgánico particulado ($\delta^{15}N \approx 3‰$ con respecto a los tratamientos control y con $^{15}N_2$ de Cambridge-Isotope), así como sobreestimaciones de las tasas de fijación de N_2 de hasta un factor de 16, cuando se utiliza la técnica del trazador isotópico estable de Montoya et al. (1996). Por tanto, las estimas de fijación de N_2 descritas en la literatura podrían ser erróneas en función de la fuente de $^{15}N_2$ usada, especialmente cuando se utilizan stocks de Sigma-Aldrich. En cualquier caso, el $^{15}N_2$ de Cambridge se utiliza en la mayoría de los estudios. Además, considerando que solamente los stocks de una casa comercial (Sigma-Aldrich) de las tres analizadas por Dabundo et al. (2014) mostraron una presencia sustancial de contaminantes marcados con ^{15}N, las tasas publicadas obtenidas con $^{15}N_2$ de los otros proveedores (Cambridge-Isotope y Campro Scientific), son a priori fiables. Por tanto, para llevar a cabo medidas correctas de fijación biológica de N_2 en el futuro será aconsejable utilizar los stocks comerciales presumiblemente libres de contaminantes según Dabundo et al. (2014), y realizar pruebas de control de pureza como las que aquí hemos descrito antes de usar el $^{15}N_2$ adquirido.

8.2.2. Magnitud y relevancia biogeoquímica de la fijación de N_2 bajo diferentes condiciones hidrográficas

Nuestros resultados demuestran una actividad de fijación biológica de N_2 detectable (hasta 0.1 µmol N m^{-3} d^{-1}) bajo diferentes condiciones hidrográficas en una región costera templada rica en nitrógeno y bajo la influencia de afloramiento. Las tasas de fijación obtenidas, que fueron máximas en aguas superficiales tanto en condiciones de afloramiento como relajación, son comparables a las tasas más bajas descritas para el Atlántico NE subtropical (Luo et al., 2012), y similares a las medidas en las proximidades de Cabo Silleiro (NO Península Ibérica) (Benavides et al., 2011). A pesar de la actividad diazótrofa relativamente baja, nuestros resultados son una evidencia más de que altas concentraciones de nitrato, ratios N:P elevadas y bajas temperaturas (<17ºC) no inhiben

la fijación de N_2, tal y como se ha observado en otras regiones de afloramiento (e.g., Benavides et al., 2014; Sohm et al., 2011; Subramaniam et al., 2013; Voss et al., 2004; Wen et al., 2017), la plataforma costera de la región templada del Atlantico NO (Mulholland et al., 2012), el Canal Inglés (Rees et al., 2009) o el Océano Ártico (Shiozaki et al., 2017, 2018). Por tanto, estos resultados son contrarios al paradigma tradicional sobre fijación de N_2 marina, el cual asume que este proceso está limitado principalmente al océano tropical y subtropical, cálido (>20ºC) y pobre en nitrógeno. Esto es debido a que el elevado suministro de nitrógeno y temperaturas superficiales las relativamente bajas típicas de los sistemas costeros templados inhibirían la actividad de cianobacterias filamentosas no heterocísticas como *Trichodesmium* (Conley et al., 2009; Howarth et al., 1988; Stal, 2009). Las evidencias de diazotrofía encontradas en zonas previamente ignoradas, junto con la amplia distribución y gran diversidad de diazótrofos (Farnelid et al., 2011; Moisander et al., 2010; Riemann et al., 2010; Zehr et al., 2000, 2003b), indican que limitar los estudios sobre fijación de N_2 exclusivamente a las zonas tropicales y subtropicales oligotróficas podría resultar en una subestimación de la magnitud global de este flujo, contribuyendo a los aparentes desequilibrios observados en el balance global de N marino (Brandes and Devol, 2002; Codispoti, 2007; Mahaffey et al., 2005; Voss et al., 2013).

A partir de nuestros datos, estimamos una entrada promedio de N nuevo asociado a la fijación de N_2 planctónica en el NO de la Península Ibérica (considerando una superficie de 3º×3º) de aproximadamente 0.4 Gg N a^{-1}. El suministro de N nuevo hacia la capa eufótica a través de la actividad diazótrofa fue entre 2 y 5 órdenes de magnitud más bajo que el suministro a través de flujos difusivos de nitrato. Por lo tanto, la contribución de la fijación de N_2 fue irrelevante (<2%) en comparación con la difusión turbulenta. Asimismo, la proporción de producción primaria bruta que podría ser explicada por la diazotrofía, asumiendo estequiometría de Redfield, fue también despreciable (<0.1%). Estas estimas de la contribución de la fijación de N_2 y difusión vertical a los flujos de N nuevo son las primeras que se realizan en un sistema costero de afloramiento. Debido a las dificultades metodológicas para cuantificar directamente la mezcla vertical (*Kz*) en el campo, pocos estudios han medido simultáneamente ambos procesos (e.g., Fernández-Castro et al., 2015; Mouriño-Carballido et al., 2011; Painter et al., 2013), motivando el uso de valores constantes de *Kz* (Capone et al., 2005), o parametrizaciones empíricas (Fernández-Castro et al., 2014; Planas et al., 1999) para estimar los flujos difusivos de

nitrato. La relevancia biogeoquímica de la fijación de N_2 en este sistema sería todavía más baja si consideramos otros suministros importantes de N nuevo, como el transporte advectivo debido al afloramiento (Pitcher et al., 2010), el transporte lateral (Torres-Valdés et al., 2009; Williams and Follows, 1998) o el aporte fluvial (Varela et al., 2005).

8.2.3. Diversidad, abundancia, variabilidad temporal y ecología de diazótrofos

La actividad de fijación de N_2 detectada en la región de estudio fue llevada a cabo por pequeños diazótrofos (<10 μm), presumiblemente unicelulares. Esta conclusión está respaldada por nuestro análisis de la biblioteca de secuencias *nifH* obtenida mediante tecnología de Next Generation Sequencing (Illumina MiSeq®), que reveló que todas las secuencias pertenecieron a diazótrofos unicelulares cianobacterianos y heterótrofos. Concretamente, la composición de la comunidad diazótrofa estuvo dominada por UCYN-A (21%, subcluster *nifH* 1B), y diazótrofos no cianobacterianos. Esto es consistente con estudios previos señalando la predominancia de UCYN-A en aguas frías y relativamente ricas en nitrógeno de latitudes templadas del Atlántico NE (Agawin et al., 2014; Rees et al., 2009). Por otro lado, los diazótrofos no cianobacterianos estuvieron representados principalmente por diversos filotipos afiliados a Gammaproteobacteria (28%, subcluster 1G), en su mayoría *Pseudomonas stutzeri*, y bacterias anaeróbicas del subcluster 3 (36%). Por el momento se desconoce la contribución de los diazótrofos no cianobacterianos a la fijación biológica de N_2. No obstante, estos fijadores de N_2 potenciales muestran una distribución más amplia que las cianobacterias, lo que pone de relieve su posible importancia biogeoquímica (Bombar et al., 2016; Delmont et al., 2018; Moisander et al., 2017).

Este estudio describe por primera vez en un ecosistema templado de afloramiento una diversa y variable temporalmente comunidad diazótrofa controlada por el forzamiento hidrodinámico. Los diazótrofos no cianobacterianos, que pertenecen principalmente a los clusters 1G (Gammaproteobacteria, en su mayoría *P. stutzeri*) y 3 (anaerobios), dominaron la comunidad durante las condición de hundimiento, caracterizada por capas profundas de mezcla y una columna de agua homogénea. Bajo estas condiciones hidrográficas, la composición de la comunidad diazótrofa mostró una variabilidad más baja y una mayor diversidad. Por el contrario, en condiciones de afloramiento y relajación observamos el predominio de UCYN-A (principalmente el sublinaje UCYN-A2 de acuerdo con el análisis de oligotyping) y una comunidad diazótrofa más heterogénea y

menos diversa. Estas condiciones se caracterizaron por una elevada estratificación vertical y una mayor variabilidad hidrográfica. Las abundancias relativas de UCYN-A más altas se cuantificaron en estas condiciones en superficie. Por tanto, nuestros resultados demuestran una comunidad diazótrofa dinámica cuyas fluctuaciones están asociadas a la variabilidad ambiental. Del mismo modo, Messer et al. (2015b) y Church et al. (2009) observaron variabilidad estacional en la composición de la comunidad diazótrofa en aguas tropicales de Australia y el giro subtropical del Pacífico Norte, respectivamente. En consonancia con todos estos hallazgos, Martin-Platero et al. (2018) demostraron, mediante una serie temporal de alta resolución en la costa templada del este de los EEUU, una rápida y brusca renovación en la composición de las comunidades planctónicas microbianas asociada a la variabilidad hidrográfica.

El método del oligotyping nos permitió investigar la diversidad enmascarada dentro de los OTUs de UCYN-A y definir oligotipos (taxones altamente depurados) que fueron asignados a sublinajes de UCYN-A. UCYN-A2 fue claramente el sublinaje más abundante (74% del conjunto de datos), seguido por UCYN-A1 (23%) y UCYN-A4 (2%), los cuales estuvieron principalmente representados por oligo3 (67%), oligo1 (18%) y oligo4 (2%), respectivamente. Estos oligotipos son algunos de los más abundantes de la biblioteca global de amplicones de *nifH* de UCYN-A (Turk-Kubo et al., 2017), que está dominada por oligotipos pertenecientes a UCYN-A1, dado que dicha base de datos incluye principalmente muestras de regiones oligotróficas de océano abierto. Los oligotipos de UCYN-A1 se detectaron a frecuencias relativamente bajas durante las tres condiciones hidrográficas, mientras que de UCYN-A2 hubo un mayor número de secuencias durante afloramiento y relajación.

Por otro lado, determinamos las abundancias absolutas a través de PCR cuantitativa (qPCR) de UCYN-A (UCYN-A1 y -A2) y el filotipo γ-24774A11 de Gammaproteobacteria. El filotipo de Gammaproteobacteria, que está globalmente distribuido, mostró las abundancias más altas durante las condiciones de hundimiento, cuando la columna de agua estaba más caliente, menos estratificada y con concentraciones bajas de nutrientes. Es probable que bajo estas condiciones una gran parte de la producción primaria se sostenga gracias a la producción de nutrientes regenerados a través de la remineralización bacteriana de la materia orgánica, como observaron Bode et al. (2004, 2011) en esta misma región. Además, Gammaproteobacteria podría verse favorecida por la materia orgánica producida después

de los pulsos de afloramiento bajo condiciones de estratificación térmica de verano, tal y como observamos en el muestreo de septiembre de 2015. De hecho, Moisander et al. (2012, 2014) sugirieron que el filotipo γ-24774A11 de Gammaproteobacteria podría depender del carbono orgánico disuelto producido por el fitoplancton. Por el contrario, UCYN-A1 y -A2 mostraron las abundancias más altas (hasta 6.7×10^2 y 1.5×10^3 copias de *nifH* L^{-1}, respectivamente) en las aguas superficiales bien iluminadas durante condiciones de afloramiento y relajación, lo que es consistente con nuestros resultados de abundancias de oligotipos. Esto indica una posible variabilidad estacional en el crecimiento de la simbiosis entre UCYN-A y la microalga primnesiofita, tal y como se observó previamente en el Pacífico SO tropical y subtropical (Bonnet et al., 2015; Moisander et al., 2010). Las abundancias absolutas de UCYN-A estuvieron en el rango medio-bajo de las abundancias globales (Benavides and Voss, 2015; Luo et al., 2012; Martínez-Pérez et al., 2016). Concretamente para el Atlántico Norte, UCYN-A es, tras *Trichodesmium*, el diazótrofo más abundante, encontrándose principalmente en la cuenca este (Benavides et al., 2016; Benavides and Voss, 2015; Ratten et al., 2015). En general, UCYN-A2 fue significativamente más abundante que UCYN-A1, tanto en términos de abundancias absolutas como de abundancias relativas de oligotipos. Esto es consistente con hallazgos recientes indicando que UCYN-A2, aunque ampliamente extendido (Cabello et al., 2016; Martínez-Pérez et al., 2016), se encuentra principalmente en áreas costeras, mientras que UCYN-A1 predomina en el océano abierto oligotrófico (Henke et al., 2018; Messer et al., 2015a, 2015b; Thompson et al., 2014; Turk-Kubo et al., 2017). Estas diferencias en la distribución global de los sublinajes de UCYN-A, así como la variabilidad temporal observada, podrían estar relacionadas con los requerimientos fisiológicos y la adaptación de los respectivos huéspedes primnesiofita a hábitats específicos y condiciones ambientales, y al hecho de que las primnesiofitas pasan a través de diferentes estadios a lo largo de su ciclo de vida (Hagino et al., 2013). La divergencia evolutiva de UCYN-A dando lugar a diferentes linajes (Cornejo-Castillo et al., 2016) les podría haber permitido dispersarse y adaptarse a diferentes ambientes.

Como hemos visto previamente, las abundancias absolutas y relativas de UCYN-A fueron máximas en aguas superficiales de las condiciones de afloramiento y relajación, coincidiendo con las tasas de fijación de N_2 más altas. De hecho, las abundancias de UCYN-A mostraron una correlación positiva significativa con la fijación, algo que no ocurrió en el caso de las Gammaproteobacteria. La relación entre UCYN-A y la actividad

diazótrofa también fue observada en la costa este de EEUU (Mulholland et al., 2012) y el Pacífico SO tropical (Bonnet et al., 2015; Turk-Kubo et al., 2015). Por tanto, la simbiosis UCYN-A–primnesiofita podría ser la principal responsable de la fijación en la región de afloramiento del NO de la Península Ibérica.

A diferencia de Gammaproteobacteria γ-24774A11 cuyas abundancias máximas fueron detectadas en aguas profundas (70 m) durante condiciones de hundimiento, las abundancias máximas de UCYN-A, principalmente del sublinaje costero UCYN-A2, fueron detectadas en aguas superficiales estratificadas y bien iluminadas bajo condiciones de afloramiento y relajación. Por tanto, nuestros hallazgos demarcan las condiciones ambientales asociadas al nicho ecológico de Gammaproteobacteria y UCYN-A en esta región de afloramiento. Además, de acuerdo con los análisis del nicho ecológico de los diazótrofos cuantificados por qPCR, UCYN-A2 fue más abundante bajo condiciones de alta concentración de clorofila *a*, mientras que Gammaproteobacteria predominó a concentraciones de clorofila más bajas.

8.2.4. Estudios futuros

En el actual escenario de cambio global, los diazótrofos están experimentando importantes cambios antropogénicos en su entorno que, en general, podrían beneficiar su crecimiento y actividad en el futuro. El calentamiento del agua de mar, el aumento de la estratificación en el océano y la expansión de las OMZs (zonas de mínima concentración de oxígeno), las cuales suministrarán aguas pobres en N a la capa fótica superficial estimulando la actividad diazótrofa (Deutsch et al., 2007; Karl and Letelier, 2008), podrían expandir el rango de distribución de los fijadores en el futuro e incrementar su actividad global (Deutsch et al., 2007; Doney, 2006; Hutchins and Fu, 2017; Karl and Letelier, 2008; Stramma et al., 2008). Concretamente para el noroeste de la Península Ibérica, la importancia relativa de la diazotrofía también podría incrementarse debido al debilitamiento del afloramiento observado en las últimas décadas (Pardo et al., 2011; Pérez et al., 2010). Por el contrario, el aumento de las entradas de N nuevo debido a una mayor deposición atmosférica y el aumento del uso de fertilizantes podrían tener el efecto opuesto (Duce et al., 2008; Naqvi et al., 2000).

Por primera vez, hemos demostrado actividad y presencia de una comunidad de diazótrofos variable en el tiempo en una región de afloramiento templada a lo largo de un

ciclo estacional. Sin embargo, estudios futuros con mayor resolución temporal incluyendo medidas de fijación de N_2 y abundancia, diversidad y expresión de genes *nifH* serán necesarios para comprender mejor los factores de control de la fijación y el papel de la variabilidad a corto plazo del forzamiento ambiental. Asimismo, una mayor cobertura espacial incluyendo transectos costa-océano permitirá caracterizar la variabilidad espacial. Los estudios de expresión del gen *nifH* permitirán determinar las abundancias absolutas y relativas de los transcriptos de *nifH* e identificar a los diazótrofos activos en este sistema, diferenciando entre fijadores cianobacterianos y heterótrofos.

La mayor parte de la fijación de N_2 en la región podría producirse bajo condiciones de limitación de nitrógeno durante el verano, cuando el fitoplancton está limitado por este elemento o al menos responde a su aporte (Martínez-García et al., 2010). De hecho, observamos que las tasas de fijación más altas, detectadas en aguas superficiales durante el verano, coincidieron con las máximas abundancias de UCYN-A bajo condiciones de ratios N:P por debajo de la estequiometría de Redfield (<11), concentraciones de clorofila *a* relativamente bajas (<1.5 mg m^{-3}) y estratificación relativamente alta ($\log_{10} N^2$ (s^{-2}) = -3.5 – -4.2). No obstante, deberían implementarse estudios observacionales y experimentales específicos, incluyendo pruebas de adición de nutrientes, para arrojar luz sobre los factores que controlan la actividad y crecimiento de los diazótrofos presentes en esta región, así como delimitar con exactitud las condiciones ambientales que definen sus nichos ecológicos.

8.3. Conclusiones

1. Los contaminantes inorgánicos marcados con ^{15}N que se encuentran en algunos stocks comerciales de $^{15}N_2$ son asimilables por organismos no diazótrofos, pudiendo producir sobreestimaciones de hasta dieciséis veces en las tasas de fijación biológica de N_2.

2. Las tasas más altas de fijación de N_2, que en general fueron bajas (hasta 0.1 µmol N m^{-3} d^{-1}) y comparables a las tasas más bajas descritas para el Atlántico Noreste subtropical, se detectaron en aguas superficiales durante afloramiento y relajación.

3. La contribución de la fijación de N_2 al suministro de N nuevo hacia la zona eufótica fue despreciable (<2%) en comparación con los flujos difusivos de nitrato.

4. La composición de la comunidad diazótrofa estuvo dominada por bacterias anaeróbicas del cluster 3 (36%), Gammaproteobacteria del subcluster 1G (28%) y diazótrofos unicelulares cianobacterianos del subcluster 1B (UCYN-A, 21%)

5. La comunidad diazótrofa mostró una importante variabilidad temporal: durante condiciones de hundimiento fue más homogénea y diversa, y estuvo dominada por diazótrofos no cianobacterianos de los clusters 1G y 3, mientras que durante afloramiento y relajación fue más heterogénea y menos diversa, con prevalencia de UCYN-A y clusters 1G y 3.

6. UCYN-A2 fue el sublinaje más abundante en términos relativos (74% de las secuencias de UCYN-A), seguido por UCYN-A1 (23%) y UCYN-A4 (2%), que estuvieron representados principalmente por los oligotipos oligo3 (67%), oligo1 (18%) y oligo4 (2%), respectivamente.

7. Gammaproteobacteria del filotipo γ-24774A11 mostró las abundancias absolutas más altas (hasta 2.4×10^4 copias de *nifH* L^{-1}) en aguas profundas durante condiciones de hundimiento, mientras que UCYN-A1 y -A2 fueron más abundantes (hasta 6.7×10^2 y

1.5×10^3 copias de *nifH* L^{-1}, respectivamente) en aguas superficiales bajo condiciones de afloramiento y relajación.

8. La correlación positiva entre las abundancias de UCYN-A y las tasas de fijación de N_2 indica que este grupo sea probablemente el principal diazótrofo activo en la región.

Universidade Vigo

Universidade Vigo

Victor Moreira Coello

Doctoral dissertation

Biological N_2 fixation in the upwelling region off NW Iberian Peninsula: magnitude, relevance and players

2018